

UNIVERSITI TEKNOLOGI MARA

**FROM WASTE TO FUEL:
CONTROLLED TORREFACTION
(MILD PYROLYSIS) OF MIXED
PLASTICS WITH
CHARACTERIZATION OF SOLID
FUEL AND BY-PRODUCTS**

SAFWAN HAFIZI BIN MASAKHOH

MSc

April 2026

UNIVERSITI TEKNOLOGI MARA

**FROM WASTE TO FUEL:
CONTROLLED TORREFACTION
(MILD PYROLYSIS) OF MIXED
PLASTICS WITH
CHARACTERIZATION OF SOLID
FUEL AND BY-PRODUCTS**

SAFWAN HAFIZI BIN MASAKHOH

Thesis submitted in fulfilment
of the requirements for the degree of
Master of Science
(Chemical Engineering)

Faculty of Chemical Engineering

April 2026

CONFIRMATION BY PANEL OF EXAMINERS

I certify that a Panel of Examiners has met on 6th January 2026 to conduct the final examination of Safwan Hafizi bin Masakhoh on his Masters of Science thesis entitled "From Waste To Fuel: Controlled Torrefaction (Mild Pyrolysis) of Mixed Plastics with Characterization of Solid Fuel and By-Products" in accordance with Universiti Teknologi MARA Act 1976 (Akta 173). The Panel of Examiner recommends that the student be awarded the relevant degree. The Panel of Examiners was as follows:

Nur Hashimah Alias, PhD
Associate Professor
Faculty of Chemical Engineering
Universiti Teknologi MARA
(Chairman)

Hazman Seli, PhD
Senior Lecturer
Faculty of Chemical Engineering
Universiti Teknologi MARA
(Internal Examiner)

Mohamad Omar Abdullah, PhD
Professor
Faculty of Engineering
Universiti Malaysia Sarawak
(External Examiner)

**PROFESSOR DR HJH ZURAEDA
IBRAHIM**

Dean
Institute of Postgraduates Studies
Universiti Teknologi MARA

Date: 3 April 2026

AUTHOR'S DECLARATION

I declare that the work in this thesis was carried out in accordance with the regulations of Universiti Teknologi MARA. It is original and is the results of my own work, unless otherwise indicated or acknowledged as referenced work. This thesis has not been submitted to any other academic institution or non-academic institution for any degree or qualification.

I, hereby, acknowledge that I have been supplied with the Academic Rules and Regulations for Post Graduate, Universiti Teknologi MARA, regulating the conduct of my study and research.

Name of Student	Safwan Hafizi bin Masakhoh
Student ID. No.	2020401142
Programme	Master of Science (Chemical Engineering) - EH750
Faculty	Chemical Engineering
Thesis Title	From Waste To Fuel: Controlled Torrefaction (Mild Pyrolysis) of Mixed Plastics with Characterization of Solid Fuel and By-Products

Signature of Student

Date April 2026

ABSTRACT

The global plastic waste crisis and the depletion of fossil fuels necessitate innovative waste-to-energy solutions. Pyrolysis remains a promising pathway, however conventional high temperature processes ($>500^{\circ}\text{C}$) are energy intensive and generate hazardous emissions, limiting their suitability for community scale adoption. This study investigates a lower temperature ($<450^{\circ}\text{C}$) mild pyrolysis approach for mixed high density polyethylene (HDPE) and polyethylene terephthalate (PET) waste using a batch reactor with extended residence times. The objectives were to characterize thermal degradation behaviour, establish wastewater-based emission profiling (COD, BOD, pH, DO, TSS and turbidity), and evaluate pyrolytic oil quality under mild pyrolysis conditions. Pure HDPE achieved oil yields of up to 68 wt% at 320°C , whereas an HDPE1:2PET blend produced 26 wt%. Thermogravimetric analysis (TGA) indicated maximum mass loss temperatures at 482°C for HDPE and 447°C for PET. A novel low cost emission monitoring method is introduced using water phase indicators where elevated COD (up to 8508 mg/L), reduced pH (down to 3.82) and suppressed DO (<4 mg/L) signalled the presence of oxygenated volatiles and acidic condensable originating primarily from PET decomposition and trace additive derived species. These observations were validated through FTIR and GC-MS analyses which identified *Ci-C25* hydrocarbons and oxygenates consistent with PET derived intermediates. Char analysis revealed fixed carbon contents of up to 21 wt% for PET rich residues. The integrated framework combining oil grading with wastewater based odour and emission profiling demonstrates a scalable and resource efficient technology particularly suitable for HDPE rich waste streams making it promising for decentralized and community level applications in resource constrained settings. Overall, the findings provide a practical pathway for the cleaner low emission conversion of mixed plastic waste into high value pyrolytic fuels using mild pyrolysis

ACKNOWLEDGEMENT

In the name of Allah, the Most Gracious, the Most Merciful. All praise is due to Allah for granting me the strength, perseverance, and patience to complete this research work successfully. I would like to express my deepest gratitude to my supervisor, Dr Zakiuddin Januri and co-supervisor Ts Prof Dr Norazah Abdul Rahman for their invaluable guidance, continuous encouragement, and constructive feedback throughout the course of this study. Their expertise and unwavering support have been instrumental in shaping this research into its present form.

My sincere appreciation also goes to the Faculty of Chemical Engineering, Universiti Teknologi MARA (UiTM), for providing the facilities, resources, and academic environment that enabled me to carry out this research. Special thanks are extended to the laboratory staff and colleagues who offered technical assistance and advice during the experimental work. I also would like to thank Prof Hussameldin Ibrahim, Director of Clean Energy Technologies Research Institute (CETRI), University of Regina, Saskatchewan, Canada as Host Supervisor while I was there as Visiting Graduate Research Student for 4 months from September 2022 to January 2023.

I am profoundly grateful to my family, especially my lovely mother, HjH , my understanding^ wife, Farizah binti Bakar, my actively daughters Hana Tasneem and Hani Syakirah for their unconditional love, prayers, and sacrifices, which have been the foundation of my academic journey. To my friends and fellow researchers, thank you for your moral support, thoughtful discussions, and encouragement during challenging moments.

Finally, I dedicate this achievement to all those who have supported and inspired me directly or indirectly in the completion of this thesis. May Allah bless you all abundantly.

TABLE OF CONTENT

	Page
CONFIRMATION BY PANEL OF EXAMINERS	ii
AUTHOR'S DECLARATION	iii
ABSTRACT	iv
ACKNOWLEDGEMENT	v
TABLE OF CONTENTS	vi
LIST OF TABLES	xii
LIST OF FIGURES	xv
LIST OF PLATES	xv
LIST OF SYMBOLS	xvi
LIST OF NOMENCLATURE	xvii
CHAPTER 1: INTRODUCTION	1
1.1 Research Background	1
1.2 Problem Statement	3
1.3 Research Objectives	5
1.4 Scope of Research	5
1.5 Significance of the Study	6
1.6 Outline of Research Work	7
1.7 Concluding Remark	8
CHAPTER 2: LITERATURE REVIEW	
2.1 Introduction	9
2.2 Current Problem in the Pyrolysis of Plastic Waste for Pyro-Fuel Production	9
2.2.1 Pollution emitted from the process	9
2.2.2 Hazardous gas released from the process	10
2.2.3 Health problems arise from the process	11
2.2.4 Root cause of the problem in pyrolysis of plastic waste	12
2.3 Types Of Plastic Affecting The Pyrolysis Process	12
2.3.1 Plastic waste characterization for pyrolysis process	12

2.3.2	Physical characterization of plastic waste	17
2.3.2.1	<i>Particle Size</i>	18
2.3.2.2	<i>Density</i>	19
2.3.2.3	<i>Thermal Properties</i>	19
2.3.2.4	<i>Moisture Content</i>	20
2.3.2.5	<i>Melting Point</i>	21
2.3.2.6	<i>Flash Point</i>	22
2.3.3	Chemical characterization of plastic waste (ac single and mix types)	22
2.3.3.1	<i>Proximate Analysis</i>	23
2.3.3.2	<i>Ultimate Analysis</i>	24
2.3.3.3	<i>Heating Value (Calorific Value)</i>	25
2.3.3.4	<i>FTIR</i>	28
2.3.3.5	<i>GC-MS</i>	29
2.3.3.6	<i>TGA</i>	30
2.3.3.7	<i>DSC</i>	31
2.3.4	Importance of choosing the mixing ratio of plastic waste types during pyrolysis process	32
2.4	Types of Reactors and Pyrolysis Process Involved for Production of Pyro-Fuel from Plastic Waste	34
2.4.1	Different types of reactors used for production of Pyro-Fuel in pyrolysis	35
2.4.2	Different types of pyrolysis process used for production of Pyro-Fuel in pyrolysis	37
2.4.3	Types of reactors and process affecting the product and by-product in Pyro-Fuel production	38
2.5	Parameter Use in Pyrolysis to Convert Plastic Waste into Pyro-Fuel That Affects Both Quality of Pyro-Fuel and Pollution Emitted	41
2.5.1	Process parameter for production of Pyro-Fuel from pyrolysis of Plastic Waste	41
2.5.2	Critical parameters that have significant effect to the process	42
2.5.3	Reaction temperature in the reactor gives significant effect to the process	44
2.5.4	Reaction time causes the runaway reaction then creates unwanted by-products	45

2.5.5	Good combination of parameters will produce high quality product with low emission of pollutants and unwanted by-products	46
2.6	Pyro-Fuel Produced from Pyrolysis of Plastic Waste	48
2.6.1	Physical properties of pyro-fuel from plastic waste	49
2.6.2	Chemical properties of pyro-fuel from plastic waste	50
2.7	Pollutant Emitted and Odour Profiling Method by Using Low-Cost Wastewater Analysis	52
2.7.1	Properties of hazardous gas released during pyrolysis of plastic waste	63
2.7.2	Odour profiling method to capture the evolution of gas during pyrolysis by using low-cost wastewater analysis method	66
2.8	Current Countermeasure to Mitigate Hazardous Waste	68
2.8.1	Use of wet scrubber in this area for mitigation and the efficient use of wet scrubber	71
2.9	Synergistic Study to Produce High Quality Pyro-Fuel with Low Emission Side Product	72
2.9.1	Combination of Critical Parameters and Pollutants Emitted to Produce High Quality Pyro-Fuel	73
2.9.2	Properties of Pyro-Fuel from Synergistic Study	75
2.10	Wastewater Generation and Profiling in Plastic Pyrolysis Processes	75
2.11	Concluding Remark	78
CHAPTER 3 RESEARCH METHODOLOGY		79
3.1	Raw Materials Preparation and Analysis	79
3.1.1	Raw Materials Preparation (HDPE and PET Samples)	79
3.1.1.1	<i>Preparation of Raw Materials for Pyrolysis according to its Mixing Ratio</i>	80
3.1.1.2	<i>Preparation of Raw Materials for Analysis Its Content</i>	81
3.1.2	Physical Characterisation of Raw Materials	81
3.1.2.1	<i>Particle Size</i>	81
3.1.2.2	<i>Density</i>	82
3.1.2.3	<i>Moisture Content</i>	82
3.1.2.4	<i>Melting Point</i>	83
3.1.3	Chemical Characterisation Of Raw Materials	83
3.1.3.1	<i>Proximate Analysis</i>	83

	3.1.3.2	<i>Ultimate Analysis</i>	85
	3.1.3.3	<i>Calorimetric Analysis</i>	85
	3.1.3.4	<i>TGA/DSC</i>	86
	3.1.3.5	<i>Fourier Transform Infrared Spectrophotometer (FTIR)</i>	86
3.2		Synergistic Pyrolysis Process of Plastic Waste	87
	3.2.1	Equipment Set-Up for Pyrolysis	87
	3.2.2	Parameter Selection for Pyrolysis	88
	3.2.3	Process Sequence and Method of Pyrolysis	88
	3.2.4	Thermal Degradation Behaviour Analysis during Pyrolysis Process	89
3.3		Odour Profiling to Determine the Level of Contamination by Using Low-Cost Wastewater Analysis	90
	3.3.1	Method analysis on the wastewater converted from gas released during the pyrolysis process of plastic waste	90
		3.3.1.1 <i>DO (Dissolved Oxygen)</i>	90
		3.3.1.2 <i>Turbidity</i>	90
		3.3.1.3 <i>Chemical Oxygen Demand (COD)</i>	91
		3.3.1.4 <i>Biochemical oxygen demand (BOD)</i>	92
		3.3.1.5 <i>pH</i>	92
		3.3.1.6 <i>Total Suspended Solid (TSS)</i>	93
	3.3.2	Basic Analysis Of Gaseous Product In Pyrolysis	93
3.4		Pyrolytic Oil Quality Evaluation (Physical And Chemical Properties)	94
	3.4.1	Yields of pyro-fuel	94
	3.4.2	Physical Characterisation of Pyro Fuel	94
		3.4.2.1 <i>Flash Point</i>	94
		3.4.2.2 <i>Density</i>	94
		3.4.2.3 <i>Calorimetric Analysis</i>	95
	3.4.3	Chemical Characterisation of Pyro-fuel	95
		3.4.3.1 <i>Gas Chromatography Mass Spectrometer (GC-MS)</i>	95
3.5		Interpretive Analysis of Correlation Between Pyro-Fuel and Wastewater Profiling, Reaction Kinetics, Emission Behaviour and Oil Quality	96
	3.5.1	Correlation Between Pyro-Fuel and Wastewater Profiling	96
	3.5.2	Error and Uncertainty Analysis	97

	3.5.2.1	<i>OFAT Analysis of the Process</i>	98
	3.5.2.2	<i>Statistical Analysis of The Process by Using Linear Regression ANOVA</i>	99
	3.5.3	Reaction Kinetics	99
	3.5.4	Emission Behaviour	100
	3.5.5	Oil Quality Assessment	101
3.6		Concluding Remark	102
CHAPTER 4 RESULTS AND DISCUSSION			103
4.1		Physical and Chemical Characteristic of Raw Materials Upon Pyrolysis	103
	4.1.1	Grain Size of Raw Material (Physical Properties)	103
	4.1.2	Density Of Raw Material (Physical Properties)	107
	4.1.3	Moisture Content Of Raw Material (Physical Properties)	108
	4.1.4	Melting Point Of Raw Material (Physical Properties)	109
	4.1.5	Proximate Analysis Of Raw Material (Chemical Properties)	110
	4.1.6	Ultimate Analysis Of Raw Material (Chemical Properties)	111
	4.1.7	Energy Content Analysis Of Raw Material (Chemical Properties)	113
	4.1.8	Thermal Degradation Analysis of Raw Material by Using TGA/DSC (Chemical Properties)	114
	4.1.9	Chemical Hydrocarbon Bond Of Raw Material By Using FTIR (Chemical Properties)	117
4.2		Pyrolysis Behaviour And Product Yields From Selected Ratio Of Plastic Waste	124
	4.2.1	Thermal Degradation Profile Analysis During Pyrolysis Process At Different Ratio Of Plastic Waste	124
	4.2.2	Product Distribution Yield Analysis During Pyrolysis Process At Different Ratio Of Plastic Waste	127
4.3		Odour Profiling by Using Low-Cost Wastewater Analysis Captured During Pyrolysis Process	129
	4.3.1	Wastewater Analysis (DO, BOD, COD, Turbidity And TSS)	130
	4.3.2	Fundamental Analysis Of Gaseous Product In Pyrolysis	132
4.4		Pyrolytic Oil Quality Evaluation (Physical And Chemical Properties)	136

4.4.1	Calorific Value Analysis Of The Pyro-Fuel (Physical Properties)	136
4.4.2	Density Analysis Of The Pyro-Fuel (Physical Properties)	137
4.4.3	Flash Point Analysis Of The Pyro-Fuel (Physical Properties)	139
4.4.4	Chemical Content Analysis Of The Pyro-Fuel (Chemical Properties)	140
4.4.5	Analysis of Char Obtained from Pyrolysis Process by Using Proximate Analysis	146
4.5	Interpretive Analysis of Correlation Between Pyro-Fuel and Wastewater Profiling, Reaction Kinetics, Emission Behaviour and Oil Quality	148
4.5.1	Correlation Between Pyro-Fuel And Wastewater Profiling	149
	4.5.1.1 <i>OF AT Analysis of the Process</i>	149
	4.5.1.2 <i>Statistical Analysis of The Process by Using Linear Regression AN OVA</i>	153
4.5.2	Reaction Kinetics	155
4.5.3	Emission Behaviour	156
4.5.4	Oil Quality Assessment	157
4.6	Concluding Remark	158
	CHAPTER 5 CONCLUSION AND RECOMMENDATIONS	159
	REFERENCES	163
	APPENDICES	176
	AUTHOR'S PROFILE	220

LIST OF TABLES

Tables	Title	Page
Table 2.1	Yield Of Pyrofuel by Using Single Type of Plastic Waste	14
Table 2.2	Yield Of Pyrofuel by Using Mixed Plastic Waste	15
Table 2.3	Yield Of Pyrofuel by Using Specific Ratio Plastic Waste	16
Table 2.4	Proximate Analysis of Different Plastics	24
Table 2.5	Ultimate Analysis Results for HDPE and PET (%)	25
Table 2.6	Heating Values of Different Type of Plastics	26
Table 2.7	Calorific Value (MJ/kg) for HDPE and PET	27
Table 2.8	Type of Reactor and Heating Medium in Pyrolysis	39
Table 2.9	Properties of Product of Pyrolytic Oil	40
Table 2.10	Pyrolytic Oil Yield Produced from Mixed or Segregated Plastic Waste	48
Table 2.11	Hazardous Gas Released During Pyrolysis of Plastic Wastes	54
Table 2.12	Non-condensable Product Yield (wt%) for Different Samples of Plastic Wastes	56
Table 2.13	Effect of Thermal and Catalytic Pyrolysis on Product Yield (%) for Different Types of Polymers	57
Table 2.14	Effect of Temperature (°C) on Gas Yield (%) for Different Type of Plastic Wastes	59
Table 2.15	Effect of Catalysts on Non-condensable Product Yield (%)	60
Table 2.16	Effect of Hazardous Gas Emission During Pyrolysis of Plastic Wastes	62
Table 2.17	Properties of Hazardous Gas Released During Pyrolysis of Plastic Waste	64
Table 2.18	Odorous Compound According to Plastic Type	66
Table 2.19	Effect of HDPE:PET Ratios on Pyrolysis By-Products	68
Table 2.20	Current Countermeasure to Mitigate Hazardous Waste	70
Table 2.21	Use of Wet Scrubber in This Area for Mitigation	72
Table 3.1	Propose Parameter for Plastic Pyrolysis	88
Table 4.1	Grain Size of HDPE, HDPE2:1PET Ratio, HDPE1:1PET Ratio, HDPE1:2PET Ratio and PET	104

Table 4.2	Density of HDPE, PET and Mixing Ratio Before Pyrolysis	107
Table 4.3	Moisture Content of HDPE, PET and Mixing Ratio Before Pyrolysis	109
Table 4.4	Melting Point of HDPE, PET and Mixing Ratio Before Pyrolysis	110
Table 4.5	The Proximate Analysis Result of HDPE, PET and Mixing Ratio Before Pyrolysis	111
Table 4.6	The Elemental Analysis Result of HDPE, PET and Mixing Ratio Before Pyrolysis Process	112
Table 4.7	Calorific Value of Sample Before and After The Pyrolysis	114
Table 4.8	FTIR Analysis Of Pyro-Oils Obtained Through Thermochemical Conversion of Different Plastic Ratio	123
Table 4.9	Percentage Yield of Product After Pyrolysis	128
Table 4.10	D.O, B.O.D, pH and C.O.D., Turbidity and TSS from Pyrolysis of HDPE and PET Ratio	130
Table 4.11	Time-Resolved Emission Characteristics (FbS, CO, and LEL) during Pyrolysis of HDPE-PET Blends	134
Table 4.12	Calorific Value of Sample After the Pyrolysis	137
Table 4.13	Density of HDPE, PET and Mixing Ratio After Pyrolysis	138
Table 4.14	Flash Point of HDPE, PET and Mixing Ratio After Pyrolysis	139
Table 4.15	Component in Liquid Fraction Obtained from Pyrolysis of HDPE and PET Ratio Using GC-MS	144
Table 4.16	The Proximate Analysis Result of HDPE, PET and Mixing Ratio After Pyrolysis	147
Table 4.17	Quadratic Trendline Equation and R ² Value from Pyrolysis of HDPE and PET Ratio	153
Table 4.18	Summarized of ANOVA Analysis from Pyrolysis of HDPE and PET Ratio	155
Table A. 1a.	GCMS Result for HDPE Pyrolytic Oil After Pyrolysis Process	177
Table A. 1b	GCMS Result for Ratio HDPE2:1PET Pyrolytic Oil After Pyrolysis Process	182
Table A. 1c.	GCMS Result for Ratio HDPE1: 1PET Pyrolytic Oil After Pyrolysis Process	187
Table A. 1d.	GCMS Result for Ratio HDPE1:2PET Pyrolytic Oil After Pyrolysis Process	193
Table A. 1e.	GCMS Result for PET Pyrolytic Oil After Pyrolysis Process	199

Table A. 3a	ANOVA Analysis Result for HDPE Pyrolytic Oil After Pyrolysis Process	215
Table A. 3b.	ANOVA Analysis Result for HDPE2:1PET Ratio Pyrolytic Oil After Pyrolysis Process	216
Table A. 3c.	ANOVA Analysis Result for HDPE1:1PET Ratio Pyrolytic Oil After Pyrolysis Process	217
Table A. 3d.	ANOVA Analysis Result for HDPE1:2PET Ratio Pyrolytic Oil After Pyrolysis Process	218
Table A. 3e.	ANOVA Analysis Result for PET Ratio Pyrolytic Oil After Pyrolysis Process	219

LIST OF FIGURES

Figures	Title	Page
Figure 1.1	Conceptual Framework	5
Figure 3.1	HDPE and PET Plastic Sample	79
Figure 3.2	Flow Diagram of Procedure Used to Prepare Raw Material for Analysis	80
Figure 3.3	HDPE and PET Plastic Waste Powder	81
Figure 3.4	Pyrolysis Mini Plant Schematic Diagram	87
Figure 4.1	TGA Result for HDPE and PET Ratio Before Pyrolysis Process	116
Figure 4.2	DTG Result for HDPE and PET Ratio Before Pyrolysis Process	116
Figure 4.3	FTIR Result For HDPE Raw Material	117
Figure 4.4	FTIR Result For HDPE2:1PET Ratio Raw Material	118
Figure 4.5	FTIR Result For HDPE1:1PET Ratio Raw Material	119
Figure 4.6	FTIR Result For HDPE1:2PET Ratio Raw Material	120
Figure 4.7	FTIR Result For PET Raw Material	121
Figure 4.8	Temperature Degradation Profile Analysis for Raw Material at Different Mixing Ratio	126
Figure 4.9	Carbon Value for Different Ratio of Plastic Waste vs % Normalized Mass	142
Figure 4.10	OFAT Analysis With Effect Of Time On Temperature For HDPE, PET and Mixing Ratio After Pyrolysis	152
Figure A. 2a	Wifi Digital Microscope	203
Figure A. 2b	Electronic Digital Precision	203
Figure A. 2c	Memmert Wisconsin Oven	204
Figure A. 2d	Digital Melting Point with Capillary Tube Red Tip G0553	204
Figure A. 2e	Mettler Toledo Analytical Balance	205
Figure A. 2f	Raw Material Sample Ratio	205
Figure A. 2g	Muffle Furnace Fisher Scientific Model 550-126	206
Figure A. 2h	Elemental Analyser Model Thermo Electron, Flash EA 1112 Series	206
Figure A. 2i	Bomb Calorimeter model PARR 6400	207

Figure A. 2j	Thermogravimetric Analyser (TGA) model Mettler Toledo	207
Figure A. 2k	Fourier Transform Infrared Spectroscopy (FTIR)	208
Figure A. 2l	Pyrolysis Mini Plant	208
Figure A. 2m	Portable Dissolved Oxygen Meter	209
Figure A. 2n	Portable Turbidity Meter	209
Figure A. 2o	COD Reactor and COD Spectrophotometer	210
Figure A. 2p	BOD bottle and BOD incubator	210
Figure A. 2q	Portable pH Meter	211
Figure A. 2r	Porcelain Funnel Buchner and Drying Oven	211
Figure A. 2s	Multi Gas Detector Leakage	212
Figure A. 2t	Magnetic Stirrer and Infrared Thermometer	212
Figure A. 2u	Glass Density Meter	213
Figure A. 2v	Bomb Calorimeter model IKAC2000 BASIC	213
Figure A. 2w	Gas Chromatography Mass Spectrometer (GC-MS)	213

LIST OF SYMBOLS

Symbols

ΔH_m

Melting Enthalpies

ΔH_c

Crystallization Enthalpies

C_p

Specific Heat Capacity

ρ

Density

LIST OF NOMENCLATURES

NOMENCLATURES

ABS	Acrylonitrile-Butadiene-Styrene
ANOVA	Analysis Of Variance
AOP	Advanced Oxidation Process
ASTM	American Society For Testing And Materials
BBD	Box-Behnken Design
BOD	Biochemical Oxygen Demand
BTX	Benzene, Toluene, And Xylene
C	Carbon
CFB	Circulating Fluidized Bed
CI	Chemical Ionization
CO ₂	Carbon Dioxide
COD	Chemical Oxygen Demand
DO	Dissolved Oxygen
DSC	Differential Calorimetry
EG	Ethylene Glycol
EI	Electron Impact
FCC	Fluid Catalytic Cracking
FTIR	Fourier Transform Infrared
GHGs	Greenhouse Gases
GC-MS	Gas Chromatography Mass Spectrometer
H	Hydrogen
HCl	Hydrogen Chloride
HDPE	High Density Polyethylene
HEPA	High-Efficiency Particulate Air
ICP-OES	Inductively Coupled Plasma Optical Emission Spectroscopy
ICPs	Intrinsically Conducting Polymers
LCAs	Life Cycle Assessment
LDPE	Low Density Polyethylene
MPW	Municipal Plastic Waste
MSW	Municipal Solid Waste

N	Nitrogen
O	Oxygen
PAC	Pyrolysis Aqueous Condensate
PBT	Polybutylene Terephthalate
PE	Polyethylene
PET	Polyethylene Terephthalate
PFR	Plastic Film Residue
PM	Particulate Matter
PMMA	Polymethyl Methacrylate
PP	Polypropylene
PPE	Personal Protection Equipment
PS	Polystyrene
PVC	Polyvinyl Chloride
RSM	Response Surface Methodology
S	Sulphur
SDGs	Sustainable Development Goals
SEM	Scanning Electron Microscopy
SO _x	Sulphur Oxides
T _c	Crystallization Temperature
T _g	Glass Transition Temperature
TGA	Thermogravimetric Analysis
T _m	Melting Temperature
TPA	Terephthalic Acid
UV	Ultraviolet
VOCs	Volatile Organic Compounds

CHAPTER 1

INTRODUCTION

1.1 Research Background

The worldwide increased demand for fuel, especially for transport and heavy machinery, is worsening the strain on the finite reserves of fossil fuels on earth. With the resources running out, the quest for alternative sources of energy and renewable energy has become more crucial. One innovative approach to solving this issue is to transform plastic waste into fuel, a measure that not only solves the increasing energy demands but also provides a prospective solution to the growing issue of plastic pollution. Plastic waste pollution has become a global environmental crisis, with over 400 million tons of plastic produced annually and less than 10% effectively recycled. To minimize the use of non-renewable resources, there is a need to use renewable energy resources or recyclable products. In addition, statistics show that Canada yields about 3.3 million tonnes of plastic waste annually. Out of this total amount, 2.8 million tonnes (which is 86%) is disposed of in landfills, and 4% is incinerated for power generation, thus promoting environmental pollution. Additionally, 1% is dumped illegally, contributing to the environmental pollution. Mechanical and chemical recycling is carried out to merely 9% of the plastic waste [1-3] . In 2018 alone, approximately 6% (20.1 million tonnes) of plastic waste was exported from North America with 11.2 million tonnes being sent to Malaysia [2, 4]. Most of this waste was directed to Southeast Asian countries, including Vietnam and Indonesia, where waste management infrastructure is inadequate. Due to limited processing capabilities, the disposal of plastic waste in these regions has led to environmental pollution [3, 5].

The utilization of biofuels as a source of clean energy aligns with the Sustainable Development Goals (SDGs), specifically SDG 7 and SDG 13, which seek to promote sustainability and protect the environment [6]. One of the most promising methods of attaining these SDGs is the pyrolysis process that enables the conversion of plastic waste into fuel. Indeed, pyrolysis can extract more than 80% fuel from plastic waste, which is a promising answer to sustainable energy generation [7]. Traditional recycling

methods are often ineffective for mixed or multilayered plastics, leading to increased interest in thermal conversion technologies such as pyrolysis. Pyrolysis offers a promising route for transforming plastic waste into fuel and value-added products, aligning with the United Nations SDGs focused on clean energy and responsible consumption. Rapid expansion in plastic to fuel technologies aligns with some of the United Nations SDGs, most importantly SDG 12 (Responsible Consumption and Production), SDG 13 (Climate Action), and SDG 15 (Life on Land).

However, conventional pyrolysis typically operates at temperatures above 500 °C, resulting in high energy consumption and the release of toxic emissions such as hydrogen chloride (HCl), volatile organic compounds (VOCs), sulphur oxides (SO_x), and polycyclic aromatic hydrocarbons (PAHs). These emissions contribute to odour pollution and pose health risks, often leading to negative public perception and resistance from local communities. Recent studies have explored alternatives to high temperature pyrolysis. For instance, Surma et al. (2025) demonstrated that low temperature catalytic pyrolysis of low density polyethylene (LDPE) at 250 °C using zeolite catalysts produced significant yields of C1-C10 aliphatic hydrocarbons, which can be fractionated into combustible gases and gasoline range products [8]. Similarly, Yao et al. (2020) conducted kinetic studies on pyrolysis of acrylonitrile-butadiene-styrene (ABS) waste using thermogravimetric analysis, revealing that decomposition occurs in distinct stages and that activation energy varies with conversion degree, emphasizing the need for tailored kinetic models for mixed plastic waste [9]. These findings underscore the complexity of pyrolysis behaviour in real world waste streams and the limitations of models based solely on pure polymers. Moreover, Harussani et al. (2020) reviewed green pyrolysis technologies and highlighted that slow pyrolysis at lower temperatures is more suitable for char production and odour control, especially when integrated with environmentally friendly reactor designs [10].

Despite these advances, most research still relies on expensive analytical tools such as Gas Chromatography Mass Spectrometer (GC-MS) and Inductively Coupled Plasma Optical Emission Spectroscopy (ICP-OES) to monitor gas phase emissions, limiting accessibility in resource-constrained settings. To address this, the research study proposes a novel approach using water-phase analysis specifically Chemical Oxygen Demand (COD), Biochemical Oxygen Demand (BOD), pH, Dissolved Oxygen (DO), and turbidity as an indirect indicator of contaminant evolution. This method

offers a low cost, scalable alternative for tracking odour intensity and emission behaviour during pyrolysis.

Additionally, controlled torrefaction or mild pyrolysis, which operates at lower temperatures and slower heating rates, has been widely studied for biomass conversion but remains relatively underexplored for plastic waste, particularly mixed plastics. Mild pyrolysis offers the potential to regulate thermal degradation behaviour, influence reaction kinetics, and affect the formation and quality of pyrolytic oil and associated by products. Understanding these effects is especially important when dealing with heterogeneous mixed plastic waste, which exhibits complex and overlapping degradation mechanisms.

By converting plastic waste into a valuable commodity, this method encourages more sustainable production and consumption patterns, lessens the environmental impact of plastic pollution, and aids in preserving natural ecosystems. Nevertheless, the process is not without its negative effects: the production process tends to produce foul smells and emit toxic gases, which raises health and environmental safety concerns. Despite all these challenges, the creation of plastic to fuel conversion technologies is a crucial milestone along the way to achieving the SDGs. It contributes to ensuring responsible waste disposal, facilitates climate action through reducing dependence on fossil fuels, and supports restoring ecosystems by taking plastic wastes away from landfills and ecosystems.

1.2 Problem Statement

The increasing generation of mixed plastic waste presents a significant challenge to existing recycling and waste management systems. Mechanical recycling methods are largely ineffective for mixed plastics due to polymer incompatibility and contamination, leading to low recycling efficiency and limited end-use applications. Consequently, pyrolysis has emerged as a promising waste-to-fuel technology for converting mixed plastics into liquid fuels.

However, most plastic pyrolysis studies prioritise high temperature operation to maximise pyrolytic oil yield, often overlooking the influence of controlled, lower temperature thermal treatment on oil formation and quality. High temperature processes typically involve high energy input and complex reaction pathways, which complicate process control and hinder understanding of the fundamental degradation behaviour of

mixed plastics. Studies have shown that co-pyrolysis can significantly alter product composition and activation energy due to these synergistic effects, and that contaminants in mixed waste streams contribute to complex VOC profiles and odour emissions [11, 12].

Moreover, the pyrolytic oil produced under such conditions often exhibits inconsistent quality, limiting its utility as a fuel or chemical feedstock. Current literature predominantly focuses on the thermal degradation of pure polymers such as high density polyethylene (HDPE), polystyrene (PS), and polypropylene (PP) under fast pyrolysis conditions. This narrow scope overlooks the complex behaviour of real-world mixed plastic waste, which frequently contains multilayered structures, additives, and halogenated compounds. As noted by Harussani et al. (2020), mild pyrolysis offers advantages in char yield and odour mitigation, yet kinetic models tailored for lower temperature (<450 °C), long residence time pyrolysis remain underdeveloped [10]. The unpredictable decomposition pathways of multi component mixtures further complicate the modelling of reaction kinetics and contaminant evolution.

Controlled torrefaction or mild pyrolysis represents a potential alternative approach, yet its application to mixed plastic waste for pyrolytic oil production remains insufficiently studied. In particular, the thermal degradation behaviour and reaction kinetics of mixed plastics under mild pyrolysis conditions are not well established. Existing kinetic models are largely based on pure polymers or fast pyrolysis conditions and therefore do not adequately describe the behaviour of heterogeneous plastic mixtures under controlled heating. Therefore, there is a need for a systematic investigation into the production of pyrolytic oil from mixed plastic waste under controlled torrefaction (mild pyrolysis) conditions, with emphasis on thermal degradation behaviour, reaction kinetics, oil characterisation, and by-product identification.

Recent innovations, such as the catalyst-free carbon column reactor developed by Yale University, demonstrate that structured pyrolysis systems can achieve up to 66% conversion of polyethylene into fuel like chemicals without relying on expensive catalysts [13]. This advancement underscores the potential of lower temperature pyrolysis for energy efficient and selective conversion. However, practical methods for monitoring and mitigating emissions particularly under slow pyrolysis conditions that are still lacking.

Furthermore, standardized benchmarks for assessing pyrolytic oil quality, especially from mild pyrolysis, are not well established. This absence of classification

systems impedes the downstream integration of pyrolytic oils into existing fuel or chemical production frameworks. To address this gap, the present study proposes the use of simple aqueous indicators namely COD, BOD, pH, turbidity, and DO that serves as novel proxies for tracking the evolution of contaminants during pyrolysis. This approach aligns with the findings of Hung et al. (2023), who demonstrated the feasibility of low temperature pyrolysis for decentralized energy systems using modular devices and integrated electromechanical controls [14].

By integrating wastewater profiling into pyrolysis research, this study aims to establish a scalable, low-cost diagnostic framework that supports cleaner and data informed pyrolysis design. Such a methodology holds promise for enhancing environmental safety, improving oil quality, and facilitating the adoption of pyrolysis technologies in diverse socio-economic contexts. Despite these advancements, a comprehensive understanding of the synergistic effects between various pyrolysis parameters remains limited.

1.3 Research Objectives

The objectives of this research are:

1. To investigate the thermal degradation behaviour and reaction kinetics of mixed plastic waste under controlled torrefaction (mild pyrolysis) conditions including the formation of gaseous by products.
2. To characterize the physicochemical properties of solid fuel produced from torrefied mixed plastics.
3. To identify and evaluate the liquid and gaseous by products generated during the torrefaction process using accessible analytical techniques.

1.4 Scope of Research

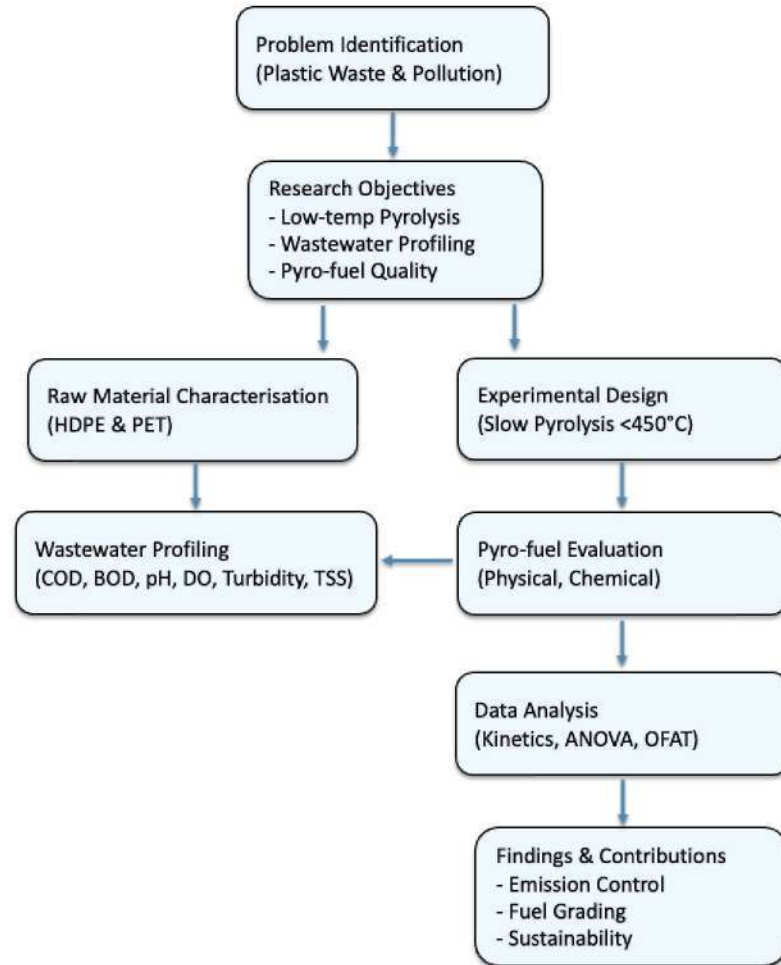


Figure 1.1. Conceptual Framework

1.5 Significance of the Study

This study makes a significant contribution to the field of plastic waste to fuel conversion by investigating the production of pyrolytic oil from mixed plastic waste using controlled torrefaction (mild pyrolysis) conditions. While most existing plastic pyrolysis studies prioritise high temperature processes to maximise oil yield, this research explores a lower temperature and controlled thermal approach to better regulate degradation behaviour and improve the understanding of oil formation pathways from mixed plastics.

The key novelty of this work lies in its systematic examination of pyrolytic oil production from mixed plastic waste under mild pyrolysis conditions rather than relying

on conventional high-temperature regimes. By focusing on controlled thermal treatment, this study provides new insight into how torrefaction level temperatures influence oil quality, composition and fuel related properties which is the area that remains insufficiently addressed in current literature.

Another important contribution is the integrated analysis of thermal degradation behaviour and reaction kinetics in relation to pyrolytic oil formation. Unlike many previous studies that derive kinetic models from pure polymers or fast heating conditions, this research investigates mixed plastics under slow and controlled heating rates, which more closely represent practical reactor operation. This approach enhances the relevance of the kinetic data for understanding oil producing reactions in heterogeneous plastic systems.

In addition, this study contributes novel experimental data on the generation of liquid and gaseous by products during controlled pyrolysis providing a more comprehensive understanding of product distribution under mild thermal conditions. The identification of these byproducts offers valuable baseline information that can inform future optimisation of oil yield, product upgrading strategies and emission monitoring methods.

Overall, the significance of this study lies in its original focus on pyrolytic oil production from mixed plastics under controlled, low temperature conditions and its integration of kinetic analysis with oil quality evaluation and its contribution of foundational data for advancing plastic to fuel research beyond conventional high-temperature pyrolysis approaches.

1.6 Outline of Research Work

Chapter 2 present the literature review offers a comprehensive overview of prior studies relevant to plastic pyrolysis. It critically examines the current problems of pollutant emissions, the influence of different plastic types and mixing ratios, reactor and process configurations, and the key parameters affecting pyro-fuel yield and quality. Special emphasis is placed on pollutant monitoring methods, with a focus on low-cost wastewater analysis as an innovative diagnostic approach. This chapter also synthesizes knowledge gaps and research opportunities that this study seeks to address.

Chapter 3 details the experimental design and methodological framework. It describes the preparation and characterization of raw materials (HDPE and PET), the

pyrolysis process design, and the parameter selection for experimentation. The methodology incorporates wastewater profiling as a proxy for emission monitoring and outlines the procedures for evaluating the physical and chemical quality of pyrolytic oil. Furthermore, it explains the analytical approaches, including statistical analysis and kinetic modelling, used to interpret the experimental results and establish correlations between process parameters, emission behaviour, and fuel quality.

Chapter 4 show the results of the experimental work are presented and critically discussed in this chapter. It includes findings on the physical and chemical properties of raw materials, pyrolysis behaviour under different mixing ratios, wastewater analysis for odour and emission profiling, and the evaluation of pyro-fuel quality. The chapter integrates these findings through interpretive analyses, highlighting correlations between fuel properties, emission characteristics, and wastewater indicators. The discussion emphasizes the synergistic effects of process parameters and validates the feasibility of the proposed low-cost diagnostic framework.

Finally, the conclusion of the overall research work and recommendation on future work has been highlighted in Chapter 5.

1.7 Concluding Remark

This study represents a research by highlighting the global challenge of plastic waste accumulation and the urgent need for sustainable energy alternatives. The potential of pyrolysis as a waste-to-fuel conversion pathway has been discussed, alongside the limitations of conventional high-temperature processes that generate significant pollutant emissions and odour nuisances. By framing the problem statement, this chapter underscores the critical research gap in achieving both high-quality pyro-fuel and reduced emissions under realistic, low-temperature conditions. The objectives and scope have been clearly defined, focusing on the pyrolysis of HDPE and PET wastes, the application of wastewater profiling as a novel diagnostic tool for emission monitoring, and the evaluation of pyro-fuel quality through integrated physical, chemical, and kinetic analyses. The significance of this study lies in its contribution to advancing cleaner and more resource-efficient pyrolysis technologies suitable for deployment in resource-constrained settings. By coupling experimental investigation with an innovative, low-cost monitoring approach, this research aims to provide both scientific insight and practical solutions that align with global sustainability goals.

CHAPTER 2

LITERATURE REVIEW

2.1 Introduction

In the previous section, issues raised due to the disposal of plastic waste have been highlighted which will result in damage to the environment. Therefore, in this section, the steps of using the pyrolysis process to eliminate the disposal of plastic waste have been explained as best as possible. Indirectly, the process of eliminating plastic waste using the pyrolysis process can produce a new source of energy that can be used as fuel for vehicles as well as other equipment that uses petroleum products as materials to power the equipment.

2.2 Current Problem in the Pyrolysis of Plastic Waste for Pyro-Fuel Production

2.2.1 Pollution Emitted from the Process

Plastics play an important role in daily life and have major contribution towards global urbanisation. Plastics are made from a variety type of polymers such as PP, PET, PS and PVC. Nowadays, plastics have been used extensively in daily life from household applications such as containers and plastic cutleries which are made from HDPE and PP respectively to construction materials such as pipes made from PVC and PS foam. Demand for plastics has increased tremendously as plastics are frequently used to meet current economic growth.

The pyrolysis of plastic waste, while offering a method for converting waste into valuable products, can emit various pollutants that pose environmental and health risks. The primary emissions include the Greenhouse Gases (GHGs). Pyrolysis processes are energy-intensive and can emit significant amounts of carbon dioxide (CO₂). Studies have shown that GHG emissions from pyrolysis are substantially higher than those from mechanical recycling methods [15]. Apart from that, the thermal degradation of plastics during pyrolysis can release VOCs, including benzene and toluene, which are hazardous

air pollutants with known health risks [16]. The content of PAHs which are a group of organic contaminants that can be produced during the pyrolysis of plastic waste. PAHs are known for their carcinogenic and mutagenic properties, posing significant health hazards. Dioxins and furans which are presence of certain additives in plastics can lead to the formation of dioxins and furans during pyrolysis, which are highly toxic and can cause serious health effects, including cancer and endocrine disruption [17]. Mitigating these emissions requires the implementation of advanced emission control technologies, such as high-efficiency particulate air (HEPA) filters and activated carbon adsorption systems, to capture and neutralize hazardous emissions. Regular environmental monitoring, adherence to stringent regulatory standards, and community engagement are also crucial components in mitigating the health risks associated with the pyrolysis of plastic waste.

2.2.2 Hazardous Gas Released from the Process

While pyrolysis offers a potential solution to plastic pollution, several factors can lead to the formation of hazardous byproducts, resulting in the release of harmful gases, unpleasant odors, and toxic materials. Different plastics, such as polyethylene (PE), PP, PS and PVC have varying chemical structures. When processed together, they can decompose unevenly, leading to unpredictable reactions and the formation of hazardous compounds. Plastics often contain additives like plasticizers, flame retardants, and colorants. During pyrolysis, these additives can break down into toxic substances, contributing to environmental pollution [18]. The configuration of the reactor influences heat distribution and residence time. Inadequate designs can cause incomplete pyrolysis, resulting in the emission of harmful byproducts. Incomplete pyrolysis can release VOCs, PAHs, and other toxic gases, posing significant health risks. Byproducts like char may contain hazardous substances, necessitating careful handling and disposal to prevent environmental contamination.

Different pyrolysis methods like thermal and catalytic operate under varying conditions. Without proper optimization, these processes can produce unwanted side products. Operating at suboptimal temperatures can lead to incomplete decomposition of plastics, generating hazardous substances like dioxins and furans. Rapid heating or insufficient residence time may prevent complete breakdown of materials, resulting in the formation of toxic intermediates. Unintended oxygen introduction can shift the

process towards combustion rather than pyrolysis, leading to the release of harmful gases. Reports indicate that pyrolysis can produce toxic byproducts, including dioxins, arsenic, mercury and benzene which contribute to air and environmental pollution [19]. These insights underscore the importance of addressing the root causes of hazardous byproduct formation in plastic pyrolysis.

2.2.3 Health Problems Arise from The Process

The pyrolysis of plastic waste, while offering a method for waste reduction and energy recovery, poses significant health risks due to the emission of hazardous substances. During the pyrolysis process, complex chemical reactions break down plastic polymers, leading to the release of various toxic compounds. VOCs have high vapor pressures at room temperature, leading to significant vaporization and subsequent inhalation exposure. Exposure to VOCs can cause respiratory issues, headaches, and, with prolonged exposure, may lead to liver and kidney damage. Other highly toxic compounds are Dioxins and Furans that can be unintentionally produced during the thermal decomposition of plastics containing chlorine. Dioxins and furans are associated with serious health effects, including immune system suppression, reproductive and developmental problems, and an increased risk of cancers [20].

Apart from that, PAHs are a group of organic compounds with multiple aromatic rings, known for their persistence in the environment and potential to bioaccumulate. PAHs are recognized carcinogens, and exposure can increase the risk of cancer, particularly lung, skin, and bladder cancers. While Particulate Matter (PM) is fine particles released during pyrolysis can penetrate deep into the respiratory tract, leading to cardiovascular and respiratory diseases, including aggravated asthma and decreased lung function[17].

In conjunction of occupational hazards, workers in pyrolysis facilities may face additional risks due to potential exposure to high concentrations of these hazardous substances, as well as risks associated with process upsets, equipment malfunctions, or accidental releases. Implementing stringent occupational safety measures, including proper ventilation, personal protective equipment, and continuous monitoring of air quality, is essential to mitigate these risks. The siting of pyrolysis plants often occurs in low-income and marginalized communities, exacerbating environmental health

disparities. These populations may experience cumulative exposure to pollutants from multiple sources, leading to a higher burden of adverse health outcomes [21, 22].

2.2.4 Root Cause of The Problem in Pyrolysis of Plastic Waste

Pyrolysis, a process that thermally decomposes plastic waste into fuels and other valuable products, has garnered attention as a potential solution to the global plastic waste crisis. However, several challenges hinder its widespread adoption and effectiveness. Pyrolysis process causes feedstock contamination where mixed and contaminated plastic waste can lead to inconsistent fuel quality and process inefficiencies. Non-plastic contaminants like metals, dirt, and organic residues will complicate the pyrolysis process [23]. Pyrolysis is energy-intensive, requiring high temperatures which is around 300 to 600°C and precise conditions. The high energy demand can reduce its net environmental benefits, especially if the energy source is non-renewable. The pyrolysis process can release harmful emissions, including VOCs and GHGs, if not properly managed. Incomplete decomposition can also result in toxic residues [24].

Malaysia has been grappling with improper solid waste management, leading to environmental pollution. The implementation of thermal treatment technologies like pyrolysis has been considered; however, challenges persist in ensuring sustainable and environmentally friendly operations [25]. Studies have been conducted to evaluate the techno-economic feasibility of pyrolysis-based plants in Malaysia indicating that while oxidative pyrolysis uses less energy, economic challenges remain in scaling up the technology [26].

2.3 Types of Plastic Affecting the Pyrolysis Process

2.3.1 Plastic Waste Characterisation for Pyrolysis Process

Plastics are a diverse group of synthetic materials categorized based on their chemical composition, physical properties, and processing behaviours. A comprehensive classification is essential for understanding their applications, recycling potential, and environmental impact. Plastics are primarily classified according to the chemical structure of their polymer backbones and side chains. This classification

includes groups such as acrylics, polyesters, silicones, polyurethanes, and halogenated plastics. Each group exhibits distinct chemical and physical properties due to variations in their molecular architecture [27].

The synthesis process of plastics also serves as a basis for classification. Key polymerization methods include condensation Polymerization where it involves the combination of monomers with the elimination of small molecules like water. Addition polymerisation entails the joining of monomers without the loss of any atoms, forming polymers such as polyethylene and polypropylene. While cross-linking of polymers creates networks of interconnected polymer chains, resulting in materials with enhanced mechanical properties. These processes significantly influence the thermal and mechanical characteristics of the resulting plastics [28].

Another classification of plastic is by its physical properties. Plastics can be categorized based on their response to heat which is Thermoplastics and Thermosetting Polymers (Thermosets). Thermoplastics are the materials that soften upon heating and can be reshaped multiple times without undergoing chemical changes. Examples include PE, PP, PS and PVC. While for thermosets, these kinds of plastics cannot be remelted or reshaped once cured. They decompose upon reheating. Examples include epoxy resins and phenolic resins. This classification is crucial for determining processing methods and end-use applications [7].

Plastics are also distinguished by their degree of crystallinity which are Amorphous Plastics, Crystalline Plastics and Semi-Crystalline Plastics. Amorphous Plastics are the plastics that lack a highly ordered molecular structure, resulting in materials like polystyrene and polymethyl methacrylate (PMMA). Crystalline plastics exhibit a regular molecular arrangement, as seen in HDPE and polybutylene terephthalate (PBT). While semi-crystalline plastics contain both amorphous and crystalline regions, including materials like polyethylene and polypropylene. The degree of crystallinity affects properties such as density, melting point, and mechanical strength [29].

Others classification of plastics is by it conductivity where most plastics are insulators, a subset known as intrinsically conducting polymers (ICPs) can conduct electricity. Examples include polyacetylene and polyaniline. However, their conductivity is generally lower than that of metals like copper. Understanding these classifications provides a framework for selecting appropriate plastics for specific

applications, optimizing processing conditions, and developing effective recycling strategies [30].

Characterizing plastic waste involves analysing its physical and chemical properties, both for individual plastic types and for mixtures with varying compositions. This characterization is crucial in the pyrolysis process, as the specific types and ratios of plastics directly influence the yield and quality of the resulting pyro-fuel. Different plastics decompose at varying temperatures due to their distinct chemical structures. For instance, PE and PP require higher temperatures for decomposition compared to PS. Therefore, the composition of the plastic feedstock significantly affects the pyrolysis outcomes [31].

Moreover, the ratio of different plastics in mixed waste streams plays a pivotal role in determining the yield and characteristics of the pyrolysis products. Studies have shown that mixed plastic wastes can produce varying amounts of pyrolysis liquid, depending on their composition. For example, during individual pyrolysis, mixed plastic wastes produced 70.6 wt% of pyrolysis liquid, which is 37.9% and 33.4% more than furniture wood and waste tyres, respectively [32]. Understanding the specific properties and compositions of plastic waste enables optimization of the pyrolysis process, leading to improved yields and quality of pyro-fuel. This knowledge is essential for developing efficient and sustainable methods for converting plastic waste into valuable energy resources.

Table 2.1
Yield of pyrofuel by using single type of plastic waste

Type of Plastic Waste	Yield (%)	Ref
HDPE	84	[33]
PP	80	[33]
LDPE	47.65	[34]
PET	28.4	[35]
PE	76.1	[36]
LDPE	43.9	[37]
PS	91.8	[38]
PP	10.91	[39]
PP	88.5	[40]
HDPE	82.5	[40]

LDPE	82	[40]
HDPE	84.7	[41]
PS	70	[42]
PE	40	[42]
PP	40	[42]

Several studies have investigated the production of high-quality pyro-fuel through the pyrolysis of plastic waste, employing various feedstock compositions, including single-type plastics, mixed plastics, and specific plastic ratios. Table 2.1 show the yield of pyro fuel by using single type of plastic waste. It was found that PS produced the highest yield of pyro fuel which was 91.8% [38] while PET had the lowest yield which was only 28.4% [35]. Most HDPE plastic waste produced pyro fuel yield which was more than 70% of the total product obtained through the pyrolysis process [33, 43]. The pyrolysis of mixed plastic waste has also been extensively studied. Table 2.1 shows the yield of pyro fuel by using mixed plastic waste. From the graph, mixture of 90% PP and LDPE produce more yield of pyrofuel which is 80% while mixture of 10% PP and LDPE produce the lowest yield of pyrofuel which is 28% [44].

Table 2.2
Yield of pyrofuel by using mixed plastic waste

Type of Plastic Waste	% mix	Yield (%)	Ref
LDPE + PP	10%PP + LDPE	28	[44]
LDPE + PP	30%PP + LDPE	68	[44]
LDPE + PP	50%PP + LDPE	72	[44]
LDPE + PP	70%PP + LDPE	78	[44]
LDPE + PP	90%PP + LDPE	80	[44]
PVC/PET/PS/PP/PE	3/4/18/35/40	72	[45]
PS/PE/PP	50/25/25	44	[42]
PS/PP/PE/PET	40/20/20/20	28	[42]
PET + PS	10%PET + PS	67.56	[46]
PET + PS	20%PET + PS	54	[46]
PET + PS	30%PET + PS	30.4	[46]
LDPE/HDPE/PP	30/30/40	76.38	[47]

Table 2.3
Yield of pyrofuel by using specific ratio plastic waste

Type of Plastic Waste	Ratio	Yield (%)	Ref
PET + PS	1:1	91.8	[48]
PP + HDPE	1:4	80	[33]
PP + HDPE	2:3	75	[33]
HDPE + PP	1:4	80	[33]
HDPE + PP	2:3	76	[33]
PP + HDPE + LDPE	1:1:1	81	[40]
PS + PE	1:1	44	[42]
PS + PP	1:1	54	[42]
PP + PE	1:1	44	[42]
PET + PE	1:1	34.4	[49]

Investigations into the effects of different plastic ratios in the feedstock have revealed significant impacts on the yield and quality of the resulting pyro-fuel. It was found that the PET1:1PS ratio produced the highest pyro fuel yield of 91.8% [48] while the PET1:1PE ratio produced the lowest pyro fuel yield of 34.4% [49]. A study by Jadhwa et al. examined the pyrolysis of mixed plastics, demonstrating that varying the proportions of different plastics influences the composition and properties of the produced oil. The findings suggest that optimizing the plastic ratios can enhance the quality of the pyro-fuel [44].

These studies collectively indicate that the selection and proportion of plastic feedstock are critical factors in the pyrolysis process, directly affecting the quality and yield of the resulting pyro-fuel. However, A comprehensive review published in the journal by Gregg T. Beckham et al. analysed the process of converting mixed plastic waste into pyrolysis oil, highlighting the challenges and potential of this approach. The study emphasized the importance of feedstock composition and process optimization in achieving desirable fuel characteristics [50].

Pyrolysis of mixed plastic waste significantly increases GHGs emissions compared to conventional manufacturing processes. For example, the production of benzene, toluene, and xylene (BTX) from mixed plastic waste results in a 2.4-fold increase in GHGs emissions per kilogram of BTX compared to virgin BTX production

. GHGs emissions are primarily associated with energy-intensive processes like electricity consumption, heating, and product separations. The process reduces total supply chain energy consumption by up to 24% compared to traditional manufacturing of some petrochemical products. However, this reduction comes at the cost of increased emissions due to higher utility and feedstock preparation requirements.

While the process reduces fossil fuel depletion and ozone depletion, it shows poorer performance in categories such as acidification, smog formation, and ecotoxicity due to emissions from utility use and feedstock preprocessing. The choice of catalysts and process configurations can significantly affect environmental outcomes. For example, high catalyst-to-feed ratios improve olefin yields but require more energy, further increasing environmental burdens [50].

2.3.2 Physical Characterization of Plastic Waste

Understanding the physical characterization of plastic waste is crucial for optimizing recycling processes and developing high-quality recycled products. Key aspects include sorting and separation, process optimization, product development, and achieving sustainability goals. Identifying physical properties such as density, melting point, and particle size enables efficient sorting of different plastic types, enhancing the purity of recycled materials. For instance, a study on electronic plastic waste utilized physical characterization to determine moisture content and composition, facilitating effective separation strategies [51].

Knowledge of physical characteristics ensures that materials are suitable for specific recycling methods like extrusion or pyrolysis. Research on recycled HDPE assessed properties such as thermal stability and extrusion rates, informing process parameters for 3D printing applications [52]. Physical characterization informs the design of recycled plastic products, ensuring they meet required standards. By understanding properties like melting temperature and mechanical behaviour, manufacturers can produce items that are both durable and functional.

Optimizing the recycling or reuse process through thorough physical characterization reduces waste and conserves resources, contributing to environmental sustainability. Accurate characterization allows for better material utilization and minimizes the environmental impact of plastic waste. Incorporating detailed physical characterization into the recycling workflow is essential for improving efficiency,

product quality, and environmental outcomes [53]. To perform the physical characterization of plastic waste, the physical properties of the plastic waste need to be evaluated first. These properties are essential for understanding how the material behaves under mechanical, thermal, and environmental conditions. The properties that can be evaluated such as particle size, density, thermal properties and moisture content

2.3.2.1 Particle Size

Particle size affects processing techniques like pyrolysis, mechanical recycling, or blending with other materials. Surface morphology (e.g., smooth, rough) influences bonding, adhesion, and material compatibility. Smaller particles can improve thermal degradation efficiency in pyrolysis while morphology affects composite formation in recycled plastic products.

The particle size of HDPE varies depending on its form and intended application. For instance, in additive manufacturing, HDPE powders typically have an average particle size around 70 μm , with a standard deviation of 22 μm , indicating a range primarily between 60 and 90 μm [54]. In composite materials, HDPE can be combined with fillers of various particle sizes. For example, one study examined HDPE composites with Tetra Pak® filler particles larger than 1000 μm [55].

The particle size of PET varies depending on its form and the processing methods used. For instance, in a study examining the impact of ball milling on PET's microstructure, scanning electron microscopy (SEM) analyses revealed that after milling for 90 minutes at 30 Hz, PET samples transformed into small lamellar particles with thicknesses less than 10 μm and diameters approximately between 40 and 60 μm [56].

In another study focusing on the effects of aging on PET microplastics, PET samples were ground in a cryogenic mill and then sieved to analyse particle size distribution. The results indicated that a significant portion of the particles had sizes greater than 500 μm [57]. Additionally, research on microplastic particle size distribution reported that PET particles exhibited a distribution maximum at approximately 255 μm , with an upper cut-off particle size around 440 μm [58]. These variations in particle size are influenced by factors such as the specific processing techniques employed and the physical properties of the PET material.

2.3.2.2 Density

Understanding the density of plastic waste is crucial for several reasons, particularly in the context of recycling and waste management. Density plays a pivotal role in the sorting and separation processes, which are essential for efficient recycling. Density-based separation techniques, such as the sink-float method, are commonly employed to segregate different types of plastics. In this process, plastic particles are placed in a fluid medium; those with densities lower than the medium float, while those with higher densities sink. For instance, polyolefins like LDPE and HDPE, which have densities less than 1 g/cm^3 , will float in water, whereas plastics like PET and PVC, with densities greater than 1 g/cm^3 , will sink. This method facilitates the effective separation of mixed plastic waste streams [59].

The study emphasizes that media density separation is fundamental for the separation and pre-concentration of recyclable plastics. However, it also notes limitations in current static media processes, such as capacity constraints and size limitations of materials that can be treated. The review suggests that alternative processing methods, like cyclone-type media separators used in coal processing, could enhance the efficiency and capacity of plastic recycling operations [60]. In summary, knowing the density of plastic waste is vital for implementing effective separation strategies, which in turn enhances the efficiency of recycling processes and contributes to better resource utilization and environmental sustainability.

2.3.2.3 Thermal Properties

Understanding the thermal properties of plastic waste is essential for optimizing recycling processes, ensuring material compatibility, and enhancing the quality of recycled products. Key thermal properties include melting temperature (T_m) which is the specific temperature at which a plastic transitions from a solid to a liquid state. Glass Transition Temperature (T_g) is the temperature range where the plastic changes from a hard, glassy material to a soft, rubbery state. For example, T_m and T_g for HDPE are 132°C and -80°C respectively [47].

Knowledge of these properties is crucial for selecting appropriate processing conditions during recycling. For instance, a study emphasizes the importance of understanding the thermal degradation behaviours of various plastics to optimize

pyrolysis processes, a method that thermally decomposes plastic waste into valuable products like fuels and monomers. The study highlights that different plastics degrade at different temperatures, and precise control of these temperatures is necessary to maximize yield and quality of the desired products [61].

Additionally, the thermal stability of various plastic wastes has been examined, including plastic bottles, bags, and straws. The study found that these materials degraded at temperatures ranging from 382°C to 456°C, indicating their thermal stability under typical environmental conditions. This information is vital for determining the suitability of recycled plastics in applications requiring specific thermal resistance [53]. In summary, understanding the thermal properties of plastic waste is essential for optimizing recycling processes, ensuring material compatibility, and enhancing the quality and safety of recycled products.

2.3.2.4 Moisture Content

Understanding the moisture content of plastic waste is crucial for optimizing recycling processes and ensuring the quality of the final products. Excess moisture can adversely affect both the processing and mechanical properties of plastics. Certain plastics, such as PET, are susceptible to hydrolysis when moisture is present during processing. This reaction can break down the polymer chains, leading to a reduction in molecular weight and deterioration of material properties. A study highlighted that PET absorbs moisture from its environment, and during processing at high temperatures, this moisture can cause hydrolytic degradation, adversely affecting the polymer's properties [62].

Moisture can lead to issues like vapor formation during melting, causing voids, bubbles, and surface defects in the final product. This not only compromises the aesthetic quality but also the structural integrity of the recycled plastic. Research indicates that excess moisture in plastic granules can result in problems such as foaming, difficulties in mold filling, and inconsistent viscosity during processing. To mitigate moisture-related issues, it's essential to thoroughly dry plastic waste before processing. This step helps in maintaining the desired material properties and ensures the production of high-quality recycled plastics. Effective drying reduces the risk of hydrolytic degradation and processing defects [63].

Moisture can act as a plasticizer, reducing the intermolecular forces between polymer chains, leading to decreased tensile strength and elasticity. A study on biodegradable polyester demonstrated that increased moisture content resulted in higher elongation at break and a slight reduction in both the elastic modulus and tensile strength [64]. In summary, monitoring and controlling the moisture content in plastic waste is vital for efficient processing and maintaining the mechanical integrity of recycled products. Implementing appropriate drying techniques can significantly enhance the quality and performance of recycled plastics.

2.3.2.5 Melting Point

Understanding the melting point of plastic waste is crucial for optimizing recycling processes and ensuring the quality of recycled products. The melting point is the temperature at which a plastic transitions from a solid to a liquid state, and this property significantly influences various aspects of plastic recycling. Different plastics have varying melting points, necessitating specific processing temperatures. For instance, HDPE melts at approximately 143°C, while PET melts around 255°C. Accurate knowledge of these temperatures is essential for selecting appropriate recycling methods, such as extrusion or injection moulding, to prevent thermal degradation and maintain material integrity [65].

Plastics with lower melting points require less energy to process, making their recycling more cost-effective. Conversely, high-melting-point plastics demand more energy, impacting the overall economics of the recycling operation [66]. Mixing plastics with different melting points can lead to processing challenges, as some polymers may degrade at temperatures required to melt others. For instance, HDPE melts at approximately 143°C, while PP melts around 261°C [65]. Processing a mixture of these plastics at the higher temperature necessary for PP can cause HDPE to degrade. Therefore, effective sorting and separation based on melting points are essential to ensure material compatibility and enhance the performance of recycled products.

In summary, knowledge of the melting points of various plastics is vital for efficient recycling operations, influencing the choice of processing techniques, energy consumption, and the quality of the final products.

2.3.2.6 Flash Point

Understanding the flash point of plastic waste is crucial for ensuring safety during storage, handling, and processing, especially when converting plastics into fuels. The flash point is the lowest temperature at which vapours of a material ignite when exposed to an ignition source. Knowledge of this property helps in assessing flammability risks and implementing appropriate safety measures.

Converting plastic waste into fuel through pyrolysis—a process of thermal decomposition in the absence of oxygen—yields products with specific flash points. A study on LDPE and PP plastic waste found that the resulting fuels had flash points ranging from 1°C to 2°C. These low flash points indicate high flammability, necessitating careful handling and storage to prevent accidental ignition. Fuels derived from plastic waste with low flash points require stringent safety protocols. Proper storage in well-ventilated areas, use of flame arrestors, and regular monitoring of storage conditions are essential to mitigate fire hazards [67].

Equipment used in the pyrolysis process must be designed to handle materials with low flash points. This includes implementing explosion-proof components and maintaining temperatures below the flash point during storage and transfer operations [68]. In summary, accurately determining the flash point of plastic waste and its derived products is vital for assessing flammability risks and ensuring the safe design and operation of processing facilities. Implementing appropriate safety measures based on flash point data helps prevent accidents and promotes the safe handling of plastic-derived fuels.

2.3.3 Chemical Characterization of Plastic Waste (According to Single and Mix Types)

Chemical characterization of plastic waste is crucial for understanding its composition, properties, and potential environmental or recycling impacts. The analysis differs depending on whether the plastic waste consists of single-type plastics or mixed plastics. Researchers have previously used various methods to analyse pyrolytic oil that has been produced from the pyrolysis process.

2.3.3.1 Proximate Analysis

Proximate analysis is a fundamental aspect of the chemical characterization of plastic waste, especially in the context of pyrolysis processes. This analytical method evaluates the distribution of a material's components into moisture content, volatile matter, fixed carbon, and ash content. Understanding these parameters is crucial for optimizing pyrolysis conditions and enhancing the efficiency of converting plastic waste into valuable products.

Moisture content refers to the amount of water present in the plastic material. High moisture levels can adversely affect the pyrolysis process by requiring additional energy to vaporize the water, thereby reducing the thermal efficiency and yield of desired products. Therefore, assessing and minimizing moisture content is essential for efficient pyrolytic conversion.

Volatile matter comprises the components of the plastic that are vaporized upon heating in an inert atmosphere, excluding moisture. Plastics with high volatile matter content are particularly suitable for pyrolysis, as they tend to produce higher yields of liquid and gaseous products. For instance, studies have shown that various plastics exhibit volatile matter content exceeding 90 wt%, indicating a high potential for conversion into valuable pyrolysis products.

Fixed carbon represents the fraction of the material that remains as solid residue after the volatile matter has been released, excluding ash. In the context of plastic pyrolysis, the fixed carbon content is typically low, resulting in minimal char formation. This characteristic is advantageous, as it implies that a greater proportion of the plastic material can be transformed into liquid and gaseous products.

Ash content denotes the inorganic residue remaining after complete combustion of the plastic material. A high ash content can negatively impact the pyrolysis process by acting as a heat sink, reducing the reactor's temperature, and potentially catalysing unwanted side reactions. Consequently, plastics with low ash content are preferred for pyrolysis to maximize the yield of desired products. Empirical data indicates that common plastics such as PE and PP have ash contents typically below 1 wt%, making them ideal candidates for pyrolytic conversion [69].

In summary, proximate analysis provides critical insights into the composition of plastic waste, directly influencing the efficiency and optimization of the pyrolysis process. By evaluating moisture content, volatile matter, fixed carbon, and ash content,

researchers and industry professionals can better predict the behaviour of plastic materials under pyrolytic conditions and tailor processes to maximize the production of valuable outputs.

Table 2.4:
Proximate Analysis of different plastics [70].

Types of plastic	Proximate Analysis (wt.%)		
	FC	VM	Ash
PET	13.15	86.85	0
HDPE	0	100	0
PVC	2.77	97.23	0
LDPE	0.02	99.98	0
PP	0.03	99.97	0
PS	0	99.80	0.20

Table 2.4 shows the value of proximate analysis and ultimate analysis for six types of plastic. It was found that HDPE's volatile matter is the highest when compared to other types of plastic. This shows that HDPE will produce a high amount of oil from the pyrolysis process when compared to other types of plastic [70]. The fixed carbon value for PET is higher when compared to other types of plastic. This shows that PET will produce high char when compared to other plastics [71]. This table also shows the hydrocarbon content found in plastic is between 43.3% to 100% where the lowest hydrocarbon content is PVC while the highest hydrocarbon content is HDPE, LDPE and PP.

2.3.3.2 *Ultimate Analysis*

Ultimate analysis or elemental analysis refers to a method used to determine the elemental composition of a substance, typically focusing on organic compounds such as fossil fuels, biomass, or other organic materials. It involves determining the percentages of carbon (C), hydrogen (H), nitrogen (N), sulphur (S), and in some cases oxygen (O), as well as other elements that may be present in trace amounts. Ultimate analysis is often performed through various techniques such as combustion analysis, where the sample is burned in a controlled environment, and the resulting gases are

analysed to determine the elemental composition. Other methods may involve spectroscopic techniques or elemental analysis instruments. The results of ultimate analysis are typically expressed as weight percentages of each element present in the sample. This information is essential for understanding the properties and behaviour of the material being analysed and for making informed decisions regarding its use or processing.

Table 2.5:
Ultimate analysis results for HDPE and PET (%)

Ref	HDPE					PET				
	C	H	O	N	S	C	H	O	N	S
[33]	83.43	15.34	1.22	0	0					
[38]	84.5	13.8	1.5	0.1	0.1	62.5	4	33.5	0.1	0
[70]	85.5	14.5	0	0	0	62.5	4.21	33.29	0	0
[72]	84.55	14.63	0.82	0	0					
[73]						63.47	4.759	0	0.72	0.189

Table 2.5 shows a comparison of the results of ultimate analysis involving HDPE and PET plastic done by the researchers. Comparatively, the hydrocarbon value for HDPE is higher when compared to PET which is over 90%. While the hydrocarbon value for PET is not more than 70%. To obtain high quality petroleum, hydrogen and carbon are essential elements when compared to oxygen or chlorine. Carbon and hydrogen are the desired components to obtain high quality petroleum products instead of oxygen or chlorine [70].

A high carbon content in a fuel will produce a high calorific value [74]. The calorific value of hydrocarbon fuel is highly dependent on the carbon element in the fuel where a high hydrogen content will increase the calorific value of the fuel [33, 74].

2.3.3.3 Heating Value (Calorific Value)

Calorific value, in the context of plastic waste pyrolysis, refers to the amount of energy released when a given amount of plastic is burned or subjected to thermal decomposition (pyrolysis) under controlled conditions. It is typically measured in units like kilojoules per kilogram (kJ/kg) or megajoules per kilogram (MJ/kg). Plastic waste

pyrolysis involves subjecting plastic materials to high temperatures in the absence of oxygen, leading to the breakdown of the long hydrocarbon chains that make up plastics into smaller molecules. This process produces a mixture of gases, liquids, and solids, which can be further refined into valuable products such as fuels or chemical feedstocks.

The calorific value of the resulting products from plastic pyrolysis is significant because it indicates the potential energy content that can be harnessed from the process. Higher calorific value means more energy can be obtained from the pyrolysis products, making them more suitable for applications such as fuel production. Understanding the calorific value of plastic waste is essential for assessing the economic viability of pyrolysis processes and determining the potential energy yield. Higher calorific value plastics can yield more energy-rich products, which may be more desirable for energy recovery or conversion into valuable chemicals.

Table 2.6
Heating values of different type of plastics

Types of plastic	Heating values (MJ/kg)	References
Commercial Diesel	46.18	[33]
PET	30.2	[75]
HDPE	46.31	[33]
PVC	17.82	[76]
LDPE	42.88	[34]
PP	44.34	[33]
PS	41.9	[75]

Table 2.6 shows the heating values for six types of plastic. It was found that the heating value of HDPE is the highest and it is very suitable for pyrolysis and will produce a high oil content [75]. At the same time, the heating value of HDPE approaches the heating value of commercial gasoline and diesel. While the heating value for PVC is the lowest and will produce low oil quality due to the presence of benzoic acid and chlorine compounds in the plastic [74].

Table 2.7
Calorific Value (MJ/kg) for HDPE and PET

References	Type of Plastic		Commercial Standard Value (ASTM 1979)	
	HDPE	PET	Gasoline	Diesel
[7]	49.4	24.13	46.8	43.0
[77]	40.5	28.2	42.5	43.0
[33]	46.31	n.a	n.a	n.a
[40]	43.19	n.a	46.86	42.51
[47]	46.43-46.81	n.a	n.a	n.a
[74]	43.92	n.a	n.a	n.a
[78]	43.646	n.a	45.94	46.951
[79]	40.5	28.2	42.5	43.0

Table 2.7 shows a comparison of the caloric value of HDPE and PET for each study conducted by other researchers. The value of petrol and diesel is also shown to compare the calorific value of plastic waste with commercial petrol and diesel. It was found that the calorific value for HDPE is high and almost equals the calorific value of commercial gasoline and diesel. While the calorific value for PET is very low, below 30MJ/kg. The production of new energy from plastic waste that has a high caloric value is a good step because the origin of plastic is from petroleum sources. Therefore, the pyrolysis process is one of the popular ways to reduce global plastic waste [79].

This study will use HDPE plastic waste and PET plastic waste because these two plastic wastes are the most popular used. A total of 67% of plastic waste of this type used the mechanical recycling method in Canada in 2016 [1]. An estimated 60 million tons of HDPE plastic waste is thrown away every year and only one third of it is reused or recycled. This has a negative impact not only on the environment but also on the production of petroleum raw materials to produce more of this type of plastic [80]. According to Recycling International, PET production is close to 20 million tons for the year 2021 alone [81]. Therefore, if these two types of plastic waste can be used in the production of petroleum products again, the disposal of this plastic waste in large quantities every year can be overcome.

2.3.3.4 FTIR

Fourier Transform Infrared (FTIR) spectroscopy is a pivotal analytical technique in the pyrolysis of plastic waste, offering detailed insights into the molecular composition and structural transformations of polymers during thermal degradation. Its application is essential for optimizing pyrolysis processes and enhancing the yield of desired products.

FTIR spectroscopy facilitates the precise identification of various plastic polymers by detecting their unique vibrational modes. Each polymer exhibits characteristic absorption bands corresponding to specific functional groups, enabling differentiation among polymer types. For instance, an inquiry-based FTIR spectroscopy experiment demonstrated the capability to distinguish common recyclable polymers through their distinct spectral signatures [82]. During pyrolysis, FTIR serves as a real-time analytical tool to monitor the decomposition pathways of plastics and the evolution of volatile products. By coupling thermogravimetric analysis with FTIR (TG-FTIR), researchers can observe the formation of specific compounds at various temperatures. For example, a study utilizing TG-FTIR revealed that low-density polyethylene (LDPE) and polypropylene (PP) predominantly produced wax-like substances at 500 °C. At elevated temperatures (above 600 °C), these waxes diminished, and the generation of light hydrocarbons increased. Notably, the formation of aromatic compounds such as benzene and toluene was observed at temperatures exceeding 700 °C [83].

FTIR spectroscopy is instrumental in evaluating the interactions between plastic waste and other materials during co-pyrolysis. By analysing the functional groups present in the pyrolysis vapours, FTIR aids in understanding synergistic effects that can enhance the production of valuable hydrocarbons. Research on the co-pyrolysis of lignin and plastics demonstrated that adding LDPE or HDPE to lignin significantly promoted the formation of aromatic compounds, as evidenced by intensified absorption peaks corresponding to aromatic vibrations in the FTIR spectra [84].

In summary, FTIR spectroscopy is an indispensable tool in the pyrolysis of plastic waste, providing comprehensive molecular-level information that is crucial for process optimization, product quality assessment, and the development of efficient recycling strategies.

2.3.3.5 GC-MS

GC-MS has been used to identify the chemical content found in the hydrocarbon product. GCMS stands for Gas Chromatography-Mass Spectrometry. It is a powerful analytical technique used to identify and quantify the components of complex mixtures of volatile substances. Gas chromatography (GC) is a separation technique where the sample is vaporized and injected into a chromatographic column. The components of the sample travel through the column at different rates based on their interactions with the column's stationary phase. As a result, the components are separated according to their volatility and affinity for the stationary phase.

Mass spectrometry (MS), on the other hand, is a technique used to measure the mass-to-charge ratio of ions. In GCMS, the eluting compounds from the gas chromatograph are ionized by various methods, such as electron impact (EI) or chemical ionization (CI), producing charged ions. These ions are then separated based on their mass-to-charge ratio in the mass spectrometer, creating a mass spectrum that represents the molecular fingerprint of the compound. By analysing the mass spectra of the separated compounds, GCMS can identify individual components within complex mixtures based on their unique fragmentation patterns and mass spectra. Additionally, the abundance of each compound's ions in the mass spectrum can be used to quantify the concentration of the compounds in the original sample. GCMS is widely used in various fields such as environmental analysis, forensic science, pharmaceuticals, food and flavour analysis, and petrochemical analysis, among others, due to its high sensitivity, selectivity, and ability to analyse a wide range of compounds.

When using HDPE as raw material, results from GC-MS show that the pyro-oils produced contain 81.5% carbon bonds which is the content of commercial diesel. The contents obtained mostly consist of alkanes and alkenes and have carbon numbers ranging from C9 to C25 [33]. The final product of the pyrolysis process found in the reactor, which is wax, has also been studied for its content and found that the carbon content found ranges from C11 to C14. As for the resulting pyro-oils, the same main compound is also found as the wax content, only in a slightly smaller part with the carbon content found is from C8 to C16 [80]. Researchers also found that pyro-oil from HDPE is suitable for use in diesel engines because it has a long aliphatic hydrocarbon [49]. J. Wang et al. have analysed HDPE at different pyrolysis temperatures and found

that when the temperature exceeds 490°C, the carbon content between C6 and C12 will increase dramatically [72].

While using PET as raw material in pyrolysis of plastic waste, the pyrolysis results from PET do not produce many aromatics or aliphatic hydrocarbons but mostly produce compounds that have oxygen in their content such as acetophenone and benzoic acid [85]. The main compound found in the liquid from the pyrolysis of PET consists of paraldehyde, ethylene glycol and benzoic acid and benzoates. This compound can be applied practically and can be separated from crude oil mixture [86]. The tar produced from the pyrolysis of PET produces substances such as 4-acetylbenzoic acid and 1,2-ethanedial, dibenzoate and it was found that these substances are toxic and can cause cancer which makes this polymer difficult to use in the European continent [87].

2.3.3.6 TGA

TGA stands for Thermogravimetric Analysis. It is a technique used in analytical chemistry to determine the changes in a material's weight as a function of temperature or time, while it is subjected to a controlled temperature program in a defined atmosphere (often inert). In atypical TGA experiment, a small amount of sample (solid or liquid) is placed in a crucible and heated at a constant rate or in steps, while its weight change is continuously monitored. As the temperature increases, various physical and chemical processes may occur, leading to decomposition, volatilization, oxidation, or other reactions within the sample. These processes result in changes in the sample's mass, which are recorded by the TGA instrument. TGA is particularly useful for studying thermal stability, decomposition kinetics, composition analysis, and reaction kinetics of materials. It finds applications in a wide range of fields including polymer science, pharmaceuticals, materials science, and environmental analysis. The data obtained from TGA experiments can provide valuable insights into the thermal behaviour and properties of materials, aiding in product development, quality control, and research endeavours.

The use of TGA is used many times by researchers especially to understand the thermal behaviour and kinetics of material as well as study the fundamental of combustion characteristic of plastic waste. From TGA results of Alawa et. al. it was found that the degradation temperature for HDPE occurs between the temperature of 448.75°C and 495.45°C where the maximum degradation occurs at 481.45°C [33].

However, the degradation temperature of HDPE studied by Das et. al. [47] is lower as compared to the samples of Alawa et. al. which is 370°C with the major weight loss being at a temperature of 475°C. While the end temperature for both analyses is the same, at a temperature of 495°C. L. Rodrguez-Luna et al. found the highest weight loss was at a temperature of 483°C [80]. J. Wang et al. has performed a TGA analysis on HDPE with different heating rates of 10, 20 and 30 °C/min and he found that the higher the heating rate is, the higher the resulting temperature where the highest rate of mass loss occurs respectively at the temperature 465°C, 480°C and 490°C [72]. It can be concluded here that maximum degradation for HDPE occurs between temperatures of 475°C to 483°C. As for PET, Hammoodi et al found that the range of degradation is between 350°C to 465°C while the study by Wang et al is almost the same as Hammoodi's which is the range between 380°C to 487°C [46].

2.3.3.7 DSC

DSC (Differential Calorimetry) measures the heat flow associated with thermal transitions in polymers, such as melting (endothermic) and crystallization (exothermic) events. By analyzing these transitions, researchers can determine key parameters including melting temperature (T_m), crystallization temperature (T_c), and the associated enthalpies (ΔH_m and ΔH_c). These parameters are indicative of the polymer's thermal stability and crystallinity, which directly influence its behavior during pyrolysis. For instance, a study on recycled polypropylene utilized DSC to assess morphological features, revealing that processing technologies significantly impact the crystallinity and predicted mechanical properties of the recycled material [88].

Accurate identification of polymer types within mixed plastic waste streams is crucial for tailoring pyrolysis conditions to specific material properties. DSC aids in this identification by generating unique thermograms that reflect the distinct thermal transitions of different polymers. An optimized DSC method, involving the creation of a thermogram library from 201 polymer reference standards, has been developed to enhance polymer identification accuracy. This approach is particularly beneficial in distinguishing polymers with similar chemical structures but differing thermal behaviours, thereby informing more effective pyrolysis strategies [89].

The specific heat capacity (C_p) of a polymer, representing the amount of heat required to raise its temperature by one degree Celsius, is a critical factor in designing energy-efficient pyrolysis processes. DSC enables precise measurement of C_p across a range of temperatures, providing data essential for modelling thermal degradation and optimizing reactor conditions. Research involving plastic waste/fly ash recycled composites demonstrated the application of DSC in determining specific heat capacities, which are vital for understanding the energy requirements and thermal behaviour of such materials during processing.

Plastic waste often contains various additives and fillers that can influence its thermal properties and pyrolysis outcomes. DSC is instrumental in detecting the presence and effects of these substances by identifying deviations in expected thermal transitions. For example, the inclusion of fillers such as fly ash in recycled composites can alter the specific heat capacity and melting behaviour of the material, as evidenced by DSC analyses. Understanding these effects allows for the adjustment of pyrolysis parameters to accommodate the modified thermal characteristics of the composite material [90].

In summary, DSC provides comprehensive thermal analysis of plastic waste, encompassing the assessment of thermal transitions, specific heat capacities, polymer identification, and the influence of additives. These insights are indispensable for optimizing pyrolysis processes, enabling the efficient conversion of diverse plastic wastes into valuable products.

2.3.4 Importance of Choosing the Mixing Ratio of Plastic Waste Types During Pyrolysis Process

The selection of an appropriate mixing ratio of plastic waste types is a crucial factor in optimizing the yield, composition, and efficiency of the pyrolysis process. The thermal degradation behaviour, chemical composition, and interaction between different plastic types significantly impact the production of pyrolysis-derived fuels and chemicals. A well-optimized mixing ratio can enhance fuel yield, improve product quality, and reduce unwanted byproducts.

The ratio of different plastic types in a pyrolysis feedstock directly affects the quantity and composition of the pyrolysis products. Different plastics exhibit varying pyrolysis behaviour, and their thermal decomposition pathways result in distinct yields

of liquid, gas, and char fractions. As per Table 2.1, high-yielding plastics such as PS and HDPE produce substantial amounts of pyro-fuel, with PS yielding up to 91.8% and HDPE yielding over 80%. In contrast, polyethylene terephthalate (PET) has a low yield of 28.4%, making it a less suitable candidate for maximizing fuel production. By adjusting the plastic composition, the pyrolysis process can be optimized to increase the liquid fuel fraction while minimizing solid residues and unwanted gaseous emissions.

The interactions between different plastic types during pyrolysis can lead to synergistic effects, where one type of plastic influences the degradation of another, resulting in enhanced fuel production. From Table 2.2, PP and LDPE mixtures exhibit higher yields when PP is present in higher proportions. A 90% PP + LDPE mixture yielded 80% pyro-fuel, whereas a 10% PP + LDPE mixture yielded only 28%. From Table 2.3, PET and PS (1:1 ratio) produced the highest pyro-fuel yield of 91.8%, suggesting that specific polymer interactions can enhance fuel production. Properly selecting and balancing different plastic types can improve the efficiency of thermal cracking, leading to higher-quality pyrolysis products.

Different plastics degrade at different temperatures, affecting the energy efficiency and effectiveness of the pyrolysis process. PE and PP degrade at 450-500°C, whereas PET degrades at lower temperatures (350-465°C) [91]. If the mixing ratio is not optimized, some plastics may degrade prematurely, leading to incomplete pyrolysis or the formation of undesirable char residues. By choosing the correct ratio, the degradation process can be synchronized, ensuring that all plastic components break down efficiently without wasting energy or producing excessive solid waste.

Research has demonstrated that adjusting the mixing ratio can significantly influence pyrolysis performance. From Table 2.3, a mixture of PP, HDPE, and LDPE (1:1:1) produced an 81% pyro-fuel yield, making it a well-balanced combination. PS and PE in a 1:1 ratio yielded only 44%, indicating that certain combinations are less favourable. While PS, PP, PE, and PET in a 40:20:20:20 ratio yielded only 28%, suggesting that high PET content reduces efficiency. These findings underscore the importance of carefully selecting plastic ratios to achieve the best fuel yields while minimizing char production and unwanted byproducts.

The choice of plastic waste mixing ratios plays a critical role in the efficiency, yield, and quality of pyrolysis products. By optimizing the composition of plastic waste, researchers and industries can, increase pyro-fuel yield, enhance the quality of the final product and improve thermal efficiency.

2.4 Types of Reactors and Pyrolysis Process Involved for Production of Pyro-Fuel from Plastic Waste

In the pyrolysis process, a reactor is a key component used to thermally degrade organic materials in the absence of oxygen to produce useful products such as bio-oil, syngas, and biochar. The design and operation of the reactor play a crucial role in determining the efficiency, product yield, and quality of the pyrolysis process. Typically used of reactors in the pyrolysis process are feeding, heating, pyrolysis reaction, production collection and residue handling. In feeding process, the organic material, which could be biomass such as wood chips, agricultural residues, or waste plastics, is fed into the reactor. The material may be in solid, liquid, or gaseous form depending on the specific pyrolysis setup. In heating, the reactor is heated to high temperatures, typically ranging from 300°C to 800°C, depending on the type of feedstock and desired products. The absence of oxygen prevents combustion and ensures that the organic material undergoes thermal decomposition through pyrolysis.

In pyrolysis reaction process, inside the reactor, the organic material undergoes thermochemical decomposition in the absence of oxygen. This process involves breaking down complex organic molecules into simpler compounds such as bio-oil, syngas (a mixture of hydrogen and carbon monoxide), and solid char (biochar). While in product collection process, the products of pyrolysis are collected from the reactor. These products may be separated using various techniques such as condensation, filtration, or scrubbing, depending on their physical properties and intended applications. In residue handling process, any remaining solid residue or ash, such as biochar or inorganic impurities, may be removed from the reactor and handled appropriately, depending on its composition and potential uses. Reactor designs for pyrolysis vary widely depending on factors such as the feedstock type, scale of operation, desired products, and process conditions. Common reactor types used in pyrolysis include fixed-bed reactors, fluidized bed reactors, rotary kilns, and microwave reactors. Each reactor type offers advantages and limitations in terms of heat transfer efficiency, residence time control, product yields, and scalability. The choice of reactor design is crucial to optimize the pyrolysis process for maximum efficiency and product quality.

2.4.1 Different Types of Reactors Used for Production of Pyro-Fuel in Pyrolysis

The production of pyro-fuel through pyrolysis is facilitated by various reactor designs, each tailored to optimize specific operational parameters and product yields. The selection of an appropriate reactor type is critical, as it influences the efficiency, scalability, and economic viability of the pyrolysis process. This discourse delineates the predominant reactor configurations employed in pyro-fuel production, elucidating their operational principles, advantages, and limitations.

Fixed bed reactors are among the most rudimentary and extensively utilized configurations in pyrolysis applications. These reactors consist of a stationary bed of feedstock through which heat is applied, initiating the pyrolytic decomposition. The simplicity of design and operation renders fixed bed reactors advantageous for small-scale applications and experimental studies. However, they are often constrained by limitations such as non-uniform heat distribution, lower heat transfer rates, and challenges in scaling up for industrial applications. These factors can impede the efficiency and consistency of pyro-fuel production [32, 92].

Fluidized bed reactors are characterized by the suspension of finely divided feedstock particles within an upward flow of gas, creating a fluid-like state that enhances heat and mass transfer. This configuration facilitates uniform temperature distribution and efficient contact between reactants, thereby optimizing the yield of pyro-fuel. The continuous operation capability of fluidized bed reactors makes them suitable for large-scale industrial applications. Nonetheless, challenges such as attrition of bed materials, complex design requirements, and potential difficulties in handling feedstocks with varying particle sizes necessitate careful consideration in their implementation [70, 92].

Circulating fluidized bed (CFB) reactors represent an evolution of the conventional fluidized bed design, incorporating a recirculation mechanism for the bed material. In CFB systems, the solid particles are continuously circulated between the reactor and a separator, promoting enhanced mixing and heat transfer. This design supports higher throughput and improved control over reaction parameters, which are advantageous for consistent pyro-fuel production. However, the increased mechanical complexity and operational costs associated with CFB reactors may pose challenges, particularly in terms of maintenance and energy consumption [70, 92].

Rotating cone reactors employ centrifugal force to facilitate the contact between the feedstock and a heated surface. In this design, biomass particles are introduced onto a rapidly rotating cone, where they are subjected to intense heat, leading to rapid pyrolysis. The absence of inert gas requirements and the compact nature of the reactor are notable advantages. However, the mechanical intricacy of the rotating components and the need for precise control systems can complicate the operational dynamics and scalability of rotating cone reactors [92].

Ablative pyrolysis reactors operate on the principle of direct contact between the biomass and a heated reactor surface. The mechanical pressure ensures that the feedstock maintains continuous contact with the hot surface, facilitating rapid heat transfer and pyrolysis. This method allows for the processing of larger biomass particles and reduces the necessity for inert gases. However, the mechanical complexity associated with maintaining consistent contact and the potential for uneven heating are challenges that must be addressed to ensure efficient and uniform pyro-fuel production [92].

Auger reactors utilize a helical screw mechanism to convey biomass through a heated reactor chamber. This design enables precise control over the residence time and temperature profiles, which are critical parameters in determining the yield and quality of pyro-fuel. The compact and modular nature of auger reactors makes them suitable for decentralized applications and the processing of diverse feedstocks. However, potential issues such as mechanical wear of the auger components, challenges in scaling up, and limitations in heat transfer efficiency necessitate careful engineering considerations [7]. Plasma pyrolysis reactors employ ionized gases (plasma) to achieve the high temperatures required for pyrolysis. The intense energy density of plasma facilitates the rapid decomposition of feedstocks into pyro-fuel and other byproducts. While plasma reactors offer the advantage of processing a wide range of feedstocks, including those with high moisture content, the significant energy requirements and associated operational costs present substantial challenges. Additionally, the technical complexity of plasma generation and control systems may limit the widespread adoption of this technology in pyro-fuel production [92].

The selection of an appropriate reactor design for pyro-fuel production is contingent upon a comprehensive evaluation of factors such as feedstock characteristics, desired product distribution, operational scale, and economic considerations.

2.4.2 Different Types of Pyrolysis Process Used for Production of Pyro-Fuel in Pyrolysis

The production of pyro-fuel via pyrolysis encompasses several distinct process types, each characterized by specific operational parameters that influence the yield and composition of the resultant products. The primary classifications include slow pyrolysis, fast pyrolysis, flash pyrolysis, and hydrothermal liquefaction. Slow pyrolysis operates at temperatures ranging from 250 to 450 °C, with prolonged vapor residence times between 10 to 100 minutes and a heating rate of 0.1 to 1 °C per second. This process is particularly effective in maximizing biochar production, yielding approximately 35% biochar, 30% bio-oil, and 35% gaseous products. The extended residence time and moderate temperatures facilitate the thorough decomposition of biomass, favouring solid char formation [93].

Fast pyrolysis is conducted at temperatures between 250 to 450 °C, with short vapor residence times of 0.5 to 5 seconds and a heating rate of 10 to 200 °C per second. This method is optimized for liquid bio-oil production, achieving yields of approximately 50%, alongside 20% biochar and 30% gases. The rapid heating and swift vapor residence time minimize secondary reactions, enhancing liquid yield [94]. Flash pyrolysis operates at elevated temperatures ranging from 800 to 1,000 °C, with extremely brief vapor residence times of less than 5 seconds and heating rates exceeding 1,000 °C per second. This process is designed to maximize bio-oil production, achieving yields of approximately 75%, with 12% biochar and 13% gaseous products. The intense thermal conditions and rapid processing time favour the swift depolymerization of biomass into liquid products [95].

The selection of a pyrolysis process for pyro-fuel production is contingent upon the desired product distribution and the specific characteristics of the biomass feedstock. Each process type offers distinct advantages, with operational parameters tailored to optimize the yield of targeted products, whether solid, liquid, or gaseous fuels.

2.4.3 Types of Reactors and Process Affecting the Product and By-product in Pyro-Fuel Production

The use of reactors in the pyrolysis process is very important in ensuring that the pyrolysis process can produce the desired product. Table 2.8 shown the type of reactor and heating medium in pyrolysis process. It was found that most researchers use batch reactors in their pyrolysis process [35, 39, 44, 46, 80, 96, 97]. Some also use semi batch reactor [36, 38, 45], fluidized bed reactor [37], tubular reactor [49] and packed bed reactor [98]. The use of batch reactors by most researchers may be due to the pyrolysis process being easy to implement in batch reactors where the parameters are easy to change [77].

However, there are researchers who state that the production of products from batch reactors is inefficient and inconsistent because it is necessary to add raw materials frequently and involves high labour costs. Therefore, some suggest fixed bed reactor is the best alternative compared to other reactors due to its simple design and more economical when compared to the operation and maintenance cost of other reactors [75]. The type of heater is also very important in ensuring that the pyrolysis process can be heated according to the desired heating speed. Most researchers use furnaces as their heating medium [36, 40, 45, 96]. Some use other heating mediums such as electrical heaters [38, 46, 49, 97, 98], stoves [35], fluidizing gas [37] and infrared heaters [39].

Table 2.8
Type of reactor and heating medium in pyrolysis

Types of plastic waste	Type of reactor	Type of heating medium	Operated Temp (°C)	Ref
PS, PP and PE	Batch	Furnace	560	[44]
PE+PP+ PS+PET+PVC	Semi batch	Furnace	600	[45]
PET	Batch	Stoves	412	[35]
Waste Packaging	Semi batch	Furnace	900	[36]
LDPE	Fluidized bed	Fluidizing gas	450	[37]
HDPE+PP+PET+PS+ LDPE	Semi batch rotary kiln	Electrical	500	[38]
PP	Batch	Infrared heaters	250, 300, 350	[39]
PP, LDPE, HDPE and PP+LDPE+HDPE	Batch	Furnace	400-550	[40]
PS. PET	Batch	Electrical	350, 400, 450	[46]
PET	Tubular	Electrical	600 - 900	[49]
PE	Batch	Furnace	200, 250, 300, 350	[96]
Dump plastic	Batch	Electrical	500, 550, 600	[97]
LDPE	Packed Bed	Electrical	300	[98]

Table 2.9 summarized properties of pyrolysis product. It has been observed that high gross calorific value produced low flash point of the product. This is due to high amount of volatile material in the product. The best density is in the range of 700-900 g/m³. Research done by Yohandri et. al. obtained product that has ideal properties such as heating value of 44.46MJ/kg, density of 774g/m³, and low flash point of 31.0°C [97]. Meanwhile, B. Sugiarto et. al. 2020 obtained 46.23MJ/kg gross calorific value for municipal plastic waste and it is comparable with commercial fuel gasoline and diesel which were 45.7MJ/kg and 47MJ/kg respectively [35]. Thus, liquid oil produced from plastic waste can be used as an alternative fuel for commercial fuel such as gasoline and diesel.

Table 2.9
Properties of product of pyrolytic oil

Types of plastic	Density (kg/m ³)	Flash Point (°C)	Gross Calorific value (MJ/kg)	Ref
PS and PET	700-770	11.6		[48]
PET	-	10.0	46.23	[35]
PP	774	31.0	44.46	[39]
PP	800	-	5.47	[96]
Dump plastic	-	69.0 (non-catalyst), 65.0(catalyst)	-	[97]
PP, LDPE, HDPE and PP+LDPE+HDPE	-	-22.0	44.37	[98]
PP	800	-	45.56	[99]
Commercial Fuel (Gasoline)	750	-	45.7	
Commercial Fuel (Diesel)	830	50	47	

A batch reactor will be used in this study where a total of 5 samples will be used in this study, namely HDPE, PET, a mixture of HDPE and PET in a ratio of 2 to 1, 1 to 1 and 1 to 2. The product produced consists of liquid, char and gas. There is a study found that HDPE produces more than 60% liquid after the pyrolysis process [100]. While for PET, there is a study stating that it does not produce liquid, however it produces 50% gas after the pyrolysis process is carried out [101]. However, the result of the mixture according to the ratio between HDPE and PET has not yet been done by any researcher. Therefore, the expectation that may be produced from this study for the mixing between HDPE and PET where the ratio that has a lot of HDPE will produce more liquid when compared to the ratio that has a small ratio of HDPE.

2.5 Parameter Use in Pyrolysis to Convert Plastic Waste into Pyro-Fuel That Affects Both Quality of Pyro-Fuel and Pollution Emitted

Pyrolysis is a thermochemical process that decomposes plastic waste in an oxygen-deprived environment to produce pyrolytic oil, commonly referred to as pyro-fuel. The efficiency and environmental impact of this process are significantly influenced by various operational parameters, including temperature, reaction time, and the use of catalysts.

2.5.1 Process Parameter for Production of Pyro-Fuel From Pyrolysis of Plastic Waste

In the pyrolysis of plastic waste to produce pyrolytic fuel, several critical parameters significantly influence both the yield and quality of the resulting fuel. These parameters include operating temperature, reaction time, catalyst selection, and feedstock composition. The operating temperature is a crucial factor in the pyrolysis process, as it directly affects the thermal degradation of plastic polymers. Studies have shown that an optimal temperature range exists for maximizing oil yield. For instance, pyrolyzing low-density polyethylene (LDPE) at approximately 350°C has been found to yield about 52.6% of oil by volume. Temperatures exceeding this optimal range may lead to increased gas production due to secondary cracking reactions, thereby reducing the liquid oil yield [102].

The duration of the pyrolysis reaction, or reaction time, influences the extent of polymer breakdown and product distribution. Extended reaction times can enhance the conversion of plastic waste into pyrolytic oil; however, excessively long durations may promote secondary reactions that decompose the oil into gaseous products, thus diminishing the liquid yield. Therefore, determining an optimal reaction time is essential to balance oil production and prevent over-cracking [103].

The use of catalysts in the pyrolysis process can significantly affect the efficiency and selectivity of the reaction. Catalysts such as natural zeolites have been employed to lower the activation energy required for polymer degradation, thereby enhancing oil yield and quality. For example, incorporating natural zeolite catalysts in the pyrolysis of plastic waste has been shown to improve the conversion rates and produce oil with properties comparable to commercial fuels [102].

The type of plastic waste used as feedstock plays a vital role in determining the characteristics of the pyrolytic oil produced. Different polymers decompose at varying rates and temperatures, influencing the yield and composition of the resulting fuel. For instance, LDPE has been found to produce a significant amount of liquid oil upon pyrolysis, with properties closely resembling those of kerosene. Understanding the composition of the plastic waste allows for better control over the pyrolysis process and optimization of the desired fuel characteristics [102].

Optimizing these parameters—operating temperature, reaction time, catalyst selection, and feedstock composition—is essential for enhancing the efficiency of the pyrolysis process and improving the yield and quality of pyrolytic fuel derived from plastic waste. A comprehensive understanding of these factors facilitates the development of effective strategies for converting plastic waste into valuable energy resources.

2.5.2 Critical Parameters That Have Significant Effect to the Process

In the pyrolysis of plastic waste, several critical parameters significantly influence both the efficiency of the process and the quality of the resulting products. These parameters include temperature, heating rate, residence time, feedstock composition, catalyst application, and reactor type. Temperature is a pivotal factor affecting the pyrolysis process. It influences the breakdown of polymer chains, thereby determining the yield and composition of the pyrolysis products. Lower temperatures (approximately 300-500°C) favour the production of liquid oils, while higher temperatures (above 500°C) enhance gas yields due to increased secondary cracking reactions. For instance, a study demonstrated that pyrolyzing polystyrene waste at 450°C yielded a maximum liquid oil output of 80.8%, whereas increasing the temperature to 500°C resulted in a higher gas yield and reduced liquid oil production. The heating rate, defined as the speed at which temperature increases during pyrolysis, plays a crucial role in determining product distribution. High heating rates (e.g., 1000°C/min) are associated with fast or flash pyrolysis, leading to increased liquid yields due to rapid depolymerization and immediate vaporization of intermediates. Conversely, slow heating rates (1-10°C/min) favour char formation as prolonged exposure allows for more extensive solid residue development [104].

Residence time, or the duration for which the feedstock remains in the pyrolysis reactor, affects the extent of thermal degradation. Short residence times are conducive to higher liquid yields, as they minimize secondary cracking of condensable vapours into non-condensable gases. In contrast, extended residence times can lead to increased gas production and reduced liquid yields due to prolonged exposure to high temperatures. The chemical nature of the plastic feedstock influences the pyrolysis process. Plastics such as polyethylene (PE) and polypropylene (PP) possess simple linear structures, requiring higher temperatures for effective degradation. In contrast, polystyrene (PS), with its aromatic ring structure, decomposes at relatively lower temperatures and tends to yield higher liquid oil fractions rich in aromatic compounds [104].

The use of catalysts in pyrolysis can lower the required reaction temperature and modify product distribution. Catalysts such as zeolites and fluid catalytic cracking (FCC) catalysts enhance the breakdown of polymer chains, increasing the yield of desirable products like liquid fuels and valuable chemicals. For example, catalytic pyrolysis has been shown to improve the quality of liquid oils by increasing the concentration of lighter hydrocarbons and reducing the formation of heavy residues. The design and configuration of the pyrolysis reactor significantly impact heat transfer, mass transfer, and residence time, thereby affecting product yields and process efficiency. Fluidized-bed reactors, for instance, offer excellent heat transfer and uniform temperature distribution, making them suitable for both thermal and catalytic pyrolysis. Batch reactors, while simpler in design, may face challenges such as uneven heating and difficulties in scaling up for continuous operations [104].

Optimizing these critical parameters such as temperature, heating rate, residence time, feedstock composition, catalyst application, and reactor type is essential for enhancing the efficiency of the pyrolysis process and improving the quality of the derived products. A comprehensive understanding of these factors facilitates the development of tailored strategies for effective plastic waste conversion.

2.5.3 Reaction Temperature in the Reactor Gives Significant Effect to the Process

In the pyrolysis of plastic waste, the reaction temperature within the reactor is a critical parameter that profoundly influences the yield and quality of the resulting pyrolytic products. Temperature dictates the thermal degradation of polymer chains, thereby affecting the distribution of gaseous, liquid, and solid fractions. Empirical studies have demonstrated that varying the pyrolysis temperature alters the proportions of pyrolytic outputs. For instance, research on polystyrene (PS) waste revealed that at 400°C, the liquid oil yield was 76% by mass, with gas and char yields at 8% and 16%, respectively. Elevating the temperature to 450°C increased the liquid oil yield to 80.8% and gas yield to 13%, while char yield decreased to 6.2%. Further temperature escalation to 500°C resulted in a higher gas yield of 16.8% and a reduced liquid oil yield, indicating that excessive temperatures may favour gas production over liquid oil [105].

The composition of the pyrolytic liquid oil is also temperature dependent. At an optimal temperature of 450°C, the liquid oil derived from PS waste predominantly comprised styrene (48%), toluene (26%), and ethylbenzene (21%). These aromatic compounds are valuable as chemical feedstocks, underscoring the importance of temperature control in tailoring product composition. Thermogravimetric analysis of PS plastic indicates a single-step decomposition process initiating at 400°C and achieving approximately 91% decomposition at 450°C. Beyond this temperature, up to 650°C, only an additional 4-5% weight loss occurs, suggesting that 450°C is an optimal temperature for maximizing liquid oil yield while minimizing energy input [105].

The optimal pyrolysis temperature can vary depending on the type of plastic feedstock. For example, pyrolysis of LDPE waste at 350°C yielded 280 ml of liquid oil from 750 grams of feedstock. This oil exhibited a density between 0.730-0.750 g/ml and contained hydrocarbon chains ranging from C7 to C12, as determined by GC-MS analysis [106]. Precise control of the reaction temperature in the pyrolysis of plastic waste is essential for optimizing product yields and tailoring the composition of pyrolytic oils. Identifying the optimal temperature specific to the plastic type ensures efficient conversion processes and the production of high-quality fuels or chemical feedstocks.

2.5.4 Reaction Time Causes the Runaway Reaction then Creates Unwanted By-Products

In the pyrolysis of plastic waste, reaction time is a critical parameter that significantly influences product distribution and quality. Prolonged reaction times can lead to secondary cracking reactions, resulting in the formation of unwanted by-products and a decrease in desirable liquid oil yields.

Extended reaction times can promote secondary cracking of primary pyrolysis products, leading to the formation of lighter hydrocarbons and non-condensable gases. This not only reduces the yield of liquid oil but also alters its composition, potentially increasing the concentration of undesired by-products. For instance, a study on the pyrolysis of polystyrene waste demonstrated that an optimal reaction time of 75 minutes at 450°C yielded a liquid oil rich in styrene, toluene, and ethylbenzene. Deviations from this optimal reaction time could lead to further degradation of these valuable compounds into less desirable products [105].

In industrial pyrolysis processes, maintaining control over reaction time is essential to prevent runaway reactions. Runaway reactions occur when exothermic secondary reactions accelerate uncontrollably, leading to excessive heat release and potential safety hazards. Such scenarios can cause thermal degradation of the reactor materials and compromise the integrity of the system. Therefore, precise monitoring and regulation of reaction time are imperative to ensure process stability and safety. Furthermore, the development of smart overpressure protection devices has been explored to adaptively respond to dynamic reaction conditions. These devices are designed to offer flexibility and precise countermeasures, thereby improving the safety and efficiency of chemical reactors during exothermic processes [107].

To mitigate the risks associated with prolonged reaction times, it is crucial to determine the optimal duration that maximizes liquid oil yield while minimizing the production of unwanted by-products. This involves conducting systematic studies to evaluate the effects of various reaction times on product distribution and quality. Implementing real-time monitoring systems can aid in promptly detecting deviations from desired reaction conditions, allowing for immediate corrective actions [105].

2.5.5 Good Combination of Parameters Will Produce High Quality Product with Low Emission of Pollutants and Unwanted By-Products

Optimizing the pyrolysis of plastic waste to produce high-quality products with minimal pollutant emissions necessitates careful control of several key parameters: temperature, residence time, pressure, and catalyst selection. Temperature is a critical determinant in pyrolysis, influencing the breakdown of polymer chains and the distribution of end products. Studies have shown that operating within a temperature range of 400-450°C favours the production of liquid oils, while higher temperatures (500-600°C) tend to increase gas yields. For instance, PS begins to degrade at approximately 300°C, with complete breakdown occurring at higher temperatures. Therefore, maintaining temperatures around 400-450°C can optimize liquid oil yields from PS pyrolysis [108].

The duration for which reactants remain in the reactor, known as residence time, significantly affects product composition. Extended residence times can lead to secondary cracking, increasing gas production at the expense of liquid yields. Research indicates that at 450°C, LDPE yields 91.1 wt% oil and 8.7 wt% gas at zero residence time. As residence time increases to 120 minutes, oil yield decreases to 61 wt%, while gas yield rises to 28.5 wt%. Thus, optimizing residence time is crucial to maximize liquid output and minimize unwanted by-products. Operating pressure influences the pyrolysis process, particularly at lower temperatures. Studies have demonstrated that increasing pressure from 0.1 to 0.8 MPa at 410°C raises gas production from 6 wt% to 13 wt%. However, at 440°C, gas production increases only from 4 wt% to 6 wt%, suggesting that pressure effects diminish at higher temperatures. Therefore, adjusting pressure appropriately can help control product distribution and quality [108].

The use of catalysts can enhance pyrolysis efficiency and product quality. Catalysts such as Zeolite, Fluid Catalytic Cracking (FCC) catalysts, and MgO have been shown to improve yields and reaction kinetics. For example, the BHZSM-5 catalyst has achieved bio-oil yields of 88% while minimizing char formation. Natural alternatives like Mabisan clay have also demonstrated effectiveness in bio-oil production [109]. Achieving a high-quality product with low emissions in the pyrolysis of plastic waste requires a synergistic approach, carefully balancing temperature, residence time, pressure, and catalyst selection. Tailoring these parameters to the specific plastic feedstock can optimize product yields and minimize environmental impact.

Recent studies have demonstrated that optimizing pyrolysis parameters can significantly enhance the quality and yield of pyro-fuel derived from plastic waste. Faisal et al. (2024) investigated focusing on the thermal pyrolysis of mixed waste plastics, including HDPE, PP, and PS. Utilizing response surface methodology (RSM) and Box-Behnken design (BBD), the researchers varied reaction temperature (460-540 °C), residence time (30-150 minutes), and feedstock particle size (5-45 mm) to maximize liquid oil yield. The study identified that a reaction temperature of approximately 536 °C, a residence time of 150 minutes, and a feedstock particle size of 24 mm resulted in the highest oil yield of 75.14 wt%. Analysis of variance (ANOVA) indicated that temperature and residence time were the most influential factors affecting oil yield, followed by feedstock size. However, the crude pyrolytic oil exhibited higher water content (0.125 wt%) and sulfur content (5.12mg/kg), along with a lower flash point (<20 °C) and cetane index (32), rendering it unsuitable for direct use as automotive fuel. The researchers suggested that post-treatment techniques, such as distillation and hydrotreatment, are necessary to upgrade the oil's quality for practical applications [110].

In a separate study, Mibei et al. (2023) explored the catalytic pyrolysis of plastic waste using a local clay catalyst. The research focused on optimizing operating variables, specifically catalyst concentration and reaction temperature, to maximize liquid oil yield from HDPE, PP, and PS waste plastics. The study employed a central composite design matrix and response surface methodology to analyse the effects of these variables. For HDPE, the optimal conditions were identified as a pyrolysis temperature of 300 °C and a catalyst concentration of 10 wt%, achieving a maximum oil yield of 87.23 wt%. The analysis of variance confirmed the significance of both temperature and catalyst concentration in influencing the oil yield. These findings underscore the potential of utilizing locally sourced catalysts to enhance pyro-fuel production from plastic waste [111]. Collectively, these studies highlight the critical role of optimizing pyrolysis parameters including reaction temperature, residence time, feedstock particle size, and catalyst concentration in producing high-quality pyro-fuel from plastic waste.

2.6 Pyro-Fuel Produced from Pyrolysis of Plastic Waste

In 2019, the value of the world plastic to fuel market is US\$972.8 million and is expected to increase by 8.2% from 2020 until 2027. The Asia Pacific region alone has dominated the world market, which is 35.5% in 2019. The increasing population and urbanization of the economy in the region is expected to cause oil consumption to increase every year. Therefore, through this pyrolysis process when compared to depolymerization and gasification, it will produce a global market of 65.3% because this technique will produce a more efficient process when compared to other processes [44].

Table 2.10
Pyrolytic oil yield produced from mixed or segregated plastic waste

Type of plastic waste	Yield of Pyrolytic Oil (wt%)	References
PET and PS	91.8	Soumya Sikdar [48]
PET	28.4	B. Sugiarto [35]
PE	67.7-76.1%	Wonjin Jeon [36]
LDPE	43.9	P. T. William [37]
3% PVC, 4%PET, 18%PS, 35%PP, 40% PE	72.0	A. Lopez [45]
PS	91.8	Y. Zhang [38]
PP	10.91	Y. Bow [39]
P S+10%/20%/3 0%PET	77.0	S. I. Hammoodi [39]
PP	21.7	M. Martynis [96]
50%PE, 50%PET	34.4	M. Al-Asadi [49]

The yield of pyrolytic oil from the non-catalytic pyrolysis process has been shown in Table 2.10. From the table, PS produces the highest yield of oil which is 91.8% due to the structure of PS containing high phenyl groups. The phenyl group produces a stable benzylic radical and produces a low hydrocarbon chain [38]. From that table also, PP produces the least yield of pyrolytic oil which is only 10.91% at a temperature of 350°C [39].

2.6.1 Physical Properties of Pyro-fuel from Plastic Waste

Pyrolysis derived fuels or pyro-fuels obtained from plastic waste exhibit physical properties that are influenced by the type of plastic feedstock and the specific pyrolysis conditions employed. These properties are critical in determining the suitability of pyro-fuels for various energy applications.

The calorific value (CV) indicates the energy content of the fuel. Pyro-fuels derived from polyolefin plastics such as high-density polyethylene (HDPE), low-density polyethylene (LDPE), and polypropylene (PP) have calorific values ranging between 39.5 and 40.8 MJ/kg, comparable to conventional diesel and gasoline fuels, which have CVs of approximately 43 MJ/kg. In contrast, fuels obtained from polystyrene (PS) exhibit higher calorific values around 43 MJ/kg, while those from polyethylene terephthalate (PET) and polyvinyl chloride (PVC) have lower CVs of 28.2 MJ/kg and 21.1 MJ/kg, respectively. The reduced energy content in PET and PVC-derived fuels is attributed to their chemical structures, which include oxygenated and chlorinated compounds [18].

Density affects the volumetric energy density and combustion characteristics of the fuel. Pyro-fuels from HDPE, LDPE, and PP have densities ranging from 0.78 to 0.89 g/cm³ at 15°C, closely aligning with conventional diesel (0.807 g/cm³) and gasoline (0.78 g/cm³). PS-derived fuels exhibit slightly higher densities around 0.96 g/cm³, while PET-derived fuels have densities approximately 0.90 g/cm³. These variations are influenced by the molecular composition and structural characteristics of the original plastic materials. Viscosity influences fuel atomization and combustion efficiency. Pyro-fuels from HDPE and LDPE exhibit viscosities between 1.63 and 5.56 mm²/s at 50°C, comparable to conventional diesel fuels, which range from 1.9 to 4.1 mm²/s. PP-derived fuels have viscosities around 2.27 mm²/s, while PS-derived fuels are lower, approximately 1.4 mm²/s. Appropriate viscosity is essential for efficient fuel injection and combustion in engines [18].

The flash point indicates the temperature at which the fuel can vaporize to form an ignitable mixture in air, reflecting its volatility and safety in handling. Pyro-fuels from HDPE, LDPE, and PP have flash points ranging from 30 to 48°C, comparable to gasoline (42°C) and diesel (52°C). PS-derived fuels have lower flash points around 26.1°C, indicating higher volatility. These values are influenced by the composition of hydrocarbons present in the pyro-fuel. The cetane number measures the combustion

quality of diesel fuels during compression ignition. PP-derived pyro-fuels have a cetane rating of 56.8, indicating good ignition properties, while PS-derived fuels have a lower cetane rating of 12.6, suggesting less favourable ignition characteristics. Cetane numbers are influenced by the structure of hydrocarbons present, with straight-chain alkanes contributing to higher values [18].

The physical properties of pyro-fuels derived from plastic waste are comparable to those of conventional fuels, with variations depending on the type of plastic feedstock. Understanding these properties is essential for optimizing pyro-fuel production and assessing their suitability for specific energy applications.

2.6.2 Chemical Properties of Pyro-fuel from Plastic Waste

Pyrolysis of plastic waste yields pyro-fuels with chemical properties that are contingent upon the feedstock composition and operational parameters of the pyrolysis process. A comprehensive understanding of these chemical characteristics is essential for evaluating the applicability of pyro-fuels in energy production and industrial applications.

Pyro-fuels derived from plastic waste predominantly consist of hydrocarbons, including paraffins, olefins, naphthenes, and aromatics. The specific distribution of these compounds is influenced by the type of plastic feedstock and the pyrolysis conditions employed. For instance, pyrolysis oils obtained from HDPE are rich in aliphatic hydrocarbons, whereas those derived from PS contain higher concentrations of aromatic compounds. Advanced analytical techniques, such as comprehensive two-dimensional gas chromatography (GC×GC), have been utilized to elucidate the detailed hydrocarbon profiles of these pyrolysis oils, facilitating the identification and quantification of various hydrocarbon classes, including linear, branched, and diolefins.

The occurrence of sulphur and nitrogen containing compounds in pyro-fuels is contingent upon the presence of heteroatom-containing additives or contaminants in the plastic waste. These compounds are undesirable due to their potential to form harmful emissions upon combustion. Analytical assessments have revealed that pyrolysis oils from mixed plastic waste may contain trace amounts of sulphur and nitrogen species, necessitating further refining processes to meet environmental and fuel quality standards [112].

The presence of oxygenated compounds in pyro-fuels is primarily attributed to the inclusion of oxygen-containing polymers, such as PET, in the plastic waste feedstock. These oxygenated species can adversely affect the stability and combustion properties of the fuel. Studies have demonstrated that pyrolysis oils derived from PET exhibit a higher abundance of oxygenated compounds compared to those obtained from polyolefin-based plastics. Therefore, controlling the composition of the feedstock and optimizing pyrolysis conditions are critical to minimizing the formation of undesirable oxygenated compounds in the resulting pyro-fuel.

The molecular weight distribution of pyro-fuels is a critical parameter influencing their viscosity, volatility, and combustion characteristics. Pyrolysis oils typically encompass a wide range of molecular weights, with the exact distribution being dependent on the plastic feedstock and pyrolysis conditions. For example, pyrolysis of polyolefin plastics tends to produce lighter hydrocarbons, whereas feedstocks containing polymers like PET may yield heavier fractions. Understanding and controlling the molecular weight distribution are essential for tailoring pyro-fuels to specific applications [113]. The chemical properties of pyro-fuels derived from plastic waste are intricately linked to the nature of the feedstock and the operational parameters of the pyrolysis process. Advanced analytical techniques are indispensable for characterizing these properties, thereby enabling the optimization of pyro-fuel production for targeted energy and industrial applications.

Recent advancements in pyrolysis technology have demonstrated the potential to convert plastic waste into high-quality pyro-fuels while minimizing the production of undesirable by-products. A notable study by Sivagami et al. (2022) explored the catalytic pyrolysis of mixed plastic waste using zeolite catalysts in a bench-scale reactor. The researchers employed both commercial and synthesized ZSM-5 zeolite catalysts to assess their efficacy in producing fuel oil from various plastic types, including LDPE, HDPE, PP and multilayer plastics. The synthesized ZSM-5 catalyst, characterized by its strong acidic properties and microporous crystalline structure, facilitated enhanced cracking and isomerization reactions [114].

This catalytic activity led to a significant increase in oil yield, achieving a maximum of 70% for LDPE feedstock, with corresponding gas and char yields of 16% and 14%, respectively. Importantly, the sulphur content in the produced oil was below detectable limits, indicating a cleaner fuel product. The study also reported that the residual char contained heavy metals, necessitating appropriate management strategies

for this by-product. These findings underscore the effectiveness of ZSM-5 zeolite catalysts in optimizing pyrolysis processes to yield high-quality pyro-fuels with minimal undesirable by-products [114].

2.7 Pollutant Emitted and Unwanted By-Products Produced from Pyro-Fuel Production

Production of plastic has grown radically due to extensive consumption and demand of plastic in daily life as can be seen in these few decades hence the production of plastic waste has increased accordingly. The increasing amount of plastic waste has raised major concern worldwide [115] because pyrolysis of plastic waste has left significant impact to human and environment caused by hazardous gas released during the process.

Hazardous gas is associated with considerable negative impacts for living organisms, climate and environment parallel with vast urbanization, expanding populations and growing economy [116]. Pyrolysis emitted hazardous gas which cause harmful effect to ecosystems such as human toxicity, climate change, aquatic ecotoxicity and many more. This issue has set an increased focus among society on reduction of hazardous gas and many research and studies have been made to encounter the problem [117]. Therefore, cleaner production during pyrolysis of plastic waste is essential to reduce the probability of global contamination. Cleaner production has been proposed as an initiative to minimize waste emissions and maximize product output. To combat the negative effects, use of hazardous waste technologies can be seen as a potential for hazardous gas mitigation as it is known to guarantee cleaner production. Wet scrubber is compatible and effective air pollution control device to capture polluting gases [118] and ensure maximum reduction of hazardous gas emission during pyrolysis of plastic waste.

From Table 2.11, it can be summarized that hazardous gas which is categorized under flammable gas is mainly produced from the pyrolysis of raw material such as polyethylene (HDPE, LLDPE, LDPE). As analyzed, polyethylene is recognized as one of the major producers of hazardous gases such as NO_x, SO₂, CO₂, CH₄, CO, dioxins, furans etc. Pyrolysis of plastic film residue (PFR) made of HDPE and LDPE produce H₂, CO, CO₂ and CH₄ as stated by Cocchi, et al. [119]. Thermal and catalytic pyrolysis by using coal fly ash (CFA) and synthesized X zeolites as catalysts are applied on PFR.

Both pyrolysis processes produce different gas yields of 25wt% at temperature of 480°C and 42wt% at temperature of 472°C by thermal and catalytic pyrolysis respectively. Same research has been found from pyrolysis of LDPE, MDPE and HDPE which emitted NO_x, SO_x, CO, CO₂ and CH₄ with gas yield between 7.3% to 11.3% as reported by Roy, et al. [120]. Besides, minor producer of hazardous gases during pyrolysis of plastic waste is polyvinyl chloride (PVC). Table 5 shows less studies on pyrolysis of PVC compared to other type of raw material or only if PVC is mixed with other raw materials. Kwon, et al. [121] found that pyrolysis of PVC releases hazardous gases such as CO, H₂ and CH₄ at a rate of 10°C/min. Hazardous gas yield of 0.22mol%, 0.36mol% and 0.24mol% at temperature 390°C, 480°C and 540°C is produced from pyrolysis of PVC. Pyrolysis of PVC with other raw materials produce different gas products and gas yield than pyrolysis of PVC alone. By referring Table 2.11, non-condensable product such as CO, H₂ and CO₂ is produced from pyrolysis of municipal solid waste (MSW) and municipal plastic waste (MPW) that contain PE, PP, PET, PS and PVC as stated by Miskolczi, et al. [97].

Table 2.11
 Hazardous gas released during pyrolysis of plastic wastes

	PE	PP	PET	P S	p V C	Type of waste	References
CO ₂ , NO _x , SO ₂	HDPE	PP				waste polymers	Stelmachowski [122]
CO ₂ , NO ₂ , H ₂ O ₂	PE	PP	PET	P S			Nishida [123]
CO ₂ , CO, CH ₄ , N ₂	bio-PE		bio- PET				Lamberti, et al. [124]
CO, HCl, Cl ₂	HDPE, LLDPE, LDPE	PP		p S			Jha and Kannan [125]
CO ₂ , CO, CH ₄ , H ₂ , C ₂ H ₆	PE	PP	PET	p S	p V C		Jeon, et al. [36]
H ₂ , CO, CO ₂ , CH ₄	HDPE, LDPE	PP				plastic film residue (PFR)	Cocchi, et al. [119]
CO ₂ , CO, NO, NO _x , SO _x , NH ₃ , CH ₄ , N ₂ O, H ₂ S, HF, HCl						(PSW)	Antelava, et al. [115]
CO ₂ , CH ₄ , H ₂ , NH ₃ , N ₂ O, dioxins, furans						MSW	Lee, et al. [116]
CH ₄ , CO ₂ , N ₂ O							Fruergaard, et al. [117]
CO ₂ , NO ₂ , SO ₂ , H ₂ , S ₂	PE	PP	PET			FPPW	Ahamed, et al. [126]
H ₂ , CO, N ₂ , CO ₂ , CH ₄	HDPE			p S			Akubo, et al. [71]
CO ₂ , CO, NO, NO _x , SO _x , N ₂ O, HCl, H ₂ S						waste tyre	Czajczyriska, et al. [127]
CO ₂ , CH ₄ , CO	PE(MB)	PP (S Y)				Syringes (SY) & medical bottles (MB)	Ding, et al. [128]
NO _x , SO ₂	PE					MPW	Gear, et al. [129]
CO ₂ , HCl, CO, H ₂	HDPE, LDPE	PP	PET	p S	p V C		Grause, et al. [130]
SO ₂		PP					Jha, et al. [131]
CO ₂ , CH ₄ , H ₂ , CO, C ₂ H ₆	PE	PP	PET	p S	p V C		Lopez, et al. [45]
CO ₂ , CH ₄ , CO	LDPE		PET			plastic bottle	Maity, et al. [132]
CO, H ₂ , CO ₂	PE	PP	PET	p S	p V C	MSW & MPW	Miskolczi, et al. [97]
dioxins, furans, O ₃ , S ₂ , NO _x , SO _x , NO ₂ , SO ₂ , N ₂ O	LDPE, HDPE	PP	PET	p S	p V C		Nkwachukwu, et al. [133]
CO, CO ₂ , H ₂ , CH ₄			PET			water bottles	Osman, et al. [16]

NO _x , SO _x , CO, CO ₂ , CH ₄	LDPE, MDPE, HDPE							Roy, et al. [120]
CH ₄ , CO ₂ , C ₂ H ₆ , C ₃ H ₈ , C ₄ H ₁₀ , CO	LDPE	PP						Sarker, et al. [134]
CO ₂ , NO _x , SO _x	LDPE, HDPE	PP	PET	P	V	waste plastics		Sikdar, et al. [48]
H ₂ , CO, CO ₂ , CH ₄ , HCl	LDPE, HDPE	PP	PET	P	S			Williams [135]
H ₂ , C ₂ H ₆ , C ₂ H ₄ , CH ₄ , CO, CO ₂	LDPE, HDPE	PP	PET	P	S	MSW		Zhang, et al. [38]

Pyrolysis of MSW and MPW through thermal and catalytic pyrolysis by using different catalysts releases different amounts of gas yield for different catalysts and at different temperatures. Thermal pyrolysis of MSW and MPW produce gas yield between 8.2% to 20.3% in the temperature range of 500°C to 600°C. Catalytic pyrolysis of MSW produces gas yield between 14.2% to 21.5% while MPW produces gas yield between 9.9% to 26.4%. Almeida and Marques [41] investigated that catalysts such as Y-zeolite, β -zeolite, equilibrium FCC, MoO₃, Ni-Mo catalysts, HZSM-5, Al(OH)₃ are used in the catalytic pyrolysis have been proven to increase the yield of products from recycling of pure or mixed plastics waste. Different sources of plastic waste or raw material produce variety of hazardous gas and gas yield at different parameters. Pyrolysis traps the gas for recycling and uses the gas for daily purposes. For example, biogas produced from pyrolysis process may be combusted in gas engines to generate heat and electricity (Fruegaard, et al. [117]) and can be used for cooking as the gas is contained in gas cylinder.

Table 2.12
Non-condensable product yield (wt%) for different samples of plastic wastes

Sample	Non-condensable product yield (wt%)	Gas products	Ref.
Waste tyres	14.1	CO ₂ , CO, NO, NO _x , SO _x , N ₂ O, HCl, H ₂ S	[127]
Syringes	75.43	CO ₂ , CH ₄ , CO	[128]
Medical bottles	98.27		
Personal protection equipment (PPE)	69.8	pyrolysis gas	[136]
Water bottles	42.8	CO, CO ₂ , H ₂ , CH ₄	[16]

Table 2.12 shows the data for non-condensable product yield (%) for different samples of plastic waste which are waste tires, syringes, medical bottles, personal protection equipment (PPE) and water bottles. From Table 2.12, it can be concluded that medical bottles made of PE produce the highest non-condensable product yield by 98.27% [128]. Pyrolysis of medical bottles produce hazardous gases such as CO₂, CH₄ and CO.

The highest gas yield production may be due to lower melting point of PE which leads to increase of gas and liquid products as degradation temperature increases. It

breaks down more easily over time, leading to higher surface areas. PE is identified as potentially toxic to humans and bad for our environment as it easily leaches when exposed to ultraviolet (UV). Pyrolysis of waste tyre at a rate of 5°C/min and heating value of 34.5MJ/kg shows much different result than medical bottles. CO₂, CO, NO, NO_x, SO_x, N₂O and H₂S are toxic gases with gas yield of 14.1% produced from pyrolysis of waste tyre at temperature of 400°C according to Czajczyhska, et al. [127] shows the lowest non-condensable product yield compared to other samples of plastic wastes. This is due to complex polymeric chain of tyre which is made up of HDPE making it a high complex tyre thus hard to decompose to gas instead to solid or liquid. Burning of tyre produces black fumes contain heavy metals which can lead to airborne pollution that linger in the air and contribute to acute chronic health hazards. Apart from that, PPE is widely used in our current situations around the world as we are facing a global pandemic where PPE is essential for self-protection. PPE is mainly made of PP fiber which has a special characteristic of trapping particles effectively and protecting its wearer from infection like face masks. Jain, et al. [136] found that pyrolysis of PPE produces non-condensable product yield of 69.8% which is higher than pyrolysis of waste tyres but lower than that of medical bottles. PPE undergoes thermal pyrolysis and has melting point of 171°C which is lower.

Table 2.13
Effect of thermal and catalytic pyrolysis on product yield (%) for different types of polymers

Type of polymers	Percentage Gas Yield %		Cras products	Ref.
	Non-Catalytic	Catalytic		
HDPE	13	63.5	pyrolysis gas	[41]
HDPE, LDPE, PP	25	42	H ₂ , CO, CO ₂ , CH ₄	[119]
PE, PP, PET, PS, PVC	8.2	26.4	CO, H ₂ , CO ₂	[97]
PP	12.5	14	non-condensable products	[137]
LDPE	50.4	54.5	pyrolysis gas	[138]

Lower melting point of PPE is favorable for thermal pyrolysis of PP due to the presence of the tertiary carbon atom that makes the chemical bond breaking easier. Pyrolysis of PPE produces harmful toxic gases that may cause respiratory irritation. Thermal pyrolysis of plastic waste is thermal decomposition of materials at elevated temperature in inert atmosphere whereby no or less oxygen is used because free oxygen

atmosphere is unavoidable. Formation of wide range hydrocarbons has resulted from the breaking down of macromolecules into smaller molecules at high temperatures [41]. Thermal pyrolysis is not very selective but catalytic pyrolysis helps in reducing these reaction conditions as it increases the yield of products through increase in process selectivity. Catalytic pyrolysis also helps in inhibiting the formation of undesirable products.

From Table 2.13, raw material that shows the largest differences between thermal and catalytic pyrolysis is HDPE with 13% of thermal pyrolysis yield and 63.5% of catalytic pyrolysis yield according to Almeida and Marques [41]. Larger gap between both gas yield for pyrolysis processes is caused by low degradation temperature of 450°C needed for product distribution in HDPE. Thermal pyrolysis yield increases as temperature increases. HDPE has rigid and durable structure which makes it harder to degrade due to greater strength while catalyst used in this process which is zeolite ZSM-5 alters the decomposition reaction for HDPE aids in larger product distribution by achieving 63.5% of catalytic pyrolysis gas yield. Next, thermal pyrolysis and catalytic pyrolysis gas yield of HDPE, LDPE and PP from plastic film residue (PFR) appear to have medium differences. Cocchi, et al. [119] found that thermal pyrolysis of PFR was conducted at temperature 480°C produces 25% of thermal pyrolysis yield. Result of using Coal fly ash (CFA) and synthesized X zeolites as catalysts for catalytic degradation of PFR produces gas yield of 42% at temperature of 472°C. As can be seen, lower temperature is needed for catalytic pyrolysis compared to thermal pyrolysis because catalysts promote decomposition reactions at low temperature and higher gas yield is achievable than thermal pyrolysis.

Pyrolysis of PP has the lowest differences between thermal and catalytic pyrolysis by 12.5% and 14% respectively. Abbas-Abadi, et al. [137] states that 10wt% fluid catalytic cracking (FCC) catalysts are used to degrade PP produce only small increases in the catalytic gas yield. This is explained by the property of PP which has good chemical resistance and corrosion resistance structure. So, it is hard to degrade PP even with presence of catalysts.

Table 2.14
Effect of temperature (°C) on gas yield (%) for different type of plastic wastes

Type of waste polymers	Temperature (°C)	Non-condensable product yield (%)	Ref.
LDPE, HDPE, PP, PET, PS, PVC	900	42	[130]
PE, PP, PET, PS, PVC	500	8.2	[97]
	550	11.1	
	600	14.5	
LDPE, PP	400	6	[134]

Pyrolysis process is conducted at temperatures from 300°C to 900°C. As per Table 2.14, the highest pyrolysis gas yield is obtained at temperature 900°C by 42% [130] and the lowest gas yield obtained at temperature 400°C by 6% [134]. Generally low temperature is favorable for production of biochar. Therefore, the increase in gas yield at high temperature subsequently decreased the char yield as the operating temperature increases. In this context, the energy contents of plastic waste are elevated to liquid and gas products at higher temperature. As pyrolysis temperature increases, polycyclic aromatic hydrocarbon (PAH) is generated and released to atmosphere. Abundant emission of Eb (unstable atom), CEL and other non-condensable gas produce large quantity of dioxins and furans which is not good for liquid fuel. Pyrolysis of plastic waste shows increasing trend and achieves peak at 900°C. At this temperature, maximum gas yield of hazardous gas up to 42% has been reported [130]. From low to moderate temperature, the hazardous gas yield rises resulting in a decrease in char yield. As observed, high temperature pyrolysis provides greater quantity of non-condensable products (synthetic gas) while lower temperatures favor the production of high-quality solid products such as charcoal.

Table 2.15
Effect of catalysts on non-condensable product yield (%)

Type of catalysts	Type of waste polymers	Percentage Gas Yield		Gas products	Ref.
		Non-Catalytic	Catalytic		
20wt% fluid catalytic cracking (FCC) catalysts	HDPE	6.7	8.8	non-condensable product	[139]
zeolite ZSM-5	HDPE	13	63.5	non-condensable product	[41]
HY zeolite	LDPE	39.1	43.9	pyrolysis gas	[138]
HZSM-5	PE, PP, PET, PS, PVC	11.1	34.6	CO, H ₂ , CO ₂	[97]

Several studies reported the use of catalysts in pyrolysis of plastic waste to increase products yield because catalysts increasing process selectivity during catalytic pyrolysis as stated by Almeida and Marques [41]. Catalyst used in pyrolysis of HDPE which is zeolite ZSM-5 increases the gas yield by 50.5%. Zeolite ZSM-5 has strong acidic property, and its microporous crystalline structure provides best selectivity in the degradation of HDPE molecules, thus increasing efficiency in cracking. Meanwhile, pyrolysis of HDPE at a rate of 25°C/min by using 20wt% FCC catalysts show the least differences between thermal and catalytic gas yield compared to other types of polymers. According to Abbas-Abadi, et al. [139], thermal pyrolysis of HDPE at temperature 420°C produces 6.7% of non-condensable product while catalytic pyrolysis of HDPE produces 8.80% of gas yield with aid of FCC catalysts. Catalytic pyrolysis gas yield of HDPE with 20wt% FCC catalysts only shows 2.1% increase which is very small if compared to catalytic pyrolysis of HDPE with zeolite ZSM-5. This may result from FCC catalysts that is less effective on the non-condensable product yield because the use of FCC catalyst only emphasizes optimization of high yield hydrocarbons production from catalytic pyrolysis of HDPE. During the process, more coke is produced due to dehydrogenation through aromatization on the catalyst surface. It can be concluded that excellent catalyst like zeolite ZSM-5 produces higher gas yield than FCC catalysts for catalytic pyrolysis of HDPE.

As shown in Table 2.16, pyrolysis of raw material from plastic solid wastes (PSW) emitted more hazardous gases product as studied by Antelava, et al. [115]. Toxic gases produced from pyrolysis of PSW are CO₂, CO, NO, NO_x, SO_x, NH₃, CH₄, N₂O, H₂S, HF and HCl which contribute to fatal impact. These hazardous gases can cause

global warming through assembled air pollutants in the atmosphere and trap the heat followed by heat wave cause the planet to get hotter. This phenomenon has led to melting glaciers at north and south pole and decreases land area caused by rise in sea level. Another effect of hazardous gas from PSW pyrolysis is acidification which is mainly caused by CO₂ absorbed by ocean and reacts with seawater to produce carbonic acid (H₂CO₃). An acidic ocean ecosystem has a lower concentration of carbonate ions, limiting the ability of marine life to build and maintain calcium-based structures such as shells and corals due to erosions. Besides, Lee, et al. [116] studied that pyrolysis of MSW associated with toxic emissions such as CO₂, CH₄, H₂, NH₃, N₂O, dioxins and furans are harmful to human health and safety. Toxic gases such as dioxins and furans have been related with a wide range of adverse health impairments. The person who may exposed to high concentration of dioxins and furans will cause these hazardous substances to enter their body through digestive or respiratory tract or through skin contact. Therefore, exposure to dioxins and furans should be kept as low as possible. Similarly, pyrolysis of PE from MPW resulting in emission of NO_x and SO₂ Gear, et al. [129].

Table 2.16

Effect of hazardous gas emission during pyrolysis of plastic wastes

Polymers	Gas products	Effect of hazardous gas emission	Ref.
PE, PP, PET (FPPW)	CO ₂ , NO ₂ , SO ₂ , H ₂ , S ₂	climate change, fossil depletion, human toxicity(cancer), ionizing radiation potentials	[126]
Plastic solid wastes (PSW)	CO ₂ , CO, NO, NO _x , SO _x , NH ₃ , CH ₄ , N ₂ O, H ₂ S, HF, HCL	global warming, human toxicity, acidification, eutrophication, photochemical oxidant formation	[115]
PE (MPW)	NO _x , SO ₂	freshwater and marine aquatic ecotoxicity, ozone depletion, human toxicity, global warming	[129]
municipal solid waste (MSW)	CO ₂ , CH ₄ , H ₂ , NH ₃ , N ₂ O, dioxins, furans	health impairments, diarrhoea, headaches, chest pains, irritation of the skin, nose and eyes, typhoid, stomach ulcers	[116]
LDPE, HDPE, PP, PET, PS, PVC	dioxins, furans, O ₃ , S ₂ , NO _x , SO _x , NO ₂ , SO ₂ , N ₂ O	endangered aquatic life, cancer, deformed offspring, reproductive failure, immune diseases, subtle neurobehavioral effects, endocrine disruption	[133]

Emissions of NO_x and SO_2 into the air, where the pollutants are transformed into acid particles namely sulphuric acid or nitric acid may be transported long distances via cloud. These acid particles may cause harmful effects on aquatic ecosystem when the hazardous particles fall to the earth as wet and dry deposition. This can include rain, snow, fog, hail or even dust that is acidic.

2.7.1 Properties of Hazardous Gas Released During Pyrolysis of Plastic Waste

Table 2.17 shows the properties of hazardous gas released during pyrolysis of plastic waste. Different hazardous gases show variety properties as studied by several researchers. Pyrolysis of waste tyre as investigated by Czajczyhska, et al. [127] is carried out under different temperatures of 400°C , 500°C and 600°C produce hazardous gases such as CO_2 , CO , NO , NO_x , SO_x , N_2O , HCL and H_2S . Heat released during the waste tyre pyrolysis is $5^\circ\text{C}/\text{min}$ which is very low indicates slow heating rate. The density of syngas is assumed to be $0.95\text{kg}/\text{m}^3$ and has high heating value of $34.5\text{MJ}/\text{kg}$. Other than that, waste polymers consist of HDPE and PP are degraded under temperature between 362°C to 423°C as mentioned by Stelmachowski [122]. Hazardous gas released from pyrolysis of waste polymers are identified as CO_2 , NO_x and SO_2 under different rate of reaction of HDPE and PP. During pyrolysis of waste polymers, rate of reactions is between 2500 to $3500\text{kg}/\text{hm}^3$ and between 3600 to $4400\text{kg}/\text{hm}^3$ for both HDPE and PP respectively. PP is less rigid than HDPE thus the rate of reaction for pyrolysis of PP is higher than HDPE. Another study made by Williams [135] reported the pyrolysis of mixed plastic wastes consist of LDPE, HDPE, PP, PET, PS and PVC are carried out under temperature between 700°C to 900°C . Pyrolysis of mixed plastic wastes produces toxic gases such as H_2 , CO , CO_2 , CH_4 and HCl have mass flowrate of $25\text{kg}/\text{h}$. Temperature of 900°C is considered as the highest temperature for pyrolysis because large amount of waste plastics from different type of polymers need to be degraded at higher temperature as lower temperature will slower the rate of degradation.

Table 2.17

Properties of hazardous gas released during pyrolysis of plastic waste

Raw material					Temperature (°C)	Gas products	Q, heat released (°C/min)	Properties	Ref.
PE	PP	PET	PS	PVC	Type of waste				
PE	PP	PET			FPPW	700	CO ₂ , NO ₂ , SO ₂ , H ₂ , S ₂	CCVD=1100MJ/kg	[126]
HDPE			PS			750, 850	H ₂ , CO, N ₂ , CO ₂ , CH ₄	20	[71]
HDPE, LDPE	PP				plastic film residue (PFR)	Thermal pyrolysis=480, Catalytic pyrolysis=472	H ₂ , CO, CO ₂ , CH ₄	E=1.47 and 2.07 MJ/kg	[119]
					waste tyre	400,500,600	CO ₂ , CO, NO, NO _x , SO _x , N ₂ O, HCl, H ₂ S	5	[127]
PE (MB)	PP (SY)				Syringes (SY)& medical bottles (MB)	SY:394.4-501°C, MB:417.9-517°C	CO ₂ , CH ₄ , CO	Ea=246.5 & 268.51 kJ/mol, HHV (SY: MB) =33.06:45.51 MJ/kg	[128]
PE	PP	PET	PS	PVC		400	CO ₂ , CO, CH ₄ , H ₂ , C ₂ H ₆	10	[36]
				PVC		390,480,540	CO, H ₂ , CH ₄	10	[121]
bio-PE		bio-PET				450,500,600	CO ₂ , CO, CH ₄ , N ₂	PET(MP=160°C), PE(GCV=46.06MJ/kg)	[124]

PE	PP	PET	PS	PVC		460,500,600	CO ₂ , CH ₄ , H ₂ , CO, C ₂ H ₆	20		[45]
LDPE		PET			plastic bottle	260	CO ₂ , CH ₄ , CO		GHSV=3000mL/hr.gr	[132]
PE	PP	PET	PS	PVC	MSW & MPW	500,550,600	CO, H ₂ , CO ₂		MSW (HV:27.1 MJ/kg)	[97]
		PET			water bottles	460	CO, CO ₂ , H ₂ , CH ₄	4	PET (CV=214 kJ/kg)	[16]
LDPE	PP					400	CH ₄ , CO ₂ , C ₂ H ₆ , C ₃ H ₈ , C ₄ H ₁₀ , CO	5		[134]
HDPE	PP				Waste polymers	HDPE:408-423/ PP=362-417	CO ₂ , NO _x , SO ₂		Rate react. (PE=2500-3500/ PP=3600-4400 kg/hm ³)	[122]
LDPE, HDPE	PP	PET	PS	PVC		700-900	H ₂ , CO, CO ₂ , CH ₄ , HCl		m=25kg/h	[135]
LDPE, HDPE	PP	PET	PS		MSW	500	H ₂ , C ₂ H ₆ , C ₂ H ₄ , CH ₄ , CO, CO ₂		F=0,5,10,15,20%, HHV (PE:PP:PS= 50:48.5:41.5 MJ/kg)	[38]

2.7.2 Odour Profiling Method to Capture the Evolution of Gas During Pyrolysis by Using Low-Cost Wastewater Analysis Method

Table 2.18
Odorous compound according to plastic type

Plastic Type	Key Odorous Compounds	Odour Characteristics	Chemical Origin
Polyvinyl Chloride (PVC)	Hydrogen chloride (HCl), chlorobenzenes	Acidic, sour, choking	Dehydrochlorination of vinyl groups
Polyethylene Terephthalate (PET)	Benzoic acid, aldehydes (formaldehyde)	Vinegar-like, sharp	Oxidative cleavage of ester bonds
Polystyrene (PS)	Styrene, benzene, toluene	Sweet, pungent, solvent-like	Aromatic ring scission
High Density Polyethylene / Polypropylene (HDPE / PP)	Alkenes, alkanes, light aromatics	Mild gasoline-like	Thermal cracking of saturated chains
Mixed Plastics	Mercaptans, hydrogen sulfide, phenols, carboxylic acids	Cheese-like, faecal, burnt rubber	Synergistic degradation and contamination

In the pyrolysis of plastic waste, gas mitigation processes, such as gas scrubbing, are employed to remove hazardous components from the produced gases. These processes generate wastewater, commonly referred to as pyrolysis aqueous condensate (PAC), which contains a variety of unwanted by-products. The composition of PAC is influenced by the type of plastic feedstock and the operational parameters of the pyrolysis process [140]. Some of the examples of key odorous compound from plastic waste is shown in Table 2.18. These emissions not only compromise environmental safety but also hinder the scalability of pyrolysis technologies in decentralized or resource constrained settings.

To mitigate the release of volatile and potentially hazardous compounds during the pyrolysis of HDPE and PET plastic waste, a water scrubber system serves as an effective post-treatment solution. In this method, the pyrolysis gas stream that is comprising hydrocarbons, oxygenates, and acid gases, is directed into a sealed column containing water or an aqueous solution. The gas is bubbled through the liquid via diffusers or packed media, promoting gas liquid interaction that facilitates the absorption of water-soluble species such as acetic acid, acetaldehyde, CO₂, and HCl. This approach is particularly relevant for PET pyrolysis, which tends to release oxygenated compounds due to its ester linkages [10]. HDPE, being a polyolefin,

contributes more to hydrocarbon rich fractions, but may still emit trace acidic gases depending on additives [141]. The scrubber operates under ambient or slightly cooled conditions to enhance solubility and condensation, and the resulting scrubber wastewater is analysed for pH, COD, BOD, DO, Turbidity and specific contaminants using UV-Vis, HPLC, or GC-MS techniques. This method not only reduces atmospheric emissions but also enables indirect profiling of gas-phase composition through wastewater diagnostics, supporting cleaner pyrolysis system design [10, 141].

PAC comprises a complex mixture of organic and inorganic compounds, including organic acids where the compounds such as acetic acid and formic acid are prevalent in PAC, contributing to its acidity and potential corrosiveness. Phenolic compounds arise from the thermal degradation of aromatic structures within the plastic material and are known for their toxicity and environmental persistence. Aromatic hydrocarbons including benzene, toluene, and xylene, these compounds are hazardous pollutants with significant health implications [11]. Nitrogenous compounds such as ammonia and various nitrogen containing heterocycles result from the breakdown of nitrogenous additives or contaminants in the plastic feedstock [142]. While PAHs have high molecular weight compounds are formed during pyrolysis and are of concern due to their carcinogenic properties [11, 17, 37]. The presence of these substances renders PAC a challenging effluent requiring careful management to mitigate environmental and health risks.

The constituents of PAC pose several environmental and health challenges where discharge of untreated PAC into water bodies can lead to bioaccumulation of toxic compounds in aquatic organisms, disrupting ecosystems [133]. Other than that, land application of PAC without proper treatment can result in the accumulation of hazardous substances, adversely affecting soil health and potentially entering the food chain. Exposure to certain PAC components, such as PAHs and phenolic compounds, is associated with carcinogenic and mutagenic effects, posing significant health hazards [11, 17]. By analysing the characteristic of wastewater, dominant gas species could identify and easy to evaluate. The data would help the industry to monitor the influence of chemical that contribute for higher chemical content from the pyrolysis process. As shown in the Table 2.18, expected characteristics of gas that will be trapped in the wastewater.

Table 2.19
Effect of HDPE:PET Ratios on Pyrolysis By-Products

HDPE:PET Ratio	Dominant Gas Species	Wastewater Characteristics	Synergistic Observation	Ref
100% (Pure HDPE)	CH ₄ , C ₂ H ₆ , C ₂ H ₄	Neutral pH, low COD, low turbidity	Hydrocarbon rich, minimal odour	[10]
75:25	CH ₄ , CO ₂ , Acetaldehyde	Slightly acidic pH (~6), moderate COD, aldehydes present	PET introduces oxygenated	[141]
50:50	CH ₄ , CO ₂ , CO, Acetaldehyde	Acidic pH (~5), high COD, moderate turbidity	Balanced release, elevated organics	[143]
25:75	CO ₂ , CO, Acetaldehyde, CH ₄	Acidic pH (-4.5), high COD/BOD, turbidity increase	PET dominates, strong contamination	[144]
100% (Pure PET)	CO ₂ , CO, Acetaldehyde	Acidic pH (<4.5), high COD, aldehyde, elevated turbidity	Oxygenated gas profile, aldehyde rich wastewater	[145]

For instance, polyethylene-derived PAC exhibited higher toxicity, with concentrations as low as 0.3 g COD/g VSS at 55 °C inhibiting carboxydrotrophic and methanogenic activities by 50% [140]. The wastewater generated from gas mitigation in the pyrolysis of plastic waste contains a complex mixture of unwanted by-products with significant environmental and health implications. Effective management of this effluent is critical to the sustainability and safety of pyrolysis-based plastic waste recycling initiatives.

2.8 Current Countermeasure to Mitigate Hazardous Waste

Efforts in reducing the release of hazardous waste to the atmosphere has aroused attention among people as this issue is very concerning to environment and ecosystems. Researchers have made new studies regarding countermeasures to mitigate hazardous waste. One of the countermeasures is adsorption of CO₂. As we know, CO₂ is the major product released by many industries nowadays. Oreggioni, et al. [146] has proposed the use of Pressure Vacuum Swing Adsorption (PVSA) unit/scrubber for adsorption of

CO₂. This unit is estimated to reduce CO₂ by 49% and is economical compared to another unit as per mentioned in Table 2.19. A small-scale oxygen production Pressure Swing Adsorption unit is deployed to produce pure oxygen required for post-treating the CO₂ product. Another study has been made by Mukherjee, et al. [147] to mitigate formation of polychlorinated dibenzo-dioxins (PCDDs) by using Thiourea. Thiourea contains high S and N which is suitable to inhibit dioxins by reducing the concentration level of dioxins. Thiourea is injected through AC injector with a flowrate of 350L/hr and maintained pressure of the nozzle at 0.50MP. This method is predicted to reduce dioxins by 91% which is very large. Mitigation of CO has involved the application of CO Preferential Oxidation (CO-PROX) reaction by one step synthesis of AuCu/TiO₂. Found that synthesis of AuCu/TiO₂ potentially reduce CO by maximum 98.4% and the catalyst is tested in fixed bed reactor. AuCu/TiO₂ catalyst is chosen for CO-PROX reaction because it exhibited good activities and selective in the range of temperature between 75°C to 100°C and presented better catalytic performance.

Table 2.20

Current countermeasure to mitigate hazardous waste

Gas released	Mitigation/Countermeasure	Equipment	Potential reduction	Author	Year	Ref.
CO ₂	Adsorption	Pressure Vacuum Swing Adsorption (PVSA) unit/Scrubber	49%	Oreggioni, et al. [146]	2015	[146]
SO _x & NO _x	Absorption (consisting of scrubbing process using aqueous acidic solutions in the advantageous presence of hydrogen peroxide which oxidizes irreversibly NO _x and SO ₂ in HNO ₃ and H ₂ SO ₄)	Scrubber	N/A	Liémans and Thomas [149]	2013	[149]
Dioxins	Injection of Thiourea (a suitable dioxin inhibitor with high S and N-content to reduce the concentration level of dioxins)	AC Injector	91%	Mukherjee, et al. [147]	2016	[147]
GHG: CH ₄ & N ₂ O	Biochar Soil Amendment (BSA)(for enhancing stable organic carbon storage with various ecosystem benefits)	Biochar	CH ₄ =26% N ₂ O=16%	Xu, et al. [150]	2019	[150]
NH ₃ & H ₂ S	Adsorption (Pilot-Scale testing of non-activated biochar)	Pilot scale manure storage simulator & non-activated biochar	NH ₃ =12.7-22.6% H ₂ S=12-30% (not significant)	Maurer, et al. [151]	2017	[151]
CO	CO-PROX reaction by one-step synthesis of AuCu/TiO ₂ (catalysts exhibited good activities and selective in the range of 75°-100°C and presented a better catalytic activity)	Fixed bed reactor (catalyst test)	max=98.4%	Alencar, et al. [148]	2020	[148]

2.8.1 Use of wet scrubber in this area for mitigation and the efficient use of wet scrubber

Wet scrubber is an air pollution control device frequently prompted in mitigating hazardous gas released by many industries. Main objectives of using wet scrubber for mitigation is to assemble the particulate matter in liquid droplets and remove harmful materials from industrial exhaust gases. A wet scrubber operates by capturing particulate or gases in the scrubbing liquid/liquid droplets. Water subsequently flows from the bottom of the scrubber and is pumped through spray pipe and liquid droplets are introduced to dirty gas stream. The particulates are allowed to settle and clarified water is circulated.

The innovation of wet scrubber with application of technology is essential to mitigate hazardous gas with high efficiency. Most industries emitting synthetic gas like CO₂ into atmosphere needs to be treated to produce cleaned gas which permits release into the environment. From Table 2.20, Koller, et al. [152] has introduced the use of spray scrubbing with monoethanolamine (MEA) of concentration 30.0wt% as an absorption solvent for CO₂ reduction estimated to mitigate CO₂ by less than 80%. MEA is preferable as solvent for CO₂ capture because it is economical and improves absorption efficiency. Next, NH₃ can be reduced by scrubbing ammonia with the concept of exergy as stated by Zisopoulos, et al. [142]. Sulfuric acid (H₂SO₄) solution is used in this concept of exergy leading to the formation of ammonium sulfate (NH₄)₂SO₄. As the concentration of sulfuric acid solution increases, exergy efficient scrubbing process increases.

The removal efficiency of acid scrubber for ammonia mitigation is estimated to be up to 87%. Si, et al. [153] has proposed new scrubbing technology which is spray-and-scattered bubble technology has efficiency of up to 99% for simultaneous SO₂/Nox removal. Ozone (O₃) is injected by ozonator into flue gas stream at the inlet of spray zone to destroy or neutralize the contaminant or odor. Liquid droplets react with mixed flue gas in a co-current mode and settle at the bottom part of the tower or bubble zone. Cleaned gas free of SO₂/Nox is allowed to release into the atmosphere after separation.

Table 2.21
Use of wet scrubber in this area for mitigation

Synthetic gas	Type of wet scrubber	Efficiency	Ref.
SO ₂	Nozzle Injection Scrubber CFD (Computational Fluid Dynamics)	>90%	[154]
SO ₂ /Nox	Spray-and-scattered bubble technology	up to 99%	[153]
NH ₃	Ammonia scrubbing with the concept of exergy	up to 87%	[142]
CO ₂	Spray scrubbing with monoethanolamine (MEA)	<80%	[152]
Dioxins and furans (PCDD/Fs)	Wet scrubber	71%	[155]

2.9 Synergistic Study to Produce High Quality Pyro-Fuel with Low Emission Side Product

Recent advancements in pyrolysis technology have focused on synergistic approaches to enhance the quality of pyro-fuels while minimizing undesirable emissions. Co-pyrolysis, which involves the simultaneous thermal decomposition of multiple feedstocks, has emerged as a promising strategy in this context.

The integration of biomass with polymeric wastes, such as plastics and rubber, during pyrolysis has demonstrated notable synergistic effects. A comprehensive study by Shahbeik et al. (2023) employed evolutionary machine learning to optimize the co-pyrolysis process of biomass and polymeric materials. The research highlighted that co-processing these feedstocks not only enhances the yield of liquid fuels but also improves their quality by increasing the calorific value and reducing the oxygen content. Moreover, the study emphasized that careful selection of feedstock ratios and process parameters is crucial to suppress the formation of harmful by-products, thereby achieving a cleaner pyrolysis process [156].

Catalytic pyrolysis has been explored to further refine pyro-fuel quality and reduce emissions. Ranizang et al. (2023) investigated the catalytic pyrolysis of fuel oil blended stock using a Ni/ZSM-5 catalyst. The study revealed that incorporating a small amount of nickel into the catalyst significantly increased the production of valuable gases, such as methane and hydrogen, while minimizing the generation of undesirable

by-products. This catalytic approach not only enhances fuel quality but also contributes to a reduction in emission-related pollutants [157].

The co-pyrolysis of diverse materials, including biomass, plastics, and waste tires, has been shown to produce synergistic effects that improve pyro-fuel yields and quality. Singo et al. (2025) conducted a study on the co-pyrolysis of waste tires, plastics and biomass, demonstrating that the combined processing of these materials leads to an enhanced production of pyro-oil with improved properties. The research highlighted that the synergistic interactions between the different feedstocks contribute to a more efficient breakdown of materials, resulting in higher-quality fuel outputs and reduced emission of harmful by-products [158].

The complexity of co-pyrolysis processes necessitates advanced optimization techniques. Chakrabarti and Shinde (2024) utilized machine learning algorithms to analyse the synergistic effects during the co-pyrolysis of algae and wood biomass. Their three-phase analysis demonstrated that machine learning models could accurately predict biochar yields and optimize process parameters, thereby enhancing fuel quality and reducing emissions. This approach underscores the potential of integrating artificial intelligence into pyrolysis research to achieve superior outcomes [159].

Synergistic strategies in pyrolysis, particularly through co-processing diverse feedstocks and employing catalytic methods, have shown significant potential in producing high-quality pyro-fuels with reduced emissions. The integration of machine learning techniques further enhances the optimization of these processes, paving the way for more efficient and environmentally friendly pyrolysis technologies.

2.9.1 Combination of Critical Parameters and Pollutants Emitted to Produce High Quality Pyro-Fuel

The production of high-quality pyro-fuel through pyrolysis is significantly influenced by critical operational parameters, which also affect the emission of pollutants. Optimizing these parameters is essential to enhance fuel quality while minimizing environmental impacts. Pyrolysis temperature is a pivotal factor determining the composition and quality of the resulting pyro-fuel. Elevated temperatures generally increase the yield of gaseous products at the expense of liquid yields. However, excessively high temperatures can lead to the formation of undesirable by-products, such as PAHs, which are environmental pollutants. Therefore, maintaining

an optimal temperature range is crucial to balance fuel quality and emission control [11].

The rate at which temperature is increased during pyrolysis affects the thermal decomposition of feedstock. Rapid heating rates can enhance the production of liquid pyro-fuels with lower viscosity and higher calorific value. Conversely, slow heating rates may favour char formation and can lead to incomplete pyrolysis, resulting in higher emissions of VOCs and other pollutants. Thus, optimizing the heating rate is essential for producing high-quality pyro-fuel with reduced emissions [11].

The duration for which the feedstock remains in the pyrolysis reactor, known as residence time, influences the extent of thermal degradation. Shorter residence times may lead to incomplete pyrolysis, increasing the emission of pollutants such as CO and VOCs. In contrast, excessively long residence times can promote secondary reactions that degrade fuel quality. Therefore, an optimal residence time must be established to ensure complete pyrolysis while maintaining high fuel quality. The inherent properties of the feedstock, including moisture content, ash content, and the presence of contaminants, significantly impact both pyro-fuel quality and pollutant emissions. Feedstocks with high moisture content require additional energy for drying, which can reduce process efficiency and increase CO₂ emissions. High ash content can lead to the formation of particulate matter during combustion. Pre-treatment processes, such as drying and contaminant removal, are therefore essential to improve fuel quality and reduce emissions [11].

The primary pollutants emitted during pyrolysis include PM, VOCs, PAHs, CO, NO_x, and SO₂. The concentrations of these pollutants are influenced by the operational parameters. For instance, suboptimal temperatures or incomplete pyrolysis can result in elevated VOC and CO emissions. Implementing gas cleaning and filtration systems, such as electrostatic precipitators and cyclone separators, can effectively reduce particulate emissions. Additionally, catalytic converters can be employed to lower NO_x and CO levels, thereby mitigating the environmental impact of pyrolysis processes [11]. The production of high-quality pyro-fuel with minimal pollutant emissions necessitates the careful optimization of operational parameters, including temperature, heating rate, residence time, and feedstock composition. By fine-tuning these factors and incorporating appropriate emission control technologies, it is possible to enhance fuel quality while adhering to environmental standards.

2.9.2 Properties of Pyro-Fuel from Synergistic Study

Recent research has explored the co-pyrolysis of biomass residues with plastic waste, revealing significant synergistic effects that enhance the properties of the resulting pyro-fuel. A study by Hongthong et al. (2024) investigated the co-pyrolysis of sawdust and hardwood biomass with polypropylene (PP) waste. The findings demonstrated that incorporating 20% PP with wood at 300°C produced a solid char with a yield of 40% by weight. This co-pyrolysis process resulted in biochar with improved properties, including increased surface area, carbon content, hydrophobicity, and aromaticity [160]. These enhancements contribute to higher calorific values, making the biochar a more efficient fuel source.

Additionally, the improved characteristics of the biochar significantly enhanced its capacity to adsorb heavy metals, indicating potential applications in environmental remediation. The synergistic interactions between biomass and plastic components during co-pyrolysis were credited for these improvements, leading to the production of fewer volatile products at elevated temperatures. This study underscores the potential of co-pyrolysis as a strategy to valorise waste materials into valuable and eco-friendly fuel products [161].

2.10 Wastewater Generation and Profiling in Plastic Pyrolysis Processes

Thermal conversion processes such as pyrolysis and mild pyrolysis inevitably generate liquid by-products in addition to pyrolytic oil and gaseous products. These liquid streams may consist of condensed organic compounds, aqueous phases, and process wastewater originating from condensation, washing, or quenching stages of the pyrolysis system. The characterization and profiling of such wastewater are essential for understanding the overall product distribution and environmental implications of plastic pyrolysis processes. Most plastic pyrolysis trains cool hot vapours immediately with water-based quench or water-cooled condensers, which inevitably generates an aqueous phase (often alongside organic condensate). Process designs from lab to pilot to industrial scale include explicit vapour quench [50] and water cooled condensation steps [162] so contact between pyrolysis vapours and water is routine.

HDPE cracking yields predominantly aliphatic hydrocarbons (C₅–C₂₅), olefins and wax which are largely hydrophobic but lighter oxygenates and dissolved gases can

dissolve to small extents and emulsified droplets can form under shear that raising value of Chemical Oxygen Demand (COD) and turbidity. Recent pilot and process scale studies show HDPE pyrolysis oils are rich in linear hydrocarbons with trace metals and additives from end-of-life plastics such as compositions favour phase separation but not zero water impact [163]. While PET behaves very differently where it is an oxygenated polyester. Under pyrolysis or steam assisted conditions it produces benzoic acid, terephthalic acid (TPA), ethylene glycol (EG) and other oxygenates which are water soluble and acidic so they strongly impact pH, COD and Biochemical Oxygen Demand (BOD) of the contacted water. Recent research documented that benzoic acid dominance and the role of steam and hydrolysis pathways yielding TPA and EG and lowering pH [164-166]. Aqueous streams in plastic pyrolysis facilities therefore tend to accumulate dissolved acids and glycols for PET plastic waste, emulsified hydrocarbons for HDPE plastic waste, light volatiles and suspended char fines each mapping directly to common wastewater [50].

Dissolved organics such as benzoic acid, terephthalic acids, EG, and aldehydes from PET plastic waste and emulsified aliphatic and light oxygenates from HDPE plastic waste entrained in the aqueous phase at low but impactful concentrations giving high COD if released to water [164]. Process schematics and life cycle assessment (LCAs) for mixed plastic pyrolysis include vapor quench and condensation stages that intentionally separate organics and water acknowledging that the aqueous side contains oxidizable content that must be treated [167]. It is expected that COD values will be higher in quench and condensate waters containing high PET content. Once measured, COD becomes a binding parameter for those facilities that require Advanced Oxidation Process (AOP) or enhanced biological binding [168]. Ethylene glycol and low molecular weight oxygenates which is PET are readily biodegradable while long chain aliphatic droplets which is HDPE are less biodegradable. Therefore, wastewater containing PET may show high BOD or COD ratios, while emulsions containing HDPE will result in lower BOD or COD. Studies on the hydrolysis process of PET have shown the formation of TPA, EG and benzoic acid in which these compounds increase the oxygen demand during biological oxidation [165, 169].

The pH of PET is expected to be low due to the presence of benzoic acid and terephthalic acid in the aqueous phase, both of which are weak acids. However, observation of their concentrations can lead to a pH value in the neutral range [164]. For HDPE, the oil content is not acidic. However, the appearance of carboxylates from

the oxidation of condensates and CO₂ dissolution from off gas can slowly lower the pH value [170]. Several mechanisms have been found to reduce the value of Dissolved Oxygen (DO) such as high BOD or COD values in a tank. In addition, oil films and emulsions have prevented aeration from occurring and hot effluent from condensation can reduce oxygen solubility. Therefore, it is ecologically proven that the effect of DO is due to high oxygen demand in wastewater. In addition, aeration control is essential to maintain DO values in the biological stage to treat the waste [171].

Turbidity can be caused by several reasons such as oil-in-water emulsions especially during HDPE condensation, fine carbon particles and acid salts precipitated from acid neutralization of PET derivatives. Apart from that, quench and condense hardware and shear conditions also promote emulsification and thus increase the turbidity level. The main sources of TSS are char fines trapped in the reactor or transfer line and demulsified droplets or scale in the quench loop. Pyrolysis systems often include cyclones or filters to prevent solids from condensing. However, char fines still appear in the quench water and must be removed to protect downstream treatment. Solids polishing is advisable to ensure that TSS is within permit limits [172].

Mild pyrolysis operates at lower temperatures and therefore produces more oxygenated liquids and fewer gases, especially for oxygen rich polymers like PET. This increases the risk of transferring partially oxidized and water soluble compounds into quench or condensation water. For PET, mild pyrolysis strongly favours benzoic acid and other oxygenates and increasing potential aqueous solubility and COD [164, 172]. For HDPE, mild conditions reduce secondary cracking which leaving more waxy and long chain compounds. These are hydrophobic, but under water quench conditions they can form stable emulsions, raising turbidity and oily COD. Although HDPE is less reactive than PET, lower temperature pyrolysis increases liquid or oil yields and prolongs residence of oxygenated trace contaminants that can partition to water. From the research of pilot scale mild HDPE, it shows the shift toward linear hydrocarbons and oxygenated contaminants in end of life HDPE feeds [170].

2.11 Concluding Remark

In conclusion, this chapter has critically reviewed the current body of knowledge on plastic waste pyrolysis, with particular emphasis on the challenges of pollutant emissions, the variability of fuel quality, and the role of process parameters in determining product outcomes. The review highlighted that while pyrolysis holds significant promise as a sustainable waste-to-fuel pathway, its effectiveness is often constrained by inconsistent yields, hazardous by-products, and limited understanding of synergistic effects in mixed plastic feedstocks.

The discussion further identified wastewater profiling as an underexplored but potentially valuable tool for odour and emission diagnostics, offering a practical alternative to more costly and complex analytical techniques. This insight establishes a clear knowledge gap that the present study seeks to address by combining slow pyrolysis, wastewater-based emission analysis, and comprehensive pyro-fuel evaluation into a unified methodological framework. The next chapter will therefore outline the research methodology designed to fill these gaps, providing a systematic approach for experimental implementation, data collection, and analytical interpretation.

CHAPTER 3

RESEARCH METHODOLOGY

This chapter describes the techniques used for obtaining and preparing raw materials for chemical and physical characterisations, heat treatment of samples by using Bomb Calorimeter, TGA and GC-MS. The sample will be decomposed using a pyrolysis plant. The result will be analysed using Bomb Calorimeter, TGA and GC-MS. The gas produced after the pyrolysis process will be analysed in terms of water quality, DO (Dissolved Oxygen), Turbidity, COD, BOD, pH and TSS (Total Suspended Solid). All experimental measurements were subjected to systematic error and uncertainty analysis, as detailed in Section 3.6 to ensure reliability and statistical validity of the results

3.1 Raw Materials Preparation and Analysis

3.1.1 Raw Materials Preparation (HDPE and PET Samples)

Raw material plastic waste has been taken from the plastic waste being dumped in a student dormitory and staff quarters of IKM Bintulu and waste recycling site in Bintulu Airport. Plastic materials will be sorted and separated according to the type of plastic. This study will use two types of plastics, which are PET and HDPE as per Figure 3.1.



HDPE plastic waste sample

PET plastic waste sample

Figure 3.1: HDPE and PET plastic sample

3.1.1.1 Preparation of Raw Materials for Pyrolysis according to its Mixing Ratio

Figure 3.2 shows the overview of the steps taken to prepare sample for analysis. Samples obtained were air dried for one day for moisture removal. The samples were then has been cut into small particle. The sample will be stored in a container where it will be used for analysis in the laboratory analyses such as different substances, proximate and calorimetric.

Raw material is dried all day

Raw material cutting and dividing

The sample is cut into small pieces to make a powder



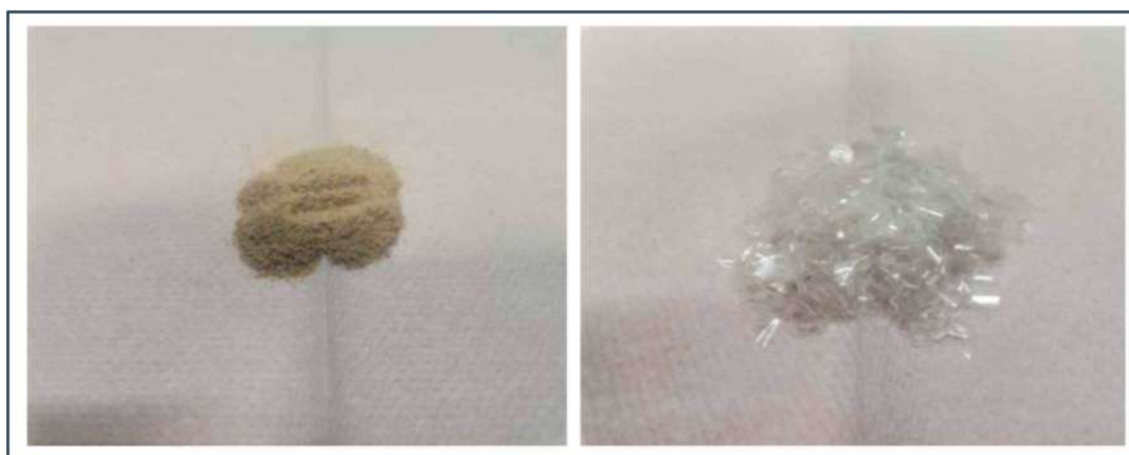
Samples are stored in containers for further analysis

Figure 3.2 Flow diagram of procedure used to prepare raw material for analysis

Raw material and Mixing ratio used in this study are pure HDPE, pure PET, ratio 2HDPE:1PET, ratio 1HDPE:1PET and ratio 1HDPE:2PET. Ratio 2HDPE:1PET and Ratio 1HDPE:2PET were chosen to compare if the quantity of HDPE exceeds PET, will it affect the pyrolysis process and vice versa. Similarly, when the ratio 1HDPE:1PET is chosen, it shows an equal amount of weight, will it also affect the pyrolysis process. After conducting experiments on these five types of ratios, the resulting data will be compared to see whether pure raw material is better or mixing ratio is better.

3.1.1.2 Preparation of Raw Materials for Analysis Its Content

To obtain raw materials to carry out analysis such as Proximate Analysis, Elemental Analysis and so on, the plastic waste that has been obtained has been cut into small pieces until it becomes a powder as shown in Figures 3.3.



HDPE plastic waste powder

PET plastic waste powder

Figure 3.3: HDPE and PET plastic waste powder

3.1.2 Physical Characterisation of Raw Materials

Characterizing the physical and chemical properties of plastic waste raw materials is essential for optimizing pyrolysis, improving product yield, and minimizing environmental impact.

3.1.2.1 Particle Size

ANESOK® 315W 2000X Wifi Handheld Digital Microscope is used in this research to determine particle size in raw plastic waste as per shown in Figure A. 2a. The plastic sample will be placed on the plate under the microscope, and the sample picture will be taken through the camera on the MacBook Air Model M1. Particle sizes will be measured according to ASTM D1921 standards for particle size distribution.

3.1.2.2 Density

Electronic Digital Precision Brand A&D Model MD-300S as per shown in Figure A. 2b has been used in this research to get density for each sample ratio of plastic waste. The sample will be placed on the densimeter's upper weighing pan and the weight displayed is record (W_{air}). The sample will submerge in the distilled water using the appropriate holder to prevent contact with the tank's sides or bottom. It has been ensured that there are no air bubbles appearing on the sample surface as they can affect buoyancy measurements. The displayed submerged weight (W_{water}) is record. The densimeter automatically calculates the sample's specific gravity (density) using the formula:

$$\text{Density, } \rho \text{ (g/cm}^3\text{)} = \frac{W_{air}}{W_{air} - W_{water}}$$

The result is displayed directly on the densimeter's screen.

3.1.2.3 Moisture Content

Moisture Content (MC) is one of the important properties that exist in plastic waste samples. Moisture content is the number of water molecules found in the plastic waste sample. The sample is put into a crucible and weighed. Then the sample with the crucible will be put into the Memmert Wisconsin Oven as in Figure A. 2b. at a temperature of 110°C for 16hrs. After that, the crucible containing the sample will be put into a desiccator for about 30 minutes. Then, the crucible will be weighed again and its weight recorded. Moisture Content % is calculated using the formula (1). The same procedure is also done for other samples.

$$\% \text{ Moisture Content}^{Li} = \frac{m_1 - m_0}{m_1 - m_0} \times 100 \quad (1)$$

Where:

m_0 = Empty crucibles weight (g)

m_1 = Crucibles weight with sample (g)

m_2 = Crucible weight with sample after heating (weight of moisture) (g)

3.1.2.4 Melting Point

Digital Melting Point brand Stuart model SMP10 has been used as per Figure A. 2d. The Capillary Tube Red Tip G0553 will be heated to sealed one of the tube holes. The sample will put in Capillary Tube and insert it in one of the holes provided on the heater stand in digital melting point. The set point will be set up as per require value and the ramp is activated and the temperature now increases linearly at the much slower ramp rate, during which time the melt analysis takes place. The melting of the sample is observed and the temperatures registered via the keypad at the appropriate time.

3.1.3 Chemical Characterisation of Raw Materials

3.1.3.1 Proximate Analysis

Proximate Analysis of plastic waste is a simple way to determine the quantity of substances found in a material. To ensure the quality of the material, several tests such as the determination of moisture content, volatile matter, ash content and fixed carbon need to be done where in this study, the ASTM E870-82 standard has been used [173-175]. To obtain the value, 1.5g sample of the plastic waste for each ratio was weighed using a Mettler Toledo Analytical Balance as shown in Figure A. 2e. The sample was weighed into five types of measurement, namely FIDPE, ratio FIDPE 2: 1 PET, ratio HDPE 1:1 PET, ratio HDPE 1:2 PET and PET as shown in Figure A. 2fi The calculation of moisture content will use the procedure as in para 3.1.2.1.3 Moisture Content.

Volatile matter (VM) is a substance that will continue to burn when oxygen is present in it. The determination of volatile matter is very important in showing that a substance is flammable. Common substances found in Volatile matter are hydrocarbons, hydrogen, CO, CO₂, CH₄, H₂O and SO₂. It can also prove that if the content is high, the material is easy to process and will produce more liquid [175]. Therefore, to obtain the value of volatile matter, the sample obtained in determining the moisture content was used again in this experiment. The closed crucibles containing the samples were put into the Muffle Furnace Fisher Scientific Model 550-126 as shown in Figure A. 2g and will be heated at a temperature of 900°C for 10 minutes. Then the

crucibles will be put in a desiccator for about 30 minutes. Volatile Matter % is calculated using the formula (2). The same procedure is also done for other samples.

$$\% \text{ Volatile Content} = \frac{m_2 - m_1}{m_1 - m_0} \times 100 \quad (2)$$

Where:

m_0 = Empty crucibles weight (g)

m_1 = Crucibles weight with sample (g)

m_2 = Crucible weight with sample after heating (weight of moisture) (g)

m_3 = Crucible weight with sample after heating (weight of volatile matter) (g)

Ash Content (AC) indicates the non-combustible material remaining after the sample has burned completely. If a material produces a high %ash content, it will produce a high char after the pyrolysis process. To obtain the value of ash content, the sample obtained in determining the volatile matter was used again in this experiment. The uncovered crucibles containing the samples were put into the Muffle Furnace Fisher Scientific Model 550-126 and heated at a temperature of 585°C for 3 hours. Then the crucibles will be put in a desiccator for about 30 minutes. Volatile Matter % is calculated using formula (3). The same procedure is also done for other samples.

$$\% \text{ Ash Content} = \frac{m_4 - m_0}{m_1 - m_0} \times 100 \quad (3)$$

Where:

m_0 = Empty crucibles weight (g)

m_1 = Crucibles weight with sample (g)

m_4 = Crucible weight with sample after heating (weight of ash) (g)

Fixed carbon (FC) is the last solid residue left after combustion which is a flammable material after the material is heated and removes the volatile matter of the material. Once MC, VM and AC have been obtained, the FC value can be obtained by using equation (4). All values obtained are in percentage.

$$\% \text{ Fixed Carbon} = 100 - (\text{MC} + \text{VM} + \text{AC}) \quad (4)$$

3.1.3.2 Ultimate Analysis

Ultimate analysis of plastic waste raw materials is crucial for understanding their composition and potential for pyrolysis. Elemental analysis of plastic waste raw materials provides essential data to tailor pyrolysis processes effectively, optimize resource recovery, and minimize environmental impact through efficient waste management strategies.

By using Elemental Analyzer model Thermo Electron, Flash EA 1112 Series, the content of carbon, hydrogen, nitrogen, sulphur and oxygen in the sample is determined as shown in Figure A. 2h. The graph obtained from this tool will produce the percentage of carbon, hydrogen, nitrogen and sulphur from the sample tested, while the oxygen content is obtained by subtracting 100 from the amount of carbon, hydrogen nitrogen sulphur and oxygen obtained from the graph. Approximately 1mg of sample was weighed using a Mettler Toledo Analytical Balance. The sample is wrapped in an aluminium foil container and placed in the sample tray. Next, the sample will be put into the reaction chamber, and it will take 20 minutes for the analysis to be completed.

3.1.3.3 Calorimetric Analysis

Calorimetric analysis is the determination of the gross heating value of a fuel. It measures the heat created by a sample when it is burned under oxidative atmosphere in a closed reactor that is surrounded by water and in controlled conditions. In this study, the calorific value analysis was performed using Bomb Calorimeter model PARR 6400 as per Figure A. 2i.

A sample weighed about 1g was put into a crucible, which was then put into a stainless-steel container. Before putting the crucible into the stainless-steel container, a cotton string is placed inside the crucible, which is tied to the ignition wire inside the container. The container is put into the combustion chamber. Combustion occurs when the sample is ignited through a cotton string connected to an ignition wire. Measurements are taken from the energy content value produced at the end of the experiment and combustion will take 15 minutes to produce results. Combustion of the pyrolytic oil was done in control environment inside the bomb and according to the ASTM D240.

3.1.3.4 TGA/DSC

Figure A. 2j shows the instrument used for determination of proximate analysis. It is a thermogravimetric analyser model TGA/DSC 1 manufactured by Mettler Toledo. In a 150ul crucible, a measured sample of 20mg was placed in the sample holder of the TGA furnace. The sample was subject to a dynamic temperature-heating programme from 25 - 1000°C, at heating rate of 10°C/min under nitrogen atmosphere with a constant flow rate of 20mL/min. Upon completion, the sample was then subjected to combustion process using purified air of a constant flow rate of 20mL/min to temperature of 1100°C at the same heating rate of 10°C/min. Thermogravimetric curve produced from the above was analysed for the moisture, ash, volatile matter and fixed carbon assays.

3.1.3.5 Fourier Transform Infrared Spectrophotometer (FTIR)

Fourier Transform Infrared Spectroscopy (FTIR) is an advanced analytical technique used to identify and characterize chemical compounds based on their interaction with infrared (IR) radiation. It is widely employed in various scientific fields, including chemistry, materials science, pharmaceuticals, and environmental analysis, due to its ability to detect functional groups and molecular structures in organic and inorganic materials. In this research, FTIR Perkin Elmer Spectrum 1 has been used to get the FTIR spectrum as per Figure A. 2k. In this analysis, each run uses approximately 1mg where the sample is placed on a sample tray and pressed using a stainless steel press at approximately 50 to 60 psi. Then, a modulated IR beam interacts with the sample, where specific wavelengths are absorbed based on the molecular bonds present. The transmitted or reflected IR signal is detected and processed using fourier transform to generate an absorption spectrum

3.2 Synergistic Pyrolysis Process of Plastic Waste

3.2.1 Equipment Set-Up for Pyrolysis

There were six types of equipment used in this experiment, namely a nitrogen gas cylinder, LPG cylinder, pyrolysis reactor, gas stove, condenser, and gas collection tank, as shown in Figure 3.4 and Figure A. 21. Nitrogen gas was used to purge the pyrolysis reactor at the start of each experimental run. The LPG cylinder supplied fuel to ignite the gas stove and provide direct heating to the reactor. The gas flow to the stove was controlled using a MILUX M-168F LPG gas regulator, with a rated flow rate of 2 kg per hour and an outlet pressure ranging from 2.8 to 3.5 kPa. The stainless-steel pyrolysis reactor served as the main vessel in which the pyrolysis process occurred, and a gasket was placed on the reactor cover to prevent gas leakage during operation. The reactor was positioned on the gas stove so that heating occurred directly from the flame. The condenser was used to cool the pyrolysis vapours and convert condensable vapours into liquid (pyro-fuel). The gas collection tank was used to channel non-condensable gases into water, and the resulting water was later analysed to evaluate changes in water quality due to gas absorption

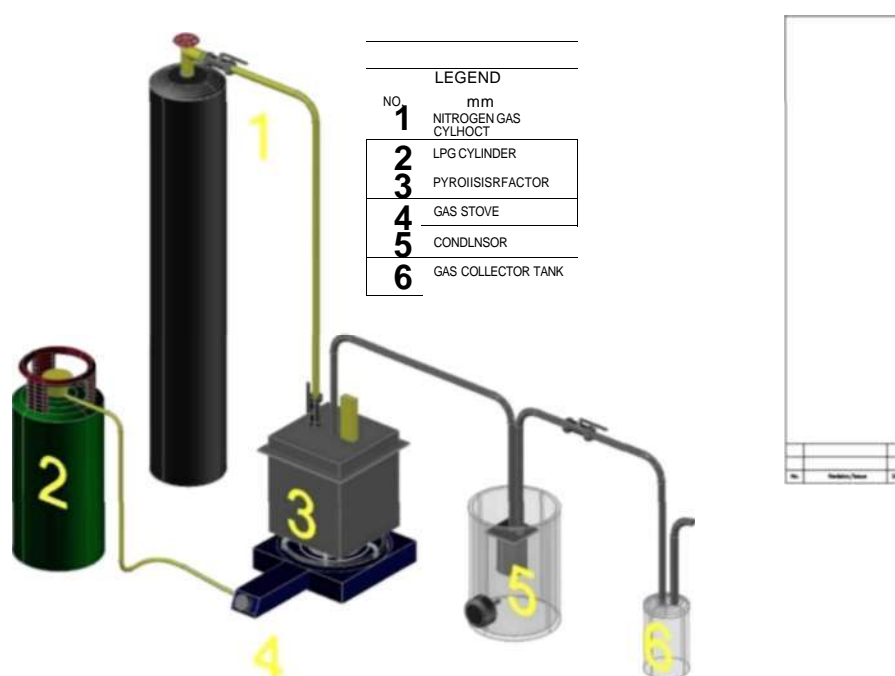


Figure 3.4 Pyrolysis mini plant schematic diagram

3.2.2 Parameter Selection for Pyrolysis

In this experiment, the study was taken to determine the time required for a change to occur in the yield tank. At the same time, the temperature will be taken when the change occurs. The parameters tested are as in Table 3.1

Table 3.1
Propose Parameter for Plastic Pyrolysis

No	Ratio Raw Material	Weight of Raw Material		
		PET	HDPE	Total Weight
1	PET	300 g	-	300 g
2	HDPE	-	300 g	300 g
3	1 PET : 2 HDPE	100 g	200 g	300 g
4	1 PET : 1 HDPE	150 g	150 g	300 g
5	2 PET: 1 HDPE	200 g	100 g	300 g

3.2.3 Process Sequence and Method of Pyrolysis

Experiment is arranged as follow; 600g as per proposed parameter in Table 3.1 was used in the experiment and fed into the pyrolysis reactor, tightly closed, and purged with nitrogen gas at the start of each experiment for 10 min. The water contained in the compressor will be placed at a temperature of 20°C. Gas collector tank will be ensured to bubble to indicate that the system is not clogged. After 10 minutes have elapsed, the nitrogen gas will be shut off while the flame from the stove which is sourced from the LPG cylinder will be ignited. The temperature on the pyrolysis reactor will be taken every 5 minutes and the temperature on the compressor will be kept at 20°C. The experiment will run for up to one hour and 30 minutes or until the resulting liquid has been fully produced. This experiment was carried out 2 more times to get an average reading of 3 readings. Data collection is going to collect in two separate phases which are in liquid product and solid product. The water in the gas collector tank will be taken and analysed to determine the quality of the water by using DO (dissolved oxygen), turbidity, COD, BOD, pH and TSS (total suspended solid) analysis.

3.2.4 Thermal Degradation Behaviour Analysis during Pyrolysis Process

In this study, thermal degradation behaviour during the pyrolysis of HDPE and PET feedstocks was systematically analysed using TGA and DTG techniques. Key indicators such as T_{onset} , T_{peak} , and T_{offset} were determined to elucidate the decomposition dynamics. For PET, TGA analysis revealed a single-stage degradation process beginning around 370 °C, peaking near 441 °C, and completing by approximately 502 °C, consistent with data reported by Alhulaybi & Dubdub (2023) [176]. When considering polymer blends, mixed thermoplastics undergo varied degradation mechanisms which are PET and PA primarily degrade via ionic intramolecular processes, in contrast to the radical chain scission mechanisms dominant in polyolefins like HDPE [177]. Additionally, structural plastics such as PET demonstrated elevated carbon residue and distinct cracking pathways evidencing the role of polymer structure in influencing both degradation profile and product yields [178]. The TGA-derived profiles were further utilised to extract kinetic parameters, serving as inputs for modeling activation energy and reaction mechanisms under slow pyrolysis conditions. This comprehensive thermal degradation analysis establishes the experimental foundation for correlating process conditions with yield patterns, emissions, and pyro-fuel quality.

3.3 Odour Profiling to Determine the Level of Contamination by Using Low-Cost Wastewater Analysis

3.3.1 Method Analysis On The Wastewater Converted From Gas Released During The Pyrolysis Process Of Plastic Waste

3.3.1.1 DO (Dissolved Oxygen)

Dissolved oxygen (DO) is the amount of oxygen that is present in water. Water bodies receive oxygen from the atmosphere and from aquatic plants. Running water, such as that of a swift moving stream, dissolves more oxygen than the still water of a pond or lake. All aquatic animals need DO to breathe. Low levels of oxygen (hypoxia) or no oxygen levels (anoxia) can occur when excess organic materials, such as large algal blooms, are decomposed by microorganisms. During this decomposition process, DO in the water is consumed. Low oxygen levels often occur in the bottom of the water column and affect organisms that live in the sediments. In some water bodies, DO levels fluctuate periodically, seasonally and even as part of the natural daily ecology of the aquatic resource. As DO levels drop, some sensitive animals may move away, decline in health or even die.

In this study, the equipment used to measure DO is a portable Dissolved Oxygen Meter Model FIVEGO F4 brand Mettler Toledo as per Figure A. 2m. The sample will be placed in a 100ml beaker. The rod containing the sensor will be dipped into the liquid being studied and ensured that it is submerged and not in contact with the bottom of the beaker. The DO reading is read on the screen on the Portable DO meter and is read in mg/l units.

3.3.1.2 Turbidity

Turbidity is the measure of relative clarity of a liquid. It is an optical characteristic of water and is a measurement of the amount of light that is scattered by material in the water when a light is shined through the water sample. Turbidity makes water cloudy or opaque. High concentrations of particulate matter affect light penetration and ecological productivity, recreational values, and habitat quality, and cause lakes to fill in faster. In streams, increased sedimentation and siltation can occur,

which can result in harm to habitat areas for fish and other aquatic life. Particles also provide attachment places for other pollutants, notably metals and bacteria. For this reason, turbidity readings can be used as an indicator of potential pollution in a water body.

In this study, the equipment used to measure turbidity is a portable turbidity meter model EUTECH TN100 brand EUTECH/USA as per Figure A. 2n. The liquid sample will be placed into the sample vial to the same level as the align index mark. Wipe the sample vial with a wiping cloth to ensure that fingerprints do not stick to the glass. The sample vial will be inserted into the sample well located on the turbidity meter and pressed until it is fully snapped in. The vial is closed with a light shield cap. Turbidity reading can be read by looking at the turbidity screen in the Ntu unit.

3.3.1.3 Chemical Oxygen Demand (COD)

Chemical Oxygen Demand (COD) is a test that measures the amount of oxygen required to chemically oxidize the organic material and inorganic nutrients, such as Ammonia or Nitrate, present in water. COD is measured via a laboratory assay in which a sample is incubated with a strong chemical oxidant for a specified time interval and at constant temperature (usually 2 h at 150°C). The most used oxidant is potassium dichromate, which is used in combination with boiling sulphuric acid. It is important to note that the chemical oxidant is not specific to organic or inorganic compounds, hence both these sources of oxygen demand are measured in a COD assay. Furthermore, it does not measure the oxygen-consuming potential associated with certain dissolved organic compounds such as acetate.

The reactor digestion method that uses the standard introduced by the US EPA has been used to evaluate the chemical oxygen demand (COD) by using COD digestion vials HR within a range of 20 to 1500 mg/L as stated in Standard Method 5220D. This analysis uses a Cole Parmer COD Reactor (Digital Reactor Block) model DRB200 and Spectrophotometer model DR2800 as per Figure A. 2o to obtain the COD value of the sample. This step is used to obtain an accurate COD value within the specified range. When the COD sample concentration exceeds its measurement capabilities, the sample will be diluted with distilled water.

3.3.1.4 Biochemical oxygen demand (BOD)

Biochemical oxygen demand (BOD) is the amount of dissolved oxygen (DO) needed by aerobic biological organisms to break down organic material present in each water sample at certain temperature over a specific time. The BOD value is most expressed in milligrams of oxygen consumed per litre of sample during 5 days of incubation at 20 °C and is often used as a surrogate of the degree of organic pollution of water. BOD reduction is used as a gauge of the effectiveness of wastewater treatment plants. BOD of wastewater effluents is used to indicate the short-term impact on the oxygen levels of the receiving water.

The reactor digestion method that uses the standard introduced by the US EPA has been used to evaluate the biochemical oxygen demand (BOD) as stated in Standard Method 5210B. This analysis uses Velp Scientifica BOD Bottle and BOD Incubator FOC2251 as per Figure A. 2p to obtain the BOD value of the sample. The sample was put into a 60ml BOD bottle and then put into a BOD Incubator for 5 days. Then the sample will be put into a beaker to get the DO value by using a Portable Dissolved Oxygen Meter.

3.3.1.5 pH

The term "pH" refers to the measurement of hydrogen ion activity in the solution. Determination of pH plays an important role in the wastewater treatment process. Extreme levels, presence of particulate matters, accumulation of toxic chemicals and increasing alkalinity levels are common problems in wastewater. As a chemical component of the wastewater, pH has direct influence on wastewater treatability regardless of whether treatment is physical/chemical or biological. Because it is such a critical component of the makeup of the wastewater, it is therefore critically important to treatment. Portable pH Meter model FIVEGO F2 as per Figure A. 2q. was used to test the sample. The sample will be put into the beaker, and the pH reading will be read on the pH meter by placing the rod into the beaker.

3.3.1.6 Total Suspended Solid (TSS)

TSS are the dry weight of suspended particles, that are not dissolved, in a sample of water that can be trapped by a filter that is analysed using a filtration apparatus. It is a water quality parameter used to assess the quality of a specimen of any type of water or water body, ocean water for example, or wastewater after treatment in a wastewater treatment plant. Total dissolved solids are another parameter acquired through a separate analysis which is also used to determine water quality based on the total substances that are fully dissolved within the water, rather than undissolved suspended particles.

The filter paper will be placed on top of the Porcelain Funnel Buchner as per Figure A. 2r. The liquid sample will be poured into the funnel Buchner and the vacuum pump will be turned on to suck the liquid that is still on the filter paper. Once found to be dry, the filter will be weighed to obtain the weight obtained. Then the filter paper will be put in a drying oven model Ecocell brand BMT for 2 hours. Then the filter paper will be reweighed to get the final TSS value obtained.

3.3.2 Basic Analysis of Gaseous Product in Pyrolysis

The pyrolysis of plastic waste involves the thermal degradation of polymers at elevated temperatures in the absence of oxygen. This process generates various gaseous by-products, including flammable, toxic, and potentially hazardous compounds. The use of a portable gas detector is crucial in ensuring operational safety, environmental compliance, and process efficiency. In this research, Multi Gas Detector Leakage brand UNI-T model UT334G as shown in Figure A. 2s. has been used to detect %LEL, O₂, H₂S and CO of air quality.

3.4 Pyrolytic Oil Quality Evaluation (Physical and Chemical Properties)

3.4.1 Yields of Pyro-fuel

Percentage of yields is an important indicator for the experiment because it will indicate the optimum condition for all parameter tested. Ultimate product yields target for this research is in the liquid because it can be future alternative fuel.

3.4.2 Physical Characterisation of Pyro Fuel

3.4.2.1 Flash Point

In this experiment, Magnetic Stirrer brand Joanlab model HS-12 and Infrared Thermometer brand Benetech model GM320 as per Figure A. 2t. has been used to determine flash point of pyro fuel of plastic waste. The sample pyro fuel will be put in the crucible. The crucible will put on aluminium countertop of magnetic stirrer. When the switch is on, the temperature of stirrer will increase by increase the thermostat knob on heating section of control panel. The pyro fuel temperature in the crucible will be taken using an infrared thermometer. At the same time, the pyro fuel in the crucible will be ignited using a long nozzle lighter. If the fire does not ignite, the temperature will be increased by moving the thermostat knob higher. When the fire is lit, the temperature recorded on the infrared thermometer is the flash point value of the pyro fuel. This method uses the ASTM D92 standard.

3.4.2.2 Density

Density of pyro-fuel is determined by using Glass Hydrometer brand Bo Li Fu Ji as per Figure A. 2u. with range of 0.700 to 1.00g/ml. The technique used to determine density of pyro-fuel is determined according to ASTM D1298

3.4.2.3 Calorimetric Analysis

To know the calorific value of the pyro-fuel, the calorific value analysis was performed using Bomb Calorimeter model IKA C2000 BASIC as per Figure A. 2v. Combustion of the pyrolytic oil was done in control environment inside the bomb and according to the ASTM D240.

3.4.3 Chemical Characterisation of Pyro-fuel

3.4.3.1 Gas Chromatography Mass Spectrometer (GC-MS)

Gas Chromatography/Mass Spectrometry, or GCMS analysis, is an analytical method that combines the features of gas chromatography and mass spectrometry to identify different substances within a sample component matrix. GCMS analysis is generally considered one of the most accurate analyses available. It is particularly beneficial for materials where low detection limits are required and can be used to evaluate samples in any size chemical state, and even when the sample quantity is limited.

Pyrolytic oil extracted from the liquid product was analysed using gas chromatography mass spectrometer (GCMS) model GC Varian 450-GC as shown in Figure A. 2w. Helium was used as a carrier gas at a flow rate of 1 mL/min. Non-polar capillary column was selected for detection of C and H atoms or C-C bonds. Oven temperature initially was set at 100 °C and then it is kept constant for 2 minutes at a heating rate of 5 °C/min. After that, it was increased to 200 °C at a heating rate of 10 °C/min. Then, it was followed by heating to 260 °C at a heating rate of 4 °C/min. Temperature was maintained at 260 °C for 15 minutes. For chromatography, injection temperature was set at 270 °C. Chemical compound in the liquid oil was traced and identified at the setting of mass per ion, $M/Z = 30 - 500$. Split ratio was set at 1:10.

3.5 Interpretive Analysis of Correlation Between Pyro-Fuel and Wastewater Profiling, Reaction Kinetics, Emission Behaviour and Oil Quality

3.5.1 Correlation Between Pyro-Fuel and Wastewater Profiling

Pyrolysis of plastic waste involves the thermal degradation of polymeric materials in the absence of oxygen to produce pyro-fuel (liquid oil), gases, and solid residues. The balance between desired and undesired products is influenced by key process parameters, including feedstock composition, temperature, heating rate, and residence time. The composition of plastic feedstock significantly influences the yield and quality of products obtained through pyrolysis. Specifically, the ratio of HDPE to PET in the feedstock mixture plays a crucial role in determining the distribution of pyrolysis products.

Pyrolysis of HDPE tends to produce higher yields of liquid oil with favourable fuel properties. For instance, a study utilizing spent FCC catalyst reported a liquid yield of 79.3 wt% from HDPE pyrolysis, with the resulting oil exhibiting properties comparable to commercial fuels [43]. In contrast, PET pyrolysis often results in increased production of solid residues and gases, leading to a reduced yield of liquid oil. Research indicates that the presence of significant amounts of PET (above 33 wt%) in mixed plastic streams negatively impacts the production of condensable products and promotes the formation of solid products beyond expected values [179]. While HDPE and PET in specific ratios can enhance liquid fuel production while minimizing unwanted solid residues. Co-pyrolysis studies have demonstrated that certain HDPE:PET ratios can lead to synergistic effects, resulting in higher oil yields than those predicted from individual pyrolysis. For example, co-pyrolysis of biomass and PET at a 40:60 ratio yielded a maximum oil yield difference of 7.78% due to synergistic interactions [180].

The yield and quality of pyro-fuel, as well as the generation of unwanted byproducts during pyrolysis, are significantly influenced by process parameters such as temperature, residence time, and heating rate. Higher temperatures (above 500°C) generally increase gas production while reducing liquid yield. Moderate temperatures (300-450°C) favour liquid fuel formation. Longer retention times can lead to secondary cracking, reducing liquid yield and increasing gaseous byproducts. Extended residence times can lead to secondary cracking reactions, resulting in decreased liquid yields and

increased gaseous byproducts. Rapid heating can enhance liquid production, while slow heating tends to increase char formation [181].

The quality of pyro-fuel and the environmental implications of the pyrolysis process are significantly influenced by various factors such as higher yield of pyro-fuel. Optimized pyrolysis conditions can produce bio-oils with high calorific values and low oxygen content, making them suitable for fuel applications. For instance, bio oils derived from forest residues and refuse-derived fuel at 450°C exhibited higher carbon and hydrogen concentrations, resulting in superior calorific values compared to typical flash pyrolysis oils [182].

Pyrolysis can generate gaseous emissions such as CO₂, CO, CH₄, and H₂S, along with wastewater byproducts characterized by high chemical oxygen demand (COD), biological oxygen demand (BOD), and total suspended solids (TSS). Proper management of these emissions is crucial to minimize environmental impact. Balancing pyrolysis conditions, including temperature, heating rate and feedstock composition, ensures maximum fuel yield with minimal pollutants. This highlights the importance of process control and feedstock selection in optimizing the pyrolysis process.

3.5.2 Error and Uncertainty Analysis

To ensure data reliability, reproducibility and statistical robustness, a systematic error and uncertainty analysis was applied throughout the experimental work. All experimental measurements including pyrolysis yields, calorific value, proximate and ultimate analyses, wastewater quality parameters (COD, BOD, pH, DO, turbidity, TSS) and kinetic data, were performed in triplicate under identical conditions. Results are reported as mean ± standard deviation (SD). Repeatability was evaluated by calculating the relative standard deviation (RSD) for each measured parameter.

$$\text{RSD(\%)} = \frac{\text{SD}}{\text{Mean}} \times 100$$

An RSD value of <5% was considered acceptable for laboratory-scale experiments.

Instrumental uncertainties were obtained from manufacturer specifications and calibration certificates. Typical uncertainties included analytical balance (± 0.01 g), temperature measurement (± 1 °C), bomb calorimeter (± 0.1 MJ/kg), and water quality meters as specified by ASTM and Standard Methods. All instruments were calibrated prior to experimentation. For calculated parameters such as product yield, fixed carbon, calorific value per mass and derived kinetic parameters, uncertainty propagation was performed using the root sum square method accounting for individual measurement uncertainties.

A One-Factor-at-a-Time (OFAT) approach was applied during parameter variation studies. Linear regression analysis and one-way ANOVA were used to evaluate statistical significance, with a confidence level of $p < 0.05$. Outliers exceeding ± 2 standard deviations from the mean were identified and excluded only when justified by experimental records. All results are presented as mean \pm SD, and error bars are included in figures where applicable, ensuring transparency and reproducibility.

3.5.2.1 OFAT Analysis of the Process

In the context of this research, study on slow pyrolysis of HDPE and PET waste, OFAT analysis refers to a classical experimental approach whereby individual process parameters such as mixing ratio, temperature, residence time or heating rate are varied independently while all other factors are held constant. This method provides a clear perspective on the singular impact of each variable on the outcomes such as pyrolytic oil yield, emission characteristics or wastewater profiling indicators. While more sophisticated optimization techniques like Response Surface Methodology (RSM) or factorial designs are often favoured, OFAT remains valuable in early stage investigations for several reasons. It allows researchers to isolate and observe the direct effects of a single variable. Other than that, it helps identify the most influential parameters before applying multivariable techniques. It also requires fewer experimental runs than full factorial designs, particularly in preliminary work.

Harussani et al. (2022) conducted pyrolysis of polypropylene-derived plastic while they primarily focused on the kinetics of char formation, their experimental design included systematic variation of single factors such as temperature or heating rate to elucidate process behaviour reflecting the principles of OFAT screening [183]. Kabeyi (2023) also provided a detailed review of plastic-to-pyrolysis oil conversion,

where the effects of catalyst presence and temperature often examined individually in screened studies were assessed to understand their influence on product yield and quality [18]. This approach offers structured, interpretable data that will later inform more comprehensive analyses such as statistical correlation models, kinetic modelling or multivariate experiments (e.g., OFAT informed RSM). It establishes a solid experimental foundation for identifying critical factors before integrating them in more complex and resource-intensive design-of-experiments frameworks.

3.5.2.2 Statistical Analysis of The Process by Using Linear Regression AN OVA

The process analysis employed both linear regression and ANOVA to elucidate the quantitative effects of independent variables—such as mixing ratios and torrefaction parameters—on pyrolysis outcomes. Linear regression models offered estimations of effect magnitude and predictive capacity, with goodness-of-fit metrics (e.g., R^2) validating their explanatory power. ANOVA was then applied to assess the statistical significance of these relationships, enabling differentiation between meaningful effects and random variation. This combined approach mirrors methods used in recent studies, such as Wang et al. (2024), who modelled the relationship between mixing ratio and pyrolysis yields using linear regression, thereby corroborating the methodological soundness of regression analysis in pyrolysis yield assessment [184].

3.5.3 Reaction Kinetics

Reaction kinetics analysis in this study was conducted using thermogravimetric (TGA) data to quantify the thermal decomposition behaviour of HDPE and PET. Both isoconversional methods (e.g., Flynn-Wall-Ozawa, Kissinger-Akahira-Sunose) and model fitting techniques (e.g., Coats-Redfern) were applied to estimate fundamental kinetic parameters—activation energy (E_a), pre-exponential factor (A), and reaction order (n). Recent literature supports this approach. A study by Das et al. (2024) used both model-free and model-fitting analyses to characterize mixed plastic waste pyrolysis, revealing E_a profiles that vary with conversion and identifying the power-law model as the best fit ($R^2 \sim 0.93-0.99$) [185]. Alhulaybi & Dubdub (2023) conducted a TGA-based kinetic investigation into PET pyrolysis comprehensively evaluating its reaction characteristics through E_a and A determination [176]. Similarly, Netsch et al. (2024) analysed pure thermoplastics (including PET and HDPE), deriving kinetic

parameters using multi-heating-rate experiments and algorithmic fitting, affirming single-step mechanisms for these materials [177]. Collectively, these techniques ensure robust kinetic modelling, enabling quantitative interpretation of thermal stability, reaction mechanisms and experimental design optimization forming a critical analytical pillar of the present research methodology.

3.5.4 Emission Behaviour

The emission behaviour during pyrolysis of plastic waste is a critical parameter that influences both the environmental footprint and the overall sustainability of the process. The types and quantities of emissions depend largely on the feedstock composition, reaction temperature, residence time and the presence of catalysts. Pyrolysis often generates a mixture of gaseous pollutants, including volatile organic compounds (VOCs), polycyclic aromatic hydrocarbons (PAHs), carbon monoxide (CO), nitrogen oxides (NO_x), sulfur oxides (SO_x), and, in some cases, persistent organic pollutants such as dioxins and furans when halogenated plastics are present.

Recent studies emphasize that uncontrolled emissions from pyrolysis plants can pose significant risks to air quality and public health. For instance, Pivato et al. (2024) conducted a systematic mapping of air-polluting emissions from pyrolysis facilities and highlighted that emissions of benzene, toluene, ethylbenzene, and xylene (BTEX) remain a major concern when plastics are processed without advanced abatement systems [24]. Similarly, Li (2024) reviewed air pollutants associated with pyrolysis of solid waste, noting that despite being a low-oxygen thermochemical conversion pathway, pyrolysis can still generate secondary emissions through incomplete degradation of polymers [11].

Mitigation strategies are therefore central to improving pyrolysis sustainability. Advanced gas-cleaning technologies such as wet scrubbers, catalytic filters, and activated carbon systems have been recommended to reduce VOCs, acid gases, and particulate matter (Moranda & Paladino, 2023) [17]. Moreover, Osman et al. (2020) demonstrated that in-situ emission monitoring, combined with kinetic modelling of plastics such as PET enables more precise prediction and control of pollutant formation [16].

From a life-cycle perspective, Graichen (2022) argued that the climate impacts of pyrolysis-derived fuels must be weighed against reuse and mechanical recycling

options, as pyrolysis tends to have higher GHG emissions per tonne of plastic processed [15]. Thus, the emission behaviour of pyrolysis not only reflects technical challenges within reactor operation but also determines the broader acceptability of the technology in circular economy frameworks.

3.5.5 Oil Quality Assessment

Oil quality assessment is a critical step in evaluating the suitability of pyrolysis-derived oil as an alternative fuel or feedstock for downstream applications. The assessment process typically involves a combination of physicochemical characterization, compositional analysis, and performance testing to ensure that the oil meets standards for stability, calorific value, and compatibility with existing fuel infrastructures.

Key parameters often evaluated include density, viscosity, calorific value, elemental composition (C, H, N, S, O), acidity and distillation range as these factors directly influence the combustion performance, storage stability, and potential environmental impacts of the oil. For example, oils with high oxygen content or acidity may exhibit instability during storage and increased corrosion risk in engines and pipelines (Mirkarimi et al., 2022)[7]. Similarly, the presence of heteroatoms such as sulfur or chlorine can contribute to higher emissions of SO_x, NO_x, or dioxins during combustion, thus necessitating pre-treatment or upgrading processes (Li, 2024)[11].

Recent studies emphasize that comprehensive characterization of pyrolysis oils not only determines their direct usability but also guides optimization of the pyrolysis process and post-treatment strategies. Mirkarimi et al. (2022) highlighted the importance of correlating operating parameters with oil yield and quality to ensure its effective application in diesel engines [7]. Likewise, Kabeyi and Olanrewaju (2023) discussed how oil properties derived from plastic pyrolysis directly affect their integration into the energy transition, particularly when comparing them with conventional fossil fuels [18].

Moreover, with the global shift toward sustainable energy, oil quality assessment also extends to evaluating environmental and economic viability. Yaqoob et al. (2025) argued that fuel characterization should include not only conventional parameters but also life cycle performance indicators such as greenhouse gas reduction potential and compatibility with renewable blending strategies [31].

In summary, oil quality assessment serves as a bridge between laboratory-scale pyrolysis research and practical industrial deployment. It enables researchers and practitioners to understand both the limitations and potential of pyrolysis oils, thereby informing upgrading techniques such as catalytic hydrotreating, blending, or fractional distillation to achieve market-ready fuels.

3.6 Concluding Remark

This chapter has outlined the methodological framework adopted to achieve the research objectives. It detailed the systematic preparation and characterization of raw materials, the design and execution of the pyrolysis experiments and the incorporation of wastewater profiling as a novel diagnostic tool for emission monitoring. Furthermore, it described the procedures for assessing pyro-fuel quality along with the analytical techniques and statistical methods employed to interpret the experimental data. By integrating physical, chemical and kinetic analyses, this methodology ensures a comprehensive understanding of the relationship between process conditions, emission behaviours and fuel properties. The subsequent chapter will present the experimental findings, interpret the results within the context of existing knowledge and evaluate their implications for emission control and fuel optimization.

CHAPTER 4

RESULTS AND DISCUSSION

Good data derives from proper raw materials preparations and standardisation of the employed techniques. This chapter describes the techniques used for obtaining and preparing raw materials for chemical and physical characterisations, heat treatment of samples by using Bomb Calorimeter, TGA and GC-MS. The sample will be decomposed using a pyrolysis plant. The final result will be analysed using Bomb Calorimeter, TGA and GC-MS. The gas produced after the pyrolysis process will be analysed in terms of water quality, DO, Turbidity, COD, BOD, pH and TSS.

4.1 Physical and Chemical Characteristics of Raw Materials Upon Raw Material Preparation for Pyrolysis



Characterization of raw material that been used in this research is divided into two (2) types which are physical characterisation and chemical characterisation.

4.1.1 Grain Size of Raw Material (Physical Properties)

Table 4.1 shows grain size of HDPE, HDPE2:1PET ratio, HDPE1:1PET ratio, HDPE1:2PET ratio and PET respectively. From Wifi Handheld Digital Microscope, size of particle. For HDPE is 95 μm , HDPE2:1PET ratio is 85 μm , HDPE1:1PET ratio is 78 μm , HDPE1:2PET ratio is 72 μm and PET is 75 μm . The results obtained are of less value than the research obtained [55, 57]. Therefore, the study obtained can be used in studying the raw material of plastic waste before pyrolysis.

Table 4.1

Grain size of HDPE, HDPE2:1PET ratio, HDPE1:1PET ratio, HDPE1:2PET ratio and PET

SAMPLE	REMARK
<p>HDPE particle before pyrolysis process</p> 	<p>Morphology & Magnification:</p> <ul style="list-style-type: none"> Likely shows smooth, rounded particles with minimal surface roughness. At moderate magnification (e.g., 500x), HDPE's semi-crystalline structure may appear as folded or layered textures. <p>Size Distribution:</p> <ul style="list-style-type: none"> Particles tend to be larger and more uniform, typically in the range of 100-500 um, due to HDPE's ductile nature during mechanical processing. <p>Pyrolysis Relevance:</p> <ul style="list-style-type: none"> Larger HDPE particles require longer residence time for complete thermal degradation. Yields aliphatic hydrocarbons with minimal char. Smooth morphology may reduce surface area, slightly slowing reaction kinetics.
<p>HDPE2:1PET ratio particle before pyrolysis process</p> 	<p>Morphology & Magnification:</p> <ul style="list-style-type: none"> Mixed morphology: HDPE dominates, but PET fragments are visible as sharper, more angular inclusions. At higher magnification, phase boundaries between HDPE and PET may be distinguishable. <p>Size Distribution:</p> <ul style="list-style-type: none"> Moderate variation in particle size, with HDPE fragments larger and PET smaller. Distribution skewed toward coarser particles, but with noticeable fine PET inclusions. <p>Pyrolysis Relevance:</p> <ul style="list-style-type: none"> PET enhances aromatic compound formation, while HDPE contributes to aliphatic oil fractions. Mixed morphology may lead to non-uniform heating, requiring careful temperature control. Potential for synergistic effects in oil composition

**HDPE1rPET particle
before pyrolysis process**



Morphology & Magnification:

- Balanced mixture with visible heterogeneity—equal presence of smooth HDPE and brittle PET particles.
- Likely shows interfacial textures or partial blending zones.

Size Distribution:

- Broad distribution, with both fine and coarse particles.
- Increased fragmentation due to PET content.

Pyrolysis Relevance:

- This ratio may yield diverse oil fractions, combining aromatics and aliphatics.
- Fragmented PET increases surface area, enhancing reaction rates.
- May produce more char and wastewater contaminants, requiring post-treatment

**HDPE1:2PET particle
before pyrolysis process**



Morphology & Magnification:

- PET dominates, with HDPE appearing as isolated smooth fragments.
- Surface features likely more angular and fractured due to PET's brittleness.

Size Distribution:

- Skewed toward smaller particles, especially PET.
- Higher surface area due to fragmentation.

Pyrolysis Relevance:

- PET-rich samples tend to produce more aromatic compounds and solid residues.
- Faster reaction kinetics due to fine particle size.
- May require temperature optimization to prevent excessive char formation

**PET particle before
pyrolysis process**



Morphology & Magnification:

- Sharp-edged, brittle particles with irregular shapes.
- At high magnification, may show crystalline domains or fracture lines.

Size Distribution:

- Typically fine particles, often <200 um, due to PET's tendency to shatter during grinding.

Pyrolysis Relevance:

- PET yields aromatic-rich oils and higher char content.

- Fine particles enhance heat transfer but may increase wastewater COD/BOD due to oxygenated byproducts.
- Requires controlled heating rates to minimize secondary reactions.

Microscopic examination shows that as PET content increases in HDPE/PET mixtures, particle morphology shifts from smooth and coarse (HDPE-dominant) to sharp and fine (PET-dominant), resulting in higher surface area and improved pyrolysis kinetics. This enhances the production of aromatic compounds but also raises char yield and the likelihood of wastewater contamination, necessitating optimized thermal conditions and post-treatment strategies.

4.1.2 Density of Raw Material (Physical Properties)

Density is a critical physical property of polymers that influences their processing, thermal behaviour, and final applications. The density of HDPE, PET, and their mixtures before pyrolysis was measured to assess the structural characteristics of the raw material. Table 4.2 presents the density values of HDPE, PET, and different mixing ratios before undergoing the pyrolysis process. HDPE exhibited a density of 0.952 g/cm^3 , which is consistent with its typical range ($0.94\text{-}0.97 \text{ g/cm}^3$). This value reflects its semi-crystalline nature and lower molecular packing compared to PET. PET had the highest density (1.298 g/cm^3), which is attributed to its rigid aromatic backbone and high crystallinity. The presence of benzene rings in its structure leads to a higher molecular packing density. HDPE2:1PET ratio which is 0.903 g/cm^3 has a lower density due to a higher HDPE fraction. 0.934 g/cm^3 which is density of ratio HDPE1: 1PET has moderate density due to equal proportions of HDPE and PET) While HDPE1:2PET ratio density which is 0.938 g/cm^3 is slightly higher density with increased of PET content.

The density values indicate that increasing the PET content in the HDPE-PET mixtures results in a gradual rise in density due to PET's higher molecular weight and structural rigidity. This trend aligns with existing literature, which reports that polymer blending can alter material properties, including density, crystallinity, and thermal stability.

Table 4.2

Density of HDPE, PET and mixing ratio before pyrolysis

Ratio Raw Material	Density (g/cm^3)
HDPE	0.952
HDPE2:1PET	0.903
HDPE1:1PET	0.934
HDPE1:2PET	0.938
PET	1.298

The density obtained is almost the same as studies conducted by other researchers with the virgin density value of HDPE being around 0.945 to 0.965g/cm³ [40, 43, 47, 72] while virgin PET is around 1.03 to 1.38g/cm³ [89, 104]. Therefore, the data obtained can be used for further studies involving mixing according to the ratio of plastic types.

Interestingly the HDPE2:1PET mixture displayed a density of 0.903 g/cm³, which is lower than that of pure HDPE despite containing a fraction of the denser PET. This outcome is consistent with the immiscible nature of HDPE and PET, where poor interfacial adhesion and phase separation give rise to interfacial micro voids and inefficient packing in the blended system thereby reducing the measured apparent (bulk) density of the powder blend. The HDPE1:1PET mixture recorded a moderate density of 0.934 g/cm³ reflecting the equal contribution of both polymers while the HDPE1:2PET ratio showed a slightly higher density of 0.938 g/cm³ with increased PET content. Notably, such measured values are influenced not only by polymer chemistry but also by powder metrology effects including particle size distribution, particle shape and bulk packing state since apparent density in powders is sensitive to handling and inter particle void age rather than representing the void free true material density [186].

4.1.3 Moisture Content of Raw Material (Physical Properties)

According to Table 4.3 presents the moisture content of HDPE, PET, and their mixtures before pyrolysis. HDPE exhibited the lowest moisture content (0.07%), reflecting its hydrophobic nature and low water absorption capacity. PET had the highest moisture content (0.27%), likely due to its polar ester groups, which can absorb atmospheric moisture. While blended samples showed intermediate moisture content, where HDPE2:1PET and HDPE1:1PET ratio shows 0.13% while HDPE1:2PET ratio shows 0.27% of moisture content which is higher due to increased PET content. The results indicate that PET contributes to higher moisture retention in plastic waste mixtures due to its hydrophilic nature, while HDPE remains relatively unaffected by moisture absorption. The moisture content values in all samples are low, suggesting minimal impact on pyrolysis efficiency.

Table 4.3
Moisture content of HDPE, PET and mixing ratio before pyrolysis

Ratio Raw Material	Moisture Content %
HDPE	0.07
HDPE2:1PET	0.13
HDPE1:1PET	0.13
HDPE1:2PET	0.27
PET	0.27

The results obtained are almost the same as studies conducted by other researchers where the moisture content obtained for HDPE is around 0 to 0.3% [7, 33, 43, 65, 75] while for PET the values obtained are in the range of 0.47 to 0.7% [7, 75]. Studies from other researchers also show that PET produces a high moisture content compared to HDPE.

4.1.4 Melting Point of Raw Material (Physical Properties)

In the melting point of a polymer is a fundamental thermal property that influences its processing, thermal stability, and behaviour under pyrolysis conditions. It represents the temperature at which the polymer transitions from a solid to a molten state, impacting its decomposition kinetics and phase transformation during pyrolysis. Table 4.4 presents the melting points of HDPE, PET, and their mixtures before pyrolysis. HDPE exhibited the lowest melting point (146.0°C), consistent with its semi-crystalline structure and strong intermolecular forces. PET had a melting point of 250.0°C, which is higher than HDPE due to its more rigid aromatic backbone but higher oxygen content, affecting its thermal behaviour [161].

Blended samples showed decreasing melting points with increasing PET content, indicating an influence of polymer interaction where HDPE2:1PET ratio is 278.0°C, HDPE1:1PET ratio is 265.0°C and HDPE1:2PET is 236.0°C. The results indicate that blending HDPE with PET reduces the overall melting point of the material, likely due to interactions between polymer chains and changes in crystallinity. Understanding the melting behaviour of polymer mixtures is essential for optimizing pyrolysis conditions and improving the efficiency of thermal conversion processes.

Table 4.4
Melting point of HDPE, PET and mixing ratio before pyrolysis

Ratio Raw Material	Melting Point (°C)
HDPE	146.0
HDPE2:1PET	278.0
HDPE1:1PET	265.0
HDPE1:2PET	236.0
PET	250.0

The data obtained is also consistent with studies conducted by other researchers where the melting point of PET is higher compared to HDPE. The melting point of HDPE is around 125.7 to 143 [47, 54, 55, 65, 80, 100, 187] while the melting point of PET is in the range of 247 to 255 [57, 65].

4.1.5 Proximate Analysis of Raw Material (Chemical Properties)

Table 4.5 summarized of proximate analysis result for HDPE, PET and mixing ratio of HDPE2:1PET, HDPE1:1PET and HDPE1:2PET. Found volatile matters for HDPE is higher when compared to plastic mixing ratio and PET. High volatile matters indicate that the material tends to produce a higher liquid after the pyrolysis process [70, 74, 75]. Therefore, HDPE will produce more liquid when compared to other ratios. High volatile matter also shows that this plastic waste is very valuable and can be used as pyrolytic oil. As for ash, it was found that PET produces the highest ash compared to other ratios. A high ash value indicates that the material tends to produce high char [74]. Therefore, PET will produce a high char when compared to other ratios.

Table 4.5

The proximate analysis result of HDPE, PET and mixing ratio before pyrolysis

Ratio Raw Material	Moisture Content %	Volatile Matters %	Ash %	Fixed Carbon %
HDPE	0.07	99.80	0.13	0.00
HDPE2:1PET	0.13	98.40	1.47	0.00
HDPE1:1PET	0.13	97.60	2.27	0.00
HDPE1:2PET	0.27	97.20	2.53	0.00
PET	0.27	96.40	3.33	0.00

Studies of other researcher show approximately the same value obtained from this study where volatile matters for HDPE are in the range of 94 to 100% [7, 31, 33, 69, 70, 74], while the volatile matters value for PET also shows almost the same value obtained by other researchers which is lower compared to HDPE which is between 85 to 92% [7, 31, 69, 70, 74]. Therefore, the value obtained from this study is relevant to use after comparing with the results obtained by other researchers.

4.1.6 Ultimate Analysis of Raw Material (Chemical Properties)

In the elemental analysis results presented in Table 4.6 provide a comprehensive breakdown of the chemical composition for pure HDPE, pure PET, and their various mixing ratios prior to pyrolysis processing. The analysis focuses on the percentage composition of key elements: Nitrogen (N), Carbon (C), Hydrogen (H), Sulfur (S), and Oxygen (O), with a calculated total C-H (Carbon-Hydrogen) content. As the PET ratio increases in the HDPE:PET blend, carbon content gradually decreases from 63.66% (HDPE) to 54.94% (PET). Hydrogen content shows a significant increase from 9.88% to a peak of 21.53% at HDPE2:1PET ratio. While oxygen content increases from 22.91% (pure HDPE) to 40.36% (pure PET). Nitrogen content reduces from 2.06% to 0% and sulphur content disappears in PET dominant mixtures.

The progressive changes in elemental composition across different mixing ratios suggest complex interactions between HDPE and PET polymers, which could significantly influence their thermal and chemical properties during subsequent processing, such as pyrolysis. This detailed elemental analysis provides crucial insights

into the molecular-level changes occurring in HDPE-PET blends, which can be instrumental in understanding their potential applications, thermal behaviour, and chemical transformations [188].

The hydrocarbon content, particularly the carbon (C) and hydrogen (H) percentages determined through ultimate analysis, plays a significant role in influencing the liquid yield during pyrolysis. Higher concentrations of these elements typically correlate with increased production of bio-oil, as they are fundamental components of hydrocarbon chains formed during thermal decomposition [189].

Table 4.6
The elemental analysis result of HDPE, PET and mixing ratio before pyrolysis process

Ratio Raw Material	N	C	H	S O	Total C-H	
HDPE	2XJ6	63.66	9 [^] 88	L49	22.91	73.54
HDPE2:1PET	0.75	61.74	21.53	0	15.98	83.27
HDPE1IPET	1.05	60.33	18.95	0	19.67	79.28
HDPE1:2PET	0	59.72	17.8	0	22.48	77.52
PET	0	54.94	1.32	3.38	40.36	56.26

The ultimate analysis in Table 4.6 shows a non-zero oxygen (O) value for HDPE, although the HDPE backbone $(C_2H_4)_n$ consists only of carbon and hydrogen. This discrepancy is mainly attributed to limitations in the elemental analysis approach and the condition of the polymer sample. In Flash-type CHNS/O analysis, C/H/N/S are measured directly, whereas oxygen may be obtained either through a separate pyrolysis run or calculated by difference. When oxygen is reported by difference, small errors from combustion efficiency, baseline drift, blank subtraction or calibration of C/H/N/S can appear artificially as "oxygen" even for oxygen free polymers.

The HDPE used in this study was sourced from post-consumer or field waste and prepared as powder. Powdered polymers are sensitive to sample heterogeneity (particle size distribution, incomplete homogenization) and residual moisture which can introduce variability during combustion and mass balance calculations. Commercial HDPE commonly contains oxygen bearing stabilizers or additives especially hindered phenolic antioxidants and related processing stabilizers used to improve thermos

oxidative resistance. Even at low dosages, such additives can contribute to a measurable oxygen fraction particularly when oxygen is computed by difference.

PE surfaces can undergo incipient oxidation during storage, weathering or processing history, producing oxygenated groups that are detectable by FTIR carbonyl index and may contribute to apparent oxygen in ultimate analysis. Therefore, the O value in Table 4.6 should not be interpreted as oxygen in the HDPE backbone, but rather as a combined effect of oxygen by difference uncertainty, sample heterogeneity, oxygen containing additives and minor surface oxidation.

4.1.7 Energy Content Analysis of Raw Material (Chemical Properties)

Table 4.7 shows the calorific value of HDPE, PET and the mixture according to the ratio of HDPE to PET which is the ratio of 2:1, 1:1 and 1:2 taken before and after the pyrolysis process. It was found that the calorific value for HDPE is the highest and is close to the calorific value for petrol and diesel which is 43,400 - 46,500J/g for petrol and 42,800 - 45,800J/g for diesel [35]. The calorific value for PET is low due to the presence of oxygen in the hydrocarbon chain. However, after going through the pyrolysis process, the calorific value for all samples increased a lot. The most significant is the calorific value for PET which increased to nearly 44%. HDPE and the mixture according to the 1:1 ratio seem suitable to be used as fuel due to its calorific value close to the calorific value of commercial petrol and diesel [74].

Plastics rich in hydrocarbons decompose more readily into smaller hydrocarbon chains during pyrolysis, leading to higher liquid yields. In contrast, plastics with higher oxygen content, like PET, tend to produce more gaseous products and char due to the formation of oxygenated compounds that are less likely to condense into liquids [16]. Therefore, the pyrolysis process is very suitable for increasing the calorific value of a material, especially plastic waste.

Table 4.7

Calorific value of sample before and after the pyrolysis

Ratio Raw Material	Before Pyrolysis (J/g)
HDPE	41,868
HDPE2:1PET	36,006
HDPE1:1PET	32,238
HDPE1:2PET	28,888
PET	22,190

4.1.8 Thermal Degradation Analysis of Raw Material by Using TGA/DCS (Chemical Properties)

Figure 4.1 show TGA result for HDPE and PET ratio before pyrolysis process with varying initial sample masses: HDPE (16.00 mg), HDPE2:1PET (10.20 mg), HDPE1:1PET (10.30 mg), HDPE1:2PET (10.80 mg), and pure PET (10.00 mg). All samples were subjected to thermal treatment from approximately 29°C to 1200°C. At initial phase which is around 29 to 350°C, all samples exhibited minimal mass loss up to 350°C where HDPE showed the highest thermal stability with only 2.82% mass loss. While mixed ratios demonstrated intermediate stability and PET maintained relatively consistent mass with minimal degradation.

At mid-temperature range which is around 350 to 500°C, HDPE initiated significant decomposition at 400°C. Most pronounced mass loss occurred between 435 to 495°C for all samples. HDPE mass reduced from 15.35 mg to 1.43 mg (90.7% loss), HDPE2:1PET mass reduced from 10.06 mg to 2.03 mg (79.8% loss) while HDPE1:1PET mass reduced from 10.21 mg to 1.85 mg (81.9% loss). HDPE1:2PET mass reduced from 10.82 mg to 2.30 mg (78.7% loss) while PET mass reduced from 10.10 mg to 1.71 mg (83.1% loss).

While at high-temperature range which is around 500 to 1200°C, secondary decomposition observed above 500°C and residual mass stabilization occurred differently for each blend where HDPE stabilized at 0.96 mg which is 6% of initial mass. HDPE2:1PET ratio stabilized at 0.84 mg (8.2% of initial mass) while HDPE1:1PET stabilized at 0.60 mg (5.8% of initial mass). HDPE1:2PET stabilized at

0.73 mg (6.8% of initial mass) while PET stabilized at 0.11 mg which is 1.1% of its initial mass.

Figure 4.2 show DTG result for HDPE and PET ratio before pyrolysis process across a temperature range from approximately 29°C to 1200°C. In Initial Degradation Phase which is from 29 to 350°C, HDPE shows minimal initial mass loss rate which is -0.0366 mg/min up to 200°C PET demonstrates even lower mass loss rates which is -0.000527 mg/min in this range. The blends exhibit intermediate behaviour, with mass loss rates correlating to their respective compositions.

At Primary Degradation Region which is from 350 to 500°C, HDPE shows its maximum degradation rate which is -7.06 mg/min at approximately 482°C while PET exhibits its peak degradation rate at -3.68 mg/min at around 447°C. The blends show two distinct degradation peaks, reflecting the presence of both polymers where HDPE2:1PET ratio shows a stronger HDPE-characteristic peak. While HDPE1:2PET ratio demonstrates a more prominent PET-characteristic peak and HDPE1:1PET ratio exhibits intermediate behaviour. At High Temperature Region which is from 500 to 1200°C, HDPE shows minimal residual degradation and PET continues to show minor mass loss. The blends demonstrate combined characteristics, with degradation patterns reflecting their compositional ratios.

In term of thermal stability comparison, HDPE appears more thermally stable at lower temperatures but undergoes more rapid degradation once initiated while PET shows more gradual degradation across a broader temperature range. The blends demonstrate intermediate thermal stability characteristics, with behaviour proportional to their composition ratios. These results indicate that the thermal degradation behaviour of HDPE:PET blends is not merely additive but shows interactions between the two polymers. The presence of PET appears to modify the degradation pattern of HDPE, and vice versa, suggesting potential molecular interactions between the polymers during the pyrolysis process.

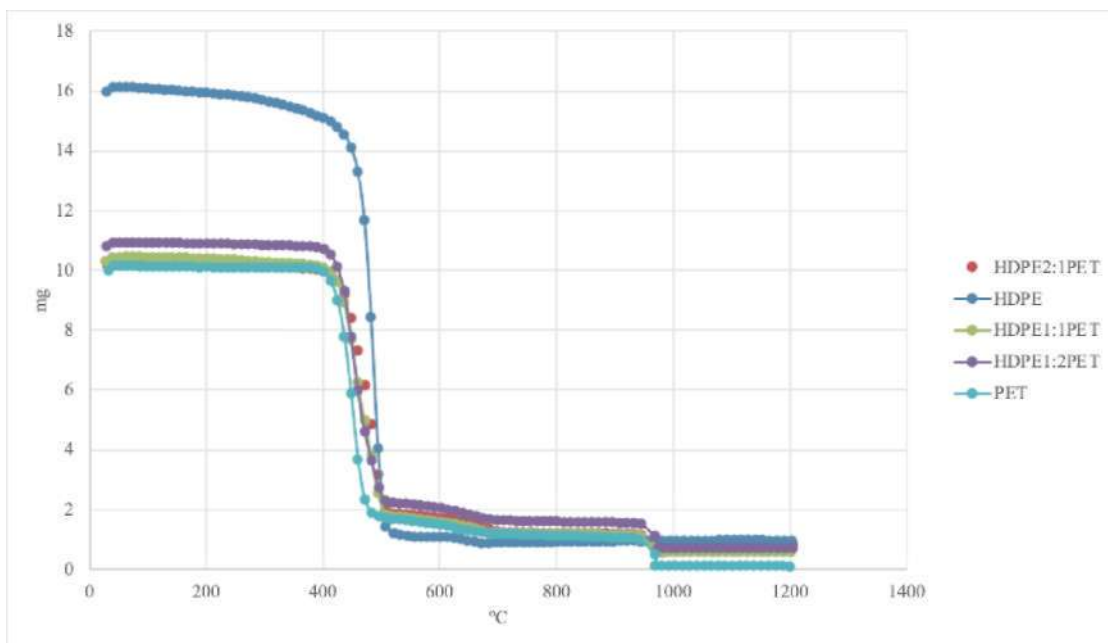


Figure 4.1 TGA result for HDPE and PET ratio before pyrolysis process

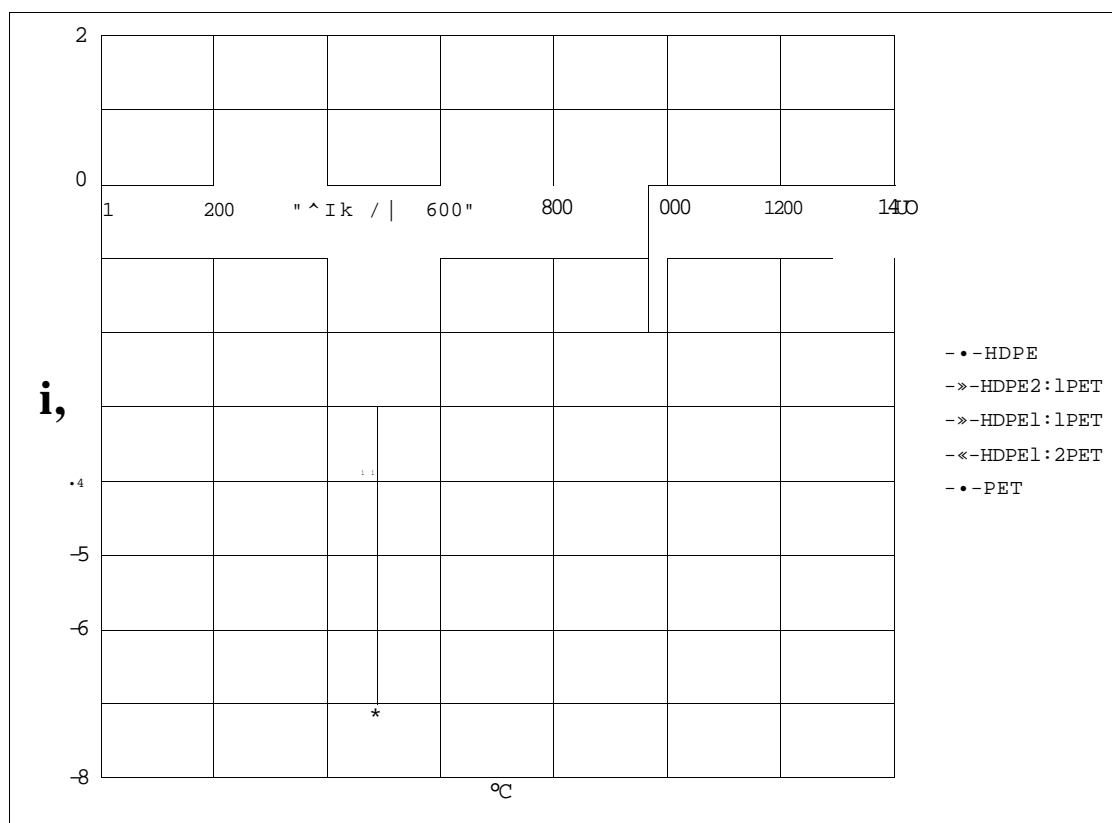


Figure 4.2 DTG result for HDPE and PET ratio before pyrolysis process

4.1.9 Chemical Hydrocarbon Bond Analysis of Raw Material by Using FTIR (Chemical Properties)

Figure 4.3 shows the FTIR spectrum of high-density polyethylene (HDPE) before pyrolysis exhibits distinct absorption bands corresponding to the characteristic functional groups of polyethylene. Key absorption peaks were observed in the wavenumber range of 2800-3000 cm^{-1} , attributed to C-H stretching vibrations in aliphatic hydrocarbons. Peaks around 2920 cm^{-1} and 2850 cm^{-1} correspond to asymmetric and symmetric stretching of C-H bonds in the methylene groups (-CH₂-). Additional peaks in the region of 1460-1475 cm^{-1} correspond to >CH- bending vibrations, while the absorption band near 720 cm^{-1} is associated with C-H rocking vibrations, confirming the presence of a long-chain polyethylene structure.

The FTIR analysis confirms that HDPE primarily consists of aliphatic hydrocarbon chains with no significant presence of oxygenated or aromatic functional groups. These findings establish a baseline chemical characterization before pyrolysis, providing essential insights into potential thermal decomposition pathways. The absence of polar functional groups further supports the non-polar nature of HDPE, influencing its interaction in pyrolysis reactions.

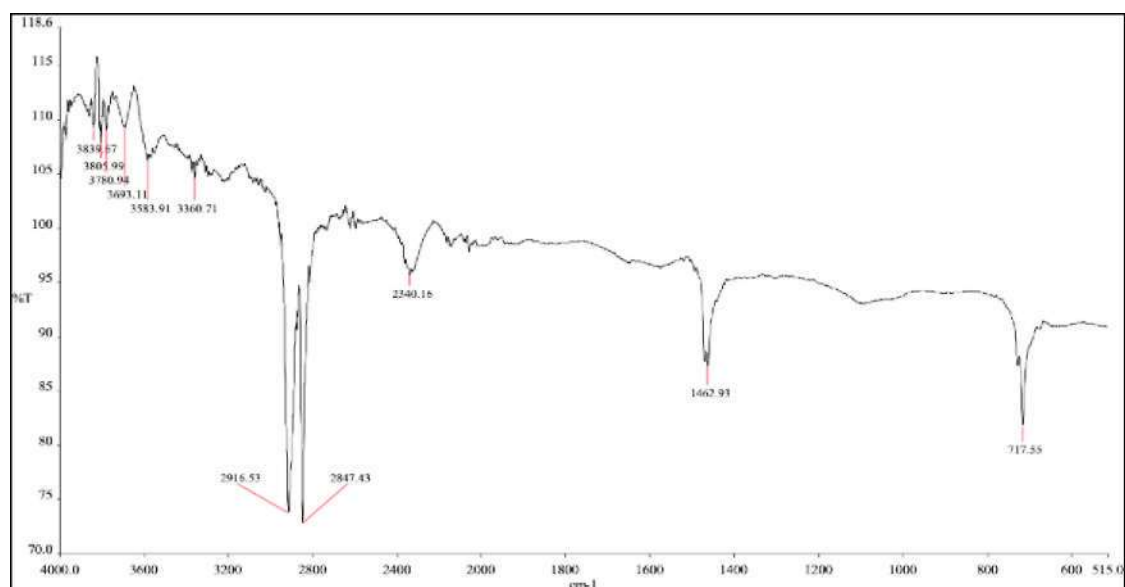


Figure 4.3 FTIR result for HDPE raw material

Figure 4.4 shows the FTIR spectrum of FIDPE2:1PET ratio raw material. Peaks associated with HDPE are typically observed at wavenumber 2920 cm^{-1} and 2850 cm^{-1} attributed to C-H stretching vibrations in aliphatic hydrocarbons. Additional peaks in the region of 1465 cm^{-1} correspond to CH_2 bending vibrations, while the absorption band near 720 cm^{-1} is associated with CH_2 rocking vibrations which is like FIDPE spectrum. While for PET component, peaks indicative of PET includes 1715 cm^{-1} correspond to C=O stretching of ester groups. Additional peaks of 1110-1240 cm^{-1} correspond C-O stretching vibrations while at wavenumber range 725-730 cm^{-1} shows aromatic C-H out-of-plane bending.

The spectrum reveals overlapping peaks due to the combination of HDPE and PET in the blend. The presence of ester groups (from PET) and methylene groups (from HDPE) suggests that the two polymers retain their individual chemical identities in the mixture. This is typical for immiscible polymer blends, where limited chemical interaction occurs between components. The FTIR analysis confirms the coexistence of HDPE and PET functional groups in the 2:1 ratio before pyrolysis. This baseline characterization is critical for assessing changes in chemical structure post-pyrolysis. The results suggest that the thermal decomposition process will likely involve distinct degradation pathways for each polymer component, leading to a variety of pyrolytic products.

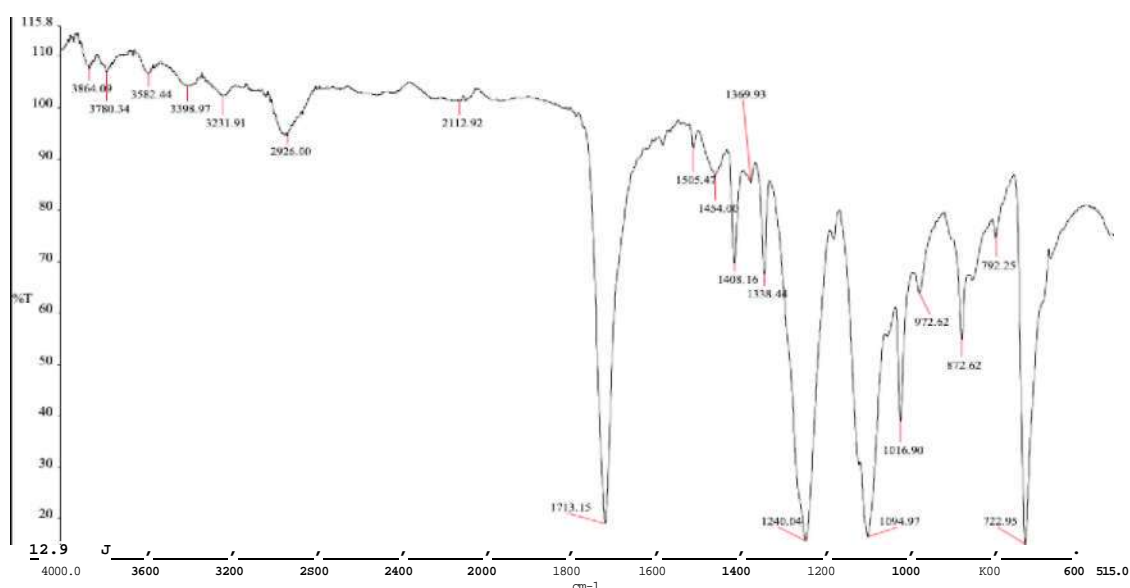


Figure 4.4 FTIR result for HDPE2:1PET ratio raw material

Figure 4.5 shows the FTIR spectrum of HDPE1:1PET ratio raw material. The FTIR spectrum of the FtDPE 1:1 PET ratio plastic waste before pyrolysis exhibits distinct absorption peaks corresponding to the characteristic functional groups of polyethylene (FtDPE) and polyethylene terephthalate (PET). At wavenumber 2800-3000 cm^{-1} strong C-H stretching vibrations from aliphatic hydrocarbons, primarily attributed to HDPE. At wavenumber 1710-1730 cm^{-1} a sharp peak indicating the presence of carbonyl (C=O) stretching, characteristic of the ester functional group in PET. While at wavenumber range 1470-1500 cm^{-1} correspond to CH_2 bending vibrations, mainly from FtDPE. At 1240-1260 cm^{-1} , C-O stretching vibrations, confirming the presence of PET ester linkages. While at wavenumber 720 cm^{-1} , CH_2 rocking vibrations, further supporting the polyethylene structure.

The FTIR analysis confirms the coexistence of FtDPE and PET components within the plastic waste. The observed peaks validate the presence of aliphatic hydrocarbons from polyethylene and ester linkages from PET, providing insight into the structural composition before pyrolysis. This characterization is crucial for understanding the decomposition behaviour of mixed polymeric waste under thermal treatment.

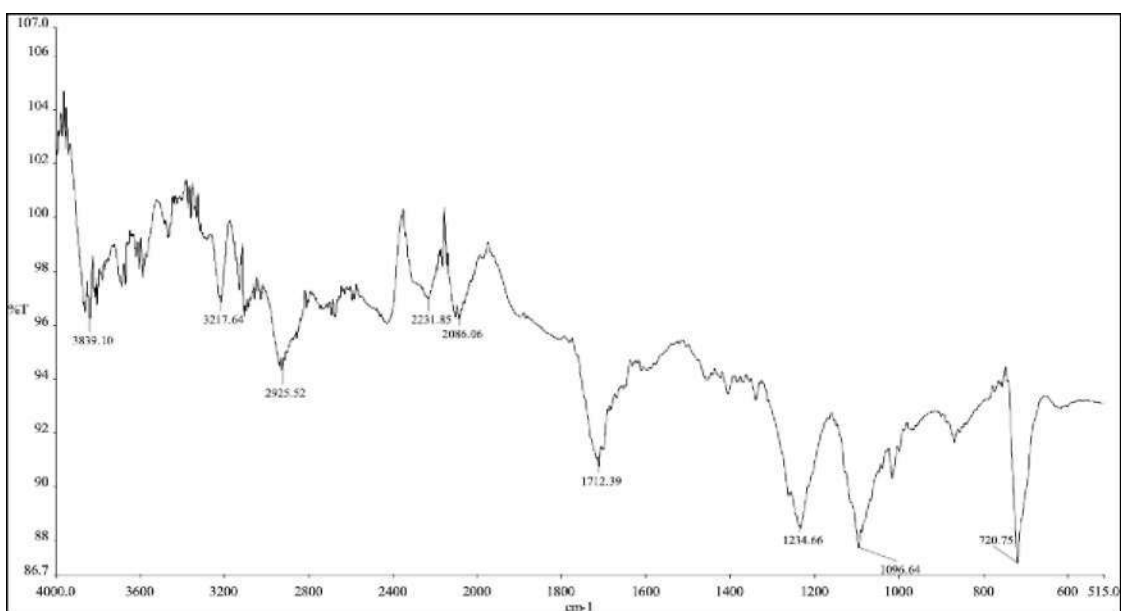


Figure 4.5 FTIR result for HDPE1: 1PET ratio raw material

Figure 4.6 shows the FTIR spectrum of HDPE1:2PET ratio raw material. From FIDPE component, peaks near 2920 cm^{-1} and 2850 cm^{-1} correspond to asymmetric and symmetric C-H stretching vibrations from methylene ($-\text{CH}_2-$) groups. A peak at 1465 cm^{-1} is attributed to CH_2 bending vibrations. While a peak around 720 cm^{-1} indicates CH_2 rocking vibrations, typical of FIDPE. On PET component, a strong peak at 1715 cm^{-1} is associated with C=O stretching vibrations from ester groups, a signature of PET. Peaks between 1240-1100 cm^{-1} are indicative of C-O stretching vibrations in ester functional groups. While peaks near 725-730 cm^{-1} correspond to aromatic C-H out-of-plane bending.

The FTIR spectrum shows overlapping peaks due to the combination of HDPE and PET. The lack of significant peak shifts or new bands suggests that the polymers retain their individual chemical identities in the blend, consistent with immiscible polymer mixtures. The higher proportion of PET in this blend results in more pronounced peaks associated with its ester and aromatic functional groups.

The FTIR analysis confirms the presence of characteristic functional groups from both HDPE and PET in the 1:2 ratio blend. The spectrum reflects a higher contribution from PET due to its greater proportion in the mixture. This baseline characterization is crucial for understanding the chemical changes during pyrolysis, where distinct degradation pathways for HDPE and PET are expected. HDPE is likely to decompose into hydrocarbons, while PET may yield aromatic compounds and other oxygenated products.

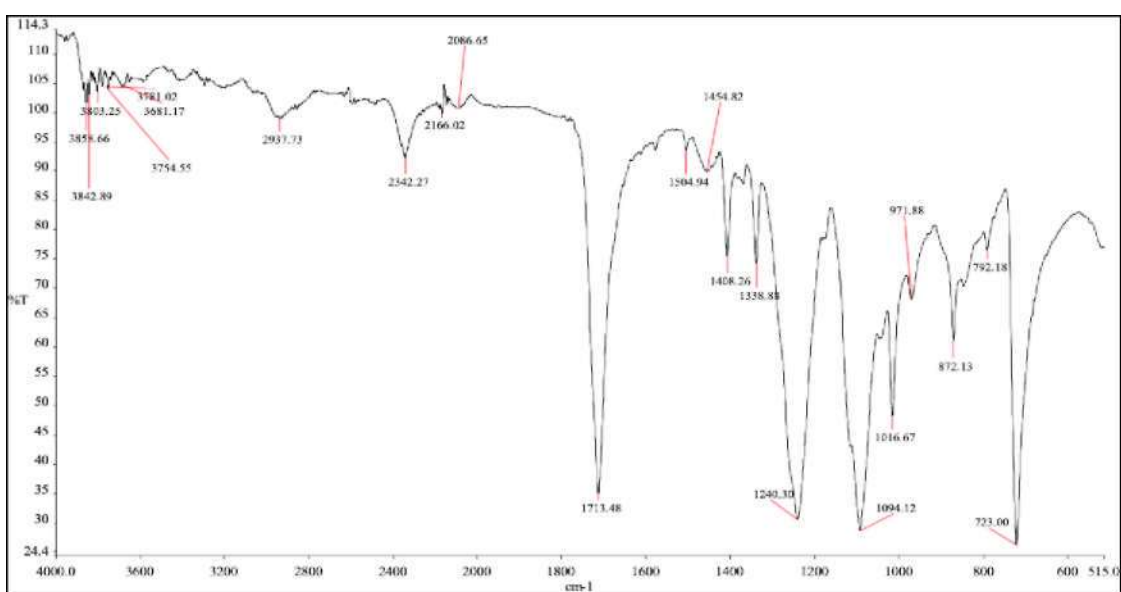


Figure 4.6 FTIR result for HDPE1:2PET ratio raw material

Figure 4.7 shows the FTIR spectrum of PET raw material. A strong absorption band is expected near 1715 cm^{-1} , which corresponds to the stretching vibration of the carbonyl group (C=O) in the ester linkage. Absorption bands in the range of $1240\text{-}1100\text{ cm}^{-1}$ are attributed to C-O stretching vibrations in the ester groups. Peaks around $725\text{-}730\text{ cm}^{-1}$ indicate aromatic C-H out-of-plane bending.

PET is known for its ester linkages and aromatic components. The prominence of peaks associated with these functional groups confirms the material's chemical structure. The spectrum shows that PET maintains its structure integrity before pyrolysis process. The FTIR analysis confirms the presence of the essential functional groups of PET plastic waste, including the ester carbonyl, C-O bonds, and aromatic C-H groups. This pre-pyrolysis characterization serves as a reference point for monitoring the chemical transformations occurring during the thermal decomposition process.

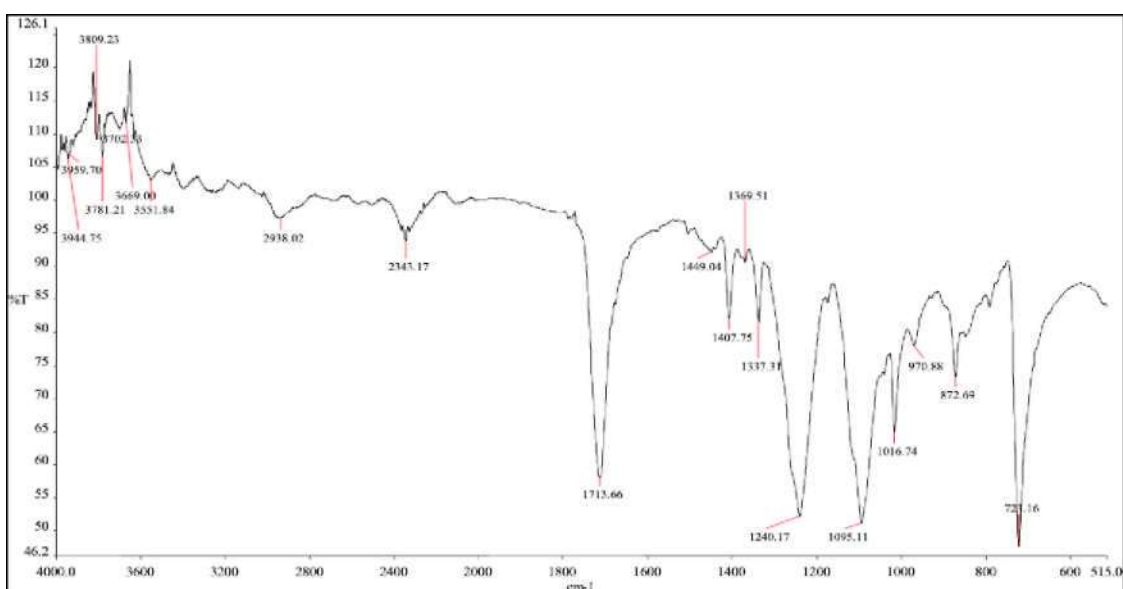


Figure 4.7 FTIR result for PET raw material

Table 4.8 shows FTIR analysis of pyro-oils obtained through thermochemical conversion of different plastic ratio. From this table, FTIR for HDPE and HDPE:PET blends (2:1, 1:1, 1:2 ratios) shows strong aliphatic C-H stretching and bending peaks (near $2920, 2850, 1460\text{ cm}^{-1}$) similar to those found in commercial diesel, indicating a hydrocarbon structure compatible with diesel-like fuels. However, as PET content increases, carbonyl (C=O) peaks (-1715 cm^{-1}) become more pronounced, reflecting the presence of oxygenated compounds from PET. PET shows strong ester/carboxylic (C=O) and aromatic peaks do not present in diesel. Oils derived from PET can contain

more oxygenates and water, which may limit their direct use as diesel substitutes without further upgrading [175]. While commercial diesel FTIR is dominated by aliphatic hydrocarbon peaks (C-H stretches and bends), with minimal oxygenated or aromatic content.

Pyrolysis of HDPE and similar plastics produces oil rich in alkanes and alkenes (C₁₀-C₂₅), closely matching the hydrocarbon profile of diesel [190]. These oils have suitable density, viscosity, and calorific values for use as diesel-like fuels. PET-derived oils can be produced, but often contain higher oxygen content (e.g., carboxylic acids, water), which may require further refining before use as diesel. While for mixing ratio of HDPE and PET, the more PET present, the more the resulting oil deviates from pure diesel characteristics due to increased oxygenates. However, blends with higher HDPE content as per HDPE₂:1PET is more diesel-like [164].

From this FTIR data, it shows that not all plastic waste is equally suitable for direct conversion to diesel-like fuel. Polyolefins (HDPE, LDPE, PP) are most compatible, while PET and other oxygen-rich plastics may require additional refining [174]. Blending plastics can dilute undesirable features, but high PET content introduces oxygenates that are not ideal for diesel engines. FTIR analysis confirms that HDPE and HDPE-rich blends yield products most like diesel, while PET and PET-rich blends deviate due to oxygenated functionalities [163].

Table 4.8

FTIR analysis of pyro-oils obtained through thermochemical conversion of different plastic ratio

HDPE			HDPE2:1PET			HDPE1:1PET		
Wavenumber (cm ⁻¹)	Group [172,174]	Class	Wavenumber (cm ⁻¹)	Group [172,174]	Class	Wavenumber (cm ⁻¹)	Group [172,174]	Class
2916	C-H stretching	alkane	2926	C-H stretching	alkane	2926	C-H stretching	alkane
2847	C-H stretching	alkane	1715	C=O stretching	a,p-unsaturated ester	1712	C=O stretching	carboxylic acid
1462	C-H bending	alkane	1240	C-O stretching	alkyl aryl ether	1235	C-O stretching	alkyl aryl ether
717	C=C bending	aklene	1095	C-O stretching	secondary alcohol	1096	C-O stretching	aliphatic ether
			723	C=C bending	aklene	720	C=C bending	aklene
HDPE1:2PET			PET			Commercial Diesel [43;173]		
Wavenumber (cm ⁻¹)	Group [172,174]	Class	Wavenumber (cm ⁻¹)	Group [172,174]	Class	Wavenumber (cm ⁻¹)	Group [172,174]	Class
2937	C-H stretching	alkane	1713	C=O stretching	carboxylic acid	2953	C-H stretching	alkane
2342	O=C=O stretching	carbon dioxide	1240	C-O stretching	alkyl aryl ether	2922	C-H stretching	alkane
1713	C=O stretching	carboxylic acid	1195	C-O stretching	ester	2870	C-H stretching	alkane
1240	C-O stretching	alkyl aryl ether	723	C=C bending	aklene	2853	C-H stretching	alkane
1094	C-O stretching	aliphatic ether				1464	C-H bending	alkane
723	C=C bending	aklene				667	C=C bending	aklene

4.2 Pyrolysis Behaviour and Product Yields from Selected Ratio of Plastic Waste

The pyrolysis behaviour of plastic waste is a critical determinant of the distribution and yield of its resulting products, namely liquid oil, gaseous fractions, and char. The thermal decomposition of polymers is highly sensitive to the feedstock composition, operating conditions, and the ratio of plastic types used in the process. Blending different polymers can either enhance or hinder pyrolytic efficiency due to synergistic or antagonistic interactions during degradation.

4.2.1 Thermal Degradation Profile Analysis During Pyrolysis Process at Different Ratio of Plastic Waste

Figures 4.8 show the temperature degradation profile analysis for raw material at different mixing ratio. Within one hour and 30 minutes, the highest temperature reached to reach a constant value is at a temperature of 320°C, which involves HDPE. While the lowest temperature reached to reach a constant value is at a temperature of 235°C, which involves a ratio of HDPE 1:1PET. Within 25 minutes, each raw material will produce its first liquid product at a temperature between 130°C to 165°C except HDPE1:2PET ratio and PET which did not produce liquid throughout the experiment. This shows that the pyrolysis process takes place at a relatively low temperature which is below 400°C within one hour and 30 minutes.

Recent studies have demonstrated that HDPE undergoes effective pyrolysis, producing significant liquid oil yields. For instance, Zein et al. (2022) reported that pyrolysis of HDPE at temperatures ranging from 400°C to 450°C resulted in substantial liquid fuel production. The study highlighted that the optimal temperature for maximizing liquid yield was around 450°C [163]. In contrast, PET tends to produce solid residues and gases rather than liquid products during pyrolysis. PET is more resistant to pyrolysis and typically requires higher temperatures for decomposition. The same study noted that PET yielded significantly less oil compared to HDPE under similar conditions. PET yields mostly gaseous products upon undergoing pyrolysis which is around 29.14-38.89 wt.% liquid oils [191]. The co-pyrolysis of HDPE and PET has been explored to enhance liquid fuel production. Blending HDPE with PET affects the pyrolysis behaviour. A study by Tuly et al. demonstrated that adding

polythene (similar to HDPE) to PET increased oil yields and improved oil characteristics. This indicates that higher PET ratios in the mixture can suppress liquid product formation [101].

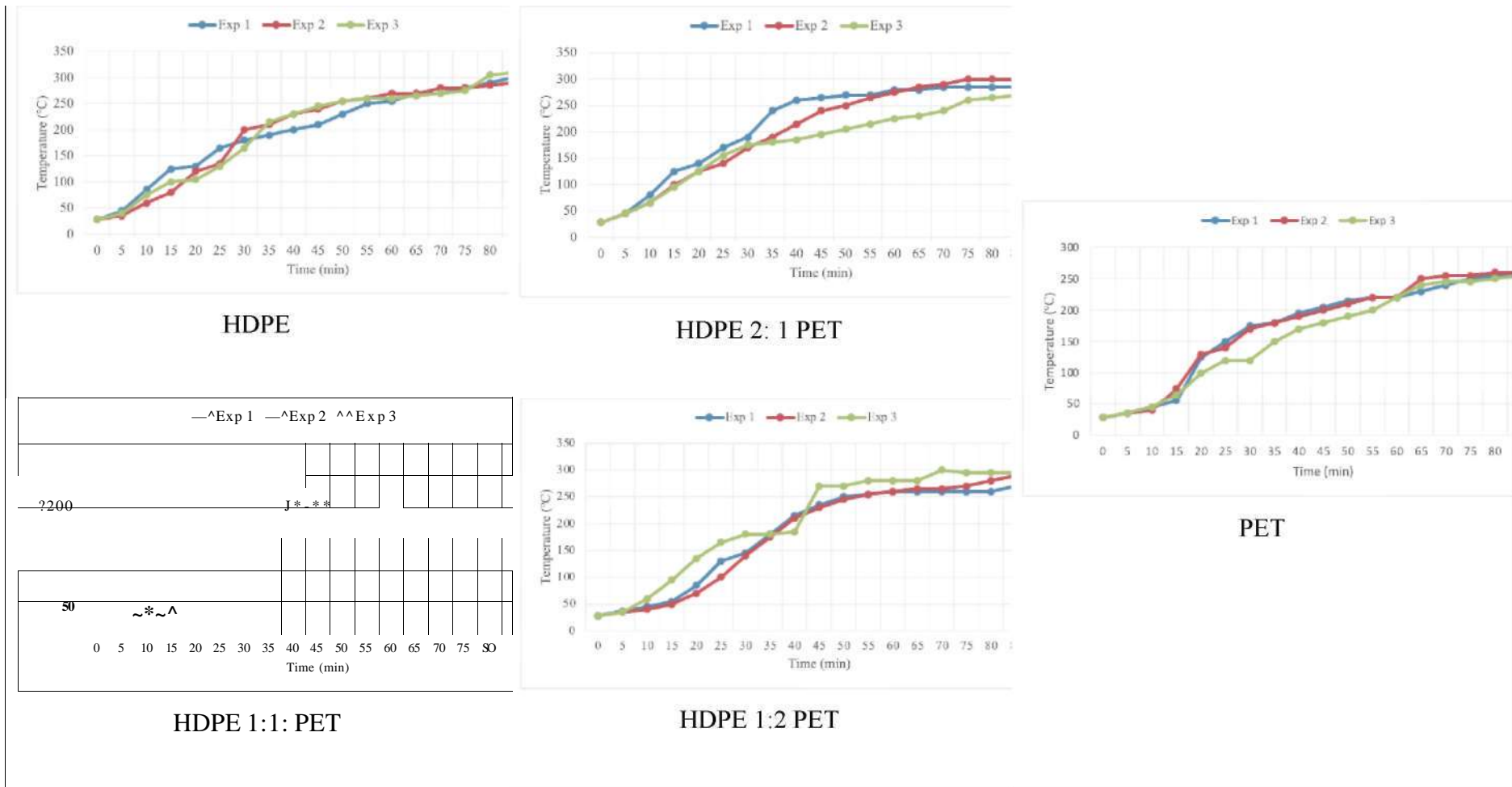


Figure 4.8: Temperature Degradation Profile Analysis for Raw Material at Different Mixing Ratio

4.2.2 Product Yield and Distribution Analysis During Pyrolysis Process at Different Ratio of Plastic Waste

Table 4.9 shows the percentage yield that results after the pyrolysis process for each raw material. Each raw material produced the first liquid between 25 to 30 minutes after the experiment was conducted except for the ratio of HDPE1:2PET and PET which did not produce pyro-fuel. The raw material that produces the highest product oil is HDPE, which on average produces as much as 68%. While PET and HDPE ratio 1:2PET do not produce liquid. The raw material that produces the highest gas content is HDPE1:2PET with an average of 73.11% while the raw material that produces the lowest gas content is HDPE with an average of 5.85%. The highest char production was recorded in the raw material HDPE2:1PET with 41.67% on average while HDPE does not produce char after pyrolysis but produces tar.

It is similar to the findings obtained from other researchers where HDPE has been shown to produce substantial amounts of liquid oil during pyrolysis. For instance, a study by Aisien et al. reported that thermal pyrolysis of HDPE at 500°C yielded 73.9 wt% liquid oil, 23.1 wt% gas, and 3 wt% char. Catalytic pyrolysis further increased the oil yield to 88.8 wt% [54]. In contrast, polyethylene terephthalate (PET) tends to produce higher gas yields and lower oil yields. A study by Kabeyi et al. indicated that pyrolysis of PET at 500°C resulted in 38.9 wt% oil, 52.1 wt% gas, and 8.98 wt% char [18]. Mixing of HDPE with PET affects the pyrolysis product distribution where mixtures with higher PET content tend to produce more gas. For example, a blend of PET and polyolefin mixed plastic waste yielded 30 wt% oil, 35 wt% gas, and 35 wt% char during pyrolysis at 450-500°C. While char yield increases with higher PET content in the mixing. For instance, a mixture of PET/FOIL/PET resulted in 10 wt% oil, 42 wt% gas, and 48 wt% char during pyrolysis at 450-500°C [114].

As a conclusion, HDPE produces the highest oil yield and minimal char [18]. PET and HDPE mixing with higher PET content yield more gas and char, with reduced oil production. It show that the composition of the feedstock significantly influences the distribution of pyrolysis products.

Table 4.9
Percentage Yield of Product after pyrolysis

Ratio raw material	Experiment	Product Yield (%)			
		Tar	Char	Oil	Gas
HDPE	1	24.33	-	70.00	5.67
	2	27.83	-	66.67	5.55
	3	26.33	-	67.33	6.33
HDPE2:1PET	1	-	39.17	28.33	32.50
	2	-	42.00	26.67	31.33
	3	-	43.83	25.00	31.17
HDPE1:1PET	1	-	37.83	2.50	59.67
	2	-	36.33	3.33	60.33
	3	-	40.00	5.00	55.00
HDPE1:2PET	1	-	19.00	-	81.00
	2	-	29.00	-	71.00
	3	-	32.67	-	67.33
PET	1	-	34.33	-	65.67
	2	-	34.00	-	66.00
	3	-	42.67	-	57.33

The pyrolysis of plastic waste leads to the thermal degradation of polymeric materials, resulting in the formation of liquid (pyro-oil), gaseous, and solid (char) products. The distribution of these products is highly dependent on factors such as feedstock composition, temperature, residence time, and heating rate.

From Figure 4.8, HDPE shows the highest constant temperature reached during pyrolysis was 320°C, and the first liquid product was obtained between 130-165°C. While HDPE 2:1 PET ratio and HDPE 1:1 PET ratio showed varying thermal behaviours, with the HDPE 1:1 PET ratio stabilizing at 235°C, which is lower than pure HDPE. The HDPE 1:2 PET ratio and PET alone did not produce liquid, indicating that PET suppresses pyrolysis oil formation in mixed waste streams. PET did not produce liquid throughout the experiment, likely due to its complex decomposition pathway and higher degradation temperature requirements. These results highlight that pyrolysis occurs at relatively low temperatures (below 400°C) within 1 hour and 30 minutes, with liquid products emerging at 130-165°C for select materials.

From product yields and its composition, liquid phase (pyro-Oil) which the primary product in HDPE pyrolysis, containing hydrocarbons ranging from gasoline to diesel-like fractions. In gas phase which consists of hydrogen (H₂), methane (CH₄), carbon monoxide (CO) and volatile hydrocarbons (C₁-C₄), contributing to the energy balance of the process. While in solid residue (char) it composed of unconverted carbonaceous material, with minimal yield from HDPE but potentially higher for PET due to its aromatic structure [112]. From the observations, PET does not easily decompose into liquid hydrocarbons due to decarboxylation of the PET produces a gas consisting mainly carbon monoxide and carbon dioxide [178], which affects the overall yield when mixed with HDPE. Higher HDPE content enhances pyro-oil production, as HDPE undergoes depolymerization at moderate temperatures. While pyrolysis temperature and residence time play a crucial role in optimizing product yields, with liquid formation initiated at relatively low temperatures. These findings emphasize the need for feedstock selection and process optimization to maximize pyro-oil production while minimizing unwanted residues.

4.3 Odour Profiling by Using Low-Cost Wastewater Analysis Captured During Pyrolysis Process

Wastewater profiling serves as an indirect diagnostic tool to monitor the release and behaviour of gaseous and soluble contaminants during pyrolysis. Instead of relying solely on expensive gas-phase instrumentation (e.g., GC-MS, FTIR), this method uses aqueous indicators to simulate and quantify the absorption of pyrolytic emissions in water that mimicking industrial scrubbing systems.

Prior to wastewater characterisation, all instruments and analytical procedures were calibrated and verified in accordance with Standard Methods for the Examination of Water and Wastewater (APHA/AWWA/WEF). pH measurement was standardised using certified buffer solutions (typically pH 4.00, 7.00 and 10.00) following the electrometric method SM 4500-H+ B. Dissolved oxygen (DO) readings were calibrated using water-saturated air (and verified where applicable) consistent with SM 4500-O (membrane/optical probe methods) prior to sample analysis to minimise drift during measurement. Biochemical oxygen demand (BOD) was conducted using the 5-day incubation protocol (20 °C) as specified in SM 5210 B, with DO calibration and measurement performed before and after incubation as required by the method.

Chemical oxygen demand (COD) analysis followed the closed reflux, colorimetric method SM 5220 D, including digestion under controlled conditions and calibration/verification using appropriate blanks and standards as defined by the method. Turbidity measurements were calibrated against formazin-traceable standards and performed using the nephelometric approach described in SM 2130 B, ensuring that readings were taken under stable optical conditions and with clean sample vials to avoid false scattering effects. Total suspended solids (TSS) was determined gravimetrically by filtration and drying at 103-105 °C according to SM 2540 D, including pre-conditioning of filters and repeated drying to constant mass [192].

4.3.1 Wastewater Analysis (DO, BOD, COD, PH, Turbidity and TSS)

Table 4.10 presents data on key water quality parameters for DO, BOD, pH, COD and turbidity which derived from the liquid fraction collected from water bath of gas released from pyrolysis processes involving HDPE and PET mixtures. These parameters were analysed for various ratios of HDPE and PET, with comparisons against the Malaysian Environment Standard for water quality. The DO concentrations ranged from 2.06 to 4.06 mg/L, with pure polymer samples (HDPE and PET) exhibiting the highest values (4.06 and 4.04 mg/L, respectively). The mixed ratios showed a consistent decline in DO, with HDPELIPET presenting the lowest value (2.06 mg/L). Critically, all samples fall significantly below the Malaysian Environment Standard of >7 mg/L, indicating potential challenges in oxygen availability and potential environmental implications.

Table 4.10
D.O, B.O.D, pH and C.O.D., Turbidity and TSS from pyrolysis of HDPE and PET ratio

Ratio	DO. (mg/L)	BOD. mg/L	pH	COD (mg/L)	Turbidity (Ntu)	TSS (mg/L)
HDPE	4.06	4.61	5.56	83.67	9.07	-0.0103
HDPE2:1PET	3.35	3.89	3.93	4993.83	20.69	0.0112
HDPELIPET	2.06	2.83	3.87	8508.56	1.29	-0.0073
HDPE1:2PET	2.24	3.09	3.82	8199.22	1.74	-0.0134
PET	4.04	3.75	4.49	3157.61	0.72	-0.0112

Malaysian Environment Standard	>7	<1	>7	<10	5	<25
--------------------------------------	----	----	----	-----	---	-----

BOD values varied between 2.83 and 4.61 mg/L, with pure HDPE demonstrating the highest value (4.61 mg/L). The mixed ratios exhibited lower BOD values, with HDPE1:1PET showing the minimum (2.83 mg/L). Notably, all samples substantially deviate from the Malaysian standard of <1 mg/L, suggesting elevated levels of biodegradable organic matter in the pyrolysis products.

The scrubber wastewater pH decreases markedly when PET is introduced into the HDPE system. Pure HDPE produced a pH of 5.56, whereas the mixed ratios showed strongly acidic conditions 3.93 (HDPE2:1PET), 3.87 (HDPE1:1PET) and 3.82 (HDPE1:2PET). In contrast, pure PET produced a pH of 4.49 which is acidic but higher than the mixed blends. These results indicate that PET governs the acidification behaviour while HDPE alone contributes minimal acidity.

HDPE is a polyolefin composed only of carbon and hydrogen ($-\text{CH}_2-\text{CH}_2$)_n and does not contain dissociable functional groups. Therefore, its pyrolysis products are predominantly neutral hydrocarbons (alkanes/alkenes) with low water solubility resulting in a comparatively higher pH in the scrubber water.

The reduction in pH after PET addition is more appropriately attributed to PET-derived oxygenated acidic compounds, particularly benzoic acid and related aromatic oxygenates which can dissolve in the scrubber water and depress pH. PET pyrolysis is widely reported to generate benzoic acid as a major product via ester bond scission and secondary reactions of aromatic fragments. This acid formation is consistent with strong acidity observed in PET containing systems.

Although PET is the source of organic acids, the mixed blends especially HDPE1:2PET with pH 3.82 are more acidic than the pure PET. This apparent inconsistency can be justified by process and partitioning effects of synergistic co-pyrolysis effect on oxygenate release. In mixed systems, the presence of molten HDPE can improve heat transfer and volatile transport increasing the release and transfer of PET derived oxygenated species into the gas stream and subsequently into the scrubber water. Such polymer interaction effects in mixed pyrolysis are commonly reported to modify product distribution compared to single-polymer behaviour. Therefore, the lower pH in the blends is interpreted as a result of higher dissolution of

PET derived organic acids into the scrubber water rather than the intrinsic acidity of PET alone.

Overall, the pH trend in Table 4.10 confirms that HDPE is largely pH neutral while PET drives acidification via organic acids notably benzoic acid and the lower pH in blended samples reflects increased absorption or transport of these acids into the scrubber water.

COD values demonstrated the most pronounced variations, ranging from 83.67 to 8508.56 mg/L. Pure HDPE exhibited the lowest COD (83.67 mg/L), while HDPE:1PET recorded the highest (8508.56 mg/L). Remarkably, all samples far exceed the Malaysian standard of <10 mg/L, suggesting extensive chemical oxidation and potential environmental concerns. Turbidity measurements ranged from 0.72 to 20.69 Ntu, with HDPE2:1PET showing the highest turbidity (20.69 Ntu) and pure PET demonstrating the lowest (0.72 Ntu). While the Malaysian standard specifies 5 Ntu, most samples deviate from this benchmark, indicating potential particulate matter and clarity issues. The TSS values appear to be minimal and show both positive and negative values (ranging from -0.0134 to 0.0112 mg/L). The variation suggests potential measurement challenges or extremely low concentrations of suspended solids.

From this data, mixed polymer ratios consistently demonstrate more challenging water quality parameters compared to pure polymer samples. The HDPE:1PET ratio appears to be particularly problematic, showing lowest DO, highest COD and significant deviations from environmental standards. The pyrolysis process generates substantial acidification across all polymer ratios. While significant variations in water quality parameters suggest complex chemical transformations during pyrolysis. This analysis provides a comprehensive overview of the water quality parameters resulting from HDPE and PET pyrolysis, highlighting the complex chemical transformations and potential environmental considerations associated with polymer thermal decomposition

4.3.2 Basic Analysis of Gaseous Product in Pyrolysis

The pyrolysis of HDPE and PET blends reveals distinct gaseous emission profiles, particularly in the evolution of carbon monoxide (CO), lower explosive limit (LEL) indicators, and hydrogen sulphide (ELS). In the present dataset as per Table 4.11, pure HDPE exhibited a pronounced increase in CO concentration, peaking at 312.9 ppm at 85 minutes, while PET alone showed no detectable emissions. This trend aligns with

findings by Al-Salem et al. (2017), who reported CO as a dominant product in HDPE pyrolysis, especially at elevated temperatures exceeding 400°C, due to chain scission and decarboxylation reactions [75]. Similarly, Brems et al. (2011) observed minimal CO formation from PET, suggesting its degradation pathway favours solid residues and aromatic compounds over gaseous outputs [193].

Moreover, LEL values were absent in pure HDPE but emerged in HDPE:PET blends, particularly in the 1:1 and 1:2 ratios, with the highest LEL observed in HDPE1:2PET at 90 minutes. This suggests that blending HDPE with PET enhances the formation of volatile hydrocarbons capable of reaching explosive thresholds. Sharuddin et al. (2016) reported comparable behaviour in mixed plastic pyrolysis, attributing increased LEL values to the synergistic generation of light hydrocarbons and aromatics [79]. Williams and Slaney (2007) further emphasized that polymer blending can significantly alter the volatile yield and composition, supporting the observed enhancement in LEL metrics within the current study [194]. The absence of ELS across all samples is consistent with the chemical nature of HDPE and PET, which are devoid of sulphur containing functional groups. Kaminsky et al. (2004) noted that ELS emissions are typically associated with sulphur rich polymers such as PVC or rubber and are not expected in the pyrolysis of polyolefins or polyesters [195]. This confirms the clean feedstock profile of the materials used and suggests minimal risk of sulphur based toxic emissions under the tested conditions. Overall, the data supports existing literature on the pyrolytic behaviour of HDPE and PET, while highlighting the nuanced effects of polymer blending on gaseous product formation.

Table 4.11
Time-Resolved Emission Characteristics (ELS, CO, and LEL) during Pyrolysis of
HDPE-PET Blends

Time (min)	Raw Material ratio															
	HDPE			HDPE2:1PET			HDPE1:1PET			HDPE1:2PET			PET			
	~th	CO	LE	m	C	LE	m	C	LE	Ifc	C	LE	Ifc	C	LE~	
	S			L	S	O	L	S	O	L	S	O	L	S	O	L
0	0	0	0	0	0	0	0	0	0	0	0	0	0	0	0	0
		24.														0~
5	0	9	0	0	0	0	0	0	0	0	0	0	0	0	0	0
		57.			15.											
10	0	4	0	0	1	0	0	0	0	0	0	0	0	0	0	0
		62.			43.			12.								
15	0	2	0	0	5	0	0	3	0	0	0	0	0	0	0	0
		86.			51.			38.								
20	0	3	0	0	6	0	0	2	0	0	8.2	0	0	0	0	0
		88.			61.			42.			15.					
25	0	8	0	0	3	0	0	1	0	0	9	0	0	0	0	0
		38.			12.											
30	0	6	0	0	1	0	0	7.9	0	0	7.9	0	0	0	0	0
		118			41.			23.								
35	0	.9	0	0	3	0	0	7	0	0	8.1	0	0	0	0	0
		48.			14.			26.								
40	0	2	0	0	5	0	0	7	0	0	9.8	0	0	0	0	0
		40.			16.			35.			13.					
45	0	6	0	0	7	0	0	6	0	0	7	0	0	0	0	0
		77.			23.			41.			17.					
50	0	1	0	0	8	0	0	2	0	0	8	0	0	0	0	0
		153			56.			48.			28.					
55	0	.4	0	0	8	0	0	7	0	0	9	0	0	0	0	0
		51.			45.			38.			35.					
60	0	8	0	0	1	0	0	1	0	0	6	0	0	0	0	0
		65.			56.			41.			39.					
65	0	5	0	0	7	0	0	2	0	0	3	0	0	0	0	0
		25.			13.			11.								
70	0	7	0	0	4	0	0	1	0	0	7.8	0	0	0	0	0
		123			61.			45.			34.					
75	0	.3	0	0	6	0	0	6	0	0	1	0	0	0	0	0
		242			78.			58.			38.					
80	0	.3	0	0	6	0	0	9	0	0	9	0	0	0	0	0

		312			81.			71.			40.				
85	0	.9	0	0	5	0	0	3	0	0	1	0	0	0	0
		282			91.			78.			45.				
90	0	.3	0	0	3	0	0	9	0	0	6	0	0	0	0

4.4 Pyrolytic Oil Quality Evaluation (Physical and Chemical Properties)

The evaluation of pyrolytic oil quality is fundamental in determining its potential as an alternative fuel and its suitability for industrial applications. Pyrolysis of plastic waste produces an oil fraction whose characteristics are strongly influenced by the type of polymer feedstock, reaction conditions, and the presence of catalytic or thermal upgrading steps. A comprehensive assessment of both physical and chemical properties is therefore required to establish benchmarks for fuel performance, stability, and environmental compatibility.

4.4.1 Calorific Value Analysis of the Pyro-Fuel (Physical Properties)

Table 4.12 shows calorific value of plastic waste after the pyrolysis process. The calorific values of all samples increased, demonstrating the concentration of energy-dense carbonaceous materials in the char. HDPE-derived char exhibited the highest calorific value (43,430 J/g), reflecting the retention of carbon-rich structures post-pyrolysis. PET-derived char showed a significant increase (from 22,190 J/g to 31,938 J/g), indicating a reduction in oxygen content and an enhancement of its energy properties. While mixed samples also exhibited higher calorific values, with HDPE1:1PET achieving 43,212 J/g, suggesting improved fuel potential compared to the raw material. If compared with the calorific value data before pyrolysis, which is the raw material of plastic waste, the values obtained from HDPE, PET and their mixing ratio are quite consistent with the values obtained after pyrolysis, which is the oil obtained because of pyrolysis.

The increase in calorific value after pyrolysis suggests that the thermal degradation process enhances the energy density of plastic-derived char. The removal of volatile components and concentration of fixed carbon contribute to this improvement. PET-based samples, despite having a lower initial calorific value, exhibited a more pronounced increase, indicating that pyrolysis effectively enhances their fuel properties.

Table 4.12
Calorific value of sample after the pyrolysis

Ratio Raw Material	After Pyrolysis (J/g)
HDPE	43,430
HDPE2:1PET	39,574
HDPE1:1PET	37,212
HDPE1:2PET	36,966
PET	31,938

4.4.2 Density Analysis of the Pyro-Fuel (Physical Properties)

Table 4.13 shows the density of HDPE, PET and mixing ratio after pyrolysis of plastic waste. HDPE exhibited a density of 0.945 g/cm³, which is slightly lower than its pre-pyrolysis value (0.952 g/cm³). This decrease suggests a reduction in mass due to the release of volatile compounds during the pyrolysis process. HDPE2:1PET ratio showed a density of 0.915 g/cm³, indicating a similar trend of reduced density post-pyrolysis. This decrease is likely due to thermal decomposition and possible structural changes in the polymer matrix [176]. While density values for HDPE1:1PET, HDPE1:2PET, and PET were not available due to lack of pyro-fuel produce after the pyrolysis. The observed decrease in density after pyrolysis for HDPE and HDPE2:1PET suggests that pyrolysis effectively reduces the solid phase mass, leading to structural modifications.

The absence of density values for PET and other mixtures may indicate their higher degradation rate, resulting in minimal solid residue. The results indicate that pyrolysis significantly alters the density of plastic waste, primarily through decomposition and the release of volatile components. The slight decrease in HDPE density suggests that while some carbonaceous char remains, a portion of the polymer degrades into volatile products [196]. The increase in HDPE2:1PET density could be due to the formation of a more compact char structure. The absence of measurable density for PET and other blends suggests a higher degradation rate, leaving minimal solid residue.

Table 4.13
 Density of HDPE, PET and mixing ratio after pyrolysis

Ratio Raw Material	Density (g/cm ³)
HDPE	0.945
HDPE2:1PET	0.915
HDPE1:1PET	n.a
HDPE1:2PET	n.a
PET	n.a

Based on Table 4.13, the density of the HDPE-PET samples after pyrolysis is reported as n.a., which appears inconsistent when compared with the pre pyrolysis densities presented in Table 4.2. Prior to pyrolysis, the incorporation of PET into HDPE resulted in an overall increase in density due to the higher intrinsic density of PET relative to HDPE. Therefore, a measurable density value for the HDPE-PET mixture after pyrolysis would be expected, provided that sufficient solid residue was obtained. The absence of density data after pyrolysis is likely attributed to experimental limitations, particularly the small amount of solid char residue produced, which was insufficient for accurate density determination using the available measurement method. Pyrolysis of HDPE-PET blends typically results in a significant reduction in solid yield due to extensive volatilisation especially at higher PET contents, thereby restricting post pyrolysis physical characterisation. Consequently, the n.a. designation reflects measurement constraints rather than the absence of density changes in the pyrolysed material.

4.4.3 Flash Point Analysis of the Pyro-Fuel (Physical Properties)

The flash point of pyro-fuel obtained from HDPE, PET and their mixtures was analysed based on different composition ratios. The results indicate that the flash point varies depending on the ratio of HDPE and PET used in the pyrolysis process. From Table 4.14, the individual pyro-fuel derived from HDPE has the lowest flash point at 12°C, whereas PET-derived pyro-fuel exhibits the highest flash point at 36°C. The mixing ratios of HDPE and PET show an increasing trend in flash points as the proportion of PET increases. Specifically, HDPE2:1PET ratio has a flash point of 15°C. While HDPE1:1PET ratio exhibits a flash point of 20°C. while HDPE1:2PET has a flash point of 24°C.

The flash point of pyro-fuel is significantly influenced by the composition of raw materials. PET-derived pyro-fuel has a higher flash point compared to HDPE-derived pyro-fuel. Increasing the proportion of PET in HDPE-PET mixtures leads to an increase in the flash point of the resulting pyro-fuel. This trend suggests that blending PET with HDPE can enhance the safety characteristics of pyro-fuel by reducing its flammability.

Table 4.14
Flash point of HDPE, PET and mixing ratio after pyrolysis

Ratio Raw Material	Flash Point (°C)
HDPE	12.0
HDPE2:1PET	15.0
HDPE1:1PET	20.0
HDPE1:2PET	24.0
PET	36.0

4.4.4 Chemical Content Analysis of the Pyro-Fuel by Using GC-MS (Chemical Properties)

Figure 4.9 describes a series of GC-MS graphs showing the relationship between carbon chain length and the normalized mass percentage of compounds for various pyrolytic oils derived from HDPE and PET mixtures. For HDPE, the normalized mass percentage values are plotted against carbon chain lengths, providing insight into the product composition. The distribution likely reflects the prevalence of specific hydrocarbon ranges, indicative of HDPE's decomposition behaviour under pyrolytic conditions. Such data is essential to determine the efficacy of HDPE pyrolysis for producing target compounds within specific carbon ranges. Oxalic acid, allyl pentadecyl ester ($C_{20}H_{36}O_4$) displays the highest peak with normalized mass of 9.09%. Main components of chemicals in this pyro-oils are in the range of C9 to C20.

For the HDPE ratio of 2:1 with PET, the graph reveals how the introduction of PET affects the carbon chain distribution in pyrolytic oil. This figure provides a comparative view of compound distribution relative to pure HDPE pyrolysis, showing shifts in mass percentage values. The results indicate how adding PET at this ratio may alter the production of longer or shorter chain hydrocarbons due to interaction effects between HDPE and PET during pyrolysis. Pentane, 2,2-dimethyl (C_7H_{16}) displays the highest peak with normalized mass of 8.9%. Main components of chemicals in this pyro-oils are in the range of C7 to C9.

The carbon chain distribution in a ratio of HDPE1: 1PET pyrolytic oil influence of equal proportions of HDPE and PET on product composition. Changes in the normalized mass percentages across the carbon range reflect a distinctive profile, suggesting that the pyrolysis pathways and the resultant hydrocarbon distribution are markedly affected at this mixture ratio. The data here aids in understanding the potential for balanced HDPE and PET blends in pyrolytic processes. Sulfurous acid, 2-ethylhexyl hexyl ester ($C_{14}H_{30}O_4S$) displays the highest peak with normalized mass of 4.85%. Main components of chemicals in this pyro-oils are in the range of C13 to C44.

In the case of a HDPE1:2PET ratio, the graph shows a significant shift in hydrocarbon chain distribution, demonstrating how a higher PET content influences pyrolysis products. The normalized mass percentages across carbon values provide an indication of enhanced or reduced production of specific hydrocarbon types. This figure suggests that increasing PET content may favour the formation of carbon chain lengths,

critical for applications targeting certain molecular weight ranges. Sulfurous acid, pentadecyl 2-pentyl ester ($C_{20}H_{42}O_3S$) displays the highest peak with normalized mass of 10.71%. Main components of chemicals in this pyro-oils are in the range of C10 to C20.

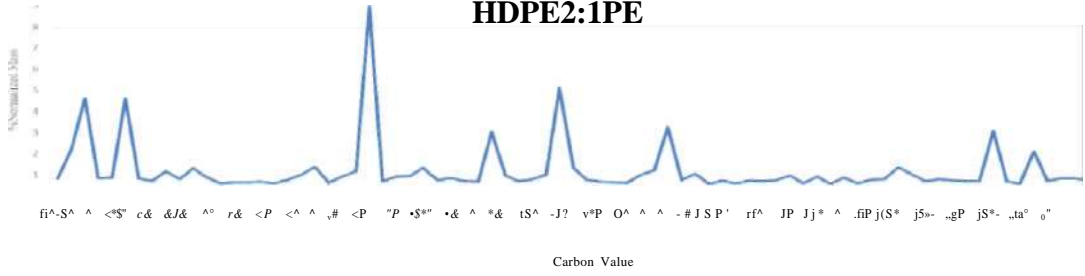
The carbon distribution in pyrolytic oil obtained from pure PET mapping the normalized mass percentages over different carbon values. The data here serves as a baseline for understanding PET's pyrolysis behaviour without HDPE influence, showing a characteristic pattern that likely differs from HDPE due to PET's aromatic and ester content. This profile is crucial for comparing PET's unique degradation pathways to mixed HDPE-PET pyrolysis processes. Acetamide, N-2-propenyl (C_5H_9NO) displays the highest peak with normalized mass of 10.31%. Main components of chemicals in this pyro-oils are in the range of C7 to C13.

Overall, this series of figures systematically shows how varying the HDPE to PET ratio impacts the carbon chain distribution and normalized mass percentage of pyrolysis products, providing valuable data for optimizing hydrocarbon yields from mixed plastic waste.

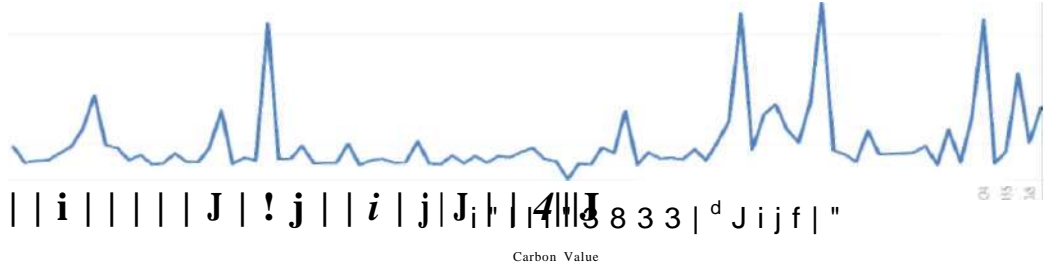
HDPE



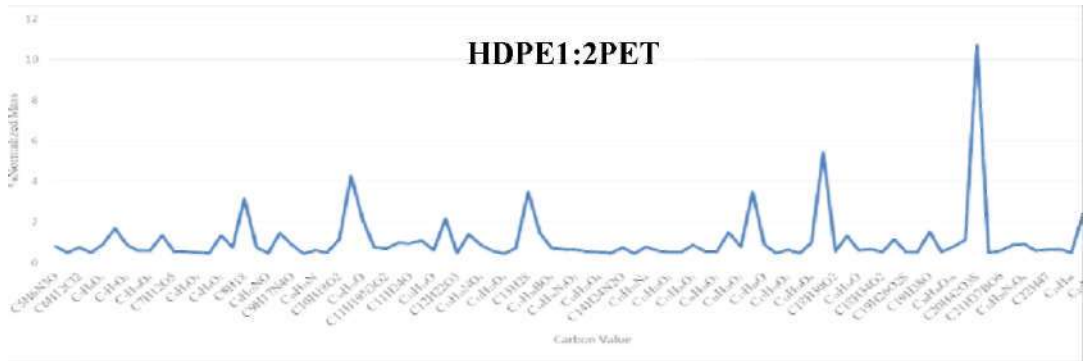
HDPE2:1PE



HDPE1:1PET



HDPE1:2PET



PET

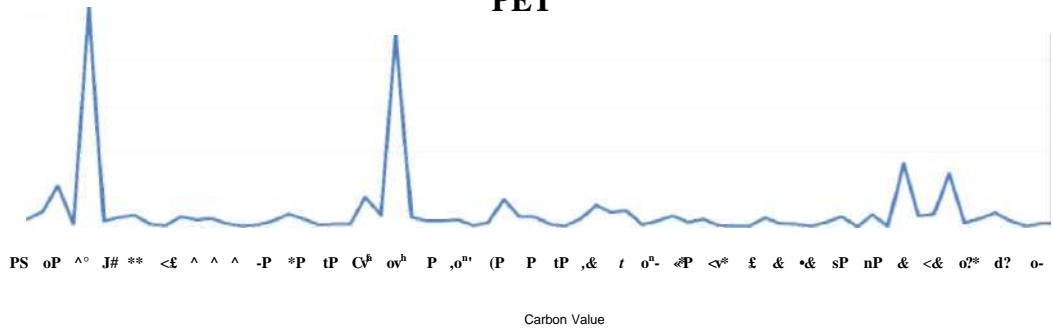


Figure 4.9
Carbon value for different ratio of plastic waste Vs % Normalized Mass

Table 4.15 outlines the GC-MS analysis of the liquid fraction from pyrolysis of HDPE and PET at different blend ratios, with data on aliphatic and aromatic components across carbon chain length categories (C5-C9, C10-C13, >C13). The GC-MS results for the liquid fraction from pure HDPE pyrolysis reveal a high percentage of aliphatic hydrocarbons across the carbon ranges. The C5-C9 range constitutes 35.13% aliphatic compounds, while the C10-C13 range holds 34.06%, and >C13 makes up 16.48%. Aromatic hydrocarbons are minimal, showing values of 1.93%, 3.35%, and 0.67% across the respective carbon ranges. This indicates that HDPE primarily decomposes into aliphatic hydrocarbons with shorter carbon chains, reflecting HDPE's straightforward structure and its tendency to produce lighter fractions.

In the 2:1 HDPE:PET pyrolysis, the liquid fraction predominantly consists of aliphatic hydrocarbons in the C5-C9 range, accounting for 64.94%). The C10-C13 range decreases to 19.83%, while the >C13 range is further reduced to 4.87%. The aromatic hydrocarbon presence is minimal, with only 0.74% observed in the C10-C13 range. These results suggest that the addition of PET at this ratio increases the proportion of shorter-chain aliphatic hydrocarbons, likely due to the interaction effects that facilitate lighter hydrocarbon formation.

With a 1:1 HDPE to PET ratio, the aliphatic distribution shifts, showing 20.21% in the C5-C9 range, 26.86% in the C10-C13 range, and a significantly higher 43.79% in the >C13 range. Aromatic compounds appear more consistently, with 3.72%, 1.08%, and 0.73% across the respective carbon ranges. This balanced ratio introduces a noticeable increase in longer-chain aliphatic hydrocarbons and a modest aromatic presence, indicating a more complex decomposition profile.

For the 1:2 HDPE:PET blend, the liquid fraction reveals a substantial proportion of longer-chain hydrocarbons. Aliphatic content in the C5-C9 range drops to 11.28%, while the >C13 range rises markedly to 42.13%). Aromatic hydrocarbons show a significant increase, with 8.51% in C5-C9, 2.55% in C10-C13, and 11.36% in >C13. These results suggest that higher PET content in the pyrolysis feedstock promotes the formation of longer-chain aliphatic and aromatic compounds, possibly due to PET's inherent aromatic structure.

The liquid fraction from pure PET pyrolysis predominantly features shorter aliphatic hydrocarbons, with 53.63% in the C5-C9 range and 30.61% in the C10-C13 range. The >C13 range accounts for only 5.52% aliphatic content. Aromatic hydrocarbons remain minimal, with 1.55% in C5-C9 and 0.76% in >C13. This

composition highlights PET's propensity to yield shorter aliphatic compounds under pyrolytic conditions, likely due to its ester linkages and aromatic backbone.

This analysis reveals how varying HDPE and PET ratios impact the carbon chain length and aromatic/aliphatic composition in the liquid pyrolysis fraction. Increasing PET content promotes longer-chain and aromatic hydrocarbons, while higher HDPE proportions favour aliphatic compounds with shorter chains. These findings are pivotal for tailoring pyrolysis processes to optimize hydrocarbon outputs based on desired carbon range and hydrocarbon type.

Table 4.15
Component in liquid fraction obtained from pyrolysis of HDPE and PET ratio using GC-MS

Component Ratio	%Normalized Mass	
	Aliphatic	Aromatic
HDPE		
C5-C9	35.13	1.93
C10-C13	34.06	3.35
>C13	16.48	0.67
HDPE2:1PET		
C5-C9	64.94	0
C10-C13	19.83	0.74
>C13	4.87	0
HDPE1:1PET		
C5-C9	20.21	3.72
C10-C13	26.86	1.08
>C13	43.79	0.73
HDPE1:2PET		
C5-C9	11.28	8.51
C10-C13	23.4	2.55
>C13	42.13	11.36
PET		
C5-C9	53.63	1.55
C10-C13	30.61	0
>C13	5.52	0.76

Table A. 1a, A. 1b, A. 1c, A. 1d and A. 1e in Appendix A show the result of GCMS for each HDPE, ratio HDPE2:1PET, ratio HDPE1:1PET, ratio HDPE1:2PET and PET. In Table A. 1a, the GC-MS results reveal various compounds in HDPE-derived pyrolytic oil, with most identified as aliphatic or aromatic hydrocarbons. Aliphatic compounds primarily include alkanes, alkenes, amines, alcohols, and esters, representing a wide range of structural types, including linear, branched, and cyclic forms. Aromatic compounds are mostly heterocyclics, indicating complex pyrolysis behaviour yielding both simple hydrocarbons and nitrogen-containing rings, with notable aromatic heterocyclics such as 1H-Tetrazole, 5-methyl-, and 1H-Pyrazole, 4-iodo.

Table A. 1b details GC-MS data for pyrolytic oil from an HDPE ratio of 2:1 of PET, highlighting aliphatic hydrocarbons as predominant. Compounds such as 1-Pentanol, 4-methyl-, and Cyclobutanemethanol signify diverse alcohols, while 1-Pentyn-3-ol, 3,4-dimethyl- represents alkyne-alcohol compounds. Notably, lactams and amines present indicate potential for functionalized hydrocarbons.

Table A. 1c shows that with an HDPE1:1PET ratio, hydrocarbons remain predominantly aliphatic with varied functionalities, including esters and alkenes, such as Pentane, 2,2-dimethyl-, and Nitric acid, nonyl ester. Noteworthy is the increased presence of alkynes and amines, reflecting a potential shift towards higher functionalization and complexity with equal proportions of PET.

Table A. 1d displays that the HDPE1:2PET ratio pyrolytic oil yields a complex mixture of aromatic and aliphatic compounds. Benzoic acid and Dextroamphetamine signify aromatic contributions, while esters and ketones like Cyclopentanecarboxylic acid and 3-Buten-1-one, 2,2-dimethyl-1-phenyl indicate functional diversification. This composition suggests that higher PET ratios may enhance aromaticity in the pyrolysis products.

Table A. 1e presents the GC-MS profile of pure PET pyrolytic oil, showing dominant aliphatic compounds and a notable concentration of nitrile, ester, and amine functionalities. The presence of compounds like 1,2-Cyclohexanediamine and Oxirane, butyl- reflects high nitrogen and oxygen content, which aligns with PET's composition, further suggesting degradation pathways that yield functionalized hydrocarbons with nitrogen and oxygen-bearing groups. This analysis provides insight into the influence of PET content in pyrolysis mixtures with higher PET ratios correlating to an increase in aromatic compounds and heterocyclic structures.

4.4.5 Analysis of Char Obtained from Pyrolysis Process by Using Proximate Analysis

Table 4.16 shows the proximate analysis result of HDPE, PET and mixing ratio after pyrolysis of plastic waste. The proximate analysis of char derived from the pyrolysis of high-density polyethylene (HDPE), polyethylene terephthalate (PET), and their blends ratio reveals significant compositional variations. The char from pyrolyzed HDPE exhibits low moisture content (0.85%), high volatile matter (82.85%), considerable ash content (12.85%), and low fixed carbon (3.45%). The char from HDPE2:1PET ratio shows low moisture content (0.65%), very high volatile matter (93.05%), moderate ash content (5.4%), and very low fixed carbon (0.9%). The char from HDPE1:1PET has low moisture content (1%), high volatile matter (88.45%), negligible ash content (0%), and moderate fixed carbon (10.55%). While the char from HDPE1:2PET ratio displays very low moisture content (0.1%), moderate volatile matter (68.99%), significant ash content (14.91%), and considerable fixed carbon (16%). The char from pyrolyzed PET exhibits a higher moisture content (2.5%), high volatile matter (76.15%), negligible ash content (0%), and substantial fixed carbon (21.35%).

The moisture content varies across different feedstock ratios, ranging from 0.10% for HDPE1:2PET to 2.50% for PET. The results indicate that the highest volatile matter content is observed for HDPE2:1PET (93.05%), while the lowest is recorded for HDPE1:2PET ratio (68.99%). The highest ash content (14.91%) is observed for HDPE1:2PET ratio, while some samples, such as PET and HDPE1:1PET contain no detectable ash. The results indicate that PET has the highest fixed carbon content (21.35%), followed by HDPE1:2PET (16.00%), while HDPE2:1PET exhibits the lowest value (0.90%). The variations in these parameters reflect the distinct chemical compositions and thermal degradation pathways of HDPE and PET. The blending ratios significantly influence the characteristics of the resulting char, which is essential for optimizing pyrolysis conditions and tailoring the properties of the char for specific applications.

If compared to before and after pyrolysis, the post-pyrolysis composition indicates the thermal decomposition of the raw materials, resulting in the release of volatile compounds and the formation of char, which is characterized by increased ash and fixed carbon content. The variations in these parameters are influenced by the composition of the raw materials used in pyrolysis. The presence of polyethylene

terephthalate (PET) increases the fixed carbon content, while high-density polyethylene (HDPE) contributes to higher volatile matter.

The results demonstrate that pyrolysis effectively transforms plastic waste by reducing volatile matter and increasing fixed carbon and ash content. The increase in fixed carbon content indicates the formation of char, which can be utilized in energy applications or as a precursor for carbon-based materials. PET derived char exhibited the highest fixed carbon content (21.35%), making it a promising candidate for high-carbon applications. The variations in ash content suggest different thermal degradation behaviours, influenced by the polymer composition [197]. Blending HDPE and PET affects the proximate composition of the resulting char where HDPE-rich blends such as HDPE2:1PET ratio have a higher volatile matter content and lower fixed carbon, indicating a greater release of volatiles during pyrolysis. While PET rich blends such as HDPE1:2PET ratio exhibit increased fixed carbon and ash content, suggesting a more significant formation of solid residues. These variations are attributed to the distinct thermal degradation pathways of HDPE and PET, where HDPE decomposes primarily into volatiles, while PET tends to form more stable char structures[198]. The shift in proximate composition following pyrolysis reflects the thermal degradation of the polymeric materials. The decrease in volatile matter and the increase in fixed carbon and ash content signify the formation of a carbonaceous residue with altered properties. These variations are influenced by the feedstock composition, blending ratios and pyrolysis conditions [199].

Table 4.16
The proximate analysis result of HDPE, PET and mixing ratio after pyrolysis

Ratio Raw Material	Moisture Content %	Volatile Matters %	Ash %	Fixed Carbon %
HDPE	0.85	82.85	12.85	3.45
HDPE2:1PET	0.65	93.05	5.4	0.90
HDPE1:1PET	1.00	88.45	0.00	10.55
HDPE1:2PET	0.10	68.99	14.91	16.00
PET	2.50	76.15	0.00	21.35

From Table 4.16, the obtained values do not exhibit a fully consistent trend across all samples. This inconsistency can be primarily attributed to experimental and material related variations rather than fundamental changes in polymer behaviour. During and after pyrolysis, HDPE-PET systems undergo extensive thermal degradation, volatilisation and phase transformation resulting in heterogeneous solid residues with non-uniform morphology and composition. Such heterogeneity can lead to variability in the measured values particularly when characterisation is performed on small sample quantities.

In addition, the low solid yield after pyrolysis especially for samples with higher PET content limits repeatability and measurement accuracy. Minor differences in char particle size, porosity and ash distribution can significantly influence bulk and apparent measurements thereby contributing to the observed fluctuations. Furthermore, manual handling, sample positioning and instrument sensitivity effects may amplify these variations when the remaining residue mass approaches the lower detection limit of the experimental setup.

Therefore, the inconsistent values reported in Table 4.16 reflect the limitations associated with post-pyrolysis characterisation of low-yield and heterogeneous residues rather than systematic errors. The overall trends should thus be interpreted qualitatively with emphasis on relative behaviour between samples rather than absolute numerical consistency.

4.5 Interpretive Analysis of Reaction Kinetics, Emission Behaviour and Oil Quality

The comprehensive evaluation of pyrolysis performance requires not only the characterization of individual parameters but also an integrated interpretation of the interrelationships between reaction kinetics, emission behaviour and oil quality. Reaction kinetics provides fundamental insights into the thermal degradation mechanisms of polymeric feedstocks, defining activation energies, decomposition pathways, and the influence of process variables such as temperature and residence time. These kinetic parameters directly affect both the rate and extent of conversion, thereby shaping the distribution and composition of products. By integrating these three dimensions which are reaction kinetics, emission profiles, and oil quality, this section seeks to provide a holistic interpretive framework. Such an approach not only enables

a deeper understanding of the fundamental science of plastic pyrolysis but also informs strategies for optimization, ensuring that the process can be scaled in a manner that is both environmentally sustainable and industrially viable.

4.5.1 Correlation Between the Wastewater Analysis Result with Temperature Profile, Reaction Time and Plastic Mixing Ratio

Wastewater generated during the pyrolysis of plastic waste provides valuable diagnostic information on the underlying reaction dynamics and product pathways. The aqueous phase often contains a complex mixture of dissolved organic compounds, acids, and trace volatiles that originate from thermal degradation and condensation processes. Analysing these constituents enables the identification of secondary reactions and degradation intermediates that are not easily captured through direct gas or oil analysis.

The correlation of wastewater characteristics with key process parameters—namely temperature profile, reaction time and plastic mixing ratio offers a unique perspective on process behaviour. Temperature governs the extent of polymer chain scission and secondary cracking, which in turn influences the concentration and type of aqueous contaminants. Reaction time determines the degree of conversion and accumulation of intermediates, while the mixing ratio of plastics such as HDPE and PET introduces synergistic or antagonistic effects that alter both emission and condensate chemistry. By establishing these correlations, wastewater analysis can serve as a complementary monitoring tool to assess pyrolysis efficiency, environmental impact, and fuel quality potential.

4.5.1.1 OF AT Analysis of the Process

The One-Factor-At-a-Time (OFAT) analysis was conducted to investigate the effect of time (independent variable) on temperature (dependent variable) during the thermal processing of HDPE, HDPE2:1 ratio, HDPE1:1PET ratio, HDPE1:2PET ratio dan PET plastic waste. The experiment was designed to maintain constant pressure at 1 atm while systematically varying the time and measuring the corresponding temperature changes.

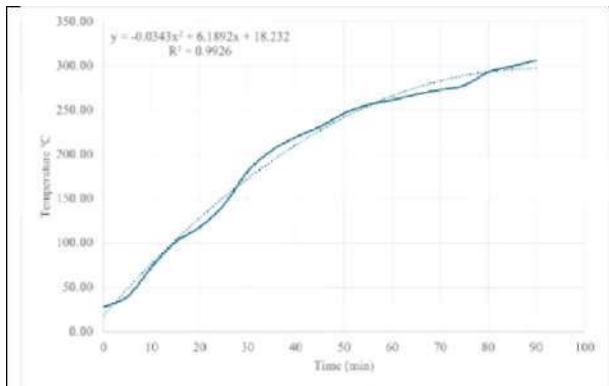
Figure 4.10 show OF AT analysis with effect of time on temperature for HDPE, PET and mixing ratio after pyrolysis. For FIDPE, the temperature increased non linearly with time, likely due to FIDPE's gradual softening and decomposition at higher temperatures. For FIDPE2:1PET and FIDPE1:1PET ratio its exhibited a similar trend, but the presence of PET altered the heating rate, likely due to PET's different thermal properties. While for HDPE1:2PET ratio, it showed a more pronounced deviation, indicating that a higher PET content significantly influences heat transfer and degradation kinetics.

The temperature profile differed from FIDPE, confirming PET's higher melting and degradation temperatures. The collected data from Figure 4.18 was analysed, and a quadratic trendline was fitted to describe the relationship between time and temperature. The quadratic equation captures the non-linear relationship between time and temperature during the thermal processing of plastics. A positive "a" value suggests that the temperature increase slows down at longer times due to heat transfer limitations or polymer degradation behaviour. A negative "a" value would indicate a decreasing trend, but this is unlikely in heating experiments. At the same time, the R^2 value which is Coefficient of Determination is also sought to measure how well the quadratic equation fits the experimental data. The objective was to understand the thermal behaviour of each plastic type and blend, which is essential for optimizing pyrolysis, recycling, or energy recovery processes.

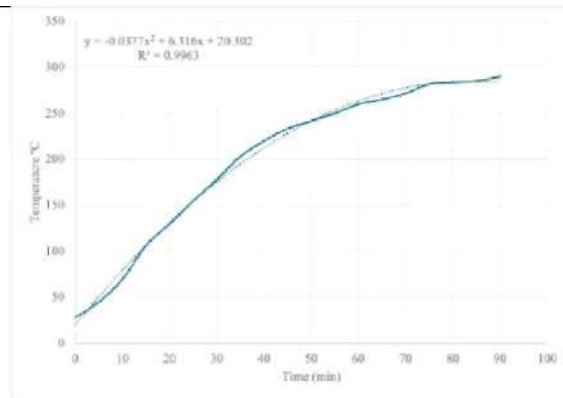
Table 4.18 shows quadratic trendline equation and R^2 value from pyrolysis of HDPE and PET ratio. The presence of a negative quadratic coefficient suggests that the rate of temperature increase gradually slows down as time progresses. The positive linear term suggests a steady temperature increase over time. HDPE2:1PET ratio has the highest R^2 value (0.9963), suggesting the most predictable temperature progression. HDPE1:2PET ratio shows the steepest temperature curve, implying greater thermal instability due to higher PET content. While pure PET and HDPE exhibit slightly different thermal behaviours, with PET requiring higher energy input for degradation.

The R^2 values are all above 0.97, indicating a highly accurate quadratic fit. The slight variations in R^2 suggest that HDPE-PET interactions affect heat distribution and thermal stability. The lower R^2 for HDPE1:2PET ratio (0.9784) may indicate greater experimental variability due to PET's higher degradation temperature. The quadratic equations effectively model the temperature evolution in pyrolysis of HDPE, PET, and their mixtures. Higher PET content increases thermal resistance, affecting temperature

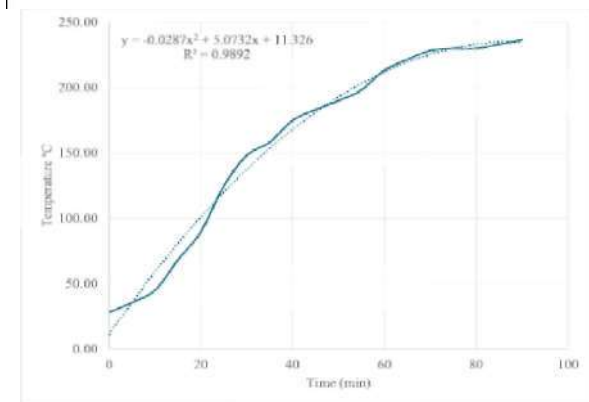
rise. While the HDPE2:1PET ratio offers the most stable heating behaviour, as indicated by the highest R^2 . The quadratic model is highly reliable, with $R^2 > 0.97$ in all cases, making it a strong predictive tool for optimizing pyrolysis conditions.



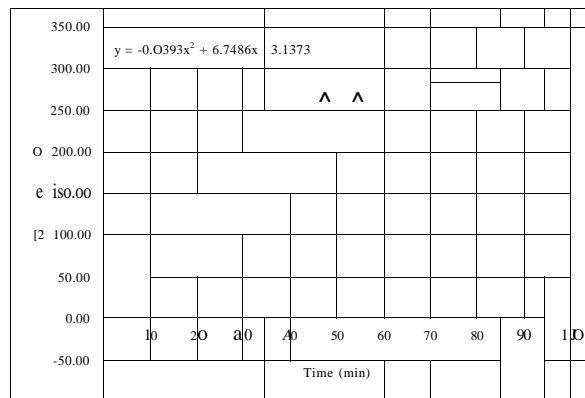
HDPE



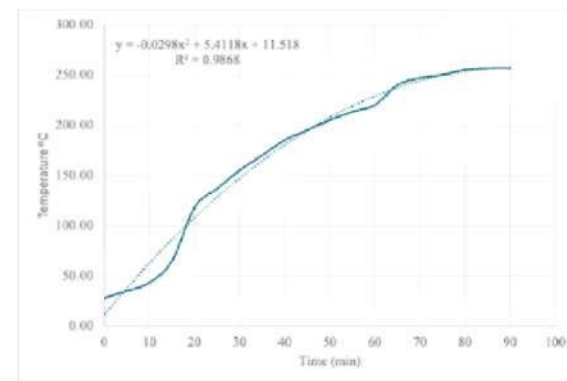
HDPE2:1PET



HDPE1:1PET



HDPE1:2PET



PET

Figure 4.10 OFAT analysis with effect of time on temperature for HDPE, PET and mixing ratio after pyrolysis

Table 4.17

Quadratic trendline equation and R^2 value from pyrolysis of HDPE and PET ratio

Ratio Raw Material	Quadratic Trendline Equation	R^2 Value
HDPE	$T = -0.0343t^2 + 6.1892t + 18.232$	0.9926
HDPE2:1PET	$T = -0.0377t^2 + 6.316t + 20.302$	0.9963
HDPE1:1PET	$T = -0.0287t^2 + 5.0732t + 11.326$	0.9892
HDPE1:2PET	$T = -0.0393t^2 + 6.7486t + 3.1373$	0.9784
PET	$T = -0.0298t^2 + 5.4118t + 11.518$	0.9868

T = temperature ($^{\circ}$ C)

t = time (minutes).

The OFAT analysis confirms that time significantly affects the thermal behaviour of HDPE, PET, and their blends. The results suggest that HDPE exhibits a smooth temperature increase, making it relatively easier to process thermally. PET requires higher temperatures for decomposition, influencing the thermal performance of mixed-plastic systems. While the HDPE-PET ratio plays a crucial role in determining the heating characteristics, with higher PET content causing a shift in the temperature profile. These insights are valuable for optimizing plastic waste pyrolysis and recycling strategies, ensuring efficient thermal conversion while minimizing energy consumption. To achieve desired thermal conditions, the model can be used to estimate processing times accurately, reducing energy consumption and improving yield quality.

4.5.1.2 Statistical Analysis of The Process by Using Linear Regression ANOVA

In the pyrolysis of plastic waste, ANOVA (Analysis of Variance) in Regression Analysis is crucial for evaluating how well different process variables (e.g., time, temperature, heating rate, and composition) affect the thermal degradation process. It helps determine the statistical significance of these factors and whether they have a meaningful impact on the pyrolysis efficiency and product yield.

Table 4.18 is summarized of ANOVA analysis from pyrolysis of HDPE and PET ratio derive from Table A. 5a, A. 5b, A. 5c, A. 5d and A. 5e from Appendix 5. High R^2 values which all raw materials are above 0.89 indicates that time and temperature strongly influence pyrolysis outcomes across all plastic compositions. The

pyrolysis process is highly predictable using the regression models. From comparison Between HDPE and PET, HDPE ($R^2 = 0.9251$) shows slightly better model predictability than PET ($R^2 = 0.9214$), suggesting more uniform degradation. PET requires higher degradation temperatures, affecting its statistical behaviour in the model. From HDPE-PET mixing ratio, HDPE2:1PET ratio ($R^2 = 0.9066$) and HDPE1:2PET ratio ($R^2 = 0.8987$) indicate that PET content alters thermal degradation, making the process slightly less predictable. Higher PET content (HDPE1:2PET) has the lowest R^2 , confirming that PET introduces more variability in pyrolysis behaviour.

The ANOVA analysis confirms that time and temperature significantly impact the pyrolysis of HDPE, PET, and their mixtures. The high R^2 values indicate that the regression models are reliable predictors of pyrolysis behaviour. HDPE exhibits more stable thermal degradation compared to PET while increasing PET content introduces more variability, requiring further process optimization. These findings can guide process control strategies to improve pyrolysis efficiency and product quality.

The p-value in ANOVA tests determines whether an independent variable (e.g., time, temperature) significantly affects the pyrolysis process of HDPE, PET, and their mixtures. A p-value < 0.05 indicates statistical significance, meaning the variable has a meaningful effect on the process. From the experiment, all p-values are significantly below 0.05, confirming that time and temperature have a statistically significant effect on pyrolysis behaviour across all plastic compositions. The lowest p-value which is PET suggests that PET has the strongest statistical significance, likely due to its higher degradation temperature affecting the pyrolysis process. All HDPE:PET mixing ratio shows significant p-values, indicating that plastic composition plays a crucial role in thermal behaviour. The extremely low p-values confirm that time and temperature strongly influence the pyrolysis of HDPE, PET and their mixtures. These results validate the regression models and highlight the importance of optimizing processing conditions for efficient thermal decomposition.

Table 4.18
Summarized of ANOVA analysis from pyrolysis of HDPE and PET ratio

	Raw Materials				
	HDPE	HDPE2:1PET	HDPE1:1PET	HDPE1:2PET	PET
Multiple R	0.961	0.952	0.957	0.948	0.960
R ²	0.925	0.907	0.917	0.899	0.921
Adjusted R ²	0.921	0.901	0.912	0.893	0.917
p-value	5.36 x 10 ⁻¹¹	3.54 x 10 ⁻¹⁰	1.33 x 10 ⁻¹⁰	7.06 x 10 ⁻¹⁰	8.1 x 10 ⁻¹¹

4.5.2 Reaction Kinetics

The thermal degradation data from this study reveal that PET undergoes decomposition at a relatively lower temperature range compared to HDPE, consistent with prior findings. As noted in the thermogravimetric results, PET degradation was observed between approximately 350 °C and 465 °C, while HDPE exhibited a higher stability range initiating decomposition at temperatures above 400 °C. When mixed at ratios such as HDPE:PET (2:1, 1:1, and 1:2), the degradation behaviour indicated synergistic effects with the onset temperature and reaction rate shifting depending on the dominance of each polymer. This observation underscores the importance of feedstock composition in determining kinetic pathways.

Furthermore, the time-dependent emission profiles (e.g., CO release reaching 312.9 ppm at 85 minutes for pure HDPE compared with lower peak values in mixed ratios) provide indirect evidence of kinetic variability. Faster degradation rates in PET rich mixtures contributed to earlier release of gaseous by-products, while HDPE rich mixtures prolonged the reaction time resulting in delayed but more sustained gas generation. These findings reinforce the correlation between kinetic parameters and observable emission behaviour.

The interpretive analysis of these results highlights that reaction kinetics not only governs the conversion efficiency of plastics into valuable products but also shapes the environmental footprint of the process. By integrating kinetic modelling with empirical gas and oil data, this study provides a framework for optimizing pyrolysis conditions to balance high product yield with reduced emissions.

4.5.3 Emission Behaviour

The emission behaviour during pyrolysis provides essential insights into the environmental implications of thermochemical conversion of plastic waste. The primary emissions observed in this study include hydrogen sulfide (H₂S), carbon monoxide (CO), and lower explosive limit (LEL) related volatile gases, each reflecting specific aspects of the degradation pathways and feedstock composition. Monitoring these parameters across different HDPE:PET ratios highlights how polymer chemistry governs both emission intensity and temporal distribution.

The data reveal that CO was the dominant gaseous emission across all feedstock compositions, with its concentration increasing significantly with reaction time. For example, pure HDPE produced peak CO concentrations of 312.9 ppm at 85 minutes, whereas PET-rich mixtures (HDPE:PET = 1:2) exhibited a lower peak of 45.6 ppm at 90 minutes. This trend indicates that HDPE undergoes more extensive thermal cracking of its C-C backbone, generating higher yields of CO while PET decomposition contributes smaller but earlier releases due to cleavage of ester linkages.

In contrast, H₂S emissions were consistently absent or negligible across all tested conditions, suggesting that the selected feedstock contained minimal sulfur bearing additives or contaminants. This result is environmentally significant as it reduces concerns related to SO_x formation and acid gas pollution which are common in the pyrolysis of mixed municipal plastics.

The LEL values while detected intermittently, reflected the accumulation of combustible volatiles during decomposition. Mixed plastic systems particularly HDPE:PET blends, exhibited moderate LEL responses compared to pure HDPE. This suggests that co-pyrolysis may dilute or redistribute the release of highly flammable volatiles thereby reducing explosion risk in controlled reactor environments.

Taken together, the emission behaviour demonstrates that feedstock composition and mixing ratios strongly influence both the scale and timing of pollutant release. Pure HDPE yields higher CO emissions and greater explosive potential, whereas PET incorporation moderates these effects by shifting degradation pathways toward oxygenated condensable and aqueous phase compounds. These findings highlight the need for integrated emission monitoring and mitigation strategies, particularly when scaling pyrolysis for industrial applications.

4.5.4 Oil Quality Assessment

The assessment of pyrolytic oil quality is an essential step in determining its potential as an alternative fuel and its compatibility with existing energy systems. In this study, the physical and chemical properties of oils derived from HDPE, PET and their blends were examined to evaluate their suitability for combustion and downstream applications. The analysis focused on key parameters including calorific value, density, viscosity, elemental composition and hydrocarbon distribution as these directly influence fuel performance, stability and environmental impact.

The results demonstrated that HDPE derived oil exhibited superior fuel quality compared to PET derived oil. Oils from HDPE were characterized by higher hydrocarbon content, dominated by long chain alkanes and alkenes which translated into higher calorific values and lower oxygenated compound fractions. In contrast, PET derived oil showed lower energy density and higher oxygen content reflecting the influence of ester linkages in PET that lead to oxygenated degradation products such as benzoic acid derivatives and aldehydes. This compositional difference is consistent with the observed pyrolysis behaviour where PET decomposition produced a greater proportion of condensable oxygenates in the aqueous phase rather than energy rich hydrocarbons in the oil fraction.

Blended HDPE:PET oils exhibited intermediate properties with the 2:1 ratio producing a more favourable balance between hydrocarbon richness and reduced oxygenated content. For example, oils from the HDPE:PET (2:1) blend showed measurable improvements in calorific value compared to the 1:1 and 1:2 blends indicating that the presence of HDPE enhances overall fuel characteristics. This synergy suggests that controlled co-pyrolysis can be strategically employed to improve oil yield and quality while simultaneously moderating emissions and by product formation.

Overall, the oil quality assessment confirms that HDPE rich feedstocks produce pyrolytic oils more suitable for use as alternative fuels, whereas PET rich blends require further upgrading or catalytic treatment to meet industrial fuel standards. The findings underscore the importance of feedstock selection and ratio optimization in designing pyrolysis processes that maximize fuel quality while minimizing environmental constraints.

4.6 Concluding Remark

This chapter has presented and critically discussed the experimental results obtained from the pyrolysis of HDPE and PET wastes. The findings demonstrated the influence of feedstock characteristics, mixing ratios and process conditions on product yields, pyro-fuel properties, and emission patterns. Wastewater profiling was shown to be a promising and cost effective approach for tracking odour and pollutant signals, offering practical advantages over conventional emission monitoring techniques. The evaluation of pyro-fuel quality, benchmarked against commercial standards revealed both strengths and limitations of the obtained products, while statistical and kinetic analyses provided further insight into the correlations between process parameters, emission behaviours, and fuel outcomes. Collectively, these results validate the research approach and highlight the synergistic potential of combining slow pyrolysis with wastewater based diagnostics. The final chapter will synthesise these findings into broader conclusions and propose recommendations for future research and practical applications.

CHAPTER 5

CONCLUSION AND RECOMMENDATIONS

5.1 Conclusions

This study has explored the pyrolysis behaviour of HDPE, PET and their blends with a focus on product yield, emission behaviour, reaction kinetics and oil quality. The findings clearly demonstrate that pyrolysis performance is strongly dependent on the type of feedstock and the ratio of plastic mixtures used. HDPE rich feedstocks consistently produced higher proportions of pyrolytic oil with favourable physicochemical properties, including greater calorific value and reduced oxygenated compounds. These qualities render HDPE-derived oils more suitable for direct use as alternative fuels. In contrast, PET and PET rich blends generated lower oil yields, higher proportions of oxygenated fractions and increased aqueous phase contaminants thereby highlighting the challenges of upgrading PET derived oils for practical applications.

Emission behaviour analysis provided additional insights into the environmental implications of the pyrolysis process. Carbon monoxide (CO) was identified as the dominant emission with pure HDPE producing the highest concentration (312.9 ppm at 85 minutes) whereas PET rich blends exhibited comparatively lower emissions but contributed to earlier release of oxygenated volatiles. Hydrogen sulfide (H₂S) emissions were negligible across all experimental conditions, indicating that the selected feedstocks contained minimal sulfur bearing additives. The lower explosive limit (LEL) values highlighted the accumulation of flammable volatiles in HDPE systems, with blended ratios showing moderated responses, thereby reducing explosion risks under controlled conditions. These findings underscore the importance of emission monitoring and control as part of pyrolysis scale-up strategies.

The principal novelty of this research lies in the application of mild pyrolysis (torrefaction) as a controlled and energy efficient approach for the valorisation of mixed plastic waste. Unlike conventional plastic pyrolysis studies that operate at high temperatures (>500 °C) and prioritise liquid fuel production, this work demonstrates that low temperature torrefaction conditions can effectively regulate thermal degradation pathways that enhance solid fuel characteristics and moderate the formation

of liquid and gaseous by products. By operating under controlled mild pyrolysis conditions, the study reveals distinct advantages in process stability that reduced secondary cracking and simplified emission behaviour. Furthermore, coupling torrefaction with accessible analytical techniques for by product assessment provides a practical and scalable framework for plastic waste conversion, particularly suited to decentralised or resource constrained applications. This positions mild pyrolysis not merely as a lower severity alternative but as a strategically advantageous and underexplored pathway for sustainable plastic-to-fuel technologies.

The experimental conditions employed in this study are closely aligned with the principles of mild pyrolysis, also referred to as low temperature or torrefaction assisted pyrolysis. Operating at temperatures below 450 °C with extended residence times allowed controlled polymer degradation while suppressing excessive secondary cracking commonly observed at higher temperatures. This approach reduced gas over production, limited the formation of highly hazardous by products, and improved reactor stability. From a technological perspective, mild pyrolysis offers advantages in terms of lower energy demand, improved operational safety, and compatibility with simple batch or semi batch reactors. The observed correlation between lower operating temperatures and reduced wastewater contamination further confirms that mild pyrolysis is a suitable technological strategy for environmentally responsible plastic to fuel conversion, particularly when emission control infrastructure is limited.

This study successfully demonstrated the application of controlled torrefaction (mild pyrolysis) for the conversion of mixed plastic waste into solid, liquid and gaseous products. The thermal degradation behaviour and reaction kinetics of FIDPE-PET mixtures showed that mild pyrolysis enables controlled polymer breakdown with the formation of gaseous by products while avoiding excessive secondary cracking. Characterisation of the solid residues confirmed that torrefaction enhances fixed carbon content and calorific value, particularly for PET rich blends that indicate the potential of the solid product as a supplementary solid fuel. In addition, the identification and evaluation of liquid and gaseous by products using accessible analytical techniques including indirect wastewater based indicators that provide meaningful insight into product distribution and emission behaviour. Overall, the findings confirm that torrefaction based mild pyrolysis is a viable, energy efficient and environmentally favourable pathway for mixed plastic waste valorisation.

5.2 Recommendations

Based on the results and interpretations, several recommendations are proposed to guide future research and industrial application. Further studies should expand the scope of feedstocks to include other widely used polymers such as PP, PS and PVC. Investigating co-processing of plastics with biomass or other organic residues could also enhance oil yield and reduce undesirable oxygenated by products.

Optimisation of process parameters including temperature, heating rate and residence time should be conducted to achieve an optimal balance between product yield, energy efficiency and emission control. Pilot scale studies are recommended to validate laboratory findings under near-industrial conditions.

Since PET derived oils contained higher oxygenated fractions, catalytic pyrolysis or post-treatment upgrading is recommended to improve fuel quality and align with conventional fuel standards. Catalysts such as zeolites or transition metal oxides could be explored for their ability to enhance hydrocarbon selectivity and reduce oxygen content.

The wastewater profiling technique demonstrated in this study should be further refined and combined with advanced analytical methods such as FTIR or GC-MS to strengthen accuracy. This integrated monitoring framework would provide deeper insights into reaction pathways and improve process control.

The study highlights the potential of decentralised pyrolysis systems with emission and odour control mechanisms for waste to fuel conversion. Stronger collaboration with policymakers and industry stakeholders is recommended to support technology adoption and align research with regulatory standards and contribute to circular economy objectives.

Future work should include systematic calibration and validation of water quality measurements used for emission and odour profiling. Although COD, BOD, pH, DO, turbidity and TSS proved effective as indirect indicators of contaminant evolution, calibration against known standard solutions and reference gas concentrations is recommended to strengthen quantitative interpretation. In particular, correlating calibrated COD and BOD values with specific gas phase compounds (e.g., organic acids, aldehydes and light aromatics) will enhance the reliability of wastewater analysis as a diagnostic tool. Regular instrument calibration following standard methods (e.g., APHA or ASTM procedures) should be incorporated to improve measurement

accuracy, reproducibility, and comparability across different pyrolysis systems. This step is essential for advancing wastewater based monitoring from a qualitative proxy toward a semi quantitative emission assessment technique.

REFERENCES

- I] J. Solly, "Economic Study of the CANADIAN PLASTIC INDUSTRY, MARKETS AND WASTE," Environment and Climate Change Canada, 2019.
- 2] J. Lewis and M. Hayes, "Reduce, reuse, recycle, rejected: Why Canada's recycling industry is in crisis mode," *The Globe and Mail*, vol. 22, 2019.
- 3] C. P. H. o. C. S. C. o. Environment, S. Development, and J. Aldag, *The last straw: Turning the tide on plastic pollution in Canada*. House of Commons Canada= Chambre des communes Canada, 2019.
- 4] M. R. f t. C. P. I. Association, "2018 Post-Consumer Plastics Recycling in Canada," Canadian Plastic Industry Association (CPIA), 2020.
- 5] G. S. Asia, "The Recycling Myth: Malaysia and the Broken Global Recycling System," 2018.
- 6] M. T. Nazari, J. Mazutti, L. G. Basso, L. M. Colla, and L. Brandli, "Biofuels and their connections with the sustainable development goals: a bibliometric and systematic review," *Environment, Development and Sustainability*, vol. 23, no. 8, pp. 11139-11156, 2021.
- 7] S. Mirkarimi, S. Bensaid, and D. Chiaramonti, "Conversion of mixed waste plastic into fuel for diesel engines through pyrolysis process: A review," *Applied Energy*, vol. 327, p. 120040, 2022.
- 8] N. Surma, G. A. Ijuo, J. I. Ona, and D. C. Ike, "Recycling Post-Consumer Waste from Low Density Polyethylene Via Low Temperature Catalytic Pyrolysis."
- 9] Z. Yao, S. Yu, W. Su, W. Wu, J. Tang, and W. Qi, "Kinetic studies on the pyrolysis of plastic waste using a combination of model-fitting and model-free methods," *Waste Management & Research*, vol. 38, no. 1_suppl, pp. 77-85, 2020.
- 10] M. Harussani, S. Sapuan, A. Khalina, R. Ilyas, and M. Hazrol, "Review on green technology pyrolysis for plastic wastes," in *Proceedings of the 7th postgraduate seminar on natural fibre reinforced polymer composites*, 2020, pp. 50-53.
- II] S. Li, "Reviewing air pollutants generated during the pyrolysis of solid waste for biofuel and biochar production: toward cleaner production practices," *Sustainability*, vol. 16, no. 3, p. 1169, 2024.
- 12] A. Cabanes, F. J. Valdes, and A. Fullana, "A review on VOCs from recycled plastics," *Sustainable materials and technologies*, vol. 25, p. e00179, 2020.
- 13] J. Yang *et al*, "Selective electrified polyethylene upcycling by pore-modulated pyrolysis," *Nature Chemical Engineering*, vol. 2, no. 7, pp. 424-435, 2025.
- 14] Y.-C. Hung, C.-H. Ho, L.-Y. Chen, S.-C. Ma, T.-I. Liu, and Y.-C. Shen, "Using a Low-Temperature Pyrolysis Device for Polymeric Waste to Implement a Distributed Energy System," *Sustainability*, vol. 15, no. 2, p. 1580, 2023.
- 15] J. Graichen, "Climate impact of pyrolysis of waste plastic packaging in comparison with reuse and mechanical recycling," 2022.
- 16] A. I. Osman, C. Farrell, H. Ala'a, A. S. Al-Fatesh, J. Harrison, and D. W. Rooney, "Pyrolysis kinetic modelling of abundant plastic waste (PET) and in-situ emissions monitoring," 2020.
- 17] A. Moranda and O. Paladino, "Controlled combustion and pyrolysis of waste plastics: A comparison based on human health risk assessment," *Recycling*, vol. 8, no. 2, p. 38, 2023.

- [18] M. J. B. Kabeyi and O. A. Olanrewaju, "Review and Design Overview of Plastic Waste - to - Pyrolysis Oil Conversion with Implications on the Energy Transition," *Journal of Energy*, vol. 2023, no. 1, p. 1821129, 2023.
- [19] E. T. Tafoya. "Don't pollute Colorado communities with plastics-to-fuel." <https://coloradonewslines.com/2024/04/28/dont-pollute-colorado-communities-with-plastics-to-fuel/> (accessed 15 May 2024, 2024).
- [20] O. Paladino and A. Moranda, "Human Health Risk Assessment of a pilot-plant for catalytic pyrolysis of mixed waste plastics for fuel production," *Journal of Hazardous Materials*, vol. 405, p. 124222, 2021.
- [21] J. L. Mernit. "As Plastics Keep Piling Up, Can 'Advanced' Recycling Cut the Waste?" *Yale Environment* 360. <https://e360.yale.edu/features/advanced-plastics-recycling-pyrolysis> (accessed 16/5/2024, 2024).
- [22] J. Meltzer. "'Chemical Recycling': Backend Fix or Toxic Technology?" *National Caucus of Environmental Legislators*. <https://ncelenviro.org/articles/chemical-recycling-backend-fix-or-toxic-technology/#> (accessed 15 May 2024, 2024).
- [23] "What is the problem with plastic pyrolysis? Overcoming Key Challenges for Sustainable Waste Conversion." *Kintek Solution*. https://kintek-tech.com/faqs/what-is-the-problem-with-plastic-pyrolysis?srsltid=AfmBOopvbAZGFQ7MgFwtaEjlxwB-RoZim618_n_qf7nWVS1CkVvkEmDN&utm_source=chatgpt.com (accessed 6/4/2025, 2025).
- [24] A. Pivato *et al*, "Air-polluting emissions from pyrolysis plants: a systematic mapping," *Environments*, vol. 11, no. 7, p. 149, 2024.
- [25] H. Chua, M. Bashir, K. Tan, and H. S. Chua, "A sustainable pyrolysis technology for the treatment of municipal solid waste in Malaysia," in *AIP Conference Proceedings*, 2019, vol. 2124, no. 1: AIP Publishing LLC, p. 020016.
- [26] M. Lim and E. S. Tan, "Techno-Economic Feasibility Study for Organic and Plastic Waste Pyrolysis Pilot Plant in Malaysia," *Sustainability*, vol. 15, no. 19, p. 14280, 2023.
- [27] "An Introduction to Plastics." [ChemicalSafetyFacts.org](https://www.chemicalsafetyfacts.org/chemistry-101/an-introduction-to-plastics/). <https://www.chemicalsafetyfacts.org/chemistry-101/an-introduction-to-plastics/> (accessed 17/5/2024, 2024).
- [28] P. SHARPE. "Making Plastics: From Monomer to Polymer." *American Institute of Chemical Engineers*. <https://www.aiche.org/resources/publications/cep/2015/september/making-plastics-monomer-polymer> (accessed 17/5/2024, 2024).
- [29] D. Li, L. Zhou, X. Wang, L. He, and X. Yang, "Effect of crystallinity of polyethylene with different densities on breakdown strength and conductance property," *Materials*, vol. 12, no. 11, p. 1746, 2019.
- [30] K. Namsheer and C. S. Rout, "Conducting polymers: a comprehensive review on recent advances in synthesis, properties and applications," *RSC advances*, vol. 11, no. 10, pp. 5659-5697, 2021.
- [31] H. Yaqoob, H. M. Ali, and U. Khali d, "Pyrolysis of waste plastics for alternative fuel: a review of key factors," *RSC Sustainability*, 2025.
- [32] I. Kumar *et al*, "Co-pyrolysis of furniture wood with mixed plastics and waste tyres: assessment of synergistic effect on biofuel yield and product characterization under different blend ratio," *Scientific reports*, vol. 14, no. 1, p. 24584, 2024.

- [33] B. Alawa, J. Choudhary, and S. Chakma, "Discernment of synergism in co-pyrolysis of HDPE and PP waste plastics for production of pyro-oil: mechanistic investigation with economic analysis and health risk assessment," *Process Safety and Environmental Protection*, vol. 169, pp. 107-131, 2023.
- [34] A. Chaudhary *et al.*, "Slow pyrolysis of low-density Poly-Ethylene (LDPE): A batch experiment and thermodynamic analysis," *Energy*, vol. 263, p. 125810, 2023.
- [35] B. Sugiarto, A. Kurniawan, and A. Perdana, "Plastic waste conversion into fuel by utilizing biomass waste as heating system on pyrolysis process," in *Journal of Physics: Conference Series*, 2020, vol. 1517, no. 1: IOP Publishing, p. 012010.
- [36] W. Jeon, Y.-D. Kim, and K.-H. Lee, "A comparative study on pyrolysis of bundle and fluffy shapes of waste packaging plastics," *Fuel*, vol. 283, p. 119260, 2021.
- [37] P. T. Williams and E. A. Williams, "Fluidised bed pyrolysis of low density polyethylene to produce petrochemical feedstock," *Journal of Analytical and Applied Pyrolysis*, vol. 51, no. 1-2, pp. 107-126, 1999.
- [38] Y. Zhang, G. Ji, C. Chen, Y. Wang, W. Wang, and A. Li, "Liquid oils produced from pyrolysis of plastic wastes with heat carrier in rotary kiln," *Fuel Processing Technology*, vol. 206, p. 106455, 2020.
- [39] Y. Bow and L. S. Pujiastuti, "Pyrolysis of polypropylene plastic waste into liquid fuel," in *IOP Conference Series: Earth and Environmental Science*, 2019, vol. 347, no. 1: IOP Publishing, p. 012128.
- [40] A. K. Panda, "Thermo-catalytic degradation of different plastics to drop in liquid fuel using calcium bentonite catalyst," *International Journal of Industrial Chemistry*, vol. 9, no. 2, pp. 167-176, 2018.
- [41] D. Almeida and M. d. F. Marques, "Thermal and catalytic pyrolysis of plastic waste," *Polímeros*, vol. 26, no. 1, pp. 44-51, 2016.
- [42] R. Miandad *et al.*, "Catalytic pyrolysis of plastic waste: moving toward pyrolysis based biorefineries," *Frontiers in energy research*, vol. 7, p. 437000, 2019.
- [43] F. A. Aisien and E. T. Aisien, "Production and characterization of liquid oil from the pyrolysis of waste high-density polyethylene plastics using spent fluid catalytic cracking catalyst," *Sustainable Chemistry for Climate Action*, vol. 2, p. 100020, 2023.
- [44] S. Jadhao and S. Seethamraju, "Pyrolysis Study of mixed plastics waste," in *IOP Conference Series: Materials Science and Engineering*, 2020, vol. 736, no. 4: IOP Publishing, p. 042036.
- [45] A. Lopez, I. De Marco, B. Caballero, M. Laresgoiti, and A. Adrados, "Influence of time and temperature on pyrolysis of plastic wastes in a semi-batch reactor," *Chemical Engineering Journal*, vol. 173, no. 1, pp. 62-71, 2011.
- [46] S. Hammoodi and R. Almukhtar, "Thermal pyrolysis of municipal solid waste (MSW)," in *IOP Conference Series: Materials Science and Engineering*, 2019, vol. 579, no. 1: IOP Publishing, p. 012018.
- [47] P. Das and P. Tiwari, "Valorization of packaging plastic waste by slow pyrolysis," *Resources, Conservation and Recycling*, vol. 128, pp. 69-77, 2018.
- [48] S. Sikdar, A. Siddaiah, and P. L. Menezes, "Conversion of Waste Plastic to Oils for Tribological Applications," *Lubricants*, vol. 8, no. 8, p. 78, 2020.
- [49] M. Al-Asadi and N. Miskolczi, "Pyrolysis of polyethylene terephthalate containing real waste plastics using Ni loaded zeolite catalysts," in *IOP*

- Conference Series: Earth and Environmental Science*, 2018, vol. 154: IOP Publishing, p. 012021.
- [50] G. Yadav *et al*, "Techno-economic analysis and life cycle assessment for catalytic fast pyrolysis of mixed plastic waste," *Energy & Environmental Science*, vol. 16, no. 9, pp. 3638-3653, 2023.
- [51] N. Othman, N. Basri, M. Yunus, and L. Sidek, "Determination of physical and chemical characteristics of electronic plastic waste (Ep-Waste) resin using proximate and ultimate analysis method," in *International conference on construction and building technology*, 2008, pp. 169-180.
- [52] S. Chong, G.-T. Pan, M. Khalid, T. C.-K. Yang, S.-T. Hung, and C.-M. Huang, "Physical characterization and pre-assessment of recycled high-density polyethylene as 3D printing material," *Journal of Polymers and the Environment*, vol. 25, no. 2, pp. 136-145, 2017.
- [53] Y. Yuriz, T. N. H. T. Ismail, I. Mohamed, and N. N. M. Hassan, "Characteristic properties of plastic wastes: possibility of reinforcing material for soil," *Jurnal Teknologi (Sciences & Engineering)*, vol. 83, no. 4, pp. 127-136, 2021.
- [54] F. M. Mwanja, J. van der Walt, L. Wu, W. Koen, and M. Maringa, "Characterisation of High - Density Polyethylene (DiaPow HDPE HX R) Powder for Use in Additive Manufacturing," *Journal of Engineering*, vol. 2024, no. 1, p. 6284961, 2024.
- [55] A. M. Kuzmin, N. Ayrlmis, F. Ozdemir, and G. Kanat, "Effect of content and particle size of used beverage carton pieces on the properties of HDPE composites," *BioResources*, vol. 18, no. 2, p. 2815, 2023.
- [56] A. Zaker and K. Auclair, "Impact of ball milling on the microstructure of polyethylene terephthalate," *ChemSusChem*, vol. 18, no. 4, p. e202401506, 2025.
- [57] J. Papac Zjadic *et al*, "Effect of aging on physicochemical properties and size distribution of PET microplastic: influence on adsorption of diclofenac and toxicity assessment," *Toxics*, vol. 11, no. 7, p. 615, 2023.
- [58] S. Richter, J. Horstmann, K. Altmann, U. Braun, and C. Hagendorf, "A reference methodology for microplastic particle size distribution analysis: Sampling, filtration, and detection by optical microscopy and image processing," *Applied research*, vol. 2, no. 4, p. e202200055, 2023.
- [59] P. Sambyal *et al*, "Plastic recycling: Challenges and opportunities," *The Canadian Journal of Chemical Engineering*, vol. 103, no. 6, pp. 2462-2498, 2025.
- [60] M. R. Gent, M. Menendez, J. Torafio, and I. Diego, "Recycling of plastic waste by density separation: prospects for optimization," *Waste management & research*, vol. 27, no. 2, pp. 175-187, 2009.
- [61] Z. A. Hussein, Z. M. Shakor, M. Alzuhairi, and F. Al-Sheikh, "Thermal and catalytic cracking of plastic waste: a review," *International Journal of Environmental Analytical Chemistry*, vol. 103, no. 17, pp. 5920-5937, 2023.
- [62] E. Pirzadeh, A. Zadhoush, and M. Haghighat, "Hydrolytic and thermal degradation of PET fibers and PET granule: The effects of crystallization, temperature, and humidity," *Journal of applied polymer science*, vol. 106, no. 3, pp. 1544-1549, 2007.
- [63] S.-C. Chen, H. Su, J. J. Mathew, H. Gunawan, C.-W. Huang, and C.-T. Feng, "An investigation to reduce the effect of moisture on injection-molded parts through optimization of plasticization parameters," *applied sciences*, vol. 12, no. 3, p. 1410, 2022.

- [64] V. Titone, A. Correnti, and F. P. La Mantia, "Effect of moisture content on the processing and mechanical properties of a biodegradable polyester," *Polymers*, vol. 13, no. 10, p. 1616, 2021.
- [65] D. Mendes *et al*, "Combustion behaviour of plastic waste-A case study of PP, FIDPE, PET, and mixed PES-EL," *Journal of Cleaner Production*, vol. 402, p. 136850, 2023.
- [66] s. yang. "Melting Point of Plastic Material: How It Affects Material Selection?" ACUTEK. <https://acutekdirect.com/melting-point-of-plastics-how-it-affects-material-selection/> (accessed 12/2/2025, 2025).
- [67] I. B. Alit, I. G. B. Susana, and I. M. Mara, "Conversion of LDPE and PP plastic waste into fuel by pyrolysis method," *Global Journal of Engineering and Technology Advances*, vol. 10, no. 3, pp. 073-078, 2022.
- [68] Y. Misra, D. J. P. Kumar, R. K. Mishra, V. Kumar, and N. Dwivedi, "Thermocatalytic pyrolysis of plastic waste into renewable fuel and value-added chemicals: A review of plastic types, operating parameters and upgradation of pyrolysis oil," *Water-Energy Nexus*, 2025.
- [69] H. H. Shah *et al*, "A review on gasification and pyrolysis of waste plastics," *Frontiers in Chemistry*, vol. 10, p. 960894, 2023.
- [70] L. Dai *et al*, "Pyrolysis technology for plastic waste recycling: A state-of-the-art review," *Progress in Energy and Combustion Science*, vol. 93, p. 101021, 2022.
- [71] K. Akubo, M. A. Nahil, and P. T. Williams, "Co-pyrolysis-catalytic steam reforming of cellulose/lignin with polyethylene/polystyrene for the production of hydrogen," *Waste Disposal & Sustainable Energy*, vol. 2, no. 3, pp. 177-191, 2020.
- [72] J. Wang, Y. Ma, S. Li, and C. Yue, "Study of HDPE plastic pyrolysis characteristics using high pressure autoclave," *Journal of the Energy Institute*, vol. 108, p. 101244, 2023.
- [73] Y. Liu, W. Fu, T. Liu, Y. Zhang, and B. Li, "Microwave pyrolysis of polyethylene terephthalate (PET) plastic bottle sheets for energy recovery," *Journal of Analytical and Applied Pyrolysis*, vol. 161, p. 105414, 2022.
- [74] S. Erdogan, "Recycling of Waste Plastics into Pyrolytic Fuels and Their Use," *Sustainable Mobility*, p. 77, 2020.
- [75] S. Al-Salem, A. Antelava, A. Constantinou, G. Manos, and A. Dutta, "A review on thermal and catalytic pyrolysis of plastic solid waste (PSW)," *Journal of environmental management*, vol. 197, pp. 177-198, 2017.
- [76] J. Zhang, L. Zhang, C. Lin, C. Wang, P. Zhao, and Y. Li, "Co-hydrothermal carbonization of polyvinyl chloride and lignocellulose biomasses: Influence of biomass feedstock on fuel properties and combustion behaviors," *Science of The Total Environment*, vol. 868, p. 161532, 2023.
- [77] S. Sharuddin, F. Abnisa, W. Daud, and M. K. Aroua, "Pyrolysis of plastic waste for liquid fuel production as prospective energy resource," in *IOP Conference Series: Materials Science and Engineering*, 2018, vol. 334: IOP Publishing, p. 012001.
- [78] H. Yaqoob, E. S. Tan, H. M. Ali, H. C. Ong, M. A. Jamil, and M. U. Farooq, "Sustainable energy generation from plastic waste: An in-depth review of diesel engine application," *Environmental Technology & Innovation*, vol. 34, p. 103467, 2024.

- [79] S. D. A. Sharuddin, F. Abnisa, W. M. A. W. Daud, and M. K. Aroua, "A review on pyrolysis of plastic wastes," *Energy conversion and management*, vol. 115, pp. 308-326, 2016.
- [80] L. Rodriguez-Luna, D. Bustos-Martinez, and E. Valenzuela, "Two-step pyrolysis for waste FIDPE valorization," *Process Safety and Environmental Protection*, vol. 149, pp. 526-536, 2021.
- [81] C. Park *et al*, "Pyrolysis of polyethylene terephthalate over carbon-supported Pd catalyst," *Catalysts*, vol. 10, no. 5, p. 496, 2020.
- [82] A. C. Leri and A. P. Pavia, "Analysis of plastic waste for sorting in recycling plants: an inquiry-based FTIR spectroscopy experiment for the organic chemistry laboratory," *Journal of Chemical Education*, vol. 99, no. 2, pp. 1008-1013, 2022.
- [83] M.-H. Cho, Y.-J. Song, C.-J. Rhu, and B.-R. Go, "Pyrolysis process of mixed microplastics using TG-FTIR and TED-GC-MS," *Polymers*, vol. 15, no. 1, p. 241, 2023.
- [84] V. Kudelyte, J. Eimontas, R. Paulauskas, and N. Striugas, "Co-Pyrolysis of Plastic Waste and Lignin: A Pathway for Enhanced Hydrocarbon Recovery," *Energies*, vol. 15, no. 2, pp. 1-19, 2025.
- [85] Y. Jiang *et al*, "Pyrolysis of typical plastics and coupled with steam reforming of their derived volatiles for simultaneous production of hydrogen-rich gases and heavy organics," *Renewable Energy*, vol. 200, pp. 476-491, 2022.
- [86] P. Straka, O. Bicakova, and M. Supova, "Slow pyrolysis of waste polyethylene terephthalate yielding paraldehyde, ethylene glycol, benzoic acid and clean fuel," *Polymer Degradation and Stability*, vol. 198, p. 109900, 2022.
- [87] A. Akgiil *et al*, "Characterization of tars from recycling of PHA bioplastic and synthetic plastics using fast pyrolysis," *Journal of Hazardous Materials*, vol. 439, p. 129696, 2022.
- [88] L. Baltes, L. Costiuc, S. Patachia, and M. Tiorean, "Differential scanning calorimetry—a powerful tool for the determination of morphological features of the recycled polypropylene," *Journal of Thermal Analysis and Calorimetry*, vol. 138, no. 4, pp. 2399-2408, 2019.
- [89] J. M. Lynch *et al*, "Differential scanning calorimetry (DSC): an important tool for polymer identification and characterization of plastic marine debris," *Environmental Pollution*, vol. 346, p. 123607, 2024.
- [90] J. Fujino and T. Honda, "Measurement of the specific heat capacity of plastic waste/fly ash recycled composite using a differential scanning calorimeter," *Heat Transfer—Asian Research: Co -sponsored by the Society of Chemical Engineers of Japan and the Heat Transfer Division of ASME*, vol. 36, no. 7, pp. 435-448, 2007.
- [91] G. Wang, Z. Zhang, D. Xu, B. Xing, L. Zhu, and S. Wang, "Insight into pyrolysis mechanism of plastic waste with CO/CN bonds in the backbone," *Science of The Total Environment*, vol. 897, p. 165359, 2023.
- [92] O. T. Ore and F. M. Adebisi, "A review on current trends and prospects in the pyrolysis of heavy oils," *Journal of Petroleum Exploration and Production*, vol. 11, no. 3, pp. 1521-1530, 2021.
- [93] A. G. Daful, M. R. Chandraratne, and M. Loridon, *Recent perspectives in biochar production, characterization and applications*. IntechOpen, 2021.
- [94] M. R. Chandraratne and A. G. Daful, "Advances in bioenergy production using fast pyrolysis and hydrothermal processing," *Biomass, Biorefineries and Bioeconomy*. London: IntechOpen, pp. 269-289, 2022.

- 95] M. R. Chandraratne and A. G. Diful, "Recent Advances in Thermochemical Conversion," *Recent perspectives in pyrolysis research*, p. 145, 2022.
- 96] M. Martynis, E. Praputri, R. Witri, and N. Putri, "The influence of temperature on the formation of liquid fuel from Polypropylene plastic wastes," in *IOP Conference Series: Materials Science and Engineering*, 2018, vol. 334, no. 1: IOP Publishing, p. 012014.
- 97] N. Miskolczi, F. Ateş, and N. Borsodi, "Comparison of real waste (MSW and MPW) pyrolysis in batch reactor over different catalysts. Part II: contaminants, char and pyrolysis oil properties," *Bioresource technology*, vol. 144, pp. 370-379, 2013.
- 98] A. A. Ajibola, J. A. Omoleye, and V. E. Efeovbokhan, "Catalytic cracking of polyethylene plastic waste using synthesised zeolite Y from Nigerian kaolin deposit," *Applied Petrochemical Research*, vol. 8, no. 4, pp. 211-217, 2018.
- 99] S. Abukasim, F. Zuhria, and Z. Saing, "Alternative management of plastic waste," in *Journal of Physics: Conference Series*, 2020, vol. 1517, no. 1: IOP Publishing, p. 012041.
- 100] S. M. Al-Salem, "Thermal pyrolysis of high density polyethylene (HDPE) in a novel fixed bed reactor system for the production of high value gasoline range hydrocarbons (HC)," *Process Safety and Environmental Protection*, vol. 127, pp. 171-179, 2019.
- 101] S. Tuly, M. M. S. Joarder, and M. E. Haque, "Liquid fuel production by pyrolysis of polythene and PET plastic," in *AIP Conference Proceedings*, 2019, vol. 2121, no. 1: AIP Publishing LLC, p. 120001.
- 102] A. T. Yuliansyah, A. Prasetya, M. A. Ramadhan, and R. Laksono, "Pyrolysis of plastic waste to produce pyrolytic oil as an alternative fuel," *International Journal of Technology*, vol. 7, pp. 1076-1083, 2015.
- 103] K. Murthy, R. J. Shetty, and K. Shiva, "Plastic waste conversion to fuel: a review on pyrolysis process and influence of operating parameters," *Energy Sources, Part A: Recovery, Utilization, and Environmental Effects*, vol. 45, no. 4, pp. 11904-11924, 2023.
- 104] S. H. Gebre, M. G. Sendeku, and M. Bahri, "Recent trends in the pyrolysis of non - degradable waste plastics," *ChemistryOpen*, vol. 10, no. 12, pp. 1202-1226, 2021.
- 105] R. Miandad *et al.*, "Influence of temperature and reaction time on the conversion of polystyrene waste to pyrolysis liquid oil," *Waste Management*, vol. 58, pp. 250-259, 2016.
- 106] F. Sulaiman, H. Prayitno, R. Ramadhani, and K. Anam, "The Effect of Temperature on the Pyrolysis PP and LDPE Plastic Waste: Implications for Pyrolysis Fuel Oil Characteristics," *Journal of Transactions in Systems Engineering*, vol. 2, no. 3, pp. 306-315, 2024.
- 107] C. Schmidt, J. Biernath, J. Schmidt, and J. Denecke, "Protection of chemical reactors against exothermal runaway reactions with smart overpressure protection devices," *Chemical Engineering Transactions*, vol. 90, pp. 493-498, 2022.
- 108] K. Paavani, K. Agarwal, S. S. Alam, S. Dinda, and I. Abrar, "Advances in plastic to fuel conversion: reactor design, operational optimization, and machine learning integration," *Sustainable Energy & Fuels*, vol. 9, no. 1, pp. 54-71, 2025.
- 109] R. Roychand, M. A. Zafar, M. Jacob, and T. Ngo, "A Comprehensive Review on the Thermochemical Treatment of Plastic Waste to Produce High Value

- Products for Different Applications," *Materials Circular Economy*, vol. 7, no. 1, p. 3, 2025.
- [110] F. Faisal, M. G. Rasul, A. A. Chowdhury, and M. I. Jahirul, "Optimisation of process parameters to maximise the oil yield from pyrolysis of mixed waste plastics," *Sustainability*, vol. 16, no. 7, p. 2619, 2024.
- [111] Z. C. Mibei, A. Kumar, and S. M. Talai, "Catalytic pyrolysis of plastic waste to liquid fuel using local clay catalyst," *Journal of energy*, vol. 2023, no. 1, p. 7862293, 2023.
- [112] H. Dao Thi, M. R. Djokic, and K. M. Van Geem, "Detailed group-type characterization of plastic-waste pyrolysis oils: by comprehensive two-dimensional gas chromatography including linear, branched, and di-olefins," *Separations*, vol. 8, no. 7, p. 103, 2021.
- [113] P. Palmay, C. Haro, I. Huacho, D. Barzallo, and J. C. Bruno, "Production and analysis of the physicochemical properties of the pyrolytic oil obtained from pyrolysis of different thermoplastics and plastic mixtures," *Molecules*, vol. 27, no. 10, p. 3287, 2022.
- [114] K. Sivagami, K. V. Kumar, P. Tamizhdurai, D. Govindarajan, M. Kumar, and I. Nambi, "Conversion of plastic waste into fuel oil using zeolite catalysts in a bench-scale pyrolysis reactor," *RSC advances*, vol. 12, no. 13, pp. 7612-7620, 2022.
- [115] A. Antelava *et al*, "Plastic Solid Waste (PSW) in the Context of Life Cycle Assessment (LCA) and Sustainable Management," *Environmental management*, vol. 64, no. 2, pp. 230-244, 2019.
- [116] R. P. Lee, B. Meyer, Q. Huang, and R. Voss, "Sustainable waste management for zero waste cities in China: potential, challenges and opportunities," *Clean energy*, vol. 4, no. 3, pp. 169-201, 2020.
- [117] T. Fruergaard, T. Astrup, and T. Ekvall, "Energy use and recovery in waste management and implications for accounting of greenhouse gases and global warming contributions," *Waste Management & Research*, vol. 27, no. 8, pp. 724-737, 2009.
- [118] A. Bhargava, "Wet Scrubbers-Design of Spray Tower to Control Air Pollutants," *Int. J. Environ. Planning and Dev*, vol. 1, no. 1, pp. 36-41, 2017.
- [119] M. Cocchie^a./., "Catalytic Pyrolysis of a Residual Plastic Waste Using Zeolites Produced by Coal Fly Ash," *Catalysts*, vol. 10, no. 10, p. 1113, 2020.
- [120] G. K. Roy, B. Kumar, and S. Jha, "Chromatographic study of the recovered gases from hydro-pyrolytic de-polymerization of LDPE, MDPE and FIDPE mix type of waste polyethylene," *Applied Petrochemical Research*, vol. 6, no. 1, pp. 65-72, 2016.
- [121] G. Kwon, D.-W. Cho, H. Wang, A. Bhatnagar, and H. Song, "Valorization of Plastics and Paper Mill Sludge into Carbon Composite and its Catalytic Performance for Azo Dye Oxidation," *Journal of Hazardous Materials*, p. 123173, 2020.
- [122] M. Stelmachowski, "Feedstock recycling of waste polymers by thermal cracking in molten metal: thermodynamic analysis," *Journal of Material Cycles and Waste Management*, vol. 16, no. 2, pp. 211-218, 2014.
- [123] H. Nishida, "Development of materials and technologies for control of polymer recycling," *Polymer journal*, vol. 43, no. 5, pp. 435-447, 2011.
- [124] F. M. Lamberti, L. A. Roman-Ramirez, and J. Wood, "Recycling of bioplastics: routes and benefits," *Journal of Polymers and the Environment*, pp. 1-21, 2020.

- 125] K. K. Jha and T. Kannan, "Recycling of plastic waste into fuel by pyrolysis-a review," *Materials Today: Proceedings*, 2020.
- 126] A. Ahamed, A. Veksha, K. Yin, P. Weerachanchai, A. Giannis, and G. Lisak, "Environmental impact assessment of converting flexible packaging plastic waste to pyrolysis oil and multi-walled carbon nanotubes," *Journal of hazardous materials*, vol. 390, p. 121449, 2020.
- 127] D. Czajczyhska, K. Czajka, R. Krzyzyhska, and H. Jouhara, "Waste tyre pyrolysis-Impact of the process and its products on the environment," *Thermal Science and Engineering Progress*, vol. 20, p. 100690, 2020.
- 128] Z. Ding, H. Chen, J. Liu, H. Cai, F. Evrendilek, and M. Buyukada, "Pyrolysis dynamics of two medical plastic wastes: Drivers, behaviors, evolved gases, reaction mechanisms, and pathways," *Journal of hazardous materials*, vol. 402, p. 123472, 2020.
- 129] M. Gear, J. Sadhukhan, R. Thorpe, R. Clift, J. Seville, and M. Keast, "A life cycle assessment data analysis toolkit for the design of novel processes-A case study for a thermal cracking process for mixed plastic waste," *Journal of cleaner production*, vol. 180, pp. 735-747, 2018.
- 130] G. Grause, A. Buekens, Y. Sakata, A. Okuwaki, and T. Yoshioka, "Feedstock recycling of waste polymeric material," *Journal of Material Cycles and Waste Management*, vol. 13, no. 4, pp. 265-282, 2011.
- 131] K. K. Jha, T. Kannan, and N. Senthilvelan, "Optimization of catalytic pyrolysis process for change of plastic waste into fuel," *Materials Today: Proceedings*, 2020.
- 132] A. Maity, S. Chaudhari, J. J. Titman, and V. Polshettiwar, "Catalytic nanosponges of acidic aluminosilicates for plastic degradation and CO₂ to fuel conversion," *Nature communications*, vol. 11, no. 1, pp. 1-12, 2020.
- 133] O. I. Nkwachukwu, C. H. Chima, A. O. Ikenna, and L. Albert, "Focus on potential environmental issues on plastic world towards a sustainable plastic recycling in developing countries," *International Journal of Industrial Chemistry*, vol. 4, no. 1, p. 34, 2013.
- 134] M. Sarker, M. M. Rashid, M. S. Rahman, and M. Molla, "Conversion of low density polyethylene (LDPE) and polypropylene (PP) waste plastics into liquid fuel using thermal cracking process," *British Journal of Environment and Climate Change*, vol. 2, no. 1, p. 1, 2012.
- 135] P. T. Williams, "Hydrogen and Carbon Nanotubes from Pyrolysis-Catalysis of Waste Plastics: A Review," *Waste and Biomass Valorization*, 2020.
- 136] S. Jain, B. Yadav Lamba, S. Kumar, and D. Singh, "Strategy for repurposing of disposed PPE kits by production of biofuel: Pressing priority amidst COVID-19 pandemic," *Biofuels*, pp. 1-5, 2020.
- 137] M. S. Abbas-Abadi, M. N. Haghighi, H. Yeganeh, and A. G. McDonald, "Evaluation of pyrolysis process parameters on polypropylene degradation products," *Journal of analytical and applied pyrolysis*, vol. 109, pp. 272-277, 2014.
- 138] Z. Chen *et al*, "Effect of volatile reactions on oil production and composition in thermal and catalytic pyrolysis of polyethylene," *Fuel*, vol. 271, p. 117308, 2020.
- 139] M. S. Abbas-Abadi, M. N. Haghighi, and H. Yeganeh, "Evaluation of pyrolysis product of virgin high density polyethylene degradation using different process parameters in a stirred reactor," *Fuel processing technology*, vol. 109, pp. 90-95, 2013.

- [140] A. Robazza, F. C. Baleeiro, S. Kleinstauber, and A. Neumann, "Two-stage conversion of syngas and pyrolysis aqueous condensate into L-malate," *Biotechnology for Biofuels and Bioproducts*, vol. 17, no. 1, p. 85, 2024.
- [141] A. y. Sabitah, I. N. Ardiyat, M. Misbachudin, I. U. Wusko, and R. P. Ningsih, "Analysis of The Pyrolysis Process of HDPE and PET Plastic Waste: The Effect of Temperature and Reaction Time in Plastic Recycling Efforts," *Scientific Journal of Mechanical Engineering Kinematika*, vol. 9, no. 1, pp. 98-106, 06/27 2024, doi: 10.20527/sjmekinematika.v9i1.318.
- [142] F. K. Zisopoulos, A. J. van der Goot, and R. M. Boom, "Exergy destruction in ammonia scrubbers," *Resources, Conservation and Recycling*, vol. 136, pp. 153-165, 2018.
- [143] N. Miskolczi, A. Angyal, L. Bartha, and I. Valkai, "Fuels by pyrolysis of waste plastics from agricultural and packaging sectors in a pilot scale reactor," *Fuel Processing Technology*, vol. 90, no. 7-8, pp. 1032-1040, 2009.
- [144] S. Al-Salem, P. Lettieri, and J. Baeyens, "Recycling and recovery routes of plastic solid waste (PSW): A review," *Waste management*, vol. 29, no. 10, pp. 2625-2643, 2009.
- [145] A. K. Panda, R. K. Singh, and D. Mishra, "Thermolysis of waste plastics to liquid fuel: A suitable method for plastic waste management and manufacture of value added products—A world prospective," *Renewable and Sustainable Energy Reviews*, vol. 14, no. 1, pp. 233-248, 2010.
- [146] G. D. Oreggioni, S. Brandani, M. Luberti, Y. Baykan, D. Friedrich, and H. Ahn, "CO₂ capture from syngas by an adsorption process at a biomass gasification CFIP plant: Its comparison with amine-based CO₂ capture," *International Journal of Greenhouse Gas Control*, vol. 35, pp. 71-81, 2015.
- [147] A. Mukherjee, B. Debnath, and S. K. Ghosh, "A review on technologies of removal of dioxins and furans from incinerator flue gas," *Procedia environmental sciences*, vol. 35, pp. 528-540, 2016.
- [148] C. S. L. Alencar, A. R. N. Paiva, J. C. M. d. Silva, J. M. Vaz, and E. V. Spinace, "One-Step Synthesis of AuCu/TiO₂ Catalysts for CO Preferential Oxidation," *Materials Research*, vol. 23, no. 5, 2020.
- [149] I. Liemans and D. Thomas, "Simultaneous NO_x and SO_x reduction from oxyfuel exhaust gases using acidic solutions containing hydrogen peroxide," *Energy Procedia*, vol. 37, pp. 1348-1356, 2013.
- [150] X. Xu, K. Cheng, H. Wu, J. Sun, Q. Yue, and G. Pan, "Greenhouse gas mitigation potential in crop production with biochar soil amendment—a carbon footprint assessment for cross - site field experiments from China," *Gcb Bioenergy*, vol. 11, no. 4, pp. 592-605, 2019.
- [151] D. L. Maurer, J. A. Koziel, K. Kalus, D. S. Andersen, and S. Opalinski, "Pilot-scale testing of non-activated biochar for swine manure treatment and mitigation of ammonia, hydrogen sulfide, odorous volatile organic compounds (VOCs), and greenhouse gas emissions," *Sustainability*, vol. 9, no. 6, p. 929, 2017.
- [152] M. Roller, D. Wappel, N. Trofaiher, and G. Gronald, "Test results of CO₂ spray scrubbing with Monoethanolamine," *Energy Procedia*, vol. 4, pp. 1777-1782, 2011.
- [153] T. Si *et al*, "Simultaneous removal of SO₂ and NO_x by a new combined spray-and-scattered-bubble technology based on preozonation: From lab scale to pilot scale," *Applied Energy*, vol. 242, pp. 1528-1538, 2019.
- [154] K. Brown, W. Kalata, and R. Schick, "Optimization of SO₂ scrubber using CFD modeling," *Procedia Engineering*, vol. 83, pp. 170-180, 2014.

- 155] T. Chen *et al*, "Removal of PCDD/Fs and CBzs by different Air Pollution Control Devices in MSWIs," *Aerosol and Air Quality Research*, vol. 20, no. 10, pp. 2260-2272, 2020.
- 156] H. Shahbeik *et al*, "Using evolutionary machine learning to characterize and optimize co-pyrolysis of biomass feedstocks and polymeric wastes," *Journal of Cleaner Production*, vol. 387, p. 135881, 2023.
- 157] W. N. A. A. W. Ranizang, S. S. M. Shukri, Z. Y. Zakaria, M. Jusoh, and M. A. M. Yussuf, "Catalytic Pyrolysis of Fuel Oil Blended Stock to Methane and Hydrogen Gases Products Using Ni/ZSM-5 catalyst," *Chemical Engineering Transactions*, vol. 106, pp. 43-48, 2023.
- 158] V. H. Singo, L. I. Fajimi, N. Seedat, and R. Roopchund, "Synergistic Effects of Waste Tires, Plastic, and Biomass in Pyro-Oil Production," *ACS omega*, vol. 10, no. 8, pp. 7609-7620, 2025.
- 159] S. Chakrabarti and S. Shinde, "A Three-Phase Analysis of Synergistic Effects During Co-pyrolysis of Algae and Wood for Biochar Yield Using Machine Learning," *arXivpreprint arXiv:2405.11821*, 2024.
- 160] S. Hongthong *et al*, "Enhanced Biochar Production via Co - Pyrolysis of Biomass Residual with Plastic Waste after Recycling Process," *International Journal of Chemical Engineering*, vol. 2024, no. 1, p. 1176275, 2024.
- 161] M. Olam, "Mechanical and thermal properties of HDPE/PET microplastics, applications, and impact on environment and life," in *Advances and Challenges in Microplastics*: IntechOpen, 2023.
- 162] I. M. A. Putrawan¹, M. Rajendra, I. K. Adi, and I. S. Rahtika¹, "Performance of Water-Cooled Spiral Type Condenser in A Plastic Waste Pyrolysis," in *Proceedings of the International Conference on Sustainable Green Tourism Applied Science-Engineering Applied Science 2024 (ICoSTAS-EAS 2024)*, 2024, vol. 249: Springer Nature, p. 259.
- 163] S. H. Zein, C. T. Grogan, O. Y. Yansaneh, and A. Putranto, "Pyrolysis of high-density polyethylene waste plastic to liquid fuels—Modelling and economic analysis," *Processes*, vol. 10, no. 8, p. 1503, 2022.
- 164] A. B. D. NANDIYANTO *et al*, "FTIR Analysis of Pyrolysis of Polyethylene Terephthalate (PET) Plastic and Its Pyrolysis Mechanism Completed With Bibliometric Literature Review for Supporting Current Issues in Sustainable Development Goals (SDGS)."
- 165] P. Pereira *et al*, "Fast hydrolysis for chemical recycling of polyethylene terephthalate (PET)," *RSC Sustainability*, vol. 2, no. 5, pp. 1508-1514, 2024.
- 166] S. Yousef, J. Eimontas, N. Striugas, A. Mohamed, and M. Ali Abdelnaby, "Pyrolysis kinetic behavior and thermodynamic analysis of PET nonwoven fabric," *Materials*, vol. 16, no. 18, p. 6079, 2023.
- 167] T. Trecakova, A. Paulu, I. Harasymchuk, H. Brunhoferova, and V. Koci, "The effects of the technological setup of plastic waste pyrolysis on its environmental performance," *Environmental Science: Advances*, vol. 4, no. 11, pp. 1796-1809, 2025.
- 168] U. Hiibner *et al*, "Advanced oxidation processes for water and wastewater treatment-Guidance for systematic future research," *Heliyon*, vol. 10, no. 9, 2024.
- 169] H. Abedsoltan, "A focused review on recycling and hydrolysis techniques of polyethylene terephthalate," *Polymer Engineering & Science*, vol. 63, no. 9, pp. 2651-2674, 2023.

- [170] M. S. Abbas-Abadi *et al.*, "Thermochemical recycling of end-of-life and virgin HDPE: A pilot-scale study," *Journal of Analytical and Applied Pyrolysis*, vol. 166, p. 105614, 2022.
- [171] D. Li, M. Zou, and L. Jiang, "Dissolved oxygen control strategies for water treatment: a review," *Water Science & Technology*, vol. 86, no. 6, pp. 1444-1466, 2022.
- [172] D. A. Agar, M. Kwapinska, and J. J. Leahy, "Pyrolysis of wastewater sludge and composted organic fines from municipal solid waste: laboratory reactor characterisation and product distribution," *Environmental Science and Pollution Research*, vol. 25, no. 36, pp. 35874-35882, 2018.
- [173] A. S. f. Testing and M. C. E. o. Biotechnology, *Standard Test Methods for Analysis of Wood Fuels*. ASTM International, 2006.
- [174] J. Yernaidu and A. K. Tripathi, "Experimental investigation on the proneness of coal samples to spontaneous heating using proximate analysis and crossing point temperature method," *Materials Today: Proceedings*, vol. 47, pp. 3387-3391, 2021.
- [175] A. Ahmed, S. Hidayat, M. S. A. Bakar, A. K. Azad, R. S. Sukri, and N. Phusunti, "Thermochemical characterisation of Acacia auriculiformis tree parts via proximate, ultimate, TGA, DTG, calorific value and FTIR spectroscopy analyses to evaluate their potential as a biofuel resource," *Biofuels*, 2021.
- [176] Z. Alhulaybi and I. Dubdub, "Comprehensive kinetic study of PET pyrolysis using TGA," *Polymers*, vol. 15, no. 14, p. 3010, 2023.
- [177] N. Netsch *et al.*, "Thermogravimetric study on thermal degradation kinetics and polymer interactions in mixed thermoplastics," *Journal of Thermal Analysis and Calorimetry*, vol. 150, no. 1, pp. 211-229, 2025.
- [178] X. Lian *et al.*, "Pyrolysis characterization and mechanism studies of different structural plastics: A comparative study at optimal temperatures," *Energy*, vol. 313, p. 133986, 2024.
- [179] H. C. Genuino, M. P. Ruiz, H. J. Heeres, and S. R. Kersten, "Pyrolysis of mixed plastic waste: Predicting the product yields," *Waste Management*, vol. 156, pp. 208-215, 2023.
- [180] A. Kumar *et al.*, "Pyrolysis behaviour and synergistic effect in co-pyrolysis of wheat straw and polyethylene terephthalate: A study on product distribution and oil characterization," *Heliyon*, vol. 10, no. 17, 2024.
- [181] "Effects of Pyrolysis Parameters on Products Yields." Pyroltech. <https://pyroltech.com/effects-of-pyrolysis-parameters-on-products-yields/> (accessed 15/8/2024, 2024).
- [182] D. Vamvuka, K. Esser, and D. Marinakis, "Characterization of pyrolysis products of forest residues and refuse-derived fuel and evaluation of their suitability as bioenergy sources," *Applied Sciences*, vol. 13, no. 3, p. 1482, 2023.
- [183] M. Harussani, S. Sapuan, U. Rashid, A. Khalina, and R. Ilyas, "Pyrolysis of polypropylene plastic waste into carbonaceous char: Priority of plastic waste management amidst COVID-19 pandemic," *Science of The Total Environment*, vol. 803, p. 149911, 2022.
- [184] S. F. Yi Wang, Bo Xu, Boqian Li "Correlation Analysis of Pyrolysis Yield Using a Linear Regression Model," *Academic Journal of Science and Technology*, vol. 12, no. 1, p. 5, 2024, doi: <https://doi.org/10.54097/6bdvn553>.
- [185] P. Das, "Pyrolysis study of a waste plastic mixture through different kinetic models using isothermal and nonisothermal mechanism," *RSC advances*, vol. 14, no. 35, pp. 25599-25618, 2024.

- [186] A. Marotta, A. Causa, M. Salzano de Luna, V. Ambrogi, and G. Filippone, "Tuning the morphology of HDPE/PP/PET ternary blends by nanoparticles: a simple way to improve the performance of mixed recycled plastics," *Polymers*, vol. 14, no. 24, p. 5390, 2022.
- [187] P. Sudalaimuthu, U. Ali, and R. Sathyamurthy, "Optimization of process parameters of catalytic pyrolysis using natural zeolite and synthetic zeolites on yield of plastic oil through response surface methodology," *Scientific Reports*, vol. 14, no. 1, p. 28442, 2024.
- [188] R. K. Singh, B. Ruj, A. K. Sadhukhan, and P. Gupta, "A TG-FTIR investigation on the co-pyrolysis of the waste HDPE, PP, PS and PET under high heating conditions," *Journal of the Energy Institute*, vol. 93, no. 3, pp. 1020-1035, 2020.
- [189] B. A. Mohamed *et al.*, "Co-pyrolysis of sewage sludge and biomass for stabilizing heavy metals and reducing biochar toxicity: A review," *Environmental Chemistry Letters*, vol. 21, no. 2, pp. 1231-1250, 2023.
- [190] G. S. P. Senthilkumar, S. Sathishkumar, S. Manigandan, "Characterisation of Waste plastic oil by Fourier Transform Infrared Spectroscopy and Gas Chromatography-Mass Spectrometry," *Journal of Science and Technology*, vol. 7, no. 02 (MAR-APR 2022), p. 11, 2022, doi: <https://doi.org/10.46243/jst.2022.v7.i02.pp270-280>.
- [191] E. C. R. Lopez, "The Present and the Future of Polyethylene Pyrolysis," *Engineering Proceedings*, vol. 37, no. 1, p. 74, 2023.
- [192] E. Rice, R. Baird, A. Eaton, and L. Clesceri, "APHA," *American Public Health Association Publisher, Standard methods for the examination of water and wastewater 23rd edition, Part*, 2012.
- [193] A. Brems, J. Baeyens, C. Vandecasteele, and R. Dewil, "Polymeric cracking of waste polyethylene terephthalate to chemicals and energy," *Journal of the Air & Waste Management Association*, vol. 61, no. 7, pp. 721-731, 2011.
- [194] P. T. Williams and E. Slaney, "Analysis of products from the pyrolysis and liquefaction of single plastics and waste plastic mixtures," *Resources, Conservation and Recycling*, vol. 51, no. 4, pp. 754-769, 2007.
- [195] W. Kaminsky, M. Predel, and A. Sadiki, "Feedstock recycling of polymers by pyrolysis in a fluidised bed," *Polymer degradation and stability*, vol. 85, no. 3, pp. 1045-1050, 2004.
- [196] H. Meng, M. Wang, Z. Wu, J. Zhao, J. Li, and S. Wang, "Physico-chemical structure and gasification performance of co-pyrolytic char produced by the pyrolysis of polyvinyl chloride blends with two rank coals," *ACS omega*, vol. 7, no. 36, pp. 32280-32291, 2022.
- [197] F. A. Ahangar, U. Rashid, J. Ahmad, T. Tsubota, and A. Alsalme, "Conversion of waste polyethylene terephthalate (Pet) polymer into activated carbon and its feasibility to produce green fuel," *Polymers*, vol. 13, no. 22, p. 3952, 2021.
- [198] N. Wantaneeyakul, K. Kositkanawuth, S. Q. Turn, and J. Fu, "Investigation of biochar production from copyrolysis of rice husk and plastic," *ACS omega*, vol. 6, no. 43, pp. 28890-28902, 2021.
- [199] M. Martín-Lara, A. Piñar, A. Ligeró, G. Blázquez, and M. Calero, "Characterization and use of char produced from pyrolysis of post-consumer mixed plastic waste," *Water*, vol. 13, no. 9, p. 1188, 2021.

APPENDICES

APPENDIX A

Table A. 1a.
GCMS result for HDPE pyrolytic oil after pyrolysis process

3	Molecular formula	Normalized mass %	Compound Name	H-C type (alkane/alkene/ester)	H-C compound type (aromatic/aliphatic)
1	C ₂ H ₄ N ₄	2.536324757	1H-Tetrazole, 5-methyl-	Aromatic Heterocycle	Aromatic
2	C ₃ H ₃ I _N ₂	1.686386142	1H-Pyrazole, 4-iodo-	Aromatic Heterocycle	Aromatic
3	C ₃ H ₄ N ₂ O	2.064136638	2-Amino-oxazole	Aromatic Heterocycle	Aromatic
4	C ₄ H ₆ N ₂ O ₂	0.690743764	Muscimol	Aromatic Heterocyclic	Aromatic
5	C ₄ H ₇ NO	1.40307327	Methacrylamide	Alkene	Aliphatic
6	C ₅ H ₈ O ₂	0.635430298	Ethanone, 1-(3-methyloxiranyl)	Ketone	Aliphatic
7	C ₅ H ₁₁ N	0.822956437	Methanamine, N-butylidene-	Amine	Aliphatic
8	C ₅ H ₁₂ O	0.938979804	1-Butanol, 2-methyl-	Alkane	Aliphatic
9	C ₆ H ₆ O ₂	1.270860597	7-Oxabicyclo[2.2.1]hept-5-en-2-one	Alkene	Aliphatic
10	CeHgBr	1.320777626	Cyclopentene, 3-(bromomethyl)-	Alkene	Aliphatic
11	CeHioO	0.701536635	Cyclopentanecarboxaldehyde	Aldehyde	Aliphatic
12	CeHioO	0.802719804	2-Ethyl-3-vinyloxirane	Epoxide	Aliphatic
13	C ₆ H ₁₀ O ₂	1.095476438	Hexanedial	Aldehyde	Aliphatic
14	C ₆ H ₈ N ₃	1.129204161	1H-Imidazole-4-ethanamine, N-methyl-	Aromatic Heterocyclic	Aromatic
15	C ₆ H ₁₂	1.416564359	Cyclopentane, methyl-	Alkane	Aliphatic

3	Molecular formula	Normalized mass %	Compound Name	H-C type (alkane/alkene/ester)	H-C compound type (aromatic/aliphatic)
17	C₆H₁₂N₂	0.648921387	Formaldehyde, (2-butenyl)methylhydrazone	Hydrazone	Aliphatic
18	C ₆ H ₁₄ O	1.224990894	1-Pentanol, 2-methyl-	Alcohol	Aliphatic
19	C ₆ H ₁₄ N ₂	0.759548318	1,3 -Cyclohexanediamine	Amine	Aliphatic
20	C ₆ H ₁₄ O ₂	0.666459803	1,5-Pentanediol, 3-methyl-	Diol	Aliphatic
21	C ₇ H ₉ N ₃ O	0.667808912	Formamide, N,N-bis(2-cyanoethyl)-	Amide	Aliphatic
22	C ₇ H ₁₀ O	0.979453071	2-Heptyne-4-one	Alkyne And Ketone	Aliphatic
23	C ₇ H ₁₀ O ₂	0.728518813	2-Propenoic acid, 2-methyl-, 2-propenyl ester	Ester	Aliphatic
24	C ₇ H ₁₂	0.800021586	1-Hexyne, 5-methyl-	Alkyne	Aliphatic
25	C ₇ H ₁₂ O	0.69479109	2-n-Butylacrolein	Alkene	Aliphatic
26	C ₇ H ₁₂ S	0.671856239	7-Thiabicyclo[4.1.0]heptane, 2-methyl	Alkane	Aliphatic
27	C ₇ H ₁₂ Si	0.674554457	Methyltrivinylsilane	Alkene	Aliphatic
28	C ₇ H ₁₃ N	0.742009902	Hexanenitrile, 5-methyl	Nitrite	Aliphatic
29	C ₇ H ₁₄ O	0.824305546	Cyclohexanol, 4-methyl-, trans-	Alcohol	Aliphatic
30	C ₇ H ₁₄ O ₂	0.696140199	1,3 -Cyclopentanedimethanol	Alcohol	Aliphatic
31	C ₇ H ₁₅ N	0.928186933	(2,2-Dimethylcyclobutyl)methylamine	Alkane	Aliphatic
32	C ₇ H ₁₆ N	0.661063368	N, 1 -dimethyl-4 -Piperidinamine	Amine	Aliphatic
33	C ₈ H ₁₂ O ₂	0.724471487	7-Octene-2,4-dione	Alkene And Dione	Aliphatic
34	C ₈ H ₁₂ N ₂ O	0.802719804	1H-Imidazole, 1-(1-oxopentyl)	Imidazole Derivative	Aromatic
35	C ₈ H ₁₄ O	0.651619605	3 -Methyl-hepta-1,6-dien-3 -ol	Alcohol	Aliphatic

	Molecular formula	Normalized mass %	Compound Name	H-C type (alkane/alkene/ester)	H-C compound type (aromatic/aliphatic)
36	C ₈ H ₄ Br ₂	1.198008715	1,1-Dibromo-2-(2,2-dimethylpropyl)cyclopropane	Alkane	Aliphatic
37	C ₈ H ₁₆	0.728518813	1-Hexene, 2,5-dimethyl-	Alkene	Aliphatic
38	C ₈ H ₁₆	0.644874061	2,3-Dimethyl-1-hexene	Alkene	Aliphatic
39	C ₈ H ₁₆	0.809465348	2,3-Dimethyl-1-hexene	Alkene	Aliphatic
40	C ₈ H ₁₆ O	0.731217031	Cyclohexanemethanol, 4-methyl-, trans-	Alcohol	Aliphatic
41	C ₉ H ₁₄ O ₂	0.661063368	Cyclopentanecarboxylic acid, allyl ester	Ester	Aliphatic
42	C ₉ H ₁₄ O ₂	0.80676713	2,4-Pentanedione, 3-(1-methyl-2-propenyl)-	Ketone	Aliphatic
43	C ₉ H ₁₆ O	0.971358418	5-Heptenal, 2,6-dimethyl-	Aldehyde	Aliphatic
44	C ₉ H ₁₈	1.148091685	Cyclopentane, (2-methylpropyl)-	Alkane	Aliphatic
45	C ₉ H ₁₉	0.841843962	Nitric acid, nonyl ester	Ester	Aliphatic
46	C ₉ H ₁₉ NO	3.11644159	Nitric acid, nonyl ester	Ester	Aliphatic
47	C ₉ H ₂₀	0.72042416	Heptane, 2,4-dimethyl-	Alkane	Aliphatic
48	C ₁₀ H ₁₂ O ₂	0.736613467	E-2-Methyl-5-(furan-3-yl)-pent-1-en-3-one	Alkene	Aromatic
49	C ₁₀ H ₁₆ O	0.924139606	2-Methyl-6-methylene-octa-1,7-dien-3-ol	Alkene And Alcohol	Aliphatic
50	C ₁₀ H ₁₆ O	0.795974259	Ethanone, 1-(4-cycloocten-1-yl)-	Ketone	Aliphatic
51	C ₁₀ H ₁₆ O	0.634081189	3-(But-3-enyl)-cyclohexanone	Ketone	Aliphatic
52	C ₁₀ H ₁₈	1.103571091	Cyclopentene, 1-(2-methylbutyl)-	Alkene	Aliphatic
53	C ₁₀ H ₁₈	0.628684754	1,5-Heptadiene, 3,3,5-trimethyl	Alkene	Aliphatic
54	C ₁₀ H ₁₈	0.849938616	1,1'-Bicyclopentyl	Ester	Aliphatic

3	NMolecular o formula	Normalized mass %	Compound Name	H-C type (alkane/alkene/ ester)	H-C compound type (aromatic/ aliphatic)
55	CioHigO	3.008512877	Butanoic acid, 3-methyl-, 3-methyl-3- butenyl ester	Ester	Aliphatic
56	CioHigO	0.735264358	3-Decyn-2-ol	Alcohol	Aliphatic
57	CioHi802	0.693441982	Cyclobutanecarboxylic acid, 3- methylbutyl ester	Ester	Aliphatic
58	C10H18N4	2.617271292	1,2,4,5-Tetrazine, 3,6-bis(1,1- dimethylethyl)-	Aromatic Heterocycle	Aromatic
59	C10H20	0.855335051	Cyclohexane, (1,1-dimethylethyl)-	Alkene	Aliphatic
60	C10H20	1.199357824	Diisoamylene	Alkene	Aliphatic
61	C10H20O	0.972707527	Decanal	Aldehyde	Aliphatic
62	C10H20O	1.307286537	2-Decen-1-ol, (E)-	Alkene And Alcohol	Aliphatic
63	C10H22	0.724471487	Octane, 2,5-dimethyl-	Alkane	Aliphatic
64	C10H22O3S	4.033835652	Sulfone, 2-hydroxyhexyl t-butyl	Sulfone	Aliphatic
65	C10H22O3S	4.087800008	Sulfone, 2-hydroxyhexyl t-butyl	Sulfone	Aliphatic
66	C10H22O3S	0.713678615	Sulfurous acid, butyl isohexyl ester	Ester	Aliphatic
67	C10H23NO	0.771690299	Hydroxylamine, O-decyl-	Alkyl Hydroxylamine	Aliphatic
68	CiiHig	0.766293863	2H-Pyran, 2-[(1,1-dimethyl-2- butynyl)oxy]tetrahydro-	Alkyne	Aliphatic
69	C11H20	0.702885744	Norbornane, 2-isobutyl-	Alkane	Aliphatic
70	C11H20	0.845891289	1,7-Nonadiene, 4,8-dimethyl-	Alkene	Aliphatic
71	C12H20O4	0.755500992	Hexanedial	Aldehyde	Aliphatic
72	C12H22	0.635430298	1-Dodecyne	Alkyne	Aliphatic
73	C12H22O2	0.679950892	Pentanoic acid, 1-cyclopentylethyl ester	Ester	Aliphatic

3	NMolecular o formula	Normalized mass %	Compound Name	H-C type (alkane/alkene/ ester)	H-C compound type (aromatic/ aliphatic)
74	C12H22O2	0.68264911	2-(1-Methylcyclohexyloxy)- tetrahydropyran	Cyclic Ether	Aliphatic
75	C12H22O4	1.686386142	Oxalic acid, butyl isoheptyl ester	Ester	Aliphatic
76	C12H22O4	0.800021586	Oxalic acid, heptyl propyl ester	Ester	Aliphatic
77	C12H24	0.747406338	Cyclohexane, (1,2-dimethylbutyl)-	Alkane	Aliphatic
78	C13H26	1.01857723	1-Decene, 3,3,4-trimethyl	Alkene	Aliphatic
79	C13H28O	0.702885744	Hexane, 1-(hexyloxy)-5-methyl- 2-Thiopheneacetic acid, 2- ethylcyclohexyl ester	Alkane	Aliphatic
80	C14H20O2S	1.103571091		Ester	Aliphatic
81	C14H24O4	0.736613467	Oxalic acid, allyl nonyl ester	Ester	Aliphatic
82	C14H28	0.647572279	7-Tetradecene, (E)-	Alkene	Aliphatic
83	C14H30O	1.484019805	Hexyl octyl ether	Ether	Aliphatic
84	C15H18O2	0.665110694	Phenylacetic acid, 2-methylcyclohex- 2-enyl ester	Ester	Aromatic
85	C18H34	0.916044952	1-Octadecyne	Alkyne	Aliphatic
86	C20H36O4	2.49585149	Oxalic acid, allyl pentadecyl ester	ester	Aliphatic
87	C20H36O4	9.092994077	Oxalic acid, allyl pentadecyl ester	ester	aliphatic

Table A. 1b.

GCMS result for ratio HDPE2: IPET pyrolytic oil after pyrolysis process

4	Molecular formula	Normalized mass %	Compound Name	H-C type (alkane/alkene/ester)	H-C compound type (aromatic/aliphatic)
1	C ₄ H ₄ N ₂	0.839650955	2-Butenedinitrile, (E)-	alkene	aliphatic
2	C ₄ H ₇ NO	2.237912669	2-Pyrrolidinone	lactam	aliphatic
3	C ₄ H ₁₁ BO ₂	4.614610621	Borinic acid, diethyl	borinic acid	aliphatic
4	C ₅ H ₈ O	0.863938379	1,4-Pentadien-3-ol	alkene	aliphatic
5	C ₅ H ₁₀ N	0.883021356	Pyrrolidine, 1-methyl-	heterocyclic amine	aliphatic
6	C ₅ H ₁₀ O	4.614610621	Cyclobutanemethanol	alcohol	aliphatic
7	C ₅ H ₁₀ O ₂	0.851794667	Butanal, 4-hydroxy-3-methyl	alkane derivative	aliphatic
8	C ₆ H ₈ O	0.74597089	Cyclopentanecarboxaldehyde	aldehyde	aliphatic
9	C ₆ H ₈ O ₂	1.190083792	Ethyl 2-butynoate	ester	aliphatic
10	C ₆ H ₁₀ O	0.827507243	1-Hexyn-3-ol	alkyne and alcohol	aliphatic
11	C ₆ H ₁₀ O ₂	1.33927797	Hexanedial	aldehyde	aliphatic
12	C ₆ H ₁₀ O ₂	0.909043596	Hexanedial	aldehyde	aliphatic
13	C ₆ H ₁₀ O ₂ S	0.634942664	1,2-Cyclohexanediol, cyclic sulfite, cis-	cyclic sulfite	aliphatic
14	C ₆ H ₁₄ O	0.681782697	1-Pentanol, 4-methyl	alcohol	aliphatic
15	C ₇ H ₁₁ NO	0.678313065	2-Propionyl-1-pyrroline	ketone	aliphatic
17	C ₇ H ₁₁ N ₃ O	0.699130857	3-Methyl-1-[(1H)-1,2,4-triazol-1-yl]butan-2-one	ketone	aliphatic
18	C ₇ H ₁₁ F ₃ O ₂	0.629738216	Acetic acid, trifluoro-, 2,2-dimethylpropyl ester	ester	aliphatic

4	NMolecular o formula	Normalized mass %	Compound Name	H-C type (alkane/alkene/ ester)	H-C compound type (aromatic/ aliphatic)
19	C ₇ H ₁₂ N	0.78934129	Bicyclo[2.2.1]heptan-2-amine, exo-	alkane	aliphatic
20	C ₇ H ₁₂ O	1.023541453	1-Pentyn-3-ol, 3,4-dimethyl-	alkyne	aliphatic
21	C ₇ H ₁₂ O	1.39132245	1-Pentyn-3-ol, 4-methyl	alkyne and alcohol	aliphatic
22	C ₇ H ₁₃ N	0.659230089	Hexanenitrile, 5-methyl-	nitrile	aliphatic
23	C ₇ H ₁₄ O	0.9420051	1-Hepten-3-ol	alkene and alcohol	aliphatic
24	C ₇ H ₁₆	1.179674895	Pentane, 2,2-dimethyl-	alkane	aliphatic
25	C ₇ H ₁₆	8.899606197	Pentane, 2,2-dimethyl	alkane	aliphatic
26	C ₇ H ₁₆ O	0.72862273	1-Pentanol, 3,4-dimethyl-	alcohol	aliphatic
27	C ₈ H ₁₄ N	0.935065836	6-[N-Aziridyl]hexadiene-1,3	alkene	aliphatic
28	C ₈ H ₁₂ O	0.966292525	2,6-Cyclooctadien-1-ol	alkene	aliphatic
29	C ₈ H ₁₂ O ₂	1.344482418	2,4-Pentanedione, 3-(2-propenyl)-	alkene	aliphatic
30	C ₈ H ₁₃ Cl	0.77199313	Cyclopropane, 3-chloro-1,1,2,2- tetramethyl	alkane	aliphatic
31	C ₈ H ₁₄	0.869142827	Cyclopentane, 1-ethyl-1-methyl-	alkane	aliphatic
32	C ₈ H ₁₄	0.725153098	Cyclopentane, 1-ethyl-2-methyl-, cis	alkane	aliphatic
33	C ₈ H ₁₄ O	0.690456777	2-n-Butylacrolein	alkene and aldehyde	aliphatic
34	C ₈ H ₁₅ N	3.03592804	Pentanenitrile, 2,2,4-trimethyl	nitrile	aliphatic
35	C ₈ H ₁₆ S	0.978436237	Cyclopentane, 1-ethyl-2-methyl	alkane	aliphatic
36	C ₈ H ₁₆ S	0.72862273	1-Pentene, 2,4,4-trimethyl-	alkene	aliphatic
37	C ₈ H ₁₆ S	0.815363531	2,3-Dimethyl-1-hexene	alkene	aliphatic
38	C ₈ H ₁₆ O	1.027011085	1-Butene, 4-butoxy-	alkene	aliphatic

4	Molecular formula	Normalized mass %	Compound Name	H-C type (alkane/alkene/ester)	H-C compound type (aromatic/aliphatic)
39	C ₈ H ₁₈	5.100359107	Hexane, 2,4-dimethyl	alkane	aliphatic
40	C ₉ H ₁₄ O ₂	1.358360946	Cyclopentanecarboxylic acid, allyl ester	ester	aliphatic
41	C ₉ H ₁₄ N ₂ O	0.787606474	Urea, N,N'-di-2-propenyl-	alkene	aliphatic
42	C ₈ H ₁₆ O	0.697396041	1-Octyn-3-ol, 3-methyl	alkyne and alcohol	aliphatic
43	C ₈ H ₁₆ O	0.688721961	5-Octen-4-one, 7-methyl-	alkene and ketone	aliphatic
44	C ₈ H ₁₆ O	0.654025641	3-Nonyn-2-ol	alkyne and alcohol	aliphatic
45	C ₉ H ₁₇ O ₂	1.025276269	Cyclohexanemethyl propanoate	ester	aliphatic
46	C ₉ H ₁₈	1.243863088	2,3,3-Trimethyl-1-hexene	alkene	aliphatic
47	C ₉ H ₁₈	3.261454123	1-Hexene, 3,5,5-trimethyl	alkene	aliphatic
48	C ₉ H ₁₈	0.778932394	1-Hexene, 3,5,5-trimethyl-	alkene	aliphatic
49	C ₉ H ₁₈	1.079055566	Pentane, 2,3,3,4-tetramethyl	alkane	aliphatic
50	C ₉ H ₁₈ N	0.617594504	(2,2-Dimethylcyclobutyl)methylamine	alkane	aliphatic
51	C ₈ H ₁₆ O	0.751175338	Cyclooctanemethanol	alcohol	aliphatic
52	C ₈ H ₁₆ O	0.631473032	Cyclooctanemethanol	n/a	aliphatic
53	C ₉ H ₁₉ Br	0.73729681	2-Bromononane	alkane	aliphatic
54	C ₉ H ₁₉ NO ₂	0.718213833	Nitric acid, nonyl ester	ester	aliphatic
55	C ₉ H ₂₀	0.76331905	Hexane, 2,2,4-trimethyl	alkane	aliphatic
56	C ₁₀ H ₁₄ O ₂	0.971496973	8-Methyloctahydrocoumarin	alkane	aliphatic
57	C ₁₀ H ₁₄ O ₂	0.638412296	2-Pentanol, 5-(2-propynyloxy)-	alcohol	aliphatic
58	C ₁₀ H ₁₆ O	0.93333102	1-Hexyne, 3-ethoxy-3,4-dimethyl-	alkyne	aliphatic

4	Molecular formula	Normalized mass %	Compound Name	H-C type (alkane/alkene/ester)	H-C compound type (aromatic/aliphatic)
59	C10H16O2	0.615859688	Propanoic acid, 2-methyl-, 3-methyl-2-butenyl ester	ester	aliphatic
60	C10H18	0.88996062	Cyclopentene, 1-(2-methylbutyl)-	alkene	aliphatic
61	C10H18	0.6280034	1,4-Heptadiene, 3,3,6-trimethyl-	alkene	aliphatic
62	C10H18Si	0.794545738	1 - Allyl-1 -but-3 -enyl-1 -silacy clobutane	alkene	aliphatic
63	G0H19N	0.825772427	2,7-Dimethyl-1,7-octadien-3 -amine	alkene	aliphatic
64	G0H19O	1.367035026	Cyclohexanone, 3-butyl	ketone	aliphatic
65	C10H20	1.046094062	Cyclohexane, (2-methylpropyl)-	alkane	aliphatic
66	C10H21NO3	0.718213833	Nitric acid, decyl ester	ester	aliphatic
67	C11H14O	0.818833163	2H-Pyran, 2-[(1,1-dimethyl-2-butynyl)oxy]tetrahydro	pyran	aliphatic
68	CnHisOz	0.77199313	4,8-Dioxatricyclo[5.1.0.0(3,5)]octane, 1 -methyl-5 -(1 -methylethyl)-	dioxatricycloalkane	aliphatic
69	C11H20O	0.719948649	2-Hexen-1-ol, 2-ethyl	alkene	aliphatic
70	C11H20O	0.719948649	Ether, 3-butenyl pentyl	alkene and ether	aliphatic
71	C11H21NO3	3.07062436	Nitric acid, decyl ester	ester	aliphatic
72	C12H16F3O2	0.730357546	Trifluoroacetyl-lavandulol	ester	aliphatic
73	C12H19NO2	0.615859688	1 -Hexyl-2-nitrocyclohexane	alkane	aliphatic
74	C12H26O	2.116475548	Hexane, 1,1'-oxybis	ether	aliphatic
75	C13H18O2	0.739031626	1,3-Benzodioxole, 2-ethenylhexahydro-	alkene	aromatic
76	C13H24O3S	0.841385771	Sulfurous acid, cyclohexylmethyl isohexyl ester	ester	aliphatic
77	C14H26O	0.843120587	Oxirane, tetradecyl-	epoxide	aliphatic

4	Molecular formula	Normalized mass %	Compound Name	H-C type (alkane/alkene/ester)	H-C compound type (aromatic/aliphatic)
78	C15H26	0.77199313	1,7-Dimethyl-4-(1-methylethyl)cyclodecane	alkane	aliphatic
79	C15H26O2	1.769512343	2,2-Dimethylpropanoic acid, oct-3-en-2-yl ester	ester	aliphatic
81	C16H36O	0.827507243	Octane, 1,1'-oxybis-	alkane	aliphatic
	C18H30O4	0.654025641	Oxalic acid, cyclohexylmethyl isohexyl ester	ester	aliphatic

Table A. 1c.

GCMS result for ratio HDPEI: IPET pyrolytic oil after pyrolysis process

5	Molecular formula	Normalized mass %	Compound Name	H-C type (alkane/alkene/ester)	H-C compound type (aromatic/aliphatic)
1	CH ₃ Br	0.925845328	Methane, bromo-	alkane	aliphatic
2	C ₃ H ₇ NO ₂ S	0.487453609	Cysteine	amino acid	aliphatic
3	C ₄ H ₆ N ₄	0.540472102	2,6 -Py razinediamine	heterocyclic	aromatic
4	C ₅ H ₇ ClO ₂	0.552341914	Furan-2-carbonyl chloride, tetrahydro	acid chloride	aliphatic
5	C ₅ H ₈ Si	0.7383023	Silacyclopent-3-ene, 3-methyl	alkene	aliphatic
6	C ₅ H ₈ Si	0.925845328	Silacyclopent-3-ene, 3-methyl	alkene	aliphatic
7	CeHgNz	1.400637805	Phenalzine	amine	aromatic
8	CeHgNz	2.318569925	Phenalzine	amine	aromatic
9	Celts Si	0.973324576	Silacyclopent-3-ene, 3-methyl	alkene	aliphatic
10	CeHioSi	0.886279289	Silacyclopent-3-ene, 3-methyl	alkene	aliphatic
11	CeHioO	0.549967952	5-Hexyn-1-ol	Alkyne alcohol	Aliphatic
12	C ₆ H ₁₁ N ₂	0.701110223	1H-Imidazole, 4,5-dihydro-2-(1-methylethyl)-	heterocyclic	aliphatic
13	CvHnNO	0.434435116	2-Propionyl-1-pyrroline	ketone	aliphatic
14	C ₇ H ₁₂ O	0.463713985	2-Ethyl-3 -vinyloxirane	alkene	aliphatic
15	C ₇ H ₁₃ N ₄	0.743050225	7-Amino-1,3,5-triazaadamantane	heterocyclic	aliphatic
17	C ₇ H ₁₆	0.502488704	Butane, 2,2,3-trimethyl-	alkane	aliphatic
18	C ₈ H ₁₂ O ₂	0.48903625	2,3'-Bifuran, octahydro	alkane	aliphatic
19	C ₈ H ₁₄ O ₂	0.894192497	2,3'-Bifuran, octahydro	Saturated ether	aliphatic
20	CsHwSi	1.91499632	Allyldimethyl(prop-1 -ynyl)silane	alkene and alkyne	aliphatic

5	Molecular formula	Normalized mass %	Compound Name	H-C type (alkane/alkene/ester)	H-C compound type (aromatic/aliphatic)
21	C ₈ H ₁₆ SiOH	0.456592098	trans-(2-Ethylcyclopentyl)methanol	alkane	aliphatic
22	C ₈ H ₁₆ Si	0.617230219	Diethyldivinylsilane	alkene	aliphatic
23	C ₈ H ₁₈	0.533350215	Pentane, 3,3-dimethyl	alkane	aliphatic
24	C ₈ H ₁₈	4.296871909	Hexane, 3,3-dimethyl	alkane	aliphatic
25	C ₉ H ₁₄ O ₂	0.573707575	2-Nonenal, 8-oxo-	alkene	aliphatic
26	C ₉ H ₁₄ O	0.596655878	2-n-Butylacrolein	alkene	aliphatic
27	C ₉ H ₁₄ O	0.933758536	3-Ethyl-1-heptyne-3-ol	Alkyne alcohol	Aliphatic
28	C ₉ H ₁₆ O	0.46846191	2-Methyl-4-octenal	alkene	aliphatic
29	C ₉ H ₁₈ O	0.482705684	Cyclooctane, methoxy-	alkane	aliphatic
30	C ₉ H ₂₂	0.47874908	Heptane, 3,5-dimethyl	alkane	aliphatic
31	C ₁₀ H ₁₆ Si	0.9970642	Triallylmethylsilane	alkene	aliphatic
32	C ₁₀ H ₁₆ Si	0.426521908	Triallylmethylsilane	alkene	aliphatic
33	C ₁₀ H ₁₆ Si	0.557881159	Triallylmethylsilane	alkene	aliphatic
34	C ₁₀ H ₁₆ O	0.583203425	<u>Bicyclo[3.1.1]heptan-3-one, 2,6,6-trimethyl-</u>	ketone	aliphatic
35	C ₁₀ H ₁₆ O	0.483497005	6,6-Dimethyl-1,3-heptadien-5-ol	alkene	Aliphatic
36	C ₁₀ H ₁₆ O	0.501697383	<u>Bicyclo[3.1.1]heptan-3-ol, 2,6,6-trimethyl-</u>	alcohol	aliphatic
37	C ₁₀ H ₁₆ Si	1.060369863	Triallylmethylsilane	alkene	aliphatic
	C ₁₀ H ₁₉ N	0.460548702	<u>2,6,6-Trimethyl-bicyclo[3.1.1]hept-3-ylamine</u>	alkane	aliphatic
39	C ₁₀ H ₂₀ O	0.439974361	Isooctane, (ethenyloxy) -	alkene	aliphatic
40	C ₁₀ H ₂₁ NO ₃	0.681327203	Nitric acid, decyl ester	ester	aliphatic

5	Molecular formula	Normalized mass %	Compound Name	H-C type (alkane/alkene/ester)	H-C compound type (aromatic/aliphatic)
41	C10H22	0.471627193	Hexane, 2,2,3,3-tetramethyl	alkane	aliphatic
42	C10H23NO	0.663126825	Hydroxylamine, O-decyl-	alkane	aliphatic
43	C11H10N2O2	0.486662288	Hydantoin, 5-ethy 1-5-phenyl-,	heterocyclic	aromatic
44	C11H17	0.661544183	Cyclopentane, 1,3-dimethyl-2-(1-methylethenyl)-	alkene	aliphatic
	CnHisN	0.61802154	Cyclopentanemethanamine, 5-amino-2,2,4-trimethyl	alkane	aliphatic
46	C12H8O4	0.780242302	Ethanone, 1,2-di-2-furanyl-2-hydroxy	ketones	aromatic
47	C12H18F3NO3	0.878366081	Butanoic acid, 2-[(triifluoroacetyl)amino]-, 1-methylpentyl ester	ester	aliphatic
48	C12H19Si	0.575290217	1-Allyl-1-but-3-enyl-1-silacyclobutane	alkene	aliphatic
49	C12H20N2	0.527810969	1,10-Dicyanodecane	alkane	aliphatic
50	C12H22O2	0.03007019	Pentanoic acid, 2-methylcyclohexyl ester, cis	ester	aliphatic
51	C12H24	0.454218135	Bicyclo[4.1.0]heptane, 7-pentyl	alkane	aliphatic
52	C12H24	0.430478512	Bicyclo[4.1.0]heptane, 7-pentyl-	alkane	aliphatic
53	C12H26	0.894192497	Cyclohexane, 1-methyl-4-(1-methylbutyl)-	alkane	aliphatic
54	C12H26	0.74779815	Decane, 2,4-dimethyl	alkane	aliphatic
55	C12H26	1.899169904	Undecane, 3-ethyl-	alkane	aliphatic
56	C12H26	0.423356625	Decane, 2,4-dimethyl	alkane	aliphatic
57	C12H28	0.768372491	Decane, 2,9-dimethyl	alkane	aliphatic
co	COH20O3	0.593490595	Methyl 8-(2-furyl)octanoate	ester	aliphatic aromatic and aliphatic

5	Molecular formula	Normalized mass %	Compound Name	H-C type (alkane/alkene/ester)	H-C compound type (aromatic/aliphatic)
59	C13H22	0.618812861	Cyclohexane, (1,2-dimethylpropyl)-	alkane	aliphatic
60	C0H22O4	0.559463801	Oxalic acid, allyl octyl ester	ester	aliphatic
61	C0H24	0.846713249	1-Tridecyne	alkyne	aliphatic
62	C0H26O3S	0.53809814	Sulfurous acid, cyclohexylmethyl <u>isohexyl ester</u>	ester	aliphatic
63	C13H28	1.060369863	Decane, 2,5,9-trimethyl	alkane	aliphatic
64	C13H28	1.630120835	Dodecane, 2-methyl	alkane	aliphatic
65	C ₁₃ H ₂₈ O	4.589660603	Hexane, 1-(hexyloxy)-5-methyl-	ether	aliphatic
66	C14H28O3S	0.838800041	Sulfurous acid, 2-ethylhexyl hexyl <u>ester</u>	ester	aliphatic
	C14H28O3S	1.804211409	Sulfurous acid, 2-ethylhexyl hexyl <u>ester</u>	ester	aliphatic
	C14H28O3S	2.081173687	Sulfurous acid, 2-ethylhexyl hexyl <u>ester</u>	ester	aliphatic
	C14H28O3S	1.384811389	Sulfurous acid, 2-ethylhexyl hexyl <u>ester</u>	ester	aliphatic
	C14H28O3S	1.044543447	Sulfurous acid, 2-ethylhexyl hexyl <u>ester</u>	ester	aliphatic
	C14H30O3S	2.14447935	Sulfurous acid, 2-ethylhexyl hexyl <u>ester</u>	ester	aliphatic
	C14H30O4S	4.850796464	Sulfurous acid, 2-ethylhexyl hexyl <u>ester</u>	ester	aliphatic
73	C14H32	0.822973625	Dodecane, 4,6-dimethyl	alkane	aliphatic
74	C15H24	0.709814752	1-Pentadecyne	alkyne	aliphatic
75	C16H28O2	0.505653987	Cyclopentanecarboxylic acid, 6-ethyl-3-octyl <u>ester</u>	ester	aliphatic
76	C16H34	1.353158557	Hexadecane	alkane	aliphatic

5	Molecular formula	Normalized mass %	Compound Name	H-C type (alkane/alkene/ester)	H-C compound type (aromatic/aliphatic)
77	C ₁₆ H ₃₄	0.715353997	Hexadecane	alkane	aliphatic
78	C ₁₈ H ₁₀ O ₈	0.727223809	(+)-Dibenzoyl-L-tartaric acid anhydride	acid anhydride	aromatic and aliphatic
79	C ₁₈ H ₃₈ O ₂	0.734345696	Hexadecane, 1,1-dimethoxy	alkane	aliphatic
80	C ₁₉ H ₃₀ O ₃ S	0.762041924	Sulfurous acid, hexyl tridecyl ester	ester	aliphatic
81	C ₁₉ H ₃₄	0.933758536	1-Nonadecene	alkene	aliphatic
82	C ₂₀ H ₄₂	0.421773983	10-Methylnonadecane	alkane	aliphatic
83	C ₂₁ H ₄₄	1.392724597	10-Heneicosene (c,t)	alkene	aliphatic
84	C ₂₂ H ₄₆	0.477957759	1-Docosene	alkene	aliphatic
85	C ₂₃ H ₃₉ O ₄	1.709252914	Oxalic acid, allyl octadecyl ester	ester	aliphatic
86	C ₂₃ H ₄₂ O ₄	4.40765682	Oxalic acid, allyl octadecyl ester	ester	aliphatic
87	C ₂₃ H ₄₆ O ₃ S	0.470044551	Sulfurous acid, cyclohexylmethyl <u>hexadecyl ester</u>	ester	aliphatic
	C ₂₃ H ₄₆ O ₃ S	0.799234001	Sulfurous acid, cyclohexylmethyl <u>heptadecyl ester</u>	ester	aliphatic
89	C ₂₄ H ₃₇ O ₃ S	2.927886936	Sulfurous acid, cyclohexylmethyl <u>heptadecyl ester</u>	ester	aliphatic
90	C ₂₄ H ₃₇ O ₃ S	1.044543447	Sulfurous acid, cyclohexylmethyl <u>heptadecyl ester</u>	ester	aliphatic
91	C ₂₄ H ₃₇ O ₃ S	2.002041608	Sulfurous acid, cyclohexylmethyl <u>heptadecyl ester</u>	ester	aliphatic
92	C ₂₄ H ₃₇ O ₃ S	1.788384993	Sulfurous acid, cyclohexylmethyl <u>heptadecyl ester</u>	ester	aliphatic
93	C ₂₄ H ₃₇ O ₃ S	2.168218974	Sulfurous acid, cyclohexylmethyl <u>heptadecyl ester</u>	ester	aliphatic
94	C ₂₄ H ₃₇ O ₃ S	2.081173687	Sulfurous acid, cyclohexylmethyl <u>heptadecyl ester</u>	ester	aliphatic

5	Molecular formula	Normalized mass %	Compound Name	H-C type (alkane/alkene/ester)	H ₃ C compound type (aromatic/aliphatic)
⁹⁵	C₂₈H₄₈O₃S C ₂₈ H ₄₈ O ₃ S	0.95749816 0.95749816	Sulfurous acid, cyclohexylmethyl octadecyl ester	ester	aliphatic
⁹⁶	C ₄₄ H ₉₀	0.453426815	Tetratetracontane	alkane	aliphatic

Table A. Id.

GCMS result for ratio HDPEI :2PET pyrolytic oil after pyrolysis process

6	Molecular formula	Normalized mass %	Compound Name	H-C type (alkane/alkene/ester)	H-C compound type (aromatic/aliphatic)
1	C ₅ H ₆ N ₃ O	0.797475617	2(1H)-Pyrimidinone, 4-amino-5-methyl-	heterocyclic	aromatic
2	C ₅ H ₇ N ₃ O	0.502964238	2-Amino-5-methyl-4-oxo-3,4-dihydropyrimidine	heterocyclic	aromatic
3	C ₆ H ₁₂ Cl ₂	0.759227386	Cyclohexane, 1,3-dichloro	alkane	aliphatic
4	C ₇ H ₅ NO ₄	0.501051826	2,6-Pyridinedicarboxylic acid	dicarboxylic acid	aromatic
5	CvHeOi	0.881621725	2,4,6-Cycloheptatrien-1-one, 2-hydroxy-	alkene	aromatic
6	CvHeOi	1.669535284	Benzoic acid	carboxylic acid	aromatic
7	C ₇ H ₇ O ₂	0.87588449	2,4,6-Cycloheptatrien-1-one, 2-hydroxy-	ketone	aromatic
8	C ₇ H ₇ NO ₂	0.587110346	5-Methyl-2-nitrophenol	phenol	aromatic
9	C ₇ H ₁₀ O ₅	0.564161408	Shikimic acid	alkene	aliphatic
10	C ₇ H ₁₂ O	1.353987378	2-Isopropyl-3-vinyloxirane	alkene	aliphatic
11	C ₇ H ₁₂ O ₅	0.545037292	endo-2,3-0-Ethylidene- α -D-erythrofuranose	Ethylidene-protected furanose	aliphatic
12	C ₇ H ₁₂ B ₂ O ₇	0.55459935	α -D-Xylofuranose, cyclic 1,2:3,5-bis(methylboronate)	ester	aliphatic
13	C ₈ H ₄ O ₃	0.483840122	1,4-Cyclohexadiene-1,2-dicarboxylic anhydride	anhydride	aliphatic
14	C ₈ H ₈ N ₂ O	0.455153949	N-(2,5-Dicyano-3,4-dihydro-2H-pyrrol-2-yl)-acetamide	amide	aromatic
15	C ₈ H ₈ Ch	1.334863263	Benzoic acid, 4-methyl	carboxylic acid	aromatic
17	C ₈ H ₁₅ NO	0.755402563	Cyclooctanone, oxime	Ketoxime	aliphatic

6	Molecular formula	Normalized mass %	Compound Name	H-C type (alkane/alkene/ester)	H-C compound type (aromatic/aliphatic)
18	C ₈ H ₁₈	3.155479059	Cyclohexane, 1,1-dimethyl	alkane	aliphatic
19	CsHisCb	0.738190859	Hexane, 1,1'-[methylenebis(oxy)]bis-	ester	aliphatic
20	C ₉ H ₁₅ NO	0.457066361	<u>Methyl-(9-oxa-bicyclo [3.3.1] non-6-en-2-yl)-amine</u>	alkene	aliphatic
21	C ₉ H ₁₅ O ₃	1.464907248	<u>2-Cyclopenten-1-one, 4-butyl-3-methoxy</u>	alkene	aliphatic
22	C ₉ H ₁₇ N ₄ O	0.900745841	1-Methyl-4-tert-butylaminocytosine	heterocyclic	aromatic
23	CsHis	0.445591891	2,4,4-Trimethyl-1-hexene	alkene	aliphatic
24	C ₁₀ H ₁₅ N	0.592847581	Dextroamphetamine	phenethylamine derivative	aliphatic
25	C ₁₀ HisO	0.495314592	6-Octen-1-ol, 3,7-dimethyl-, (n)-	alkene	aliphatic
26	C ₁₀ H ₁₈ O ₂	1.128322815	6-Octenoic acid, 3,7-dimethyl	alkene	aliphatic
27	C ₁₀ HisSi	4.283801874	<u>>1-Allyl-1-but-3-enyl-1-silacyclobutane</u>	alkene	aliphatic
28	C ₁₀ H ₁₉ O	2.141900937	Cyclohexanone, 3-butyl-	ketone	aliphatic
29	C ₁₀ H ₁₉ BO ₆	0.761139797	<u>a-d-Gulofuranose, 2,3:5,6-di-O-(ethylboranediy 1) -</u>	Boronate ester	aliphatic
30	C ₁₁ H ₁₉ N ₃ O ₂	0.703767451	<u>5-Ethyl-6-imino-5-(1-methyl-butyl)-dihydro-pyrimidine-2,4-dione</u>	Pyrimidine derivative	aromatic
31	C ₁₁ H ₂₂ N ₂ O	0.969592656	<u>N-(2,2,6,6-Tetramethylpiperidin-4-yl)acetamide</u>	amide	aliphatic
32	C ₁₁ H ₂₄ O	0.946643718	1-Hexanol, 2-ethyl-2-propyl	alcohol	aliphatic
33	C ₁₂ H ₁₁ ClO ₂	1.082424938	4-Chlorobutyl benzoate	ester	aromatic and aliphatic
34	C ₁₂ H ₁₄ O	0.613884108	3-Buten-1-one, 2,2-dimethyl-1-phenyl-	alkene	aromatic and aliphatic
35	C ₁₂ H ₂₂ O ₂	2.161025053	<u>2-(1-Methylcyclohexyloxy)-tetrahydropyran</u>	ether	aliphatic

6	Molecular formula	Normalized mass %	Compound Name	H-C type (alkane/alkene/ester)	H-C compound type (aromatic/aliphatic)
³⁶	C ₁₂ H ₂₂ O ₃	0.462803595	3,7-Dimethyl-6-nonen-1-ol acetate	alkene	aliphatic
³⁷	C ₁₂ H ₂	1.401797667	3-Heptene, 2,2,3,5,6-pentamethyl-	alkene	aliphatic
38	CoHisNOs	0.852935552	L-Isoleucine, N-benzoyl	benzoylated amine	aromatic and aliphatic
39	C ₁₃ H ₂₂ O ₃	0.567986231	Dasycarpidan-1-methanol, acetate (ester)	ester	aliphatic
40	C ₁₃ H ₂₂ O ₃	0.430292599	Dasycarpidan-1-methanol, acetate (ester)	ester	aliphatic
⁴¹	C ₁₃ H ₂	0.722891566	1,1'-Bicyclohexyl, 2-methyl-, trans	alkane	aliphatic
⁴²	C ₁₃ H ₂	3.480589023	Dodecane, 2-methyl	alkane	aliphatic
⁴³	C ₁₀ H ₂	1.441958309	Decane, 2,2,8-trimethyl-	alkane	aliphatic
44	C ₁₃ H ₂₈ BO ₉	0.709504685	a-D-Xylofuranose, cyclic 1,2:3,5-bis(butylboronate)	boronate ester	aliphatic
45	C ₁₄ H ₁₁ NO ₂	0.65404475	Cyclohexanone, 4-(benzoyloxy)-oxime	ester and oxime	aromatic and aliphatic
46	C ₁₄ H ₁₆ N ₂ O ₂	0.646395104	1,2-Diaminoethane, 1,2-bis(2-hydroxyphenyl)-	diamine	aromatic and aliphatic
⁴⁷	C ₁₄ H ₂₂ O ₂	0.55459935	E-2-Hexenyl E-2-octenoate	ester	aliphatic
48	C ₁₄ H ₂₂ O ₄	0.522088353	5-Hydroxy-2,2-dimethyl-5,6-bis-(2-oxopropyl)-cyclohexanone	ketone and alcohol	aliphatic
49	C ₁₄ H ₂₃ O ₅	0.457066361	3-Oxobutyric acid, 2-(2-oxocycloheptyl)methyl-, ethyl ester	ester	aliphatic
50	C ₁₄ H ₂₄ N ₂ O	0.734366036	1-Methyl-8-propyl-3,6-diazahomoadamantan-9-ol	amine	aliphatic
51	C ₁₅ H ₁₁ FO ₃	0.437942245	Benzoic acid, 3-yluro-, 2-oxo-2-phenylethyl ester	ester	aromatic
⁵²	C ₁₅ H ₁₅ N ₄	0.787913559	2-(4-Methylphenyl)-5-phenyltetrazole	tetrazole	aromatic

6	Molecular formula	Normalized mass %	Compound Name	H-C type (alkane/alkene/ester)	H-C compound type (aromatic/aliphatic)
53	C ₁₅ H ₂₀ O ₄	0.564161408	2,3-Dioxabicyclo[2.2.2]oct-7-en-5-one, 1-(3-oxo-1-butenyl)-6,6,7-trimethyl	alkene	aliphatic
54	C ₁₅ H ₂₂ O ₂	0.522088353	5-Hydroxy-2,3,3-trimethyl-2-(3-methyl-buta-1,3-dienyl)-cyclohexanone	alkene	aliphatic
55	C ₁₅ H ₂₅ O ₂	0.522088353	7-(1-Hydroxy-cyclohexyl)-2,2-dimethyl-hept-5-en-3-one	alkene	aliphatic
56	C ₁₅ H ₂₆ O ₂	0.852935552	Geranyl isovalerate	ester and alkene	aliphatic
57	C ₁₆ H ₂₄ O ₂	0.541212469	2,5-Furandione, 3-(dodecenyl)dihydro-	dione	aliphatic
58	C ₁₆ H ₂₄ O ₂	0.55459935	2H-Pyran, tetrahydro-2-(2,5-undecadienyloxy)-	ether	aliphatic
59	C ₁₆ H ₂₄ O _{Si}	1.476381717	1,1-Di(but-3-enyl)-1-silacyclobutane	alkene	aliphatic
60	C ₁₆ H ₂₈ O ₂	0.780263913	7-Methyl-Z-tetradecen-1-ol acetate	ester	aliphatic
61	C ₁₆ H ₃₄	3.480589023	Hexadecane	alkane	aliphatic
62	C ₁₇ H ₂₈ O	0.891183783	13-Heptadecyn-1-ol	alkyne alcohol	aliphatic
63	C ₁₇ H ₂₈ O	0.474278065	13-Heptadecyn-1-ol	alkyne alcohol	aliphatic
64	C ₁₇ H ₃₂ O ₂	0.64065787	10-Methyl-8-tetradecen-1-ol acetate	ester	aliphatic
65	C ₁₇ H ₃₄ O ₈	0.455153949	Hexanoic acid, 2-ethyl-, oxybis(2,1-ethanedioxy-2,1-ethanediyl) ester	ester	aliphatic
66	C ₁₈ H ₁₄ O ₈	0.975329891	(+)-Dibenzoyl-L-tartaric acid anhydride	anhydride	aromatic and aliphatic
67	C ₁₈ H ₁₄ O ₉	5.393000574	>(+)Dibenzoyl-L-tartaric acid anhydride	ester	aromatic
68	C ₁₈ H ₃₀ O ₂	0.539300057	Valeric acid, tridec-2-ynyl ester	ester	aliphatic
69	C ₁₈ H ₃₂ O ₅	1.31956397	2-Butyloxycarbonyloxy-1,1,10-trimethyl-6,9-epidioxydecalin	ester	aliphatic
70	C ₁₈ H ₃₄ O	0.610059285	2-Methyl-E,E-3,13-octadecadien-1-ol	alkene	aliphatic

6	Molecular formula	Normalized mass %	Compound Name	H-C type (alkane/alkene/ester)	H-C compound type (aromatic/aliphatic)
71	C ₁₈ H ₃₄ O	0.65404475	4-Octadecenal	alkene	aliphatic
72	C ₁₈ H ₃₄ O ₂	0.522088353	Oleic Acid	Carboxylic acid	aliphatic
73	C ₁₈ H ₃₆	1.135972461	Cyclopropane, 1-(1,2-dimethylpropyl)-1-methyl-2-nonyl	alkane	aliphatic
74	C ₁₉ H ₂₆ O ₂ S	0.512526296	2-Thiopheneacetic acid, tridec-2-ynyl ester	ester	aromatic and aliphatic
75	C ₁₉ H ₃₂ O ₂	0.512526296	(7R,8RS)-7-hydroxymethyl-8-ethoxy-trans-bicyclo [4.3.0] -3 -nonene	alkene	aliphatic
76	C ₁₉ H ₃₈ O	1.510805125	9-Octadecene, 1-methoxy-,	alkene	aliphatic
77	C ₂₀ H ₂₁ NO ₂	0.524000765	Fenretinide	alkene and amide	aromatic
78	C ₂₀ H ₃₀ O ₁₀	0.770701855	Phorbol	unknown	unknown
79	C ₂₀ H ₃₈ O ₂	1.120673169	Ethanol, 2-(9-octadecenyloxy)-, (Z)-	alcohol and alkene	aliphatic
80	C ₂₀ H ₄₂ O ₃ S	10.70950469	Sulfurous acid, pentadecyl 2-pentyl ester	ester	aliphatic
81	C ₂₁ H ₂₆ N ₂ O ₆	0.502964238	Heptanediamide, N,N'-di-benzoyloxy	amide	aromatic and aliphatic
82	C ₂₁ H ₃₇ BO ₆	0.567986231	a-D-Mannofuranoside, 2,3:5,6-di-ethylboranediyl-cis-nerolidyl	Boronate ester	aliphatic
83	C ₂₁ H ₄₂ O ₃	0.858672786	>[1,1 '-Bicyclopropyl] -2-octanoic acid, 2'-hexyl-, methyl ester	ester	aliphatic
84	C ₂₂ H ₂₄ N ₂ O ₆	0.929432014	Octanediamide, N,N'-di-benzoyloxy	ester	aromatic and aliphatic
85	C ₂₂ H ₄₂ O ₂	0.589022758	1,2-15,16-Diepoxyhexadecane	alkane	aliphatic
86	C ₂₂ H ₄₇	0.646395104	Heptadecane, 9-hexyl	alkane	aliphatic
87	C ₂₃ H ₄₉	0.65404475	Heptadecane, 9-hexyl-	alkane	aliphatic

6	Molecular formula	Normalized mass %	Compound Name	H-C type (alkane/alkene/ester)	H-C compound type (aromatic/aliphatic)
	C ₂₆ H ₄₈	0.495314592	Cyclohexane, 1,4-dimethyl-2- <u>octadecyl-</u>	alkane	aliphatic
	C ₂₆ H ₄₈	2.390514439	Cyclohexane, 1,4-dimethyl-2- <u>octadecyl-</u>	alkane	aliphatic
	C ₂₇ H ₅₄	0.65404475	Cyclohexane, 1,3,5-trimethyl-2- <u>octadecyl</u>	alkane	aliphatic
	CseHesOl	0.613884108	9-Hexadecenoic acid, eicosyl ester, <u>(Z)-</u>	ester	aliphatic
⁹²	C ₃₇ H ₆₇ O	1.453432779	1-Heptatriacotanol	alkane	aliphatic
⁹³	C ₄₁ H ₆₄ O ₁₃	0.548862115	Digitoxin	ester	aliphatic

Table A. 1e.
GCMS result for PET pyrolytic after pyrolysis process

7	Molecular formula	Normalized mass %	Compound Name	H-C type (alkane/alkene/ester)	H-C compound type (aromatic/aliphatic)
	CH3O3P	1.072225674	Methylphosphonic acid	Phosphonic	aliphatic
2	C2H2F4	1.398955385	Norflurane	alkane	aliphatic
3	C2H3N3O	2.48498654	3H-1,2,4-Triazol-3-one, 1,2-dihydro	heterocyclic	aromatic
4	C4H6N2O	0.860541635	H-Imidazole-2-methanol	alcohol	aromatic
5	C5H9NO	10.30809231	Acetamide, N-2-propenyl	alkene	aliphatic
6	C5H9NO2	0.991693702	Cyclopentane, nitro-	alkane	aliphatic
7	C5H9NO3	1.150456731	Cyclopentanol, nitrate	nitrate ester	aliphatic
8	C5H11NO2S	1.237891443	4-Methylthiomorpholine-1, 1-dioxide	sulfone	aliphatic
9	C5H12B	0.858240722	Borane, ethylisopropylmethyl	alkane	aliphatic
10	C6H7BO2	0.780009664	Boronic acid, phenyl	organoboron	aromatic
11	CeHnN	1.166563126	1-(2-Methylpropenyl)aziridine	aziridine	aliphatic
12	CeHiZo	1.042313799	Oxirane, butyl-	alkene	aliphatic
13	CeHnNz	1.104438462	trans-1,2-Cyclohexanediamine	alkane	aliphatic
14	C6H14N2	0.865143462	1,3-Cyclohexanediamine	amine	aliphatic
15	C7H9N	0.768505097	2-Furanmethanamine, N-methyl-	amine	aromatic
17	C7H10O	0.816824279	2-Propen-1-one, 1-cyclopropyl	alkene	aliphatic
18	C7H11NO	0.977888222	4,4-Dimethyl-3-oxopentanenitrile	ketonitrile	aliphatic
19	C7H12O	1.279307885	5-Methyl-1-hexyn-3-ol	alkyne	aliphatic
20	C7H12O	1.060721106	5-Methyl-1,5-hexadien-3-ol	alkene	aliphatic

7	Molecular formula	Normalized mass %	Compound Name	H-C type (alkane/alkene/ester)	H-C compound type (aromatic/aliphatic)
21	C7H12O	0.826027933	2-n-Butylacrolein	alkene	aliphatic
22	C7H12O	0.8375325	Oxirane, [(2-propenyloxy)methyl]-	alkene	aliphatic
23	C7H14	0.842134327	2-Pentene, 3,4-dimethyl-, (Z)-	alkene	aliphatic
24	C7H14O	2.001794713	Oxirane, (1-methylbutyl)-	Epoxide	aliphatic
25	C7H14O	1.258599664	2-Hepten-1-ol, (E)-	alkene	aliphatic
26	C7H16	9.134626447	Pentane, 2,2-dimethyl	alkane	aliphatic
27	C ₈ H ₁₂ N ₂	1.152757645	1H-Imidazole, 4,5-dihydro-2-(1-methylethyl)-	alkane	aliphatic
	C ₈ H ₁₄	0.973286395	Cyclopropane, 1,1-dimethyl-2-(2-propenyl)-	alkene	aliphatic
29	C ₈ H ₁₄	0.996295529	1-Pentene, 3,3-dimethyl	alkene	aliphatic
30	C ₈ H ₁₆ O	1.049216539	Cycloheptanemethanol	alcohol	aliphatic
31	C ₉ H ₁₄ Si	0.789213318	Divinyldimethylsilane	alkene	aliphatic
32	C ₈ H ₁₄ O ₂	0.911161731	4-Octyne-3,6-diol	alkyne	aliphatic
33	C ₈ H ₁₆ O	1.932767309	Octanal	Aldehyde	aliphatic
34	C ₈ H ₁₆ O	1.166563126	Hexanal, 4,4-dimethyl	aldehyde	aliphatic
35	C ₈ H ₁₈ O	1.18266952	1-Pentanol, 2,3-dimethyl	alcohol	aliphatic
36	C ₉ H ₁₄ O	0.844435241	7-Oxabicyclo[4.1.0]heptane, 1,5-dimethyl-	alkane	aliphatic
37	C ₉ H ₁₄ O	0.773106923	spiro [4.4] nonan-1-one	alkane	aliphatic
38	C ₉ H ₁₆ O	1.056119279	Cyclooctanemethanol	alcohol	aliphatic
39	C ₉ H ₁₉ N	1.672764087	4-Propylcyclohexylamine	alkane	aliphatic
40	C ₉ H ₁₉ NO ₃	1.373645337	Nitric acid, nonyl ester	ester	aliphatic

7	Molecular formula	Normalized mass %	Compound Name	H-C type (alkane/alkene/ester)	H-C compound type (aromatic/aliphatic)
41	C10H16O	1.42196452	Hex-4-yn-3-one, 2,2-dimethyl	Alkyne	aliphatic
42	C10H15N	0.826027933	2-Bicyclo[3.3.1]nonene, 6-methylamino	alkene	aliphatic
43	C10H18O	0.996295529	5,5-Dimethyl-cyclohex-3-en-1-ol	alkene	aliphatic
44	C10H16O2	1.212581395	4,8-Dioxatricyclo[5.1.0.0(3,5)]octane, 1-methyl-5-(1-methylethyl)-	alkane	aliphatic
	C10H18	0.927268125	Cyclopentane, 2-isopropyl-1,3-dimethyl	alkane	aliphatic
46	C10H18O	1.06302202	4-Ethyl-1-hexyn-3-ol	Alkyne	aliphatic
47	C10H20	0.786912404	Cyclohexane, (1,1-dimethylethyl)-	alkane	aliphatic
48	C10H22	0.752398702	Pentane, 3-ethyl-2-methyl	alkane	aliphatic
49	C11H15N	0.754699616	2,6,6-Trimethyl-bicyclo[3.1.1]hept-3-ylamine	alkane	aliphatic
	CnHieN	1.127447597	2-Bicyclo[3.3.1]nonene, 6-methylamino	alkene	aliphatic
51	C11H20	0.865143462	4-t-Pentylcyclohexene	alkene	aliphatic
52	C11H20O2	0.858240722	2-(1-Methylcyclopentyloxy)-tetrahydropyran	ether	aliphatic
53	C11H21B	0.766204183	Borane, ethyldipropyl	Organoboron	aliphatic
54	C11H24	0.929569039	Hexane, 2,4,4-trimethyl	alkane	aliphatic
55	C12H18	1.187271347	Cyclopropane, 1,1-dimethyl-2-(2-propenyl)-	alkene	aliphatic
	C12H20O	0.747796875	1-Propanone, 1-(3-cyclohexen-1-yl)-2,2-dimethyl-	alkene	aliphatic
57	C12H22	1.267803318	2,4,4-Trimethyl-1-hexene	alkene	aliphatic
58	C12H22O	0.759301443	2-n-Heptylcyclopentanone	ketone	aliphatic

7	Molecular formula	Normalized mass %	Compound Name	H-C type (alkane/alkene/ester)	H-C compound type (aromatic/aliphatic)
59	C12H23NO2	3.474379329	1-Hexyl-1-nitrocyclohexane	alkane	aliphatic
60	C12H24	1.214882308	Cyclohexane, (1,3-dimethylbutyl)-	alkane	aliphatic
61	C12H24	1.279307885	3-Decene, 2,2-dimethyl-, (E)-	alkene	aliphatic
62	CoHis	3.060214905	4-t-Pentylcyclohexene	alkene	aliphatic
63	CoHis	0.908860818	Cyclohexane, (4-methylpentyl)-	alkane	aliphatic
64	C13H24	1.099836635	Cyclohexane, (3,3-dimethylpentyl)-	alkane	aliphatic
65	C13H26	1.334529808	1-Decene, 3,3,4-trimethyl	alkene	aliphatic
66	C13H26	0.984790962	Hexane, 3,3,4-trimethyl-	alkane	aliphatic
67	C14H10N3O3	0.759301443	Acetophenone, 2-[(p-nitrophenyl)imino]-	ketone	aromatic
	C14H24O4	0.869745289	Methoxyacetic acid, 10-undecenyl ester	ester	aliphatic
	C14H26O2	0.888152597	3-Methyl-2-butenic acid, oct-3-en-2-yl ester	ester	aliphatic
70	C15H28	1.424265433	Cis-1-methyl-3-n-nonylcyclohexane	alkane	aliphatic
71	C15H28O4	1.327627068	Oxalic acid, cyclohexylmethyl isohexyl ester	ester	aliphatic
72	C23H48O3	1.005499183	Carbonic acid, heptadecyl propyl ester	ester	aliphatic

APPENDIX B



Figure A. 2a. Wifi Digital Microscope



Figure A. 2b. Electronic Digital Precision

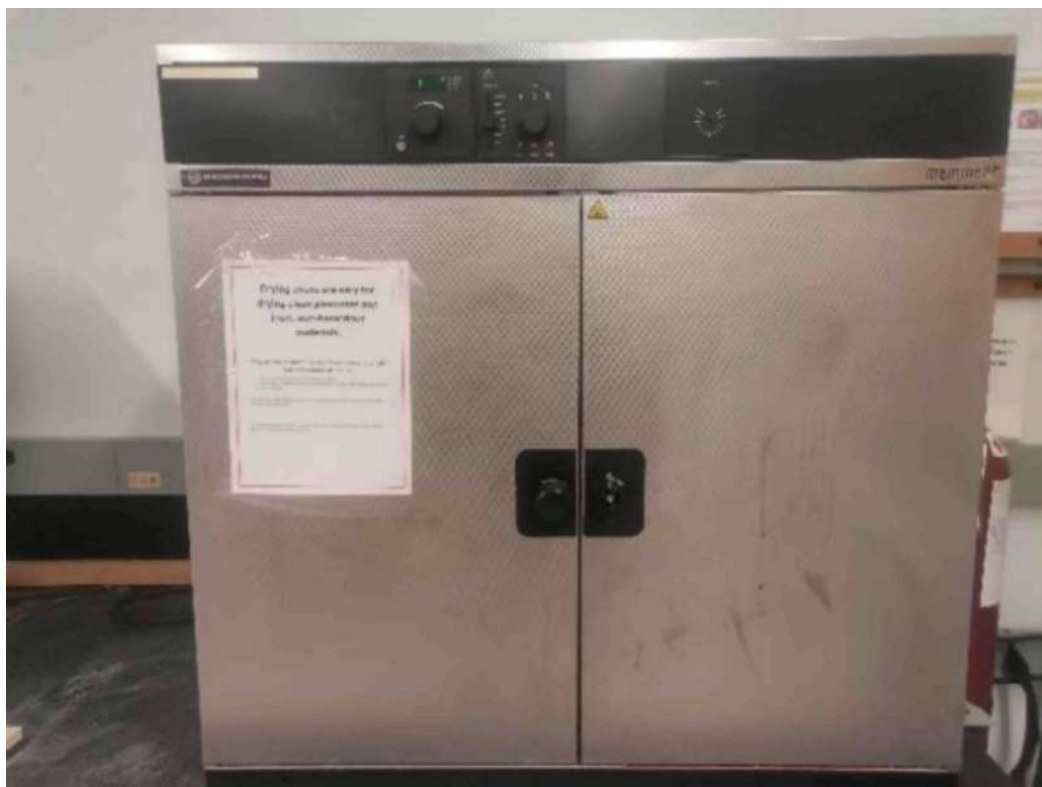


Figure A. 2c. Memmert Wisconsin Oven



Figure A. 2d. Digital Melting Point with Capillary Tube Red Tip G0553

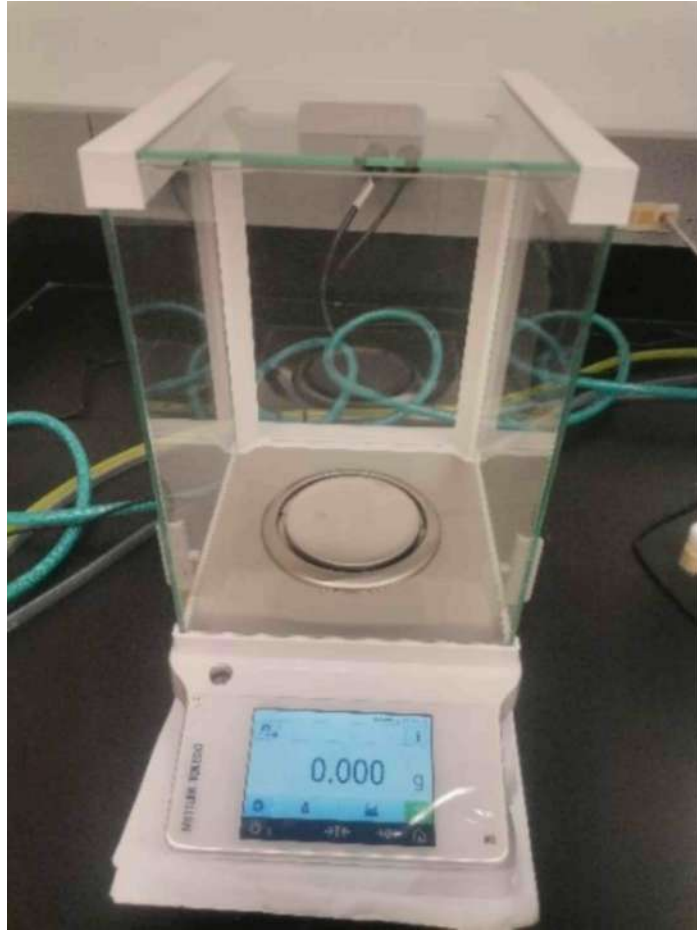


Figure A. 2e. Mettler Toledo Analytical Balance

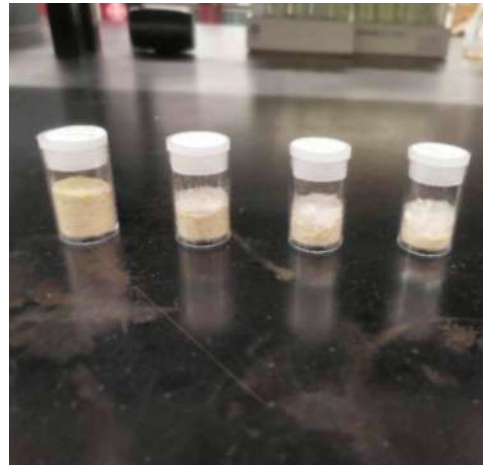


Figure A. 2f. Raw material sample ratio



Figure A. 2g. Muffle Furnace Fisher Scientific Model 550-126



Figure A. 2h. Elemental Analyser Model Thermo Electron, Flash EA 1112 Series



Figure A. 2i. Bomb Calorimeter model PARR 6400



Figure A. 2j Thermogravimetric Analyser (TGA) model Mettler Toledo



Figure A. 2k. Fourier Transform Infrared Spectroscopy (FTIR)



Figure A. 2l. Pyrolysis mini plant



Figure A. 2m. Portable Dissolved Oxygen Meter



Figure A. 2n Portable Turbidity Meter



COD Reactor (Digital Reactor Block)



COD Spectrophotometer

Figure A. 2o COD Reactor and COD Spectrophotometer



Sample is put into the BOD bottle brand Velp Scientifica



BOD Incubator Model FOC 2251 brand Velp Scientifica

Figure A. 2p BOD bottle and BOD incubator



Figure A. 2q. Portable pH meter



Porcelain Funnel Buchner



Drying Oven

Figure A. 2r. Porcelain Funnel Buchner and Drying Oven



Figure A. 2s. Multi Gas Detector Leakage



Figure A. 2t. Magnetic Stirrer and Infrared Thermometer



Figure A. 2u. Glass Hydrometer



Figure A. 2v. Bomb Calorimeter model IKAC2000 BASIC



Figure A. 2w. Gas Chromatography Mass Spectrometer (GCMS)

APPENDIX 3

Table A. 3a.
ANOVA analysis result for HDPE pyrolytic oil after pyrolysis process

Regression Statistics	
Multiple R	0.961814596
R Square	0.925087317
Adjusted R Square	0.920680689
Standard Error	25.53481136
Observations	19

ANOVA					
	df	SS	MS	F	Significance F
Regression	1	136880.507	136880.507	209.9308662	5.35954E-11
Residual	17	11084.45205	652.026591		
Total	18	147964.9591			

	Coefficients	Standard Error	t Stat	P-value	Lower 95%	Upper 95%	Lower 95.0%	Upper 95.0%
Intercept	62.00526316	11.26825627	5.50264936	3.88276E-05	38.23132055	85.77920576	38.23132055	85.77920576
X Variable 1	3.099298246	0.213907111	14.4889912	5.36E-11	2.647993691	3.5506028	2.647993691	3.5506028

Table A. 3b.
ANOVA analysis result for HDPE2:1PET ratio pyrolytic oil after pyrolysis process

Regression Statistics	
Multiple R	0.952130261
R Square	0.906552035
Adjusted R Square	0.901055096
Standard Error	8.850501828
Observations	19

ANOVA					
	df	SS	MS	F	Significance F
Regression	1	12918.3665	12918.3665	164.9194239	3.54121E-10
Residual	17	1331.633504	78.33138261		
Total	18	14250			

	Coefficients	Standard Error	t Stat	P-value	Lower 95%	Upper 95%	Lower 95.0%	Upper 95.0%
Intercept	-17.0028045	5.237667913	-3.246254788	0.004750049	-28.0533179	-5.95229118	-28.0533179	-5.95229118
X Variable 1	0.310177274	0.024153166	12.84209578	3.54121E-10	0.259218548	0.361136	0.25921855	0.361136

Table A. 3c.
ANOVA analysis result for HDPE1:1PET ratio pyrolytic oil after pyrolysis process

Regression Statistics	
Multiple R	0.957396340
R Square	0.916607751
Adjusted R Square	0.911702325
Standard Error	8.360761105
Observations	19

ANOVA					
	df	SS	MS	F	Significance F
Regression	1	13061.66045	13061.6605	186.8558767	1.33891E-10
Residual	17	1188.339546	69.9023263		
Total	18	14250			

	Coefficients	Standard Error	t Stat	P-value	Lower 95%	Upper 95%	Lower 95.0%	Upper 95.0%
Intercept	-13.90447593	4.716791924	-2.94786714	0.009000126	-23.85603701	-3.95291485	-23.856037	-5.95229118
X Variable 1	0.368314516	0.02694421	13.6695236	1.33891E-10	0.311467202	0.42516183	0.311467202	0.361136

Table A. 3d.
ANOVA analysis result for HDPE1:2PET ratio pyrolytic oil after pyrolysis process

Regression Statistics	
Multiple R	0.947993614
R Square	0.898691891
Adjusted R Square	0.892732591
Standard Error	9.215206572
Observations	19

ANOVA					
	df	SS	MS	F	Significance F
Regression	1	12806.3595	12806.35945	150.8049294	7.06251E-10
Residual	17	1443.64055	84.92003216		
Total	18	14250			

	Coefficients	Standard Error	t Stat	P-value	Lower 95%	Upper 95%	Lower 95.0%	Upper 95.0%
Intercept	-8.55762958	4.84666941	-1.76567223	0.095403577	-18.7832082	1.66794903	-18.783208	1.66794903
X Variable 1	0.279533457	0.02276282	12.28026585	7.06251E-10	0.231508109	0.32755881	0.23150811	0.32755881

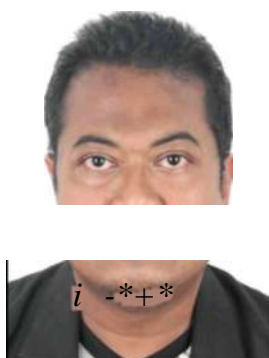
Table A. 3e.
ANOVA analysis result for PET ratio pyrolytic oil after pyrolysis process

Regression Statistics	
Multiple R	0.959904482
R Square	0.921416614
Adjusted R Square	0.916794062
Standard Error	8.116117763
Observations	19

ANOVA					
	df	SS	MS	F	Significance F
Regression	1	13130.18675	13130.18675	199.3307144	8.06279E-11
Residual	17	1119.813248	65.87136754		
Total	18	14250			

	Coefficients	Standard Error	t Stat	P-value	Lower 95%	Upper 95%	Lower 95.0%	Upper 95.0%
Intercept	-13.17727934	4.521804388	-2.91416395	0.009667836	-22.7174527	-3.63710601	-22.7174527	-3.637106008
X Variable 1	0.337551397	0.023908526	14.11845298	8.06279E-11	0.287108817	0.387993977	0.287108817	0.387993977

AUTHOR'S PROFILE



Safwan Hafizi bin Masakhoh received his Bachelor of Eng. (Hons) Chemical Engineering at School of Chemical Engineering, Universiti Sains Malaysia in 2005. He started his career in 2005 at the Tractors Malaysia as Management Trainee. In 2006 he continue his journey at TMA-Joy Industries (Asia Pasific) Sdn Bhd as Design Engineer. Then after 2 years he continue his career from technical to teaching as Technical Training Officer in German Malaysian Institute under Department of Industrial Electronic. Three years later he continue with Majlis Amanah Rakyat (MARA) as Vocational Training Officer at Institut Kemahiran MARA Bintulu, Sarawak. In 2020, he continue his study as a full-time master student with support of MARA and will continue his career with MARA after complete his study.

LIST OF PUBLICATIONS

- S.H. Masakhoh, Z. Januri, N.A. Rahman, Characterization of Pyrolytic Oil from Different Blending Ratio of HDPE and PET Plastic Waste Through Gasification Pyrolysis Process. *Proceeding of International Exchange and Innovation Conference on Engineering & Sciences (IEICES) 10*, 1277-1284 (2024); <https://doi.org/10.5109/7323420>. Published Online: 17.10.2024
- S.H. Masakhoh, Z. Januri, L.C. Lau, N.A. Rahman, Pyrofuel Extraction From Polyethylene Terephthalate (PET) Plastic Waste. *AIP Conference Proceedings*

2496, 040001 (2022); <https://doi.org/10.1063/5.0090704>. Published Online:
18.05.2022

Awards:

1. Malaysia Technology Expo (MTE 2023), Kuala Lumpur, Malaysia. *Silver Medal: Pyrofuel*
2. Malaysia Technology Expo (MTE 2022) SDG International Innovation Awards & Expo, Kuala Lumpur, Malaysia. *Silver Medal: Pyrofuel*
3. SIRFM Invention, Innovation & Technology Expo 2022 (SI2TE 2022), Kulim, Kedah, Malaysia. *Silver Medal: Pyrofuel*
4. International Intellectual Property, Invention, Innovation and Technology Exposition 2020 (TPITEX'20), Bangkok, Thailand. *Silver Medal: PYROLYSIS: From Plastic Waste to Petroleum Product.*

Patent:

System for Converting Plastic Waste into Fuel Using Pyrolysis (IP No: UI 2020005316)

Scholarship and Academic Exchange:

Canada-ASEAN Scholarship and Educational Exchanges for Development (SEED)
(13.09.2022-08.01.2023)

- Canada Host Institution: University of Regina, Saskatchewan, Canada.
- Scholarship value: CAD10,800.